METEOR-Berichte 09-2

# *SUBFLUX*

## Cruise No. 66

August 12 – December 22, 2005, Las Palmas (Spain) – Talcahuano (Chile)


**Warner Brückmann, Monika Rhein, Gregor Rehder,
Jörg Bialas, Achim Kopf**

Editorial Assistance:

Andreas Krell
Alfred-Wegener-Institut für Polar- und Meeresforschung, Bremerhaven

Leitstelle METEOR
Institut für Meereskunde der Universität Hamburg

2009

The METEOR-Berichte are published at irregular intervals. They are working papers for people who are occupied with the respective expedition and are intended as reports for the funding institutions. The opinions expressed in the METEOR-Berichte are only those of the authors. The reports can be obtained from:

Universität Hamburg
Zentrum für Meeres- und Klimaforschung
Institut für Meereskunde
Leitstelle METEOR/MERIAN
Bundesstr. 53
20146 Hamburg
Germany

The reports are available in PDF format from http://www.dfg-ozean.de/.
The METEOR expeditions are funded by the *Deutsche Forschungsgemeinschaft* and the *Bundesministerium für Bildung und Forschung*.

Addresses of the editors:

Dr. Warner Brückmann
Leibniz-Institut für Meereswissenschaften
IFM-GEOMAR
Wischhofstr. 1-3
24148 Kiel
Germany
Tel: +49 (0)431 600 2819
Fax: +49 (0)431 600 2916
Email: wbrueckmann@ifm-geomar.de

Prof. Dr. Monika Rhein
Universität Bremen
Institut für Umweltphysik (IUP)
Abteilung Ozeanographie
Otto-Hahn-Allee
28359 Bremen
Germany
Tel: +49 (0)421 218 2408
Fax: +49 (0)421 218 7018
Email: mrhein@physik.uni-bremen.de

Prof. Dr. Gregor Rehder
Leibniz-Institut für Ostseeforschung
Seestraße 15
18119 Rostock
Germany
Tel: +49 (0)381 5197 336
Fax: +49 (0)381 5197 302
Email: gregor.rehder@io-warnemuende.de

Dr. Jörg Bialas
Leibniz-Institut für Meereswissenschaften
IFM-GEOMAR
Wischhofstr. 1-3
24148 Kiel
Germany
Tel: +49 (0)431 600-2329
Fax: +49 (0)431 600-2922
Email: jbialas@ifm-geomar.de

Prof. Dr. Achim Kopf
MARUM
Zentrum für Marine Umweltwissenschaften
Universität Bremen
Postfach 330 440
28334 Bremen
Germany
Tel: +49 (0)421 218 65800
Fax: +49 (0)421 218 65805
Email: akopf@uni-bremen.de

Citations:

Brückmann W, Rhein M, Rehder G, Bialas J, Kopf A (2009) (Eds) SUBFLUX, Cruise No. 66, August 12 - December 22, 2005. METEOR-Berichte 09-2, 158 pp, Universität Hamburg.

ISSN 0936-8957

METEOR-Berichte 09-2

# *SUBFLUX*

## Cruise No. 66

August 12 – December 22, 2005, Las Palmas (Spain) – Talcahuano (Chile)


**Warner Brückmann, Monika Rhein, Gregor Rehder,
Jörg Bialas, Achim Kopf**

Editorial Assistance:

Andreas Krell
Alfred-Wegener-Institut für Polar- und Meeresforschung, Bremerhaven

Leitstelle METEOR
Institut für Meereskunde der Universität Hamburg

2009

**Table of Contents** **Page**

**Table of Contents Part 1 (M66/1)** **Page**

**Table of Contents Part 2 (M66/2)** **Page**

**Table of Contents Part 3 (M66/3)** **Page**

**Table of Contents Part 4 (M66/4)** **Page**

## Abstract

The R/V METEOR M 66 cruise was carried out primarily in support of the "SFB" 574 (Volatiles and Fluids in Subduction Zones), a Cooperative Research Center dedicated to understanding the budget, reactions, and recycling of volatile elements in subduction zones and their role in climate forcing. To address the short- and long-term variability of the Earth's climate, the geochemical evolution of the hydrosphere and atmosphere, and related processes that are all connected to the return flow of volatiles and fluids from subduction zones, the SFB 574 is studying the Central American forearc off Costa Rica and Nicaragua (Fig 1).

The goals of the initial, oceanographic leg of cruise M 66 were to obtain part of a 2-year time series of the transport of southern hemispheric water through the passages into the Caribean, to study the circulation and variability of the flow in the deep western boundary current and in the interior of the basin, and to calculate time scales of deep water spreading from the Labrador Sea to 16°N.

## Zusammenfassung

Die Reise M 66 von FS METEOR wurde in erster Linie zur Klärung von Fragestellungen des Sonderforschungsbereichs SFB 574 (Fluide und Volatile in Subduktionszonen) durchgeführt. Das Hauptziel des SFB 574 ist es, das Budget, die Reaktionen und die Rückführung volatiler Elemente in Subduktionszonen und ihre Wirkung auf das Klima zu verstehen. Für das Studium der kurz- und langfristigen Klimavariabilität, der geochemischen Evolution der Hydro- und Atmosphäre sowie verwandter Prozesse, die mit dem Recycling von Volatilen und Fluiden aus Subduktionszonen verbunden sind, fokussiert der SFB 574 seine Untersuchungen auf den zentralamerikanischen Kontinentalrand vor Costa Rica und Nicaragua (Abb. 1).

Das Ziel des ersten, ozeanographischen Fahrtabschnitts von M 66 war die Erhebung von Daten im Rahmen einer 2jährigen Zeitserie des Transports von Südhemisphären-Wassermassen durch Passagen in die Karibik, die Untersuchung der Wasserzirkulation und Variabilität im "Deep Western Boundary Current" und im Inneren des Beckens, sowie die Abschätzung von Zeitskalen der Tiefwasserausbreitung von der Labrador-See bis 16°N.

## Research Objectives

*SFB Objectives*

The RV METEOR M66 cruise is of central importance to the "Sonderforschungsbereich 574". The multi-disciplinary analysis of the volatile phases (water, carbon, sulfur and halogens) and their complex effects on the exosphere is an ambitious task, and one of the highest priority objectives of today's geoscience.

Volatiles are mainly introduced into subduction zones via the sediments, the altered products of oceanic crust, and the trench fill from down-slope mass wasting. The output is via fluid venting at the deformation front, by gas hydrate formation/dissociation, and by volcanic degassing at the forearc. Inside the subduction zone the incoming material is transformed, mobilized or fractionated into different volatile reservoirs and phases. These phases are either ejected into the exosphere through the upper plate, accreted to the leading edge of the continental plate, or are transported into the lower mantle. The tectonic style of subduction, the structure of

the margin wedge, and the properties and configuration of the downgoing plate all exert a first order control on volatile budget, its transformation, and return pathway.

The basic data acquisition for the investigations aboard RV METEOR was done by geophysical surveys, multibeam and side scan sonar surveys, sediment coring, water column sampling for methane, video-guided sea floor observations and lander deployments.

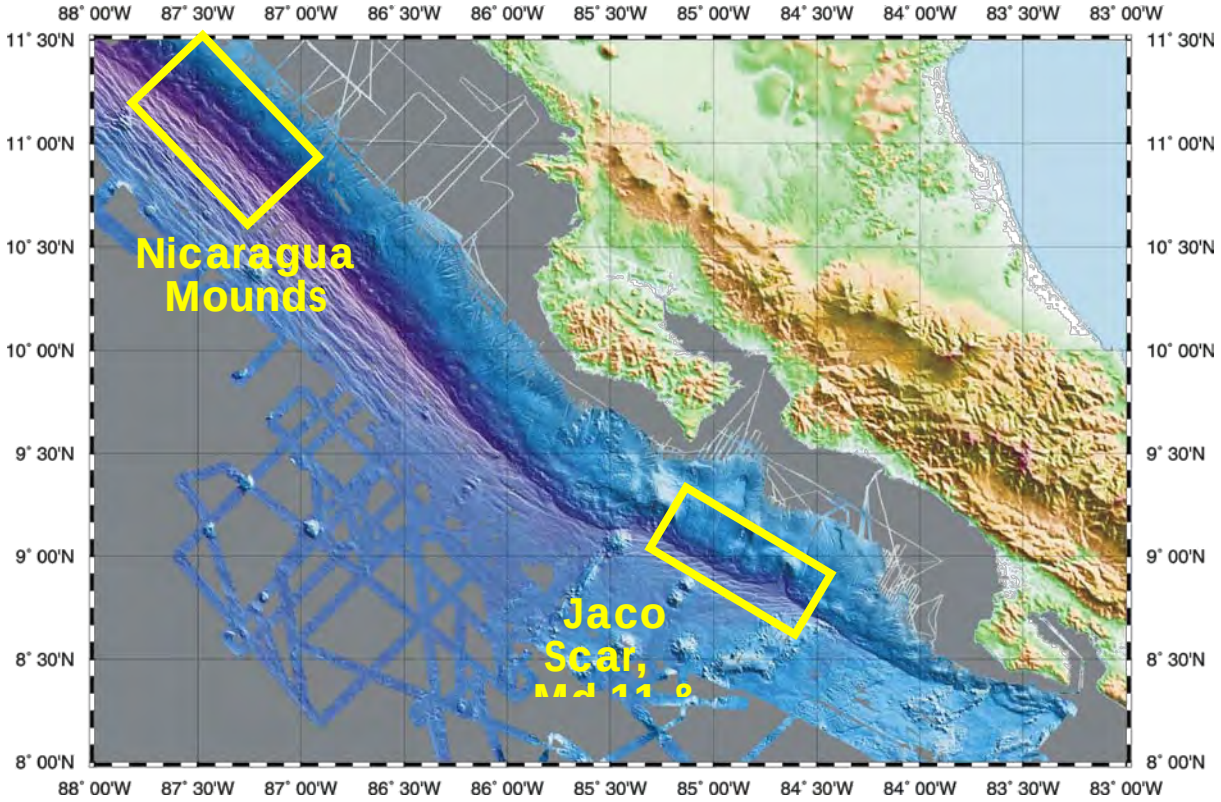


**FIG. 1:** General structure of the seafloor at the Costa Rica/ Nicaragua Pacific margin.

*Objectives of Leg 1*

The objectives of Leg 1 of M66 were unrelated to the SFB 574. It was an oceanographic leg focussing on upper ocean circulation. The goal was to obtain a 2-year time series of the transport of southern hemispheric water through the passages into the Caribbean. Further objectives were to determine the variability of the fraction of South Atlantic water east and north of the islands and to estimate the transport of southern hemispheric water east of the islands across 16°N.

With regard to deep circulation the goal was to study the circulation and variability of the flow in the deep western boundary current and in the interior of the basin and to calculate time scales of deep water spreading from the Labrador Sea to 16°N.

For this purpose, CTDO sensors were used to determine the distribution of water mass characteristics (pressure, temperature, salinity, oxygen) and analyses were performed to trace chlorofluorocarbon components CFC-11 and CFC-12 in water samples from 10L bottles. In addition, measurement of the velocity field were performed with ADCPs (Acoustic Doppler Current Profilers) attached to the CTDO system and with the vessel-mounted ADCPs (75kHz and 38.5kHz). A further objective was the recovery of the CARIBA mooring array instruments, i.e. acoustic current meters, T/S sensors and Inverted Echo Sounders (PIES) east of the Caribbean.

*Objectives of Leg 2*

Leg 2a was primarily dedicated to the transit to the working area off Central America. After the ship had passed the Panama Canal, a geophysically oriented program was carried out in the SFB574 working area off Costa Rica, with deployments of OBS/OBH stations and recovery of previously deployed stations.

The scientific program of Leg 2b comprised several detailed investigations of sites where active fluid venting occurs. The ROV Quest operated by the University of Bremen was used to sample and monitor mud extrusions, slides, and scarps generated by seamount subduction off Costa Rica and Nicaragua. The work complemented earlier work using standard and towed video-guided equipment. In addition, 2 different lander systems were deployed and several CTD/Rosette casts were performed to extend time series of the methane inventory at several stations and to quantify the inventory of the vent-derived methane at the shallow, very active Quepos Slide.

*Objectives of Leg 3*

The foremost objective of the work performed during Leg 3 was deep sampling of mud diapirs and carbonate mounds, large numbers of which have been found off Costa Rica and Nicaragua. These structures are considered to be a major element in the recycling of volatiles and fluids in this erosive continental margin – for this reason they are the focus of work for several subprojects of the SFB 574. Clear evidence has been found that fluids are transported upwards from deep sources as well as shallower sources.

Previous SFB work resulted in a differentiation between several types of authigenic carbonates: chemoherms and crusts associated with fluid expulsion at the sediment surface, gas hydrate – associated carbonates as well as limy and dolomitic concretions. Complete cores of all depths of these carbonate caps would enable a high-resolution temporal reconstruction of the devolatilisation history and fluid drainage. In addition, the pore water chemistry of the sediments can be expected to be less contaminated by sea water below the carbonate caps, as suggested by earlier samples from the marginal areas of mounds. This would allow for a better assessment of the source depth of fluids by geochemical and isotope geochemical methods, providing answers for one of the central SFB 574 objectives. Coring was performed by a portable drilling device, the BGS Seabed Rockdrill and Vibrocorer, which was deployed via METEOR's A frame.

Mound Culebra, Mound 10, Mounds 11 and 12 as well as a group of large mounds off Nicaragua discovered during SONNE cruise SO173 are already well known by preliminary SFB sampling using gravity corers and piston corers as well as OFOS surveys performed on cruises SONNE 163 and SONNE 173. For Leg 3a, representative profiles from the top of each structure as well as two further cores from the flanks were recovered in order to examine if potential earlier phases of stagnation during the formation of the mounds are documented within the carbonate layers.

*Objectives of Leg 4*

The major aim of Leg 4a was to understand the processes occurring in the other rise. To study the impact of outer rise faulting on the hydration of the oceanic crust approaching the Central American trench offshore Nicaragua two different techniques were used.

(i) a network of ocean bottom seismometers and hydrophones were left on the seafloor to record the natural seismicity in the outer rise area during leg M66/2a. The aim of this approach is to define active faults and the depth down to which they are active. This depth may provide an initial assessment of the depth down to which fluids can penetrate into the upper mantle.

(ii) active seismic wide-angle and refraction work was used to test the hypothesis that the mantle is hydrated or serpentinized. Typically, the upper mantle has velocities between 8.0 to 8.2 km/s. If the mantle is hydrated or serpentinized, seismic velocities are much lower. A serpentinization of 20 % would change the seismic velocities in the mantle to 7.6 km/s.

Furthermore, high resolution active seismic profiling was applied along three profiles to support deep-towed seismic streamer data analysing the structure and formation of mound structures along the continental margin. Cruise SO173-1 mapped a large number of mound locations by deep-towed sidescan and multichannel seismic streamer recordings. Seismic images of the structures indicate that they are related to faults or ridge-like tectonic features. A BSR has been mapped within the entire area of investigation with varying amplitude strength. Additional seismic data are to verify the variability of the BSR reflectivity and investigate the causes of BSR uplift or disappearance underneath the various mound structures and the relation to the tectonic setting.

Leg 4b was entirely dedicated to testing a new CPT (cone penetration testing) free fall lance. The overall objective when studying active convergent margins is to unravel the complex fluid processes and their ramifications for natural hazards such as submarine landslides and earthquakes. The understanding of such processes may be severely deepened if the crucial controlling parameters are measured in situ. For that purpose, a free fall CPT lance has been built. This device allows a time- and cost-effective characterization of both pore pressure and sediment strength in the uppermost ocean floor sediments. CPT measurements are usually carried out with a cylindrical lance, either motor-driven or as a free fall instrument. Penetration depth is controlled by sediment composition/grain size as well as the weight of the lance. In our case, it is a few meters. During penetration, frictional forces at the tip and along the sleeve of the lance are measured. The amount of frictional resistance allows for a classification of the sediment. In addition to these first order strength measurements, a piezometric cell is measuring pore pressure in the sediment.

Meteor-Berichte 09-2

# *SUBFLUX*

## PART 1

## Meridional Overturning in the subtropical Atlantic

Cruise No. 66, Leg 1

August 12 – September 19, 2005, Las Palmas (Spain) – Willemstad (Curacao)


**Monika Rhein**, Jan Aschmann, Oliver Bislich, Ramon Brentführer, Klaus Bulsiewicz, Reinhard Drews, Sandra Erdmann, Gerhard Fraas, Karin Fraas, Jann Grahlmann, Thor Hansteen, Kerstin Kirchner, Andreas Klügel, Christian Kreutzmann, Jon-Olaf Krisponeit, Anna Ksienzyk, Xin Li, Christian Mertens, Michael Oschmann, Reiner Steinfeldt, Uwe Stöber, Maren Walter, Torsten Truscheit, Gesa Voehrs

Editorial Assistance:

Andreas Krell
Alfred-Wegener-Institut für Polar- und Meeresforschung, Bremerhaven

Leitstelle METEOR
Institut für Meereskunde der Universität Hamburg

2009

**Table of Contents Part 1 (M66/1)** Page

## 1.1 Participants

| Name | Discipline | Institution |
|---|---|---|
| 1 . Rhein, Monika, Prof. Dr. | Chief scientist | IUPHB |
| 2 . Bulsiewicz, Klaus | CFC-analysis | IUPHB |
| 3 . Fraas, Gerhard | Moorings | IUPHB |
| 4 . Fraas, Karin | CTD/ADCP watch | IUPHB |
| 5 . Voehrs, Gesa | CTD/ADCP watch, dust sampling | IUPHB |
| 6 . Erdmann, Sandra | CFC-watch | IUPHB |
| 7 . Bislich, Oliver | CTD/ADCP watch | IUPHB |
| 8. Kirchner, Kerstin | CTD/ADCP | IUPHB |
| 9 . Krisponeit, Jon-Olaf | CTD/ADCP watch | IUPHB |
| 10. Aschmann, Jan | CTD/ADCP watch | IUPHB |
| 11. Kreutzmann, Christian | Meteorology | DWD |
| 12. Mertens, Christian, Dr. | vm-ACPs,moorings | IUPHB |
| 13. Drews, Reinhard | CFC watch | IUPHB |
| 14. Oschmann, Michael | oxygen analysis, dust sampling | IUPHB |
| 15. Grahlmann, Jann | CTD/ADCP watch, dust sampl. | IUPHB |
| 16. Steinfeldt, Reiner, Dr. | CTD/Salinometer | IUPHB |
| 17. Walter, Maren, Dr. | LADCP | IUPHB |
| 18. Li, Xin | CTD/ADCP watch | IUPHB |
| 19. Brentführer, Ramon | LADCP | IFM-GEOMAR |
| 20. Stöber, Uwe | CTD/ADCP watch | IUPHB |
| 20. Torsten Truscheit | Meteorology | DWD |
| *21. Klügel, Andreas, Dr. | Geology | IFM-GEOMAR |
| *22. Ksienzyk, Anna | Geology | IFM-GEOMAR |
| *23. Hansteen, Thor, Dr. | Geology | IFM-GEOMAR |

*participants from August, 12. to 15. 2005.

**IUPHB** Universität Bremen, Institut für Umweltphysik, Abt. Ozeanographie, Otto-Hahn-Allee, NW1, 28359 Bremen, Germany

**DWD** Deutscher Wetterdienst, Geschäftsfeld Seeschifffahrt, Bernhard-Nocht-Str. 76, 20359 Hamburg, Germany

**IFM-GEOMAR** Leibniz Institut für Meeresforschung, Wischhofstrasse, 24105 Kiel, Germany

## 1.2 Research Program

The warm branch of the Atlantic meridional overturning circulation is important for the role of the North Atlantic in European climate and climate change. Yet, no time series has been made so far of the transport of southern hemispheric water after crossing the Atlantic. In this project, we have obtained a 2-year time series of the transport of southern hemispheric water through the passages into the Caribbean and determined the variability of the fraction of South Atlantic water east and north of the islands. Moreover we have estimated the transport of southern hemispheric water east of the islands across 16°N. The deep circulation encompasses the major part of the cold path of the overturning circulation. We have studied the circulation and variability of the flow in the deep western boundary current and in the interior of the basin and calculated time scales of deep water spreading from the Labrador Sea to 16°N.

CTDO sensors were applied to determine the distribution of water mass characteristics (pressure, temperature, salinity, oxygen), and water samples from 10-L bottles were analyzed for the chlorofluorocarbon components CFC-11 and CFC-12. The velocity field was measured with ADCPs (Acoustic Doppler Current Profilers) attached to the CTDO system and with the vessel-mounted ADCPs (75kHz and 38.5kHz). The Bremen mooring array CARIBA, which had been deployed east of the Caribbean equipped with acoustic current meters, T/S sensors and Inverted Echo Sounders (PIES), was recovered. The moored time series was combined with the shipboard measurements.

The data set complemented by our measurements from recent years and by historical data allows estimating the strength and the pathways of the warm path of the Atlantic meridional overturning at the inflow into the Caribbean between the Windward Islands and east of the Islands across 16°N in the western Atlantic.

## 1.3 Narrative of the cruise

RV METEOR departed on August 13, 9 UTC from Las Palmas and headed towards the Henry Seamount at 27°18.5'N, 17°47.0'W. Dredging began at August 14, 1 UTC, and ended at August 15, 1 UTC. The weather was favourable for dredging in the southern section of the seamount. The METEOR reached Hierro at August 15, 6:30 UTC, and the three geologists and one technician departed while METEOR stayed near Puerto de la Estaca.

At August 15, 7:30 UTC, the METEOR headed towards the easternmost CTD station (51°W) of the 16°N section. With the trade winds from the back the speed of the METEOR was around 12 kn most of the time. During the transit of about 2000nm, a CTD test station was carried out successfully at August 17, 15:30 UTC. The CTD was lowered to 2000m depth. At August 20, 16 UTC, the 22 Niskin bottles were tested for CFC contamination by closing them all in the CFC minimum zone at 2500m depth. In the eastern Atlantic, very small concentrations are expected at this depth level. The test was successful, all bottles closed and no contamination could be found. This result was supported by the oxygen analysis. A second test was done on August 21, 17 UTC.

The 16°N section began at August 22, 15 UTC at the flank of the Midatalantic Ridge (CTD 4, 15°15'N, 51°20'W) at a water depth of 4000m. In order to resolve the flow-field of the Antarctic Bottom Water (AABW) at the bottom of the flank, the station spacing was at first 10nm, and then increasing to 20nm. The chosen spatial distance allows the resolution of the flow field with

the LADCP profiles measured parallel to the CTD casts. The LADCP profiles had good quality throughout the water column, but the expected northward flow of the AABW was not observed. The subsequent stations also showed the tidal velocities in the order of 3-4cm/s. The weather and sea remained calm and provided excellent working conditions. In the early morning (5UTC) of August, 25 the METEOR reached the longitude of 55°W, which on former cruises was the boundary between a net southward flow of North Atlantic Deep Water west of 55°W and a more sluggish and uncoordinated flow east of that longitude. Between 55°30'W and 57°40'W (Aug 25, 11UTC – Aug 26, 20UTC) we encountered an eddy. These eddies are called NBC rings, because of their creation at the retroflection of the North Brasil Current (NBC) into the North Equatorial Counter Current off the coast of Brazil. These rings are crucial for the transport of water from the South Atlantic across 16°N. The ring was subsurface intensified with highest velocities of 25-35cm/s between 400m and 600m depth, the fraction of South Atlantic water (SAW) was higher than 70% in the intermediate and central water masses. The signal at the surface was weak, so that most likely the ring cannot be seen by remote sensing.

During CTD 27 on August 27, one of the LADCP workhorses from RD Instruments (San Diego) failed, so that unfortunately we were unable to measure the deep velocity distribution in the western boundary region, where we expected the strongest signals. This instrument was sent to RD Instruments (RDI, San Diego) for refurbishment in February 2005. It failed after 20 profiles in June 2005 during our cruise with N/O Thalassa . The instrument was then sent back to RDI at July, 12 and after repair was delivered to RV METEOR to Las Palmas. Presumably, the instrument was not properly repaired. Due to the many parallel research cruises we were unable to take a backup instrument with us. For the remaining work in the deep western boundary current no deep velocity measurements could be carried out. With one instrument remaining, only velocity profiles to water depths shallower than 3000m are possible.

The 16°N section was finished with CTD 38 at August, 29, 4:30UTC. The METEOR headed south to carry out CTD stations every 9nm on the way to the mooring position B10 east of Saint Lucia and then to B8 north of Tobago. B10 was reached at August 30, 12 UTC (CTD 54), and B8 at September 1, 2UTC. Near that position, the surface water was murky and down to about 5m very fresh with salinities of about 27.0. Both features indicated the presence of river outflow from the Amazon and/or Orinoco. Although low salinities are frequently observed in that area especially a few months after the maximum of the river outflow, they are usually not below 32.

The METEOR turned towards Barbados, i.e. to the position of mooring B9 on the western side of Barbados. After finishing the CTD section, the remaining time was used to repeat the northern part of the section from Tobago to Barbados down to 12°35'N, 60°0'W with the two vessel mounted ADCPs. In the early morning of September, 2 (9:40UTC), CARIBA mooring B9 was released. 7 minutes after release the top float was seen and at 11 UTC the mooring was completely recovered. The top element, moored in 70m depth, showed severe signs of fishing activities but fortunately was not lost.

The CTD section from Barbados to St. Lucia began at September 2, 11:50 UTC, the station spacing was like on the last section about 9nm. When finished, a transport section to 13°40.0'N, 60°30.0'W was carried out. At September 3, 8:34 UTC the PIES at 13°47.50'N, 60°41.82'W was released. The instrument didn't respond. The release-code was repeatedly sent, but no acoustic nor radio or visual (flashlight) signals were received, although the flashlight should be easily seen in the darkness. Most likely, the PIES was not released. The search was interrupted at

10:25 UTC. CARIBA mooring B10 at 13°48.00'N, 60°41.50'W was released. Both releasers responded immediately, and the mooring was sighted 7 minutes later. The complete mooring was on board about at 11:30 UTC. This mooring showed also signs of fishing activities. The construction of the top float was damaged and the mooring contained several pieces of fishing gear. It turned out that a few months after deployment, the mooring had been hauled several 100m nearer to the shore, where the bottom was 30m shallower. The top float was then located in 35m depth instead of 70m.

Afterwards the search for the PIES was continued. Several items were found, but not the PIES. The search was abandoned at 12:20 UTC, and the METEOR headed towards Tobago. Early at September 4, 7:15 UTC the PIES was contacted and after several attempts the releaser worked at 8:45 and the PIES surfaced. It was dark, the flashlight of the PIES made it very easy to find the instrument at 9:20. After the PIES was brought on board (9:30), CARIBA mooring B8 was released at 9:35, detected at 9:40 and recovered completely. The releasers were on deck at 10:50. At the former mooring position B8 a CTD (CTD 91) was carried out at 11:30 UTC.

This (CTD 91) was the first station on the way to St. Vincent, the station spacing was 10.5nm. The section was finished with CTD 102 at September 5, 12 UTC. After 11nm, the work in the passage between St. Vincent and St. Lucia began. The CTD section (CTD 103-108) was complemented by several ADCP transects to study the influence of the tides on the velocity distribution. The vessel mounted ADCP reached down to the bottom so that we received velocity data in the passage with full continuous coverage. After finishing the passage work, the METEOR was on her way to 13°47.50'N 60°41.80'W, the PIES position off St. Lucia. The METEOR drifted towards the PIES, and the instrument was acoustically released. It took about an hour from September 6, 6 UTC to 7 UTC before the PIES responded, and the instrument surfaced 30minutes later. The PIES was brought on deck at 7:54 UTC. Both PIES carried out the measurements successfully.

The METEOR continued her track to the passage between St. Lucia and Martinique. After 5 CTD stations (CTD 109-113), the 12nm wide passage was also studied with several shipboard ADCP transects. The METEOR left the passage at September 6, 20 UTC and sailed leewards of Martinique to the passage between Martinique and Dominica. Unfortunately Dominica refused the research within the 3nm zone, so that we could not achieve full coverage of the passage. The work in the passage was finished at September 7, 15 UTC. In order to reach deeper well mixed water needed to calibrate the moored MicroCats with the CTD, a CTD station was carried out in the Caribbean at 15°N, 61°23'W with a water depth of 2356m at 17UTC. Only 4 10L bottles were attached at the carousel, the others were replaced by the MicroCats.

Work continued when the passage between Dominica and Guadeloupe was reached at Sep. 7, 23 UTC with CTD stations (CTD 121-125) followed by ADCP transects. The 3nm zone of Dominica has been left out. At September 8, 13 UTC the METEOR stopped near Pointe a Pitre (Guadeloupe) to obtain the replacement for the leaking ADCP workhorse. The Leibniz Institute for Marine Research in Kiel, Germany was able to provide us with an instrument with short notice. The instrument was brought at 11:30 UTC and the METEOR set course to the 16°N section to repeat the stations in the Deep Western Boundary Current with 2 ADCP workhorses attached to the CTD/carousel. The station work started at 19 UTC and was finished at September 9, 13 UTC. In order to study deep mixing in the western boundary current, a CTD/LADCP YoYo station was carried out at 16°17'N, 60°35'W which lasted for 12 hours and 6 complete profiles

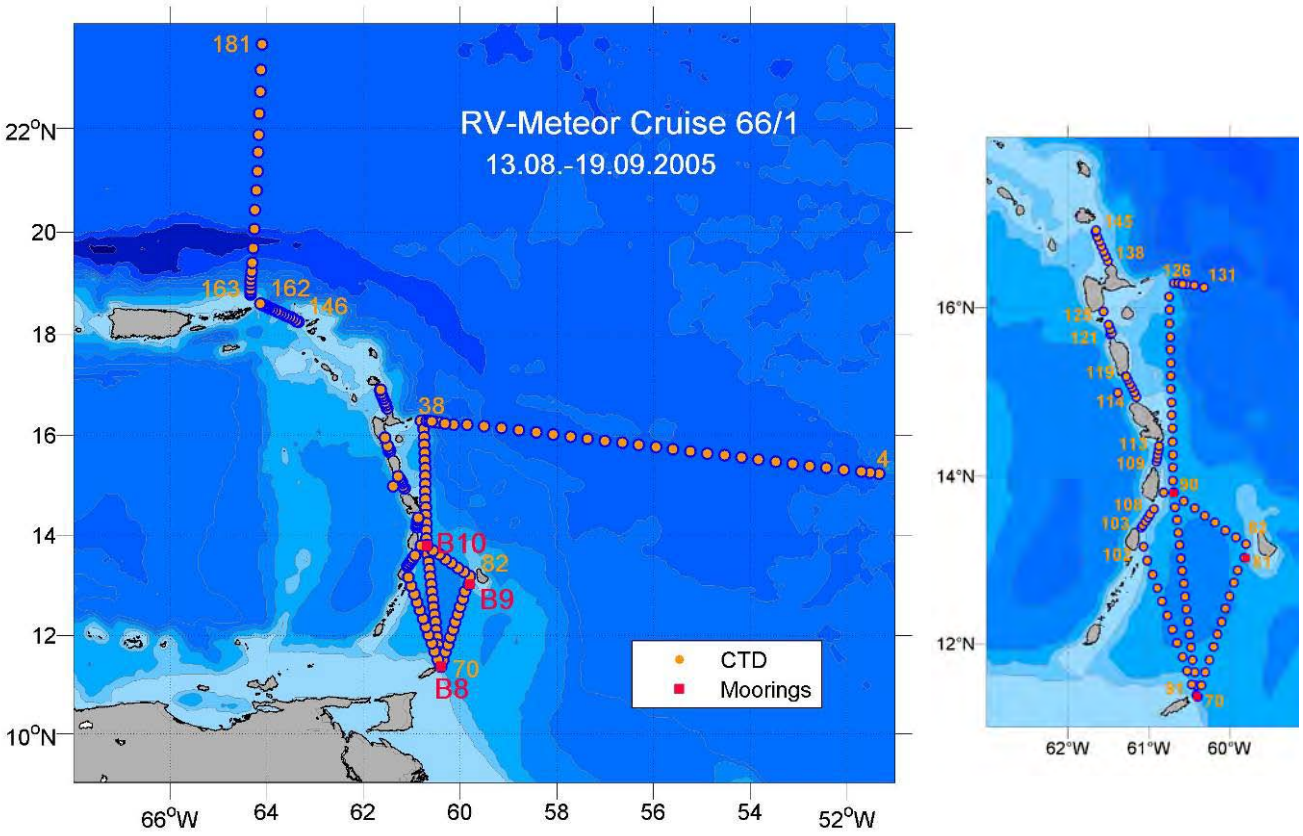


**FIG. 1.1:** Stations between Tobago and Antigua, METEOR cruise M66/1.

(CTD 132-137) could be taken in that time period. The results will be compared to microstructure measurements of K. Polzin, Woods Hole, USA, taken at about the same position.

Whether water from the South Atlantic also flows through the passages north of Guadeloupe was studied with CTD stations and ADCP transects in the passage between Guadeloupe and Antigua as well as between Anguilla and Anegada (Sombrero Passage) The latter is more than 2000m deep. The measurements in the Guadeloupe-Antigua passage (CTD 138-145) were finished at September 10, 21 UTC. The water between the two passages is very shallow, so that only ADCP sections were carried out. The work in the Sombrero Passage lasted from September 11, 9 UTC to September 12, 17:30 UTC (CTD 146 – 162). No CFC data have been taken in the Sombrero Passage. Several valves of the analysis system failed and through the unusual high failure rate the CFC sampling was stopped to be able to cover the following deep western boundary section. The velocity field in the passage was strongly influenced by tides. The detided total transport through the relatively large Sombrero Passage was small with 0.9 Sv inflow.

At September 12, 19 UTC, the CTD 163 marked the beginning of the meridional boundary section from Anegada across the Puerto Rico Trench to 23°N, 64°W. The measurements stopped at 5700m depth, although the trench is much deeper. The station spacing was at the slope 2.5 – 5nm, and further offshore the distance increased to 22nm. The deep water was devoid of scatterers leaving not enough signals for the LADCPs. The two instruments were removed after reaching water deeper than 5200m.

The last station of the boundary section at 23°36'N 64°06'W (CTD 181) was finished on September 16, 11:30 UTC, Shortly before the CTD was back on board, the CFC analysis system

had to be shut down because of problems in the gas supply line, and the CFC samples were taken 'offline'. The glass ampoules were flame sealed and will be analysed in our lab in Bremen.

The METEOR set course to Curacao, where we arrived at September 19, 11 UTC. During the entire cruise, the METEOR always experienced weather and sea conditions suitable for work.

## 1.4 Preliminary Results

### 1.4.1 CTD-$O_2$ Measurements

(R. Steinfeldt)

Measurements of conductivity, temperature, pressure and dissolved oxygen were performed with a Sea-Bird 911 plus system. The CTD was operated on a water sampler carousel together with 22 10 l Niskin bottles and 2 LADCPs. CTD data quality was good throughout the whole cruise. Some of the Niskin bottles, however, showed leakages at the bottom or the outlet. CTD data were calibrated by minimizing the difference between CTD values and salinity and oxygen samples from the Niskin bottles measured on board. The number of direct measurements was 1047 for oxygen and 498 for salinity, i.e about 6 and 3 samples per profile.

Oxygen measurements were carried out by the Winkler titration method. The standard did not show a remarkable drift, and the mean standard deviation between double samples was 0.020 ml/l. The difference between the directly measured and calibrated CTD oxygen data is 0.048 ml/l (0.046 ml/l) for all (below 1000 dbar) samples. At the beginning, the CTD oxygen sensor showed temporal fluctuations, but from profile 13 on identical calibration coefficients were used.

Salinities of the water samples were determined by means of a Guildline Autosal salinometer of type 8400A. The rms differences between the measured and calibrated CTD values amounted to 0.0029 (0.0024) for all (below 1000 dbar) samples. The mean deviation between measurements of substandard was in the range of 0.001.

IAPSO Standard Seawater of batch 145 was used for calibrating the salinometer. The salinities in the Antarctic Bottom Water (AABW) are in good agreement with former cruises if an offset of 0.003 is subtracted as was also done for salinity calibrations with batch 141.

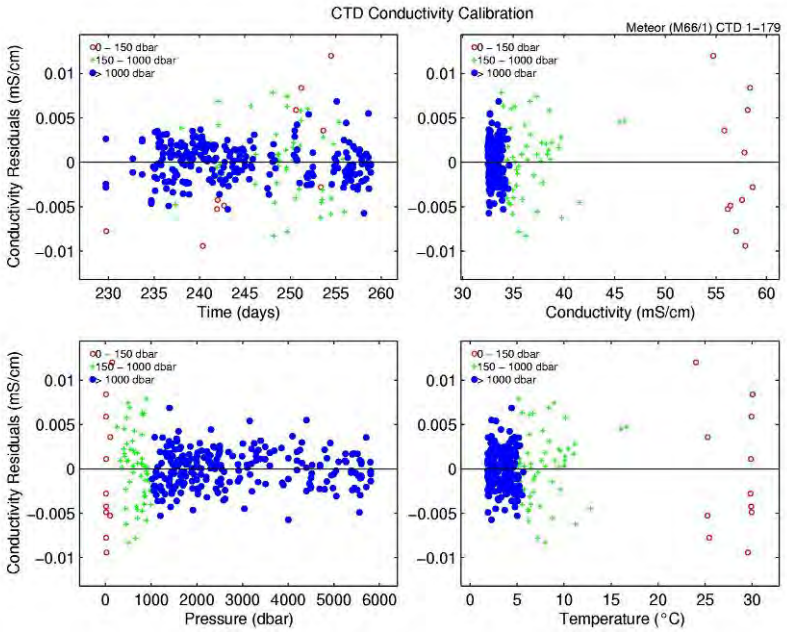


**FIG. 1.2:** Calibration of the conductivity sensor.

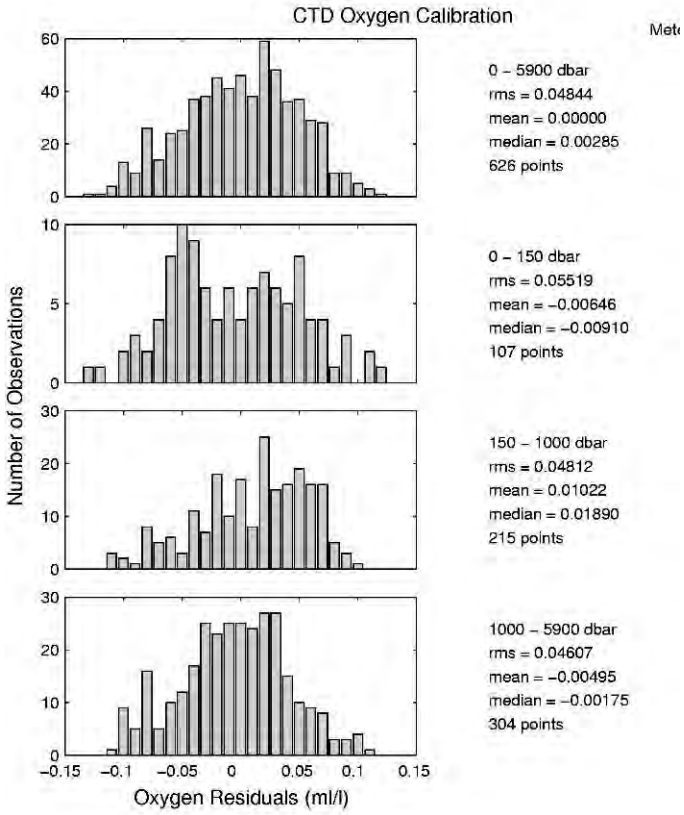


**FIG. 1.3:** Calibration of the oxygen sensor.

The oxygen values in the deep water are low compared with older data (differences between 0.05 and 0.1 ml/l). The surface oxygen saturation, on the other hand, is about 104 % and thereby in the same range as was measured the years before. An anomal large amount of samples (about one third) could not be used for the calibration routine both for oxygen and salinity, as the difference against the CTD values was too large. One reason could be the leakage of some of the Niskin bottles and/or problems at the oxygen sampling.

### 1.4.2 Analysis of Chlorofluorocarbons

(K. Bulsiewicz)

During cruise M66/1 water samples have been collected from 10l Niskin bottles for the analysis of the chlorofluorocarbons CFC-11 and CFC-12. Measurements of the CFC concentration in the water samples have been performed on board using a gas chromatographic system with capillary column and Electron Capture Detector (ECD). CFC sampling has been performed on 125 stations. A total of 1300 CFC data have been obtained.

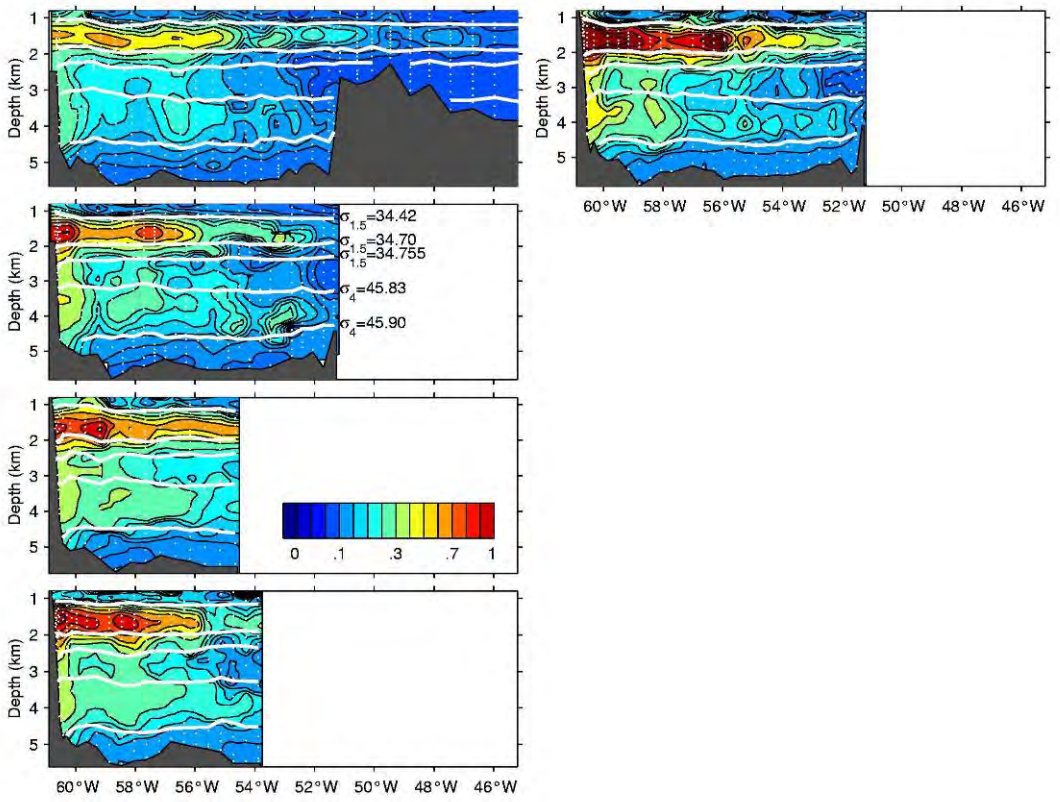


**FIG. 1.4:** CFC-11 distribution at 16°N, 2000 – 2005. Distributions 2000-20004 published in Rhein et al., 2004. Left column from top to bottom: 2000 – 2004; right column: 2005.

On the last station, CFC samples were sealed in glass ampoules for later measurements on land, as the remaining amount of pure nitrogen was not sufficient to run the automatic extraction system.

The sampling blank for CFC-11 and CFC-12 was estimated at a test station where all bottles were tripped at the same depth. This water is 'old', exhibiting zero CFC-concentrations. For CFC-11 and CFC-12 the resulting sampling blank was 0.005 pmol/kg. Accuracy was checked by analysing 33 water samples at least twice. It was found to be 0.6% for CFC-11 and 0.4% for CFC-12. The CFC concentration of the gas standard used to calibrate the water samples are reported on the SIO98 scale.

### 1.4.3 Lowered Acoustic Doppler Current Profiler LADCP

(M.Walter)

Most of the hydrographic stations were accompanied by current measurements with a lowered acoustic Doppler current profiler (LADCP) system attached to the CTD and water sampling carousel. Throughout the cruise, three instruments (RDI 300 kHz Workhorse Monitor) were used, partly two together or one as a single instrument.

Two instruments were used in a synchronized Master-and-Slave mode, with the upward looking as Slave and the downward looking as Master. When only one instrument was used, it was mounted downward looking. The instruments were powered by an external battery supply, consisting of 35 commercial quality 1.5V batteries assembled in a pressure resistant Aanderaa housing. The system was set to a ping rate of 1 ping/s and a bin length (= vertical resolution) of

10 m with a nominal range of 200 m for both operating modes, Master-and-Slave as well as single.

In total, 160 LADCP profiles were obtained during the 181 CTD stations of the cruise. The profiles from 132 to 137 were taken at the same position as a time series station.

During profile 26 on the 16° N transect, a water leakage (probably through the transducers) occurred in the upward looking instrument. Two of the transducers were damaged and severe corrosion was evident on one of the electronic boards of the unit. Unfortunately, there was no backup instrument on the ship at the time. With a water depth greater than 5000 m and very clear water (= few backscatterer), the data from a single instrument were not sufficient for a good-quality profile. Thus, the ensuing profiles up to CTD cast 33 were done without an ADCP. From cast 34 onwards, in the shallower and more productive waters close to the Antilles, a single instrument was used for profiling. A backup instrument shipped to Guadeloupe from the IFM-GEOMAR was available from profile 126 onwards, and was used for the rest of the cruise as a Slave.

From profile 114 onwards, beam 1 of the downward looking instrument started switching on and off. When the beam was working, it worked fine (normal range etc, no signs of any problem), but it stopped working for large stretches of time (several minutes) during profiles.

The problem occurred mainly in shallow water, and we suspect an electronic connection problem related to outside pressure. After profile 117, the instrument was dismounted and checked for leakage, but everything was fine (except the occasional beam failure), therefore the instrument was remounted for profile 119 and used for the rest of the cruise. 3-beam solutions were used for the velocity calculation for the periods where beam 1 failed.

The stations from 169 up to the end of the cruise (a transect across the Puerto Rico Trench) were again deeper than 5000 m and extremely scarce in backscatterers for depth greater than 2000 m, so that even the range of the combined instruments was to small to obtain velocity profiles.

The different types of environments lead to large differences in instrument range during the cruise. For the shallower (up to 2500 m water depth) stations close to the Antilles and in the passages, there was a vast amount of backscatterers, and the range of the instrument (Master only) was up to the nominal 200 m in the upper 1000 m, and scarcely falling below 60 m (again for the single instrument). With lowering and heaving velocities between 0.8 and 1.2 m/s of the instrument package this resulted in at least 200 shear estimates per depth bin and very good quality profiles.

In the deep stations of the 16°N and the Puerto Rico Trench sections, there were virtually no backscatterers below 2000 m, and the range was reduced to 2 bins (20 -30 m) for each instrument (50 m total for the package) in those parts of the profiles. With less than 100 shear estimates per depth bin no reliable velocity profile was obtained.

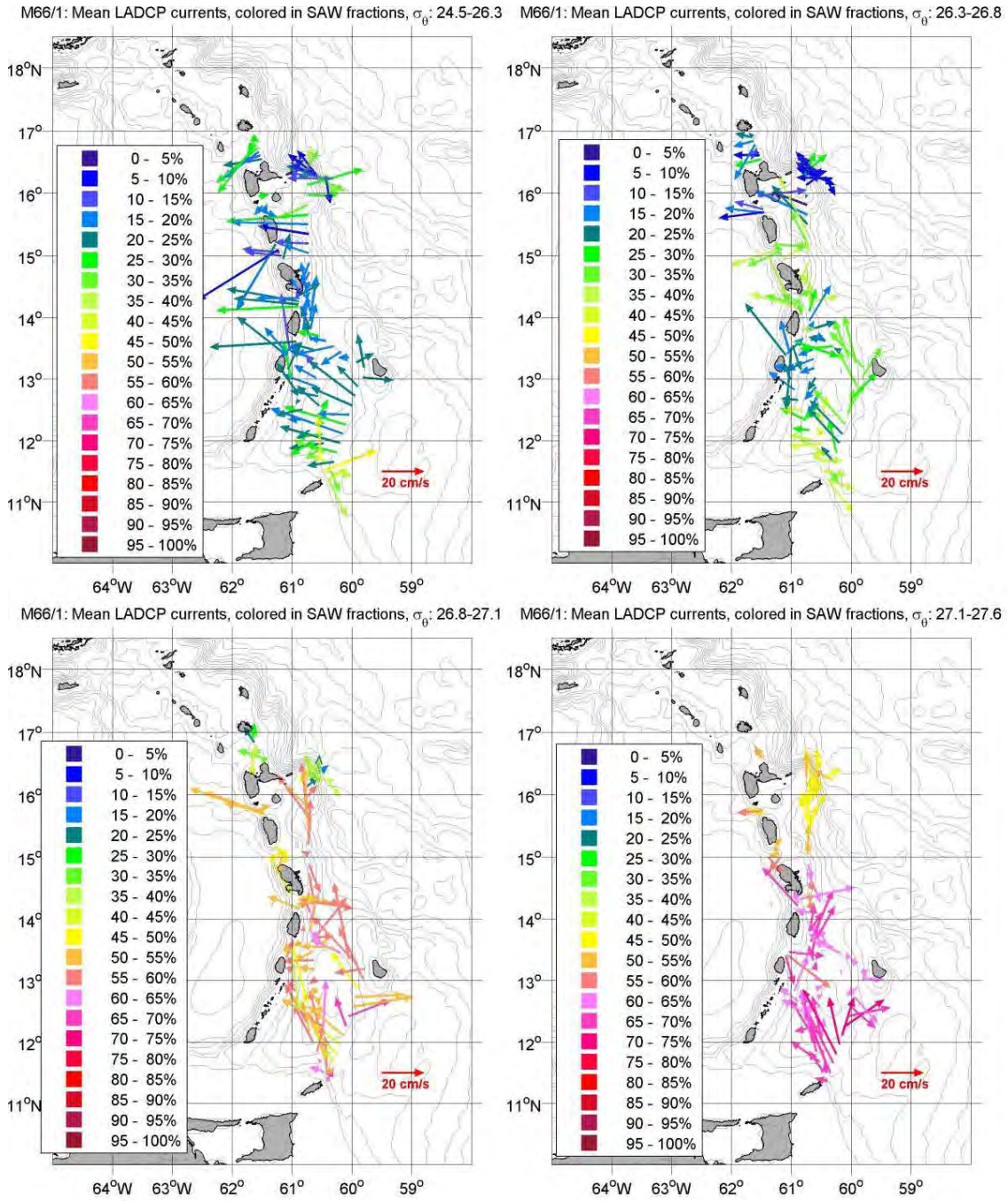


**FIG. 1.5:** Velocity distribution from LADCP measurements in the passages between Tobago and Guadeloupe for the water masses as defined in Rhein et al., 2005. The colour denotes the fraction of South Atlantic Water. The vertical and horizontal distribution of the SAW fractions in all passages measured during M66/1 are presented in Fig.1.6.

Post processing of the raw data was done using an inverse method which incorporates the measured velocity shear, the surface drift of the ship during the cast, and the bottom track velocities measured by the downward looking instrument to produce profiles of velocity and shear. This resulted in high quality velocity profiles, even for profiles with very weak current velocities (<0.05 m/s) and zero mean. Larger errors occur in the profiles deeper than 4000 m with few backscatterers and weak velocities, where not enough information is available for a good inversion.

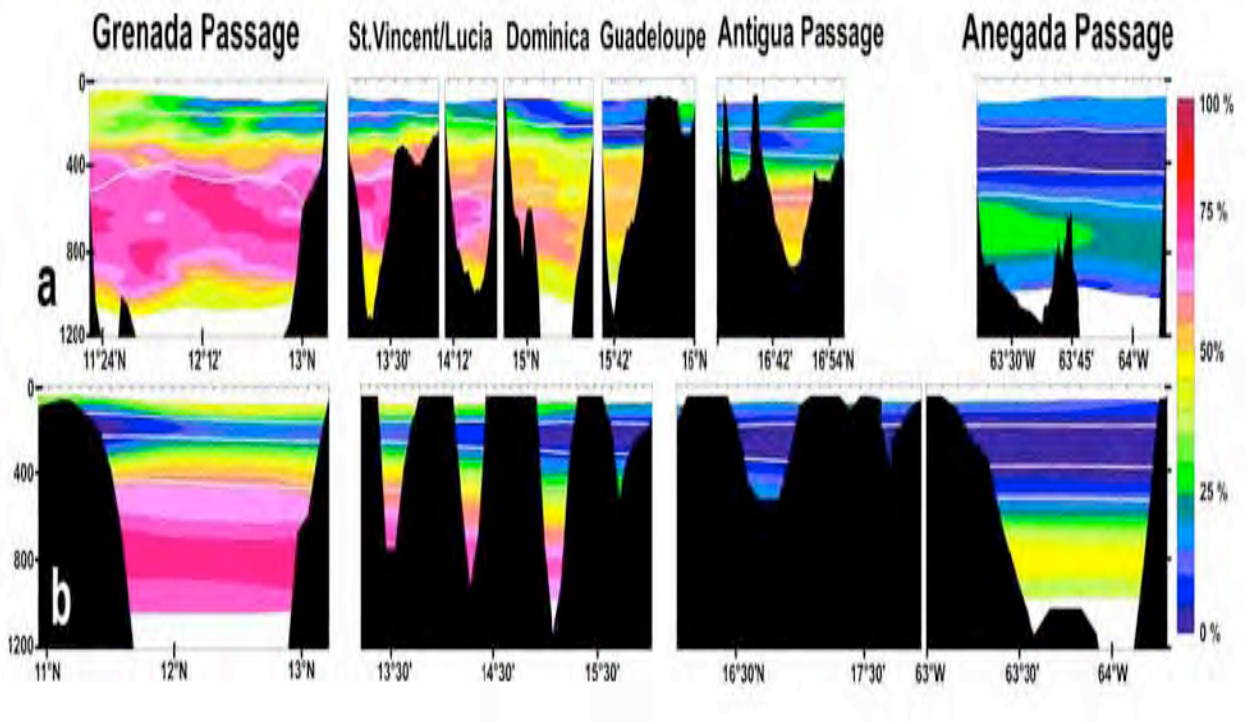


**FIG. 1.6:** *a)* Distribution of the SAW fraction in the passages. b) the mean SAW distribution in the FLAME model. The passage width is shown proportional except for Anegada Passage (twice as wide). The topography is derived from echosounder data (a) or the model grid (b). Fig. from Kirchner et al., 2008.

### 1.4.4 Shipboard Acoustic Doppler Current Profiler SADCP

(C. Mertens)

Simultaneous single-ping data were recorded from two RD Instruments Acoustic Dopplers current profilers: A 75 kHz and a 38 kHz Ocean Surveyor (OS) model, both with flat phased-array transducers. The 75 kHz OS was mounted into the hull of the ship in July 2004, and the 38 kHz instrument was lowered in the ship's well at the beginning of the cruise.

Both instruments were configured to collect narrow bandwidth water-profile data throughout the cruise. The data from the 75 kHz OS was recorded in 8 m bins to get high vertical resolution data in the upper water column. To achieve maximum range the 38 kHz OS data were collected in 32 m bins. Both systems operated flawless throughout the cruise. The ship's 78 kHz Doppler log is known to cause strong interference with the 75 kHz Ocean Surveyor which results in a reduced range of about 250 m and a deterioration of the data quality. During station work the Doppler log was needed for navigational purposes, but it was switched off when the ship was underway.

Navigation and heading information were recorded together with the velocities. Both ADCPs used the synchro version of the Fiber Optic Compass (FOG) heading connected directly to the chassis of the ADCP to transform the measured velocities into earth coordinates although it has been found on an earlier cruise (M47/1) that the FOG has a heading dependent error. Because of this error the data were corrected by substituting the syncro-FOG heading values of each single ping with heading values from the Ashtech receiver. The Ashtech receiver operated continuously throughout the cruise, delivering reliable heading data.

A water-track calibration of the angle between the transducers and the Ashtech antenna system has been carried out for both instruments. For the 38 kHz OS a misalignment angle of -1.03° and an amplitude factor of 1.004 were determined. For the 75 kHz OS the calibration resulted in a misalignment angle of -1.27° and an amplitude factor of 1.008, which is very close to the calibration carried out during Meteor cruise M62/1.

The range of the 75 kHz OS was of about 700 m, and the 38 kHz OS achieved ranges of 1200 to 1400 m. The sea state was generally calm throughout the cruise and most of the time the ship didn't had to steam against the waves which resulted in a very good quality of shipboard ADCP data for this cruise.

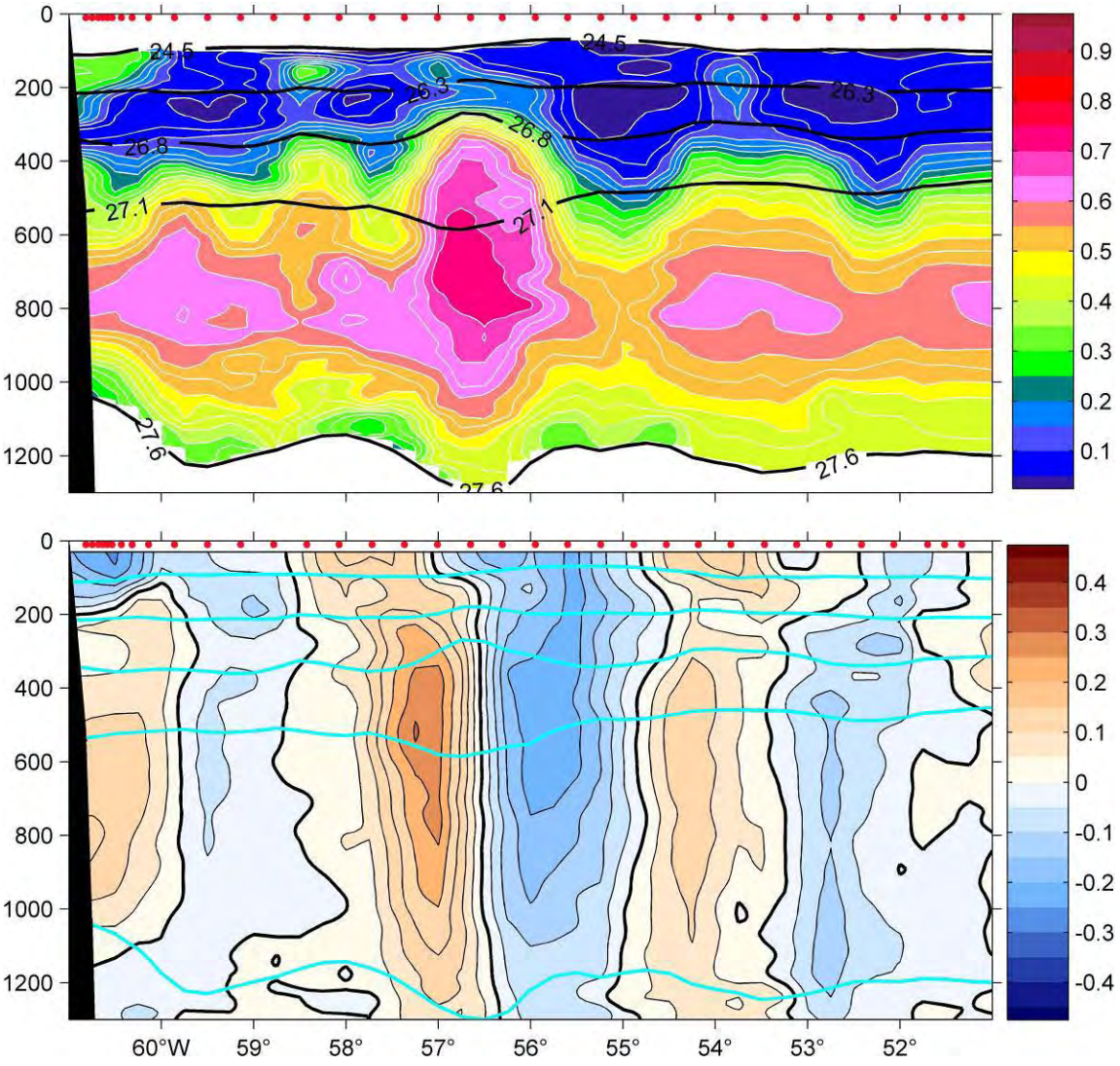


**FIG. 1.7:** Upper panel: distribution of SAW fraction at 16 °N during M 66/1. Lower panel: meridonal velocity component from shipboard ADCP measurement. The conspicuous feature centred at about 56°W is a North Brazil Current ring, transporting SAW to the north, especially in the Intermediate Water and the lower central water range. The black and blue lines are isopycnals, used to separate the water masses. The NBC rings seem to be a frequent feature at 16°N and we observed these rings on all our cruises.

### 1.4.5 Preliminary Results From the Bremen Moored CARIBA Array

(C. Mertens)

The Bremen CARIBA array consists of 2 Inverted echo sounders with bottom pressure sensors (PIES) which have been deployed for 2 years. The southernmost instrument was located north of Tobago and the northern instrument east of St. Lucia, both in about 1000m depth (Table 1, more details see Table 3). The PIES encompass the major inflow paths of South Atlantic Water (SAW) into the Caribbean and thus measure the integral transport through Grenada passage as well as St. Vincent passage. The acoustic travel time measured by the PIES were converted into T/S profiles, using our shipboard CTD measurements and the moored Microcats, which were deployed near the PIES and additionally south of Barbados (Table 1).

**TAB. 1.1:** CARIBA Moorings on cruise M66/1.

| Name | Latitude | Longitude | Depth | Deployment Date | Retrieval |
|---|---|---|---|---|---|
| B8 | 11°21.70‘N | 60°24.00‘W | 1130m | 17.7.2004, 14:48 | **4.9.2005** |
| PIES75 | 11°21.70‘N | 60°23.60‘W | 1123m | 17.7.2004, 15:15 | **4.9.2005** |
| B9 | 13°01.60‘N | 59°47.60‘W | 1007m | 21.7.2004, 18:57 | **2.9.2005** |
| B10 | 13°48.00‘N | 60°41.50‘W | 1002m | 22.7.2004, 11:00 | **3.9.2005** |
| PIES56 | 13°47.50‘N | 60°41.80‘W | 993m | 22.7.2004, 13:50 | **6.9.2005** |

PIES: Inverted Echo Sounder with Pressure sensor Time in UTC
**Bold dates: work done during M66/1 cruise**

Both time series show an increase in the SAW fraction by about 10-20%, especially in the Intermediate Water and the lower central water (Fig.1.9). Since the total transport did not change, the transport of SAW into the Caribbean did increase within these tow years.

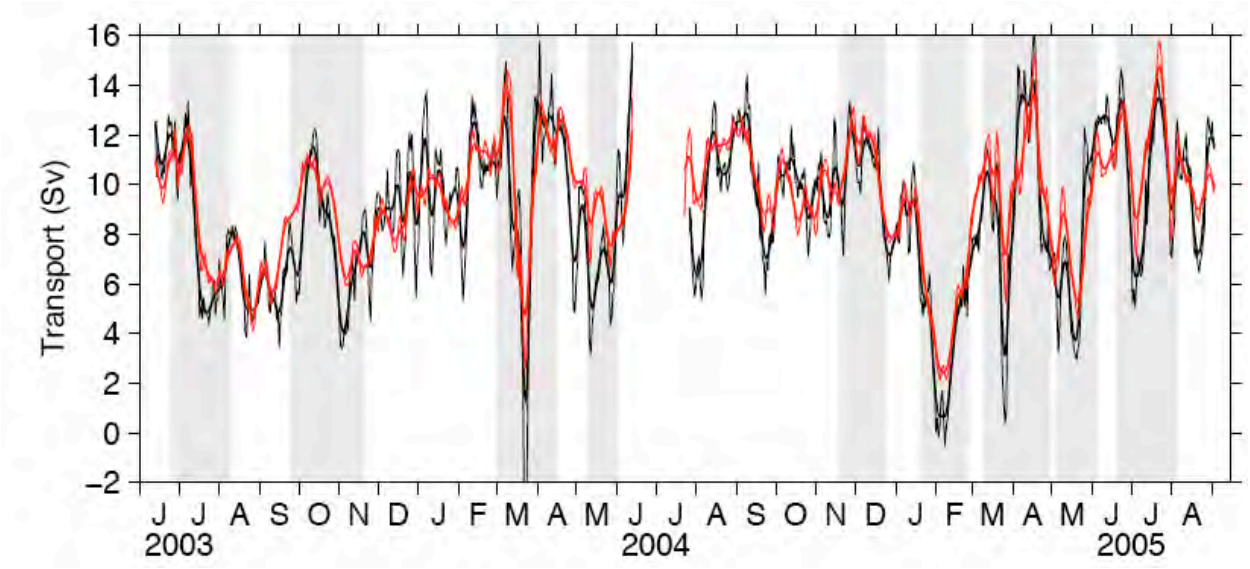


**FIG. 1.8** Two-year transport time series of SAW into the Caribbean through Grenada and St. Vincent passage, inferred from the PIES. Positive: inflow into the Caribbean. The gray shaded areas denote periods of elevated energy: black: total transport, the transport relative to 1000nm is red. From Mertens et al., 2008.

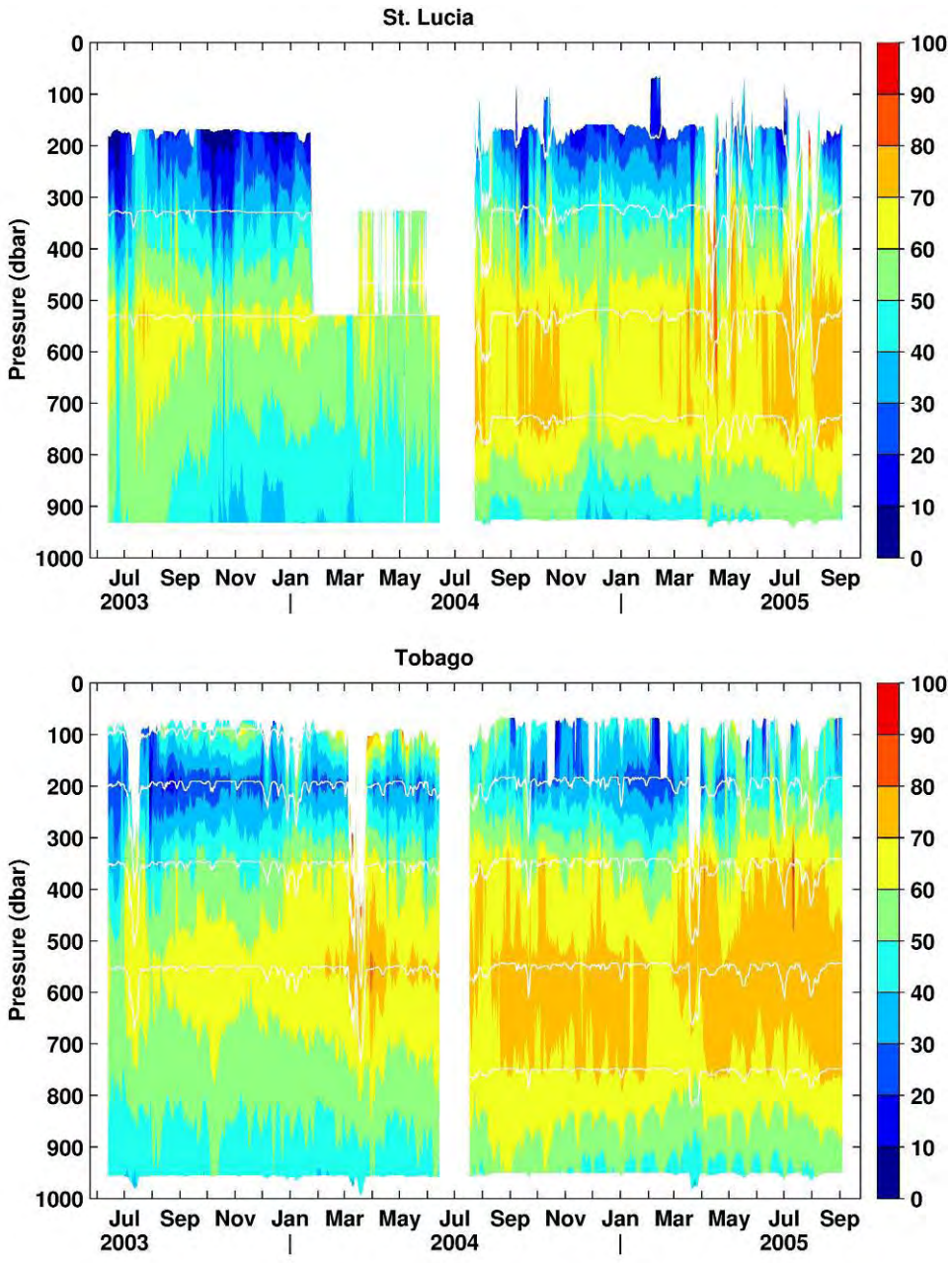


**FIG. 1.9**: Fraction of South Atlantic Water (SAW) at St. Lucia (upper figure) and Tobago (lower figure), Inferred from the T/S data of the Microcats. The depth of the Microcats are shown by the white lines. The data gap at St. Lucia in the first year was caused by a loss of the top buoy by fishing activities.

### 1.4.6 Sampling of Henry Seamount

(Andreas Klügel, Thor H. Hansteen)

Henry Seamount, an 8-km wide and 660-m tall volcano rising from 3700 m deep seafloor southeast of El Hierro (Fig. 1.10), was sampled by six dredge hauls:

**TAB. 1.2** Dredge stations during M66/1

| Date | Station | Dredge type | *on bottom:* Latitude | Longitude | Depth | *off bottom*: Latitude | Longitude | Depth |
|---|---|---|---|---|---|---|---|---|
| 14.8.05 | 392 | Chain bag | 27°18,50N | 17°47,01W | 3460 | 27°18,71N | 17°46,78W | 3330 |
| 14.8.05 | 393 | Chain bag | 27°18,89N | 17°46,78W | 3270 | 27°19,32N | 17°46,62W | 3160 |
| 14.8.05 | 394 | Chain bag | 27°17,82N | 17°45,05W | 3600 | 27°18,26N | 17°45,07W | 3350 |
| 14.8.05 | 395 | Drum | 27°17,97N | 17°45,18W | 3500 | 27°18,62N | 17°44,78W | 3410 |
| 14.8.05 | 396 | Drum | 27°19,80N | 17°47,75W | 3540 | 27°20,17N | 17°47,49W | 3380 |
| 14.8.05 | 397 | Drum | 27°19,85N | 17°45,92W | 3050 | 27°20,39N | 17°45,96W | 3160 |

Overall, dredging bites were extremely scarce confirming the previously inferred meter-thick sediment coverage (Gee et al., 2001). Only the drum dredge recovered hard rocks but all dredge hauls yielded soft silty to sandy sediment. The southern slopes of Henry Seamount apparently show thicker sediment coverage than the steeper northern slopes, which may be the result of deep-sea currents from northern directions. The dredged samples include:

- Trachytic rock fragments and pebbles with few phenocrysts (plagioclase, amphibole, titanite). The samples range from fresh to strongly altered and are covered by thin Mn-crust.
- Vesicular fragment of glassy basalt.
- Volcaniclastic sandstones with abundant Globigerina foraminifers.
- Fragments of cm-thick layered Mn-crusts.
- Fresh porous fragment of almost pure barite underlying a deep-sea coral stem (Fig. 1.10).
- Small fragments of porous biogenic or abiogenic carbonates.
- Abundant shell fragments of vesicomyid clams up to 15 cm in size that are mildly corroded (Fig. 1.11)).

The presence of shells from vesicomyid clams is surprising since this species is always associated with active hydrothermal vents or seep areas. To our knowledge, this is the first reported finding of vesicomyid clams and also the first direct or indirect evidence of submarine venting activity within the Canary Archipelago. Their preservation state suggests that the shells are not very old, probably less than 100.000 years. Texture, porosity and extreme freshness of a barite fragment recovered from the summit plateau also indicate a recent origin. The fragment is considerably larger than other marine or diagenetic barites suggesting that it originated by some focussed fluid flow.

As a preliminary interpretation, Henry Seamount may represent a recently active volcanic system related to the present location of the hotspot near El Hierro. This would be supported by the small degree of alteration of the freshest dredged trachytes. Alternatively and more likely, fluid discharge at the seamount may be related to seawater recharge at the neighbouring island of El Hierro followed by lateral flow and heating in the warm and permeable crust (Harris et al., 2004). But how can recent venting be reconciled with the presence of some meters of sediment drape? Does Henry Seamount currently show some kind of rejuvenated activity? Geochemical investigations and age determinations of rocks and shells will be carried out to resolve these questions.

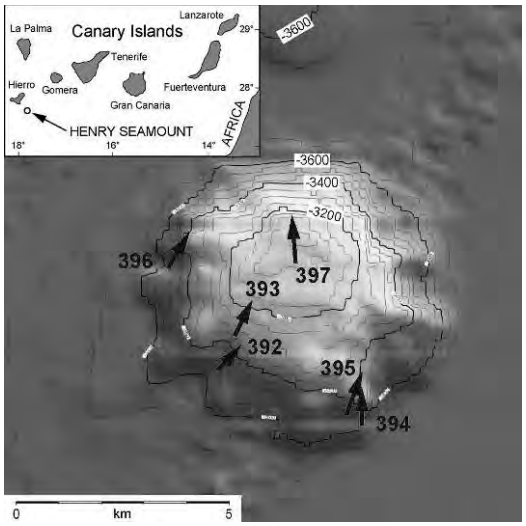


**FIG. 1.10:** Detailed bathymetric map (50 m contours) of Henry Seamount.

**FIG. 1.11:** Fresh barite fragment with coral stem (left) and shell of vesicomyid clam (right).

## 1.5 Ship's Meteorological Station

(C. Kreutzmann)

*First section from Las Palmas de Gran Canaria (Spain, August 13th) to Hierro (Spain, August 15th)*

Weather was dominated by the subtropical high west of Bay of Biscay with a ridge to the southeastern Azores and a later connection to a new predominant high to the southsouthwest of Azores. The dynamic counterpart was a heat low near Mauritania, shifting to South-Algeria with a trough to Portugal. In between METEOR was under strengthening gradient of atmospheric pressure with persistent north to northeasterly trade wind and corresponding sea (increasing from Bft 5, sea 1.5m to Bft 6, sea 2.5m). It was modified by local effects near Canary Islands, so plus Bft 1 in the nozzles between islands, veering wind around Bft 3 in the lee as well as northerly Bft 7 with gusts up to Bft 11 and rough sea around 3m close southeast to steep coast of Hierro. Water temperature was about 22 to 23°C.

*Transit to 15.2°N 51.2°W until August 22th*

The strengthening subtropical high shifted northeast to the outer Bay of Biscay with later return to the Azores. A ridge of high pressure turned to northwest from 20°N 40°W to Florida. The cruise area was along its south-eastern side in the regular trade wind, starting with north-north-easterly Bft 6 at August 15th, abating to east-north-easterly Bft 4 until August 19th and then veering to east-southeast. Sea started with 2.5m from north-northeast and finished with 1 to 1.5m from easterly direction. A weak easterly wave left Senegal at August 16th. Fringes of an upper level low entered the cruise area with freshening wind and scattered showers in the early August 19th. From then there was some tendency to local trade wind showers in the course of the following days. The easterly wave reached METEOR at August 22th. During the transit there was a rise in water temperature from 23 to 28°C. The ITCZ was continued to lying between 9 and 12°N.

*Section to 16.3°N 60.8°W until August 29th*

The steering subtropical high near Azores weakened along its way to 31°N 40°W. The ridge to the Bahamas did the same and was replaced by a connection to a new high southeast of Nova Scotia from August 27th on. Weather conditions around METEOR was made by a second ridge, slowly shifting from 15°N 47°W to METEOR at August 24th and farther to the Greater Antilles. Firstly wind blew with moderate force (Bft 4 to 5) from the east and decreased down to variable Bft 3 in the course of the section with temporary backing to northeast at August 26th and later veering to southeast. From August 24th some weak and scattered showers with gusts up to Bft 5, poor visibility and cooling down to 25°C occurred in the ship environment on the back side of the second ridge. Swell up to 2m veered from east to northeast with a decrease down to 1 - 1.5m. Water temperature showed further warming nearly up to 30°C. Tropical waves remained east of the cruise area, one weak system with embedded cyclonic circulation (close upper level trough prevented stronger development) approached METEOR up to 200 nm until August 29th. Branches of the ITCZ were situated far away between 9 and 11°N with decay from August 25th.

*Section between Guadeloupe (France), St. Lucia (France), Barbados and Tobago until September 4th*

The centres of subtropical high southeast of Newfoundland and southwest of Azores united to one extensive core close to the northwest of Azores. METEOR sailed along its southern flank with a regular change of easterly waves and weak ridges - in each case with an north-south axis. First easterly wave crossed the cruise area early in the August 29th with showers and gusts up to Bft 5. At August 30th the formerly Tropical Depression No.13 passed north of the cruise area, the accessory trough stretched out to Tobago and touched METEOR with showery gusts up to Bft 7. The Tropical Depression No.14 was also leaded by subtropical high and was upgraded to Tropical Storm MARIA north of METEOR at September 2nd (further upgrade to Hurricane No.5 near 28°N 55°W at September 4th). Only its trough reached far to the south and at September 1st a separated and westward moving cloud cluster nearby a 15°N ITCZ-branch touched the cruise area with showers, gusts to Bft 7 and temporary poor visibility. Completely dry conditions without any trade shower activity you could only expect directly in front of and under a strong ridge of high pressure. Variable south-easterly winds around Bft 3 turned to eastnortheast from August 30th on and showed a temporary rise up to Bft 5 during night to September 1st. The swell came always from east to northeast with about 1.5m and a maximum of 2.5m at September 1st. Water temperature was between 29 and 30°C.

*Section from Tobago along Windward and Leeward Islands to Anegada (British Virgin Islands) until September 12th*

Subtropical high started northwest of Azores and finished the section west of Cape Finisterre. A wide ridge stretched out across eastern Caribbean Sea, shifting northwest to Cuba with following stationarity due to three tropical storms MARIA, NATE and OPHELIA to the north. At September 10th a further high pressure core developed north of METEOR near 27°N 60°W. Until September 12th a steering upper level high close east of low-level high shifted to cruise area and finished shower activity: During this section four easterly tropical disturbances with showers and sheet lightning crossed METEOR, namely in the night to September 6th, daytime at September 6th, in the night to September 9th (with frontal upper-level low and following ITCZ-cluster) and

finally at September 11th with surrounding cloud of Saharan dust. Easterly trade winds blew with Bft 3 to 4, in combination with passing waves there were increasing winds up to Bft 5 as well as veering and backing. In lee of the islands you found calm regions. Southern nozzles showed no increasing winds due to the weak mean wind of about Bft 3. Nozzle-effects of plus Bft 1 were found only under more windy conditions in the Guadeloupe- and Anegada-Passages with further increases in its southern parts parallel to the steep coasts. Gusts up to Bft 7 occurred during passages of first three waves. From September 6th branches of ITCZ moved up to 15°N in connection with crossing waves. Sea around 1.5m came from northeast to east with maximum up to 3m in connection with swell of Ex-Hurricane MARIA during night to September 10th. Water temperature was unchanged near 30°C.

*Section to 23.6°N 64.2°W until September 16th*

First, an upper level high crossed cruise area with dry air masses and very good visibility, wind blew with Bft 3 to 4 from northeast to east with sea of about 1.5m. Simultaneously a strong stationary cyclone developed across Central Atlantic southeast of Newfoundland. A huge trough on its back moved unusually far to the south down to Puerto Rico and divided low level subtropical high into one part across southeastern North Atlantic and a second part between Bermudas and Gulf of Mexico. From September 14th METEOR approached low level trough with following passing cold upper level trough with strong vertical wind shear. Direction of low level trade winds was further predominated by the north-western subtropical high. Wind from easterly directions subsequently increased up to Bft 5 to 6 until September 15th, at the same time sea state was rougher with wave heights up to 3m from northeast. There were cloudy skies, heavy showers and thunderstorms with gusts up to Bft 9 as well as partly poor visibility. Water temperature declined a little to 29°C.

*Transit to Willemstad/Curacao (Netherlands) until September 19th*

Until early September 17th cruise area remained nearby an upper-level low at 23°N 66°W with easterly Bft 4 to 6, thunder showers, gusts to Bft 9 and wave heights around 2.5m. During further transit METEOR sailed into more dry conditions between subtropical high to the north between Gulf of Mexico as well as northeast of Bermudas and low pressure across the south-western Caribbean Sea. Easterly to south-easterly trade winds of around Bft 4 brought a weak tropical wave to the cruise area until September 18th. Wave heights decrease to 1.5m, Water temperature reached again 30°C.

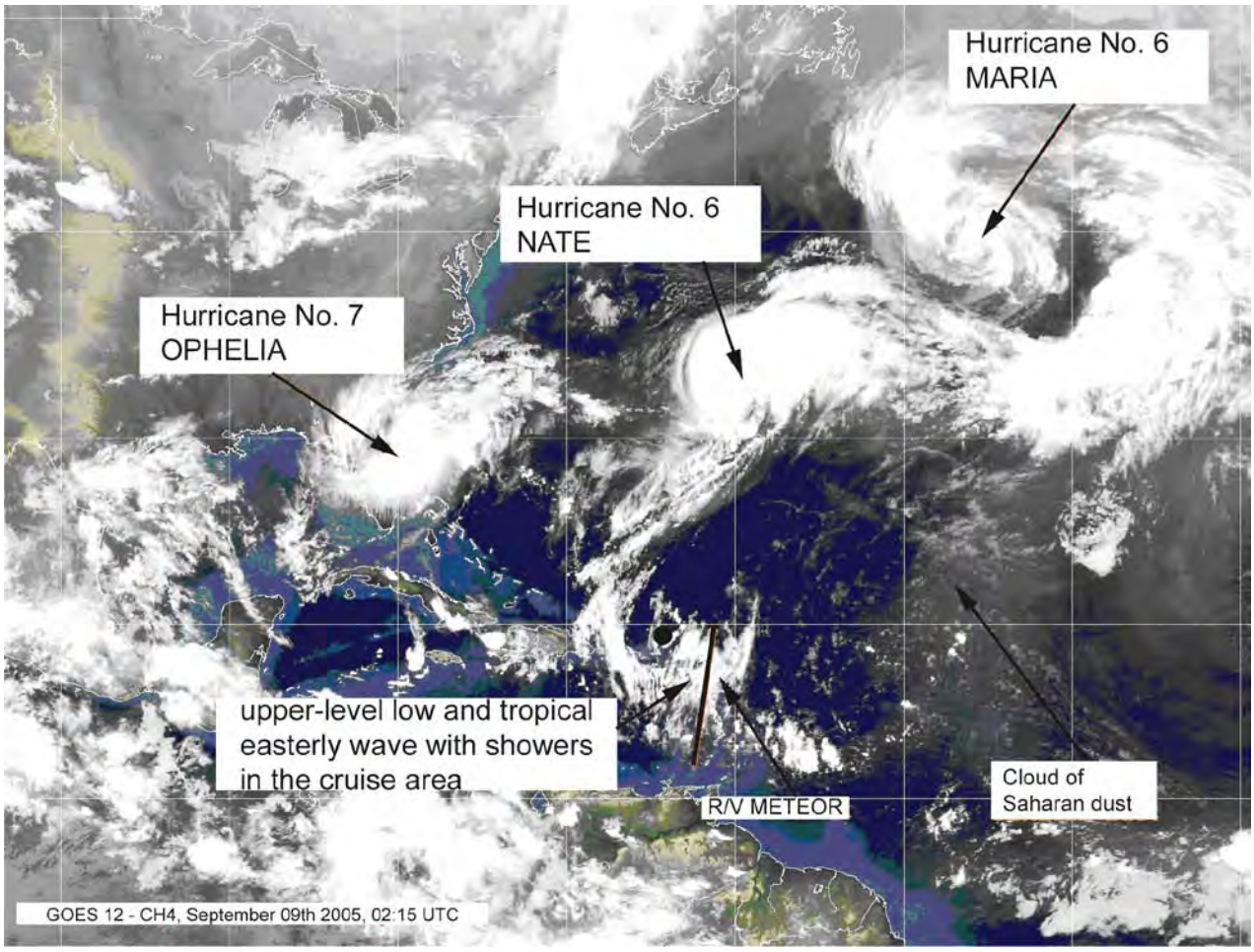


**FIG. 1.12:** Meteorological conditions at September 9, 02:15 UTC.

## 1.6 List of Stations

### List of moored instruments

**TAB. 1.3:** Recovered CARIBA Mooring B8/Tobago.

| Instrument | Number | Depth | Comments |
|---|---|---|---|
| Releaser | AR517 | 1055m | |
| Releaser | AR798 | 1055m | |
| MicroCat C,T | 2476 | 953m | |
| MicroCat C,T | 2454 | 753m | |
| MicroCat C,T | 2438 | 552m | |
| RCM11 | 93 | 350m | |
| MicroCat C,T | 2377 | 352m | |
| MicroCat C,T | 2277 | 195m | |
| RCM11 | 91 | 93m | |
| MicroCat C,T | 2051 | 78m | |

Sampling rate for all instruments : 30min.
RCM: Anderaa Acoustic Current Meter, +P: with pressure sensor
MicroCat C,T : SBE, measurement of temperature and conductivity
no radio transmitter, no flashlight

**TAB. 1.4:** Recovered CARIBA Mooring B9/Barbados.

| Instrument | Number | Depth | Comments |
|---|---|---|---|
| Releaser | RT520 | 985m | |
| Releaser | RT521 | 985m | |
| MicroCat C,T | 2050 | 952m | |
| MicroCat C,T | 1943 | 751m | |
| MicroCat C,T | 1931 | 550m | |
| RCM11 | 89 | 449m | |
| MicroCat C,T | 1933 | 342m | |
| MicroCat C,T | 1915 | 193m | |
| RCM11 | 94 | 90m | no data |
| MicroCat C,T | 1888 | 73m | |

RCM: Anderaa Acoustic Current Meter, +P: with pressure sensor
MicroCat C,T : SBE, measurement of temperature and conductivity
no radio transmitter, no flashlight

**TAB. 1.5:** Recovered CARIBA Mooring B10 / St. Lucia.

| Instrument | Number | Depth | Comments |
|---|---|---|---|
| Releaser | RT531 | 955m | |
| Releaser | AR810 | 955m | |
| MicroCat C,T | 3199 | 949m | |
| MicroCat C,T | 3198 | 748m | |
| MicroCat C,T | 3197 | 547m | |
| MicroCat C,T | 1936 | 346m | |
| RCM11 | 92 | 344m | |
| MicroCat C,T | 1934 | 189m | |
| RCM11 | 95 | 87m | |
| MicroCat C,T | 1932 | 71m | |

Sampling rate for all instruments : 30min.
RCM: Anderaa Acoustic Current Meter, +P: with pressure sensor
MicroCat C,T : SBE, measurement of temperature and conductivity
Radio frequency: 160.785 MHz

## Lists of CTD/ LADCP stations

Prof: Profile, Sta: station, Water depth and Profile depth in m, CFCs: chlorofluorocarbons, LADCP: Lowere Acoustic Doppler Current Profiler, Time in UTC.

| Meteor M66/1 | | | CTD Stations | | | | | Page 1 | | |
|---|---|---|---|---|---|---|---|---|---|---|
| Prof. | Sta. | Date | Time | Latitude | Longitude | Water Depth | Prof. Depth | Measurements CFCs | Measurements LADCP | Comment |
| 1 | 398 | 2005/08/17 | 16:30 | 23° 36.78' N | 28° 59.49' W | 5601 | 2001 | | x | |
| 2 | 399 | 2005/08/20 | 15:01 | 18° 27.59' N | 42° 53.82' W | 4748 | 2503 | x | x | |
| 3 | 400 | 2005/08/21 | 16:03 | 16° 45.80' N | 47° 22.65' W | 4081 | 2472 | x | x | |
| 4 | 401 | 2005/08/22 | 15:11 | 15° 14.49' N | 51° 20.04' W | 3998 | 3961 | x | x | |
| 5 | 402 | 2005/08/22 | 19:12 | 15° 16.01' N | 51° 31.09' W | 5251 | 5270 | x | x | |
| 6 | 403 | 2005/08/23 | 00:01 | 15° 17.04' N | 51° 41.96' W | 5421 | 5427 | x | x | |
| 7 | 404 | 2005/08/23 | 05:49 | 15° 19.00' N | 52° 4.04' W | 4960 | 4961 | x | x | |
| 8 | 405 | 2005/08/23 | 11:03 | 15° 21.98' N | 52° 25.10' W | 5150 | 5161 | x | x | |
| 9 | 406 | 2005/08/23 | 16:07 | 15° 23.99' N | 52° 46.01' W | 5150 | 5148 | x | x | |
| 10 | 407 | 2005/08/23 | 20:59 | 15° 26.46' N | 53° 7.14' W | 5310 | 5303 | x | x | |
| 11 | 408 | 2005/08/24 | 02:07 | 15° 29.03' N | 53° 28.04' W | 5413 | 5420 | x | x | |
| 12 | 409 | 2005/08/24 | 07:29 | 15° 31.51' N | 53° 50.02' W | 5475 | 5477 | x | x | |
| 13 | 410 | 2005/08/24 | 12:37 | 15° 33.97' N | 54° 11.01' W | 5452 | 5462 | x | x | |
| 14 | 412 | 2005/08/24 | 18:26 | 15° 36.51' N | 54° 31.87' W | 5496 | 5499 | x | x | |
| 15 | 413 | 2005/08/24 | 23:42 | 15° 38.84' N | 54° 53.02' W | 5489 | 5500 | x | x | |
| 16 | 414 | 2005/08/25 | 05:08 | 15° 41.51' N | 55° 14.47' W | 5487 | 5496 | x | x | |
| 17 | 415 | 2005/08/25 | 10:20 | 15° 43.91' N | 55° 36.09' W | 5484 | 5497 | x | x | |
| 18 | 416 | 2005/08/25 | 15:41 | 15° 46.47' N | 55° 57.05' W | 5591 | 5466 | x | x | |
| 19 | 418 | 2005/08/25 | 21:03 | 15° 48.98' N | 56° 18.50' W | 5333 | 5335 | x | x | |
| 20 | 419 | 2005/08/26 | 02:12 | 15° 51.48' N | 56° 39.03' W | 5287 | 5290 | x | x | |
| 21 | 420 | 2005/08/26 | 07:34 | 15° 53.95' N | 57° 0.54' W | 5184 | 5177 | x | x | |
| 22 | 421 | 2005/08/26 | 12:37 | 15° 56.51' N | 57° 22.03' W | 5286 | 5304 | | x | |
| 23 | 423 | 2005/08/26 | 18:15 | 15° 59.08' N | 57° 43.00' W | 5379 | 5414 | x | x | |
| 24 | 424 | 2005/08/26 | 23:23 | 16° 1.53' N | 58° 4.56' W | 5364 | 5379 | x | x | |
| 25 | 425 | 2005/08/27 | 04:36 | 16° 4.05' N | 58° 25.55' W | 5590 | 5606 | x | x | |
| 26 | 426 | 2005/08/27 | 09:54 | 16° 6.48' N | 58° 47.07' W | 5760 | 5780 | x | x | |
| 27 | 427 | 2005/08/27 | 15:24 | 16° 9.03' N | 59° 8.54' W | 5328 | 5353 | x | x | |
| 28 | 428 | 2005/08/27 | 20:23 | 16° 11.46' N | 59° 30.07' W | 4995 | 4992 | x | x | |
| 29 | 429 | 2005/08/28 | 01:14 | 16° 12.95' N | 59° 51.51' W | 5031 | 5018 | x | x | |
| 30 | 430 | 2005/08/28 | 05:53 | 16° 13.01' N | 60° 8.45' W | 4844 | 4836 | | x | |
| 31 | 431 | 2005/08/28 | 09:50 | 16° 14.43' N | 60° 18.97' W | 4460 | 4449 | x | x | |
| 32 | 432 | 2005/08/28 | 13:24 | 16° 15.88' N | 60° 25.97' W | 4778 | 4769 | | x | |
| 33 | 433 | 2005/08/28 | 17:08 | 16° 16.51' N | 60° 31.97' W | 4359 | 4363 | x | x | |
| 34 | 434 | 2005/08/28 | 20:15 | 16° 16.95' N | 60° 35.02' W | 3060 | 3068 | | x | |
| 35 | 435 | 2005/08/28 | 22:52 | 16° 17.45' N | 60° 37.99' W | 2540 | 2482 | x | x | |
| 36 | 436 | 2005/08/29 | 01:00 | 16° 17.53' N | 60° 40.98' W | 1742 | 1520 | x | x | |

| Meteor M66/1 | | CTD Stations | | | | | Page 2 | | | |
|---|---|---|---|---|---|---|---|---|---|---|
| Prof. | Sta. | Date | Time | Latitude | Longitude | Water Depth | Prof. Depth | Measurements CFCs | Measurements LADCP | Comment |
| 37 | 437 | 2005/08/29 | 02:49 | 16° 17.55' N | 60° 44.98' W | 1100 | 780 | x | x | |
| 38 | 438 | 2005/08/29 | 04:16 | 16° 17.45' N | 60° 49.00' W | 549 | 539 | x | x | |
| 39 | 439 | 2005/08/29 | 05:59 | 16° 7.97' N | 60° 45.03' W | 1019 | 1049 | | x | |
| 40 | 440 | 2005/08/29 | 07:51 | 15° 58.56' N | 60° 44.55' W | 995 | 985 | | x | |
| 41 | 441 | 2005/08/29 | 09:37 | 15° 48.99' N | 60° 44.55' W | 1652 | 1634 | x | x | |
| 42 | 442 | 2005/08/29 | 11:48 | 15° 39.57' N | 60° 43.99' W | 2227 | 2201 | x | x | |
| 43 | 443 | 2005/08/29 | 14:20 | 15° 30.47' N | 60° 44.09' W | 2519 | 2491 | | x | |
| 44 | 444 | 2005/08/29 | 17:15 | 15° 20.95' N | 60° 43.56' W | 2012 | 1992 | | x | |
| 45 | 445 | 2005/08/29 | 19:37 | 15° 11.89' N | 60° 43.55' W | 1770 | 1758 | | x | |
| 46 | 446 | 2005/08/29 | 21:49 | 15° 2.47' N | 60° 43.54' W | 917 | 920 | | x | |
| 47 | 447 | 2005/08/29 | 23:33 | 14° 53.03' N | 60° 43.04' W | 537 | 532 | | x | |
| 48 | 448 | 2005/08/30 | 01:02 | 14° 43.98' N | 60° 43.01' W | 527 | 522 | | x | |
| 49 | 449 | 2005/08/30 | 02:30 | 14° 34.46' N | 60° 42.52' W | 631 | 635 | x | x | |
| 50 | 450 | 2005/08/30 | 04:18 | 14° 25.01' N | 60° 42.49' W | 1250 | 1234 | x | x | |
| 51 | 451 | 2005/08/30 | 06:23 | 14° 15.47' N | 60° 42.00' W | 1435 | 1415 | x | x | |
| 52 | 452 | 2005/08/30 | 08:22 | 14° 6.52' N | 60° 42.04' W | 1033 | 1021 | x | x | |
| 53 | 453 | 2005/08/30 | 10:11 | 13° 57.02' N | 60° 42.01' W | 974 | 957 | x | x | |
| 54 | 454 | 2005/08/30 | 11:54 | 13° 49.05' N | 60° 41.48' W | 986 | 973 | x | x | |
| 55 | 455 | 2005/08/30 | 13:50 | 13° 38.04' N | 60° 40.55' W | 1247 | 1227 | x | x | |
| 56 | 456 | 2005/08/30 | 15:50 | 13° 28.94' N | 60° 38.96' W | 1658 | 1635 | x | x | |
| 57 | 457 | 2005/08/30 | 18:03 | 13° 19.95' N | 60° 38.03' W | 1899 | 1872 | x | x | |
| 58 | 458 | 2005/08/30 | 20:19 | 13° 10.99' N | 60° 37.00' W | 2106 | 2078 | x | x | |
| 59 | 459 | 2005/08/30 | 22:49 | 13° 1.52' N | 60° 36.04' W | 2241 | 2217 | x | x | |
| 60 | 460 | 2005/08/31 | 01:27 | 12° 52.69' N | 60° 35.11' W | 2360 | 2335 | x | x | |
| 61 | 461 | 2005/08/31 | 04:13 | 12° 43.56' N | 60° 34.06' W | 2461 | 2432 | x | x | |
| 62 | 462 | 2005/08/31 | 06:51 | 12° 34.05' N | 60° 33.07' W | 2460 | 2434 | x | x | |
| 63 | 463 | 2005/08/31 | 09:30 | 12° 24.98' N | 60° 32.05' W | 2437 | 2411 | x | x | |
| 64 | 464 | 2005/08/31 | 12:11 | 12° 16.02' N | 60° 30.59' W | 2383 | 2355 | | x | |
| 65 | 465 | 2005/08/31 | 14:52 | 12° 6.53' N | 60° 29.59' W | 2402 | 2373 | x | x | |
| 66 | 466 | 2005/08/31 | 17:29 | 11° 57.51' N | 60° 28.60' W | 2029 | 2007 | | x | |
| 67 | 467 | 2005/08/31 | 19:52 | 11° 48.48' N | 60° 27.52' W | 1477 | 1453 | x | x | |
| 68 | 468 | 2005/08/31 | 22:03 | 11° 39.46' N | 60° 26.01' W | 1214 | 1193 | x | x | |
| 69 | 469 | 2005/09/01 | 00:03 | 11° 30.02' N | 60° 25.06' W | 1113 | 1088 | x | x | |
| 70 | 470 | 2005/09/01 | 01:51 | 11° 23.01' N | 60° 24.57' W | 1191 | 1171 | x | x | |
| 71 | 471 | 2005/09/01 | 03:37 | 11° 30.10' N | 60° 21.04' W | 1415 | 1388 | | x | |
| 72 | 472 | 2005/09/01 | 05:44 | 11° 39.51' N | 60° 18.09' W | 1457 | 1392 | x | x | |

| Meteor M66/1 | | CTD Stations | | | | | Page 3 | | | |
|---|---|---|---|---|---|---|---|---|---|---|
| Prof. | Sta. | Date | Time | Latitude | Longitude | Water Depth | Prof. Depth | Measurements CFCs | Measurements LADCP | Comment |
| 73 | 473 | 2005/09/01 | 07:49 | 11° 48.48' N | 60° 15.06' W | 1596 | 1571 | x | x | |
| 74 | 474 | 2005/09/01 | 10:03 | 11° 57.98' N | 60° 12.03' W | 1823 | 1800 | x | x | |
| 75 | 475 | 2005/09/01 | 12:24 | 12° 6.96' N | 60° 9.10' W | 2010 | 1985 | x | x | |
| 76 | 476 | 2005/09/01 | 14:48 | 12° 15.92' N | 60° 6.06' W | 2205 | 2183 | x | x | |
| 77 | 477 | 2005/09/01 | 17:17 | 12° 25.55' N | 60° 3.03' W | 2301 | 2270 | x | x | |
| 78 | 478 | 2005/09/01 | 19:47 | 12° 34.47' N | 60° 0.01' W | 2100 | 2135 | x | x | |
| 79 | 479 | 2005/09/01 | 22:19 | 12° 43.99' N | 59° 57.02' W | 1930 | 1901 | x | x | |
| 80 | 480 | 2005/09/02 | 00:39 | 12° 52.96' N | 59° 54.07' W | 1706 | 1683 | x | x | |
| 81 | 481 | 2005/09/02 | 02:53 | 13° 1.98' N | 59° 49.04' W | 1242 | 1218 | x | x | |
| 82 | 485 | 2005/09/02 | 11:50 | 13° 11.54' N | 59° 48.02' W | 1087 | 1064 | x | x | |
| 83 | 486 | 2005/09/02 | 13:31 | 13° 16.49' N | 59° 55.53' W | 1659 | 1634 | x | x | |
| 84 | 487 | 2005/09/02 | 15:41 | 13° 21.50' N | 60° 3.01' W | 1888 | 1863 | x | x | |
| 85 | 488 | 2005/09/02 | 17:56 | 13° 27.10' N | 60° 11.04' W | 2088 | 2064 | x | x | |
| 86 | 489 | 2005/09/02 | 20:10 | 13° 32.07' N | 60° 18.52' W | 2000 | 1973 | x | x | |
| 87 | 490 | 2005/09/02 | 22:30 | 13° 37.52' N | 60° 26.04' W | 1850 | 1818 | x | x | |
| 88 | 491 | 2005/09/03 | 00:46 | 13° 42.51' N | 60° 34.08' W | 1396 | 1377 | x | x | |
| 89 | 492 | 2005/09/03 | 02:45 | 13° 48.53' N | 60° 41.54' W | 991 | 980 | x | x | |
| 90 | 493 | 2005/09/03 | 04:21 | 13° 48.50' N | 60° 48.97' W | 582 | 469 | | x | |
| 91 | 504 | 2005/09/04 | 11:33 | 11° 21.70' N | 60° 23.78' W | 1112 | 1101 | | x | |
| 92 | 505 | 2005/09/04 | 13:20 | 11° 30.60' N | 60° 27.98' W | 925 | 910 | | x | |
| 93 | 506 | 2005/09/04 | 15:11 | 11° 40.54' N | 60° 31.51' W | 1162 | 1138 | | x | |
| 94 | 507 | 2005/09/04 | 17:15 | 11° 50.50' N | 60° 35.07' W | 1663 | 1636 | | x | |
| 95 | 508 | 2005/09/04 | 19:29 | 12° 0.47' N | 60° 39.04' W | 2300 | 2262 | | x | |
| 96 | 509 | 2005/09/04 | 22:15 | 12° 10.47' N | 60° 42.52' W | 2300 | 2228 | x | x | |
| 97 | 510 | 2005/09/05 | 00:58 | 12° 20.33' N | 60° 46.05' W | 2311 | 2283 | x | x | |
| 98 | 511 | 2005/09/05 | 03:36 | 12° 30.56' N | 60° 50.06' W | 2110 | 2086 | x | x | |
| 99 | 512 | 2005/09/05 | 06:09 | 12° 40.05' N | 60° 53.49' W | 1548 | 1529 | x | x | |
| 100 | 513 | 2005/09/05 | 08:20 | 12° 49.99' N | 60° 57.02' W | 1300 | 1219 | x | x | |
| 101 | 514 | 2005/09/05 | 10:20 | 12° 59.99' N | 61° 1.00' W | 600 | 588 | x | x | |
| 102 | 515 | 2005/09/05 | 11:50 | 13° 9.98' N | 61° 4.03' W | 437 | 438 | | x | |
| 103 | 517 | 2005/09/05 | 13:37 | 13° 23.41' N | 61° 5.60' W | 483 | 498 | x | x | |
| 104 | 518 | 2005/09/05 | 14:30 | 13° 25.14' N | 61° 4.43' W | 1005 | 994 | x | x | |
| 105 | 519 | 2005/09/05 | 15:50 | 13° 28.04' N | 61° 2.36' W | 869 | 852 | x | x | |
| 106 | 520 | 2005/09/05 | 17:07 | 13° 30.78' N | 61° 0.38' W | 351 | 348 | x | x | |
| 107 | 521 | 2005/09/05 | 18:00 | 13° 33.06' N | 60° 58.84' W | 333 | 324 | x | x | |
| 108 | 522 | 2005/09/05 | 19:11 | 13° 36.75' N | 60° 56.02' W | 373 | 360 | | x | |

| Meteor M66/1 | | CTD Stations | | | | | Page 4 | | | |
|---|---|---|---|---|---|---|---|---|---|---|
| Prof. | Sta. | Date | Time | Latitude | Longitude | Water Depth | Prof. Depth | Measurements CFCs | Measurements LADCP | Comment |
| 109 | 531 | 2005/09/06 | 12:26 | 14° 10.81' N | 60° 54.14' W | 415 | 419 | | x | |
| 110 | 532 | 2005/09/06 | 13:16 | 14° 13.08' N | 60° 53.77' W | 780 | 777 | x | x | |
| 111 | 533 | 2005/09/06 | 14:18 | 14° 15.70' N | 60° 53.30' W | 902 | 897 | x | x | |
| 112 | 534 | 2005/09/06 | 15:31 | 14° 18.99' N | 60° 52.75' W | 878 | 840 | x | x | |
| 113 | 535 | 2005/09/06 | 16:42 | 14° 21.71' N | 60° 52.35' W | 329 | 330 | x | x | |
| 114 | 544 | 2005/09/07 | 07:24 | 14° 56.76' N | 61° 9.07' W | 413 | 420 | | x | |
| 115 | 545 | 2005/09/07 | 08:22 | 14° 59.97' N | 61° 10.68' W | 631 | 594 | x | x | |
| 116 | 546 | 2005/09/07 | 09:28 | 15° 3.39' N | 61° 12.42' W | 1460 | 1422 | x | x | |
| 117 | 547 | 2005/09/07 | 11:07 | 15° 5.91' N | 61° 13.71' W | 2057 | 2043 | x | x | |
| 118 | 548 | 2005/09/07 | 13:05 | 15° 9.06' N | 61° 15.26' W | 1464 | 1456 | x | | |
| 119 | 549 | 2005/09/07 | 14:33 | 15° 11.13' N | 61° 16.77' W | 856 | 844 | x | x | |
| 120 | 551 | 2005/09/07 | 16:34 | 14° 59.94' N | 61° 22.98' W | 2369 | 2354 | | x | |
| 121 | 552 | 2005/09/07 | 23:04 | 15° 41.32' N | 61° 28.43' W | 788 | 866 | x | x | |
| 122 | 553 | 2005/09/08 | 00:14 | 15° 42.08' N | 61° 27.39' W | 1084 | 1071 | x | x | |
| 123 | 554 | 2005/09/08 | 01:40 | 15° 44.77' N | 61° 28.43' W | 707 | 631 | x | x | |
| 124 | 555 | 2005/09/08 | 02:45 | 15° 48.03' N | 61° 29.85' W | 470 | 467 | x | x | |
| 125 | 556 | 2005/09/08 | 04:42 | 15° 57.30' N | 61° 33.41' W | 513 | 250 | | x | |
| 126 | 560 | 2005/09/08 | 19:11 | 16° 17.51' N | 60° 41.03' W | 1737 | 1704 | x | x | |
| 127 | 563 | 2005/09/08 | 20:55 | 16° 17.51' N | 60° 38.03' W | 2480 | 2504 | | x | |
| 128 | 562 | 2005/09/08 | 23:18 | 16° 17.01' N | 60° 35.11' W | 3165 | 3120 | x | x | |
| 129 | 563 | 2005/09/09 | 02:00 | 16° 16.53' N | 60° 32.09' W | 4305 | 4334 | | x | |
| 130 | 564 | 2005/09/09 | 05:50 | 16° 16.00' N | 60° 26.07' W | 4771 | 4765 | x | x | |
| 131 | 565 | 2005/09/09 | 10:03 | 16° 14.49' N | 60° 19.02' W | 4459 | 4449 | | x | |
| 132 | 566 | 2005/09/09 | 14:56 | 16° 17.00' N | 60° 35.09' W | 3152 | 3101 | | x | Yo-Yo |
| 133 | 566 | 2005/09/09 | 16:55 | 16° 16.98' N | 60° 34.98' W | 3358 | 3093 | | x | Yo-Yo |
| 134 | 566 | 2005/09/09 | 18:48 | 16° 16.98' N | 60° 34.98' W | 3124 | 3073 | | x | Yo-Yo |
| 135 | 566 | 2005/09/09 | 20:59 | 16° 16.99' N | 60° 35.02' W | 3134 | 3075 | | x | Yo-Yo |
| 136 | 566 | 2005/09/09 | 23:07 | 16° 16.99' N | 60° 35.01' W | 3138 | 3088 | | x | Yo-Yo |
| 137 | 566 | 2005/09/10 | 01:12 | 16° 17.00' N | 60° 34.98' W | 3138 | 3097 | | x | Yo-Yo |
| 138 | 567 | 2005/09/10 | 08:22 | 16° 32.94' N | 61° 30.50' W | 458 | 453 | x | x | |
| 139 | 569 | 2005/09/10 | 09:24 | 16° 36.48' N | 61° 32.02' W | 433 | 431 | | x | |
| 140 | 570 | 2005/09/10 | 10:22 | 16° 39.98' N | 61° 33.53' W | 417 | 411 | x | x | |
| 141 | 571 | 2005/09/10 | 11:50 | 16° 43.33' N | 61° 35.06' W | 190 | 674 | x | x | |
| 142 | 572 | 2005/09/10 | 12:54 | 16° 46.90' N | 61° 36.54' W | 853 | 844 | x | x | |
| 143 | 573 | 2005/09/10 | 14:03 | 16° 50.43' N | 61° 38.09' W | 427 | 421 | | x | |
| 144 | 574 | 2005/09/10 | 14:58 | 16° 53.92' N | 61° 39.54' W | 478 | 466 | | x | |

| Meteor M66/1 | | CTD Stations | | | | | | Page 5 | | |
|---|---|---|---|---|---|---|---|---|---|---|
| Prof. | Sta. | Date | Time | Latitude | Longitude | Water Depth | Prof. Depth | Measurements CFCs | Measurements LADCP | Comment |
| 145 | 575 | 2005/09/10 | 15:48 | 16° 54.91' N | 61° 39.02' W | 418 | 412 | | x | |
| 146 | 582 | 2005/09/11 | 08:56 | 18° 15.00' N | 63° 21.04' W | 438 | 433 | | x | |
| 147 | 583 | 2005/09/11 | 09:50 | 18° 16.02' N | 63° 23.51' W | 852 | 844 | | x | |
| 148 | 584 | 2005/09/11 | 11:05 | 18° 18.53' N | 63° 27.03' W | 901 | 891 | | x | |
| 149 | 585 | 2005/09/11 | 12:18 | 18° 20.11' N | 63° 30.48' W | 1001 | 987 | | x | |
| 150 | 586 | 2005/09/11 | 13:35 | 18° 21.56' N | 63° 34.00' W | 1064 | 1052 | | x | |
| 151 | 587 | 2005/09/11 | 14:50 | 18° 23.01' N | 63° 37.51' W | 1136 | 1124 | | x | |
| 152 | 588 | 2005/09/11 | 16:19 | 18° 24.52' N | 63° 40.97' W | 863 | 857 | | x | |
| 153 | 589 | 2005/09/11 | 17:33 | 18° 26.05' N | 63° 44.57' W | 709 | 617 | | x | |
| 154 | 590 | 2005/09/11 | 18:41 | 18° 27.43' N | 63° 47.97' W | 995 | 1390 | | x | |
| 155 | 591 | 2005/09/11 | 20:12 | 18° 28.98' N | 63° 51.56' W | 1436 | 1420 | | x | |
| 156 | 592 | 2005/09/11 | 21:47 | 18° 30.45' N | 63° 55.04' W | 1559 | 1563 | x | x | |
| 157 | 593 | 2005/09/11 | 23:26 | 18° 31.95' N | 63° 58.49' W | 2191 | 2173 | x | x | |
| 158 | 594 | 2005/09/12 | 01:21 | 18° 32.88' N | 64° 0.01' W | 2072 | 2072 | | x | |
| 159 | 595 | 2005/09/12 | 03:16 | 18° 34.03' N | 64° 2.07' W | 1458 | 1492 | x | x | |
| 160 | 596 | 2005/09/12 | 04:57 | 18° 34.44' N | 64° 3.99' W | 1921 | 1916 | | x | |
| 161 | 597 | 2005/09/12 | 07:00 | 18° 35.47' N | 64° 6.52' W | 1168 | 1157 | x | x | |
| 162 | 598 | 2005/09/12 | 08:16 | 18° 36.50' N | 64° 8.04' W | 416 | 412 | | x | |
| 163 | 601 | 2005/09/12 | 19:04 | 18° 47.49' N | 64° 20.02' W | 622 | 607 | | x | |
| 164 | 602 | 2005/09/12 | 20:03 | 18° 50.00' N | 64° 20.02' W | 1312 | 1292 | x | x | |
| 165 | 603 | 2005/09/12 | 21:29 | 18° 52.98' N | 64° 20.03' W | 1858 | 1841 | x | x | |
| 166 | 604 | 2005/09/12 | 23:26 | 18° 58.40' N | 64° 20.04' W | 2926 | 2905 | x | x | |
| 167 | 605 | 2005/09/13 | 02:10 | 19° 3.42' N | 64° 20.04' W | 3832 | 3812 | x | x | |
| 168 | 606 | 2005/09/13 | 05:39 | 19° 8.94' N | 64° 19.54' W | 4851 | 4865 | x | x | |
| 169 | 607 | 2005/09/13 | 09:46 | 19° 13.95' N | 64° 19.02' W | 5256 | 5280 | x | x | |
| 170 | 608 | 2005/09/13 | 14:07 | 19° 23.93' N | 64° 18.02' W | 5390 | 5473 | x | | |
| 171 | 609 | 2005/09/13 | 19:36 | 19° 41.46' N | 64° 17.02' W | 6938 | 5700 | x | | |
| 172 | 610 | 2005/09/14 | 01:45 | 20° 3.92' N | 64° 15.52' W | 5998 | 5701 | x | | |
| 173 | 611 | 2005/09/14 | 08:03 | 20° 26.01' N | 64° 14.53' W | 4960 | 4967 | x | | |
| 174 | 612 | 2005/09/14 | 13:16 | 20° 48.49' N | 64° 13.06' W | 5146 | 5155 | x | | |
| 175 | 613 | 2005/09/14 | 18:51 | 21° 10.62' N | 64° 11.43' W | 5339 | 5355 | x | | |
| 176 | 614 | 2005/09/15 | 00:23 | 21° 32.47' N | 64° 10.51' W | 5574 | 5602 | x | | |
| 177 | 615 | 2005/09/15 | 06:11 | 21° 52.52' N | 64° 10.06' W | 5741 | 5691 | x | | |
| 178 | 616 | 2005/09/15 | 12:13 | 22° 16.90' N | 64° 9.09' W | 5791 | 5701 | x | | |
| 179 | 617 | 2005/09/15 | 18:23 | 22° 42.04' N | 64° 8.02' W | 5806 | 5686 | x | | |
| 180 | 618 | 2005/09/16 | 00:25 | 23° 6.92' N | 64° 7.01' W | 5803 | 5695 | x | | |
| 181 | 619 | 2005/09/16 | 07:20 | 23° 36.48' N | 64° 6.09' W | 5805 | 5688 | x | | |

## 1.7 References

Gee, M.J.R., D.G. Masson, A.B. Watts, and N.C. Mitchell, 2001. Offshore continuation of volcanic rift zones, El Hierro, Canary Islands. Journal of Volcanology and Geothermal Research, 105, 107-119

Harris, R.N., A.T. Fisher, and D.S. Chapman, 2004. Fluid flow through seamounts and implications for global mass fluxes. Geology, 32, 725-728

Kirchner, K., M. Rhein, C. Mertens, C. W. Böning, and S. Hüttl, 2008. Observed and modeled MOC related flow into the Caribbean. Journal of Geophysical Research, 113, C03028

Mertens, C., M. Rhein, K. Kirchner, and M. Walter, 2008. Modulation of the Inflow into the Caribbean Sea by North Brazil Current Rings. Deep-Sea Research Part I, submitted

Rhein, M., M. Walter, C. Mertens, R. Steinfeldt, and D. Kieke, 2004. Circulation of North Atlantic Deep Water at 16°N, 2000-2003. Geophysical Research. Letters, 31, LI4305

Rhein, M., K. Kirchner, C. Mertens, R. Steinfeldt, M. Walter and U. Fleischmann-Wischnath, 2005. The transport of South Atlantic Water through the Passages south of Guadeloupe and across 16°N, 2000-2004. Deep Sea Research Part I, 52, 2234-2249

METEOR-Berichte 09-2

# *SUBFLUX*

## PART 2

Cruise No. 66, Leg 2a
September 22 – October 1, 2005, Willemstad (Curacao) – Corinto (Nicaragua)

Cruise No. 66, Leg 2b
October 2 - October 23, 2005, Corinto (Nicaragua) – Caldera (Costa Rica)


**Gregor Rehder**, Viola Beier, Jörg Bialas, Nikolaus Bigalke, Ramon Brentführer, Emelina Corrales Cordero, Bettina Domeyer, Tanja Fromm, Dieter Garbe-Schönberg, Peter Linke, Helge Niemann, Enoma Omoregie, Martin Pieper, Volker Ratmeyer, Ulrike Schacht, Tina Schleicher, Karen Stange, Matthias Türk, Klaus Wallmann, Ulrike Westernströer, and the shipboard scientific parties

Editorial Assistance:

Andreas Krell
Alfred-Wegener-Institut für Polar- und Meeresforschung, Bremerhaven

Leitstelle METEOR
Institut für Meereskunde der Universität Hamburg

2009

**Table of Contents Part 2 (M66/2)** **Page**

### 2.1.1 List of Participants M66/2

### 2.1.2 List of Participants Leg M66/2a

| Name | Discipline | Institution |
|---|---|---|
| 1 . Rehder, Gregor, Dr. | Chief scientist | IFM-GEOMAR |
| 2 . Bannert, Bernhard | Lander/ electronics | OKTOPUS |
| 3 . Bialas, Jörg, Dr. | Geophysics | IFM-GEOMAR |
| 4 . Bigalke, Nikolaus | $CH_4$ chemistry | IFM-GEOMAR |
| 5 . Brentführer, Ramon | $CH_4$ chemistry | SFB 574 |
| 6 . Buhmann, Sitta | ROV QUEST | MARUM |
| 7 . Domeyer, Bettina | Pore water geochemistry | IFM-GEOMAR |
| 8 . Fromm, Tanja | Mapping/ documentation | SFB 574 |
| 9 . Gossler, Jürgen, Dr. | Geophysics | KUM |
| 10. Hüttich, Daniel | ROV QUEST | MARUM |
| 11. Klar, Steffen | ROV QUEST | MARUM |
| 12. Linke, Peter, Dr. | Lander | IFM-GEOMAR |
| 13. Mason, Pete | ROV QUEST | IFM-GEOMAR |
| 14. Pieper, Martin | SFB 574 | IFM-GEOMAR |
| 15. Queisser, Wolfgang | Lander/ TV MUC | IFM-GEOMAR |
| 16. Ratmeyer, Volker, Dr. | ROV QUEST | MARUM |
| 17. Schleicher, Tina | Biology | SFB 574 |
| 18. Schmidt, Werner | ROV QUEST | MARUM |
| 19. Seiter, Christian, Dr. | ROV QUEST | MARUM |
| 20. Stange, Karen | $CH_4$ analytics | SFB 574 |
| 21. Steffen, Klaus-Peter | Geophysics | IFM-GEOMAR |
| 22. von Neuhoff , Holger | Press documentation | NDR |
| 23. Westernströer, Ulrike | Pore water geochemistry | CAU |
| 24. Zarrouk, Marcel | ROV QUEST | MARUM |
| 25. Quintanilla Mendoza, E. | Observer | UCR |
| 26. Aguilar Chavarria, Jorge E. | Observer | UCR |
| 27. Rojas Solano, Eduardo E. | Observer | UCR |

### 2.1.3 List of Participants Leg M66/2b

| Name | Discipline | Institution |
|---|---|---|
| 1 . Rehder, Gregor, Dr. | Chief scientist | IFM-GEOMAR |
| 2 . Beier, Viola | Microbiology | MPI |
| 3 . Bigalke, Nikolaus | $CH_4$ chemistry | IFM-GEOMAR |
| 4. Brentführer, Ramon | $CH_4$ chemistry | SFB 574 |
| 5 . Buhmann, Sitta | ROV QUEST | MARUM |
| 6 . Corrales Cordero, Emelina | Observer | NGO |
| 7 . Domeyer, Bettina | Pore water geochemistry | IFM-GEOMAR |
| 8 . Omoregie, Enoma | Microbiology | MPI |
| 9 . Fromm, Tanja | Mapping/ documentation | SFB 574 |

| | | |
|---|---|---|
| 10. Garbe-Schönberg, Dieter, Dr. | Pore water geochem./ carbonates | CAU |
| 11. Hüttich, Daniel | ROV QUEST | MARUM |
| 12. Klar, Steffen | ROV QUEST | MARUM |
| 13. Linke, Peter, Dr. | Lander | IFM-GEOMAR |
| 14. Mason, Pete | ROV QUEST | IFM-GEOMAR |
| 15. Niemann, Helge | Mikrobiologie | MPI |
| 16. Pieper, Martin | SFB 574 | IFM-GEOMAR |
| 17. Queisser, Wolfgang | Lander/ TV MUC | IFM-GEOMAR |
| 18. Ratmeyer, Volker, Dr. | ROV QUEST | MARUM |
| 19. Schacht, Ulrike | Pore water geochemistry | SFB 574 |
| 20. Schleicher, Tina | Biology | SFB 574 |
| 21. Schmidt, Werner | ROV QUEST | MARUM |
| 22. Seiter, Christian, Dr. | ROV QUEST | MARUM |
| 23. Stange, Karen | $CH_4$ analytics | SFB 574 |
| 24. Türk, Matthias | Lander | IFM-GEOMAR |
| 25. von Neuhoff , Holger | Press documentation | NDR |
| 26. Wallmann, Klaus, Dr. | Pore water geochemistry | IFM-GEOMAR |
| 27. Westernströer, Ulrike | Pore water geochemistry | CAU |
| 28. Zarrouk, Marcel | ROV QUEST | MARUM |
| 29. Seibold, Jörg | TV documentation | DWTV |
| 30. Kassube, Hans-Jürgen | TV documentation | DWTV |
| 31. Cee, Dagmar | TV documentation | DWTV |

**CAU** Institut für Geowissenschaften der Christian-Albrechts-Universität zu Kiel, Ludewig-Meyn-Str. 10, 24118 Kiel, Germany

**DWD** Deutscher Wetterdienst, Geschäftsfeld Seeschifffahrt, Bernhard-Nocht-Str. 76, 20359 Hamburg, Germany

**DWTV** Deutsche Welle TV, Voltastr. 6, 13355 Berlin Germany

**GEOB** Fachbereich Geowissenschaften; Universität Bremen Postfach 330440, 28334 Bremen, Germany

**IFM-GEOMAR** Leibniz Institut für Meeresforschung, Wischhofstrasse, 24105 Kiel, Germany

**KUM** Umwelt- und Meerestechnik Kiel GmbH, Wischhofstr. 1-3, Geb. D5, 24148 Kiel, Germany

**MARUM** Zentrum für marine Umweltwissenschaften der Universität Bremen, Leobener Str., 28359 Bremen, Germany

**MPI** Max-Planck Institut für Mikrobiologie, Celsiusstr. 1, 28359 Bremen, Germany

**NGO** Escuela de Ciencias Biologicas, Facultad de Ciencias Exactas y naturales, Universidad Nacional Heredia, Costa Rica

**OKTOPUS** Oktopus GmbH, Kieler Str. 51, 24594 Hohenweststedt, Germany

**SFB 574** Sonderforschungsbereich 574, Christian-Albrechts-Universität zu Kiel, Wischhofstrasse 1-3, 24148 Kiel, Germany

**UCR** Universidad de Costa Rica, San Pedro de Montes de Oca, 2060-1000

## 2.2 Research Program

Leg 2a was primarily dedicated to the transit to the working area off Central America. After passing the Panama Canal, a geophysically oriented program was carried out in the SFB574 working area off Costa Rica, with the deployment and recovery of various OBS/OBH stations.

The scientific program of Leg 2b comprised several detailed investigations of sites where active fluid venting occurs. The ROV Quest operated by the University of Bremen was used to sample and monitor mud extrusions, slides, and scarps generated by seamount subduction off Costa Rica and Nicaragua. The work complemented earlier work using standard and towed video-guided equipment. In addition, 2 different lander systems were deployed and several CTD/Rosette casts were performed to extend time series of the methane inventory at several stations and to quantify the inventory of the vent-derived methane at the shallow, very active Quepos Slide.

## 2.3 Narrative of the cruise

### 2.3.1 Narrative of the Cruise Leg M66/2a

After all scientific material had been installed, R/V METEOR left the port of Curacao at 09:00 on September 22nd. During the transit to Cristobal, five shallow (1000 m) CTD/rosette stations at a spacing of 120 nm along the southern rim of the Columbia Basin were completed. The samples were taken to determine the concentrations of nutrients as well as the trace gases methane and $N_2O$. The programme was completed by continuous monitoring of methane concentrations within surface waters and the marine atmosphere. We found an oversaturation by 10-20 percent which, according to the data from the CTD samples, can be attributed to methane concentration maxima at water depths between 30 and 100 m.

At 09:00 in the morning of September 25th we arrived in Cristobal. The scientific crew of M66/2a was completed by five members of the Bremen ROV team and 3 students from Costa Rica joining us. The passage through the Panama Canal started on September 25th. The passage ended on September 26th at 04:00 local time. Another one and a half days of transit later, around noon of September 27th, we started recovering some of the OBS/OBT (Ocean Bottom Seismometers/ Pressure Samplers) that had been deployed west of Osa Peninsula in April 2005. They are part of a teleseismic transect across the southern part of Costa Rica that has been designed with the objective of studying the relationship between fronts of metamorphic fluid venting and seismicity on the one hand and the seismic structure of crust and upper mantle on the other hand. The instruments serve as the seaward prolongation of an on-land transect that is currently being monitored by an array of 16 seismometers.

The teleseismic transect passes the immediate vicinity of Mound 12, a mud diapir on the summit of which several fluid samplers were deployed by US colleagues in cooperation with the SFB 574, using the ALVIN submersible. These instruments are recording the activity of fluid vents and the composition of the fluids venting from Mound 12. Two OBS were deployed

immediately next to fluid samplers with the aim of establishing correlations between microseismic activity and the extent of fluid flow. Within 8 hours, 7 instruments were recovered and 2 OBS were deployed 20 nm away at Mound 12.

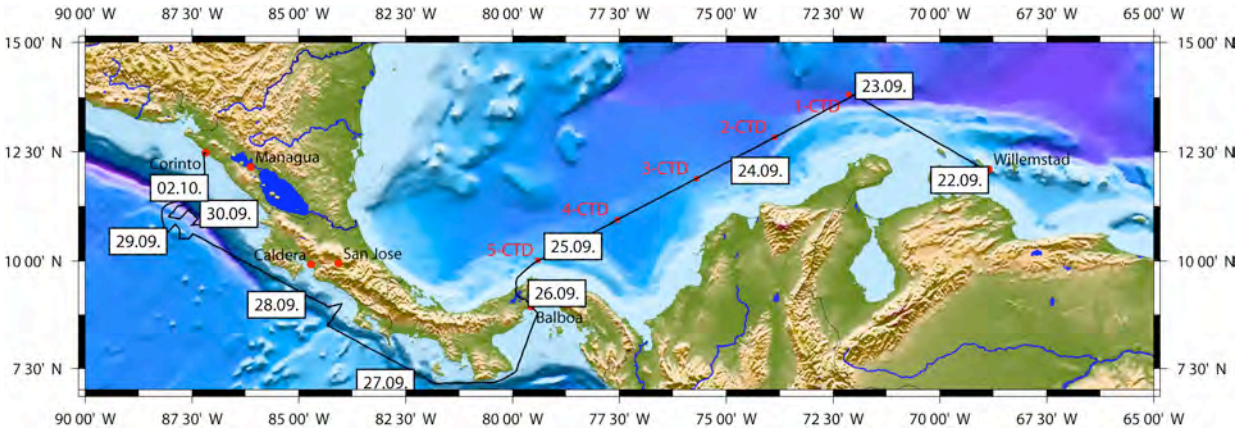


**FIG. 2.1:** Cruise track of Leg 66-2a with positions as 0:00 UTC indicated. Most of the geophysical work was performed in the area north of Corinto, ~ 29-30. September.

Afterwards, R/V METEOR went on a 213-nm-transit for our next working area off the Nicaraguan coast, where 24 OBH/S were deployed in a symmetric rectangular pattern to form a seismological network at 10°40'N and 80°W above the summit of the Outer Rise. This experiment focuses on recording local earthquakes taking place in the oceanic crust below this area. Previous studies have shown that a large number of local earthquakes are triggered in the area of the Outer Rise. This network was designed to constrain the distribution of depth and the source area of these earthquakes.

As the geophysical program went extraordinarily well, we were able to schedule a first 13-hour QUEST dive above Mound Iguana at 11°12'N;087°09'W at a water depth of about 1200m. Mound Iguana's topographic elevation above the surrounding seafloor is not very pronounced, yet it is characterized by a large carbonate-dominated area. The carbonates are partly exposed and partly covered by sediments. Due to a failure of the GAPS subpositioning system, mapping of the seafloor could not rely on exact positioning. In the southwestern part of the structure several bacterial mats were found as well as fields of calyptogenae and some accumulations of mytilidae. QUEST observation added a completely new dimension to our understanding of the spatial distribution of active areas along faults and rupture zones. In addition, some first water and sediment samples were taken.

The scientific programme of leg M66/2a was complemented by a CTD/rosette station on September 30$^{th}$ at 23:50. After an 8-hour transit, the leg ended in the port of Corinto, Nicaragua in the morning of October 1$^{st}$.

### 2.3.2 Narrative of the Cruise Leg M66/2b

After leaving Corinto in the morning of October 2nd, we headed straight back for Mound Iguana. Due to the swell caused by Hurricane "Stan", the ROV dive scheduled for the evening had to be postponed. The TV-MUC was deployed for 6 hours, yet samples were not taken, as the seafloor was mainly covered by carbonates. After detailed PARASOUND mapping and

sampling of one CTD station, QUEST was deployed for a 24-hour-dive at Mound Iguana. Extensive mapping of the mound showed that mytilidae are far more common in this region than bacterial mats, the latter being mostly small and sometimes growing directly on the carbonates. At the end of the dive, however, a large bacterial mat was found and identified as a target for the following deployment of the Benthic Chambers. In addition, further push cores and water samples were taken. On October 4th, first the DOS lander and, after sampling of another CTD station, the Benthic Chamber mooring were deployed. Unfortunately, one of the floats was torn off during the deployment. In the evening of October 4th, QUEST was deployed for Dive 66 with the aim of getting samples from a line of sites crossing a bacterial mat in order to complement our standard set of samples. The dive was successful, yet in the morning of October 5th, after a very fruitful sampling programme it showed that the chambers had toppled over because the seafloor was carbonated and very hard and thus, did not allow the chambers to penetrate to full sediment depth (12cm). Two of the chambers could be recovered and placed into the mooring with its reduced buoyancy. The third was latched into a shackle that had been lowered on the winch rope and could thus be recovered using the ROV and the ship, The subsequent attempt to retrieve the mooring failed in spite of a double release.

Afterwards, we performed a CTD sampling and a long OFOS track 2 nm away at Mound Quetzal. Mound Quetzal is a circular mound with a distinct topography and steep downslope flanks, while the upslope flanks are markedly less steep. CTD samples taken above the south-eastern part of the structure show a strong $CH_4$ plume. The OFOS survey revealed that in a small area in the north-east of the structure, scattered between massive and sometimes piled-up carbonates, there are larger accumulations of pogonophora and single fields of bacterial mats and calyptogenae. Following a successful deployment of the TV-MUC and CTD sampling above Mound 12, QUEST was deployed for dive 67, during which first of all the benthic chamber mooring was freed and recovered. The first deployment of a new system for in-situ measurement of sulfate reduction (N'Sync) designed by the Bremen MPI that had been fixed to the mooring turned out to have been successful. Afterwards, further sampling was performed on Mound Iguana. The work in the northern study area was preliminarily completed by one more CTD sampling in the morning of October 7th, after which we headed for Mound 12 in the southern working area.

The data from Mound Iguana, including a total of 11 pore water profiles, indicate some interesting results. A strong decrease of sulfate concentrations and production of sulfide indicate active AOM. In addition, the distribution of nutrients and chloride does not suggest a transport of deep fluids, so that it can be assumed that methane ascends in the form of a free gas phase, analogous to the situation found, for example, at Hydrate Ridge off Oregon. Furthermore, three cores show a slight enrichment of chloride and bromide concentrations in depth, corroborating the suspicion of near-surface gas hydrate formation.

After a transit of almost one day to Mound 12, two of our long-term CTD stations that we have been revisited consistently for years were sampled. Afterwards, a deployment of the bottom water sampler was performed, followed by a QUEST dive above the already well-studied Mounds 11 and 12. A mass spectrometer of our Hawaiian colleagues, which was positioned on the seafloor was checked as we had promised to recover it within the next days. Subsequently, several extended bacterial mats located in the south-west of Mound 12 along a central fault were mapped. We then went on to Mound 11 and some sediment cores along a bacterial mat. First

results show a clear zoning of geochemical parameters along a gradient, which will serve as data basis for two-dimensional modelling of the fluid venting. October 9th was used for OFOS mapping along the north-western flank of Parrita Scarp, which is located 20 nm away from Mds 11 and 12. However, we did not find a location that seemed suitable for an ROV dive, although single communities of calytpogena were found in the area between 1400m and 1700m water depth.

In the evening of October 9th, we resumed our work with QUEST Dive 69 at Mound 12. The sampling program was preceded by the successful recovery of the in situ mass spectrometer that had been deployed in April during an ATLANTIS/ALVIN leg with participation of the SFB 574. For this manoeuvre, a second rope was lowered and the ROV was used to attach the instrument to a shackle directly at the seafloor. Following some further mapping of Mound 12, several push cores were taken from a bacterial mat. Additional cores were taken away from the mat for reference. Fluid sampling was performed along a longish bacterial mat. Three stations were additionally used for sampling with a newly developed pressure-retaining water sampler that worked successfully.

On October 10th, a CTD cast was performed directly above the active south-western part of Mound 12, yet the enrichment of methane in the near-bottom water column was markedly less than found in the bottom values of the seemingly much less active north-western station. The Benthic Chamber shuttle was deployed with three chambers, again complemented by the sulfate measuring device N'Sync, and in the evening the next QUEST dive (70) was performed. The BC chambers were deployed at the beginning of the dive to be recovered at the end, a manoeuvre that was a great challenge for the ROV team. Two of the chambers worked flawlessly, but in the third one the program controlling the penetration of the chamber into the sediment failed. Again, a push core was taken for the N'Sync tracer addition, complemented with a second push core taken next to it. In both cases, coring was accompanied by an ascent of free gas from the sediment, which was a confirmation of our assumption from the geochemical data that we are dealing with a system controlled by the ascent of gas. Further coring and sampling of fluids/water with the KIPS fluid sampler was designed to form a transect from the centre of a bacterial mat to its edge. The retrieval of the BC mooring meant a preliminary conclusion of our work at Mound 12 in the afternoon of October 11th and we headed for Quepos Slide.

Quepos Slide is a slide in the upper area of the continental slope. It resulted in the formation of a plateau at a water depth of approximately 400m that had already been sampled extensively during cruise SO 173. The presence of bacterial mats and venting of deep, salt-depleted fluids has been documented here. Its geochemical environment is distinct. Due to the hydrographic conditions, active fluid venting meets an almost anoxic water column. In the afternoon, the Quepos Slide scientific program started with CTD deployments at three successive stations. They were part of an extensive sampling program from October 11th to 14th, comprising a total of 14 CTD stations on Quepos Slide in order to make a survey of the methane emitted into the water column from this structure. In the evening of October 11th, QUEST was deployed for its first dive (71) at Quepos Slide. Mapping the slide, we found that especially in the north-western part of the plateau, some areas are almost completely covered with bacterial mats. In north-eastern direction towards the slope, there is a slight depression filled with sediments where there are no bacterial mats. Above 400 m, there are only single spots of bacterial mats, especially in the direction of the north-western slope, which is less steep. White and orange mats alternate,

with the orange ones often concentrating in the centre. Therefore, sampling focused on a 1.5-m-broad extended bacterial mat that was transected by a series of sediment cores and water samples. The zoning of the bacterial mats from orange (inner area) to white (outer area) was given attention as well. After the dive had ended in the morning of October 12th, the day was used for further CTD sampling and a deployment of the DOS lander. The latter is used to record currents within the water column as a basis for later interpretation. Apart from a camera directed at the seafloor, it is equipped with an array of ADCPs with various frequencies, providing for a whole range of different coverages and resolutions. The BC lander was deployed on a bacterial mat on Quepos Slide as well. It was equipped with two chambers, yet as we were encountering very soft seafloor, one of the chambers was completely filled with sediment. In the night of October 12th, a long OFOS survey was run on Parrita Scarp, yet apart from some single calyptogenae there was no indication of active fluid venting, so that Parrita Scarp was no longer considered as a potential QUEST site. On October 13th, the water column program was continued during daytime, the BC lander was deployed once more with two chambers as well as an additional oxygen optode and the subbottom of Quepos Slide was mapped with PARASOUND.

A subsequent dive above Quepos Slide was first used for further mapping of the active area in north-western direction. It showed that, starting from the longish bacterial mats, the active structures found here show a transition to round, sometimes slightly elevated structures that often show black depressions in their centre, which are not covered by bacterial mats but rather enclosed by centric rings of bacterial mats. Again, we took bottom-near water samples using KIPS and push core samples along a transect across a bacterial mat with a breadth of just under one meter. Special attention was paid to the gradient into the marginal area and the surrounding sediments.

In the course of October 14th, the CTD program was continued. It now covers the entire active area. The BC lander and the DOS lander were recovered and the deployments were found to be successful. After a transit of 40 nm a QUEST dive at Jaco Scarp was scheduled in the evening. Jaco Scarp is a slide that originates from subduction of a seamount on the subducting plate. Dive 73 was focused on detailed mapping and sampling of an area known from previous cruises. Here, large fields of Pogonophora have accumulated around the faulted area, the water column above which also shows a strong emission of methane. The dive started 700 m to the north-west. More active areas were found here, smaller but often showing large outcrops of calyptogena and also bacterial mats. On this occasion, we were able to retrieve the first sediment samples taken from this area ever. The rest of the dive was mainly dedicated to measuring the depth range of the pogonophora field and video mapping. Numerous water samples were taken directly within the field using the KIPS system, and some specimens were taken from the vent fauna, among them pogonophora of more than 1m in length.

October 15th was used for CTD sampling at a site above Jaco Scarp that had already been visited several times in earlier years, and deploying the DOS lander at the debris fan south of the active area. In addition, CTD data were collected in order to search for indications of fluid venting at a circular, crater-like structure of about 500 m in diameter 10 nm west of Parrita Scarp that we call "mud pie" so far. The structure does not show strong bathymetric characteristics, however, in the DTS data it stands out for its high backscatter. The CTD showed a clear elevation of methane concentrations in the bottom water. In the evening of October 15th, QUEST was launched for Dive 74 above Jaco Scarp, with the main objective of mapping the horizontal

extension of the pogonophora field. The program was complemented by recording detailed video mosaic pictures and finding additional fields in the north-west. While the sediment was too compact to allow for further push coring, samples could be taken with the pressure-retaining system. The sample was taken directly from the field of pogonophora, and on sampling there was a spontaneous degassing that stressed the importance of pressure-retaining sampling. Our scientific program in this area was concluded when QUEST surfaced in the morning of October 16th and the water column had been sampled at our second long –term station at Jaco Scarp by CTD/rosette.

After finishing our work on Jaco Scarp, we returned to the Quepos Slide working area for two more days. The first day was dedicated to a concerted program with the aim of finding out if there is a physiological necessity for bacterial mats that are found in an almost anoxic environment (< 2µmole of oxygen in the bottom water) to produce oxygen. This question had come up due to observations made during a lander deployment on SO173 and from the data gained by the oxygen optode a few days earlier during our expedition. It was approached by taking some CTD profiles and bottom water samples followed by ROV Dive 75 in the evening of October 16th, which was mainly used for a deployment of the oxygen consumption chamber "ELINOR" and for taking 10 sediment cores for incubation experiments. A deployment of the Benthic Chamber Lander performed on the next day was also dedicated to this question. Yet, the results remained contradictory.

On October 17th, a three-person television team from the Deutsche Welle joined us in order to document our onboard "everyday life". Further CTD stations were sampled above Quepos slide to extend our coverage of the methane plume of this area. In the night of October 17th, a last dive (76) was performed above Quepos Slide. During the dive, a structure was examined that shows a black center encircled by bacterial mats in an almost concentrical pattern. Again, we made a transect across the gradient with a series of fluid samples and sediment cores. In addition, a video mosaic was recorded for visual documentation of a larger area to enable a better spatial understanding. The BC lander was then recovered from its site at Quepos Slide and the DOS lander from Jaco Scarp, 49nm away. The rest of the night was used for a long OFOS survey of the "mud pie" (8:59.6N; 84:43.7W). At the northern margin of the area, we mapped a steep flank covered by carbonates. Larger areas showing fields of calyptogena and pogonophora were documented. The work was completed at two o'clock in the night, and we set course for the last site of investigation of this cruise, Mound Culebra, which is located 130 nm in the north-west. We arrived there in the afternoon of October 19th. Mound Culebra is a mound with a strong morphological expression, about 100 m high and 1.6 km x 1 km wide, and it is crossed by a fault in NW-SE direction. We started by taking samples from two long-term stations with the CTD/rosette, followed by QUEST Dive 77. Mound Culebra is especially interesting because here, vent-specific and ordinary deep-sea fauna exist simultaneously. Sampling turned out to be difficult. Bacterial mats were not found, and the abundant calyptogenae often sat on hard, carbonated ground. However, we managed to use the pressure-retaining water sampler and to position "ELINOR" above a field of calyptogenae for a long-term deployment. The course of the last two days made us change our plans for the remaining time of the cruise and we made a transit back to the the "mud pie" in the south-west, where on the basis of the data collected previously, a final dive was made in the evening of October 20th. As documented by OFOS before, we found large fields of calyptogena and pogonophora. The most important discovery

was a depression similar to a pockmark, several meters large and located on the southern extension of the carbonate flank. Its sides as well as its bottom were covered by bacterial mats. The area was mapped by a video mosaic, water samples were taken with the KIPS system as well as with the pressure-retaining sampler. The sediment showed to be rich in water, yet we managed to take some samples. The program was complemented by further samples of bacterial mats and an "ELINOR" deployment. In the morning of October 21st, a last CTD was run directly above the "pockmark", and in the afternoon the DOS lander was deployed on mound 12 to sit for a few weeks in the immediate vicinity of the SCRIPPS fluid samplers and our seismometers that had been placed there at the beginning of M66 Leg 2a. During this period, rates of fluid venting, seismic events, and hydrographic parameters will thus be recorded simultaneously at the site. After a 14 hour HYDROSWEEP survey to close some gaps in our high-resolution bathymetric data of the Costa Rican continental margin we reached the roadstead of Caldera on October 23rd at 07:00 am.

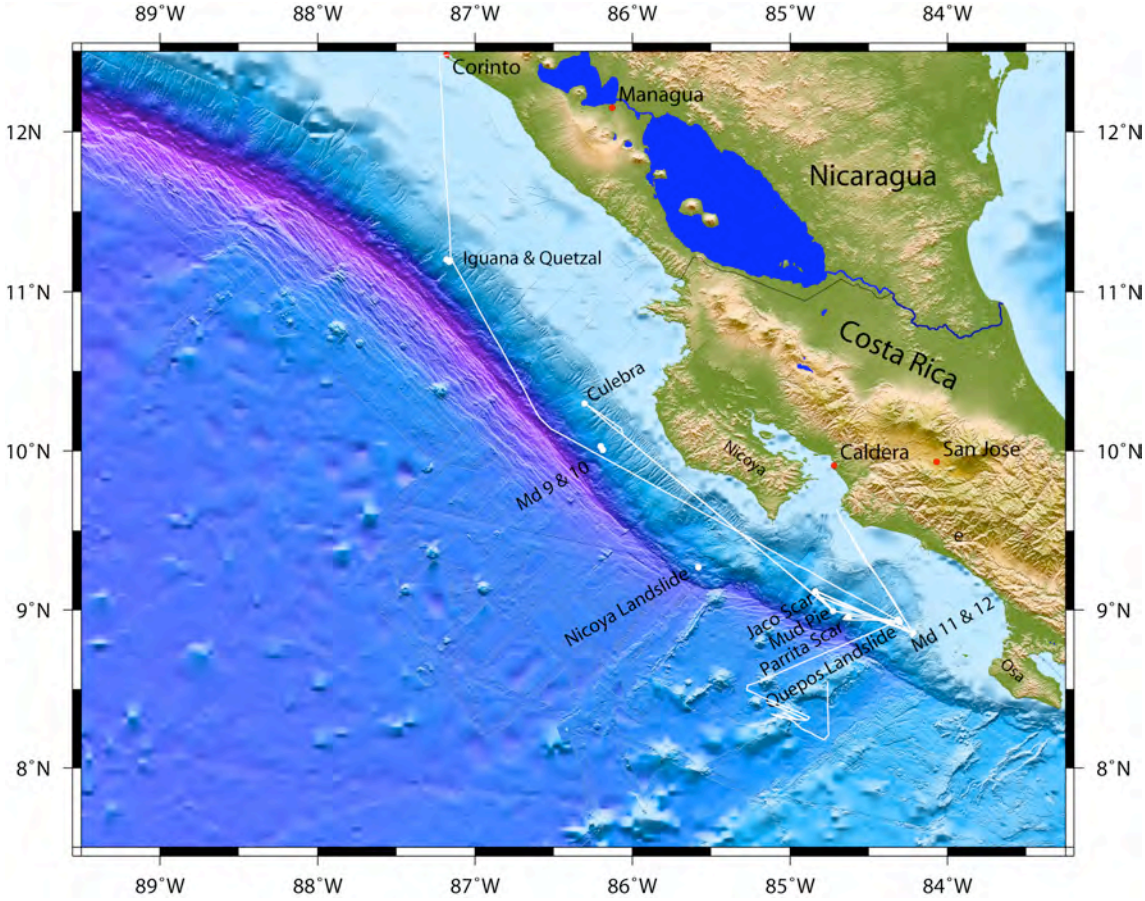


**FIG. 2.2:** Cruise track of Leg 66-2b in the target area of SFB 574. Dots indicate known sites of active fluid seepage.

## 2.4 Preliminary Results

### 2.4.1 Dive Mission Protocols and ROV Sampling

**Mound Iguana:** Dive # 64 (St. 37 ROV), Dive # 65 (St. 42 ROV), Dive # 66 (St. 45 ROV), Dive # 67 (St. 51 ROV)

Dives #64 through #67 explored the seafloor and sampled successfully a number of bacterial mats, authigenic carbonates, and biota at Mound Iguana. From the first test dive (#64) during leg M66/2a samples of Bathymodiolus and Calyptogena were recovered along with a large piece of

authigenic carbonate. Water samples above a bacterial mat, and above clam fields were taken with Niskin bottles (Niskin-3, -4 and –portside), the same spots were probed with pushcores PC-1 (bacterial mat) and -2 (Calyptogena). The first regular dive #65 during leg M66/2b sampled bacterial mats with 5 push cores and 8 water samples and recovered another piece of authigenic carbonate. The sampling program during dive #66 escorted the deployed BCL lander: push cores PC-19 to -24, and KIPS-9, sampled the bacterial mat close to the West BCL chamber, and PC-25 to -28, and KIPS-11, close to the East chamber, with PC-29, -30, and PC-31, -32 representing background stations in barren sediment remote from chambers East and West, respectively. KIPS-1 and -3 sampled bottom water close above patches of white bacteria on authigenic carbonates. A patch of greyish bacteria could be sampled with the shovel. The beginning of dive #67 was dedicated to the recovery of the BCL elevator. An attempt to transfer to Mound Quetzal had then to be cancelled because of a strong bottom current. KIPS-1 and -3 sampled bottom water close above patches of white bacteria on authigenic carbonates, the latter being sampled with the manipulator. Push cores PC-2 to -4 sampled sediment with bacterial mats.

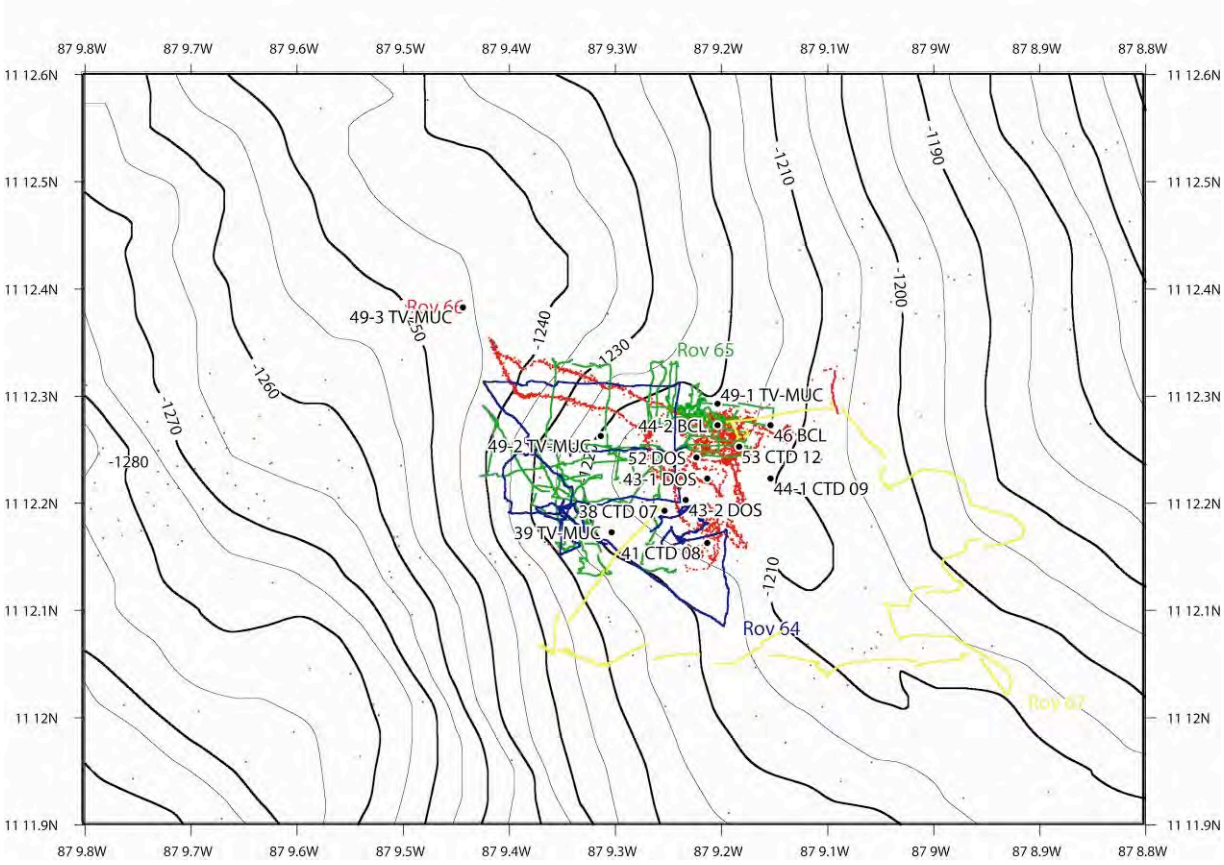


**FIG. 2.3:** ROV-tracks and sampling stations at Mound Iguana.

***Mound 11 & Mound 12:*** *Dive # 68 (St. 58 ROV), Dive # 69 (St. 60 ROV), Dive # 70 (St. 64 ROV)*

The seafloor at Mound # 12 was searched for a suitable landing site for the BCL lander. Small and medium sized patches, some with "blackened" areas, are common. ELINOR is deployed within a grey bacterial mat (EL-1), another mat is sampled with PC-1 and -2 and KIPS-1. After recovery of ELINOR the ROV transfers to Mound #11. Large bacterial mats with white and orange colors are abundant. ELINOR is dispatched on a white mat (EL-2). Push cores PC-3 to -10

sample the center part of an orange bacterial mat, PC-11 to -16 and PC-7 form a transect towards N. Bottom water 1-3 cm above seafloor along this transect is sampled with KIPS-3 to -9.

The first task of Dive # 69 was the recovery of the Deep Ocean Mass Spectrometer (DOMS, built by the Scripps Institution of Oceanography (SIO) and School of Ocean and Environmental Science and Technology (SOEST) which had been positioned during the ALVIN dive in May 2005. A huge field of bacterial mats with dead clams overgrown by bacteria was found (sampled with the shovel), being replaced at the SW end by pure bacterial mats with only a few dead clams. Sampling of a bacterial mat-transect, in close distance to the flow meter of Kevin Brown, with PC-17 to -28. Seeping fluids/ bottom water were sampled across another mat in the vicinity with KIPS-1 to -17 and autoclave sampler (PFS -1 to -3).

Dive #70 complemented bottom chamber station 63-1 BCS. All three incubation chambers were removed from the elevator and placed within a bacterial mat, at a clam site near the border of the first bacterial mat, and within another bacterial mat. Next task was the positioning of the MPI-Bremen in-situ incubation module (INSINC) within a bacterial mat. A massive release of gas bubbles was observed during the insertion of the device into the sediment. This gas release was repeatedly observed during sampling with push cores (PC-1 and -2) at this site. The same mat was then extensively sampled with push cores PC-3 through -16, and, later, with a bottom water transect (KIPS-1 to -11). The dive ended with the retrieval of all three bottom chambers and recovery of the elevator.

***Quepos Slide:*** *Dive # 71 (St. 68 ROV), Dive # 72 (St. 81 ROV), Dive # 75 (St. 97 ROV), Dive # 76 (St. 99 ROV)*

Dive # 71 had first bottom sight in an area where the seafloor was largely covered with both clam fields and yellowish bacterial mats. Further to the N, bacterial mats were elongated and parallel to the walls of outcropping sediments, with some massive carbonates. Few mats had black patches with expulsed material in the center. Gradients across a large color-zoned bacterial mat (10m long, 2 m wide) with orange to yellowish colors in the centre and white colors in the outer rims was sampled with a 6 points high-resolution transect (10-40 cm) with push cores PC-17 to PC-32 and KIPS-1 to -13. Video mosaicing documents the spatial distribution of the mats. The dive ended with further exploration of the headwall area to the N.

Dive # 72 started with 2 deployments of the MPI-Bremen ELINOR incubation experiment (EL-1, EL-2) within bacterial mats. Special morphological features first seen here were dome-like elevations covered with bacterial mats and, sometimes, with crater structures on-top. Another feature was a knoll-like structure, some 5 m high, completely paved with bacterial mats. Further up-hill to the N no bacterial mats were observed in water depths shallower than 400 m. A reference background sediment was sampled with PC-1, followed by detailed sampling of a transect across an orange-white zoned bacterial mat with PC-2 to PC-16 (microbiology, porewater chemistry) and KIPS-1 to -11. EL-3 was deployed for 5 hours within an orange mat. A rat fish could be catched with the NET sampler.

Data on dissolved oxygen from earlier BCL lander deployments surprisingly suggested that oxygen was produced in the benthic chamber rather than being consumed from biological activity. Objectives of dive # 75 focused on this theme “oxygen depletion vs. oxygen production” by bacterial mats. Dense white and orange-yellow bacterial mats were sampled in high-resolution transects (20-30 cm resolution) with push cores (PC-1 to -9) and KIPS (1-9),

complemented by ELINOR incubations on white and yellow mats. For reference, a background station was sampled with EL-4, KIPS-11, and push cores PC- 13, -14, -34. The spatial distribution of bacterial mats was mapped with video mosaicing. Towards the end of the dive a small cave formed by a overhanging thin carbonate crust was sampled with KIPS (#9) and push core (PC-28). Carbonate and the floor inside the cave were covered with white filamentous and white/yellow-orange bacterial mats, respectively.

The beginning of dive # 76 was dedicated to monitoring the deployment site of the BCL lander (St 98 BCL). New results from BCL Lander and ELINOR deployments during the previous stations on this site seemed to prove that oxygen in benthic chambers was not depleted during *in situ* incubations on bacterial mats but showed an increase. In order to validate these observations, and to test the optode oxygen probe, a series of bottom water profiles going from 10 m above seafloor down to 0.5 m was performed with ELINOR. Two other deployments of ELINOR were on a dense white, and a thick orange-yellowish bacterial mat, respectively. Transects across a white-orange-black zoned bacterial mat were sampled with KIPS (1-7) and push cores (PC-17 – PC-26). The site was covered by video mosaicing, as well as two other areas with abundant bacterial mats. Bacterial mats again were sampled with PC-28, and a massive carbonate sample was taken. The third deployment of ELINOR was on a background site.

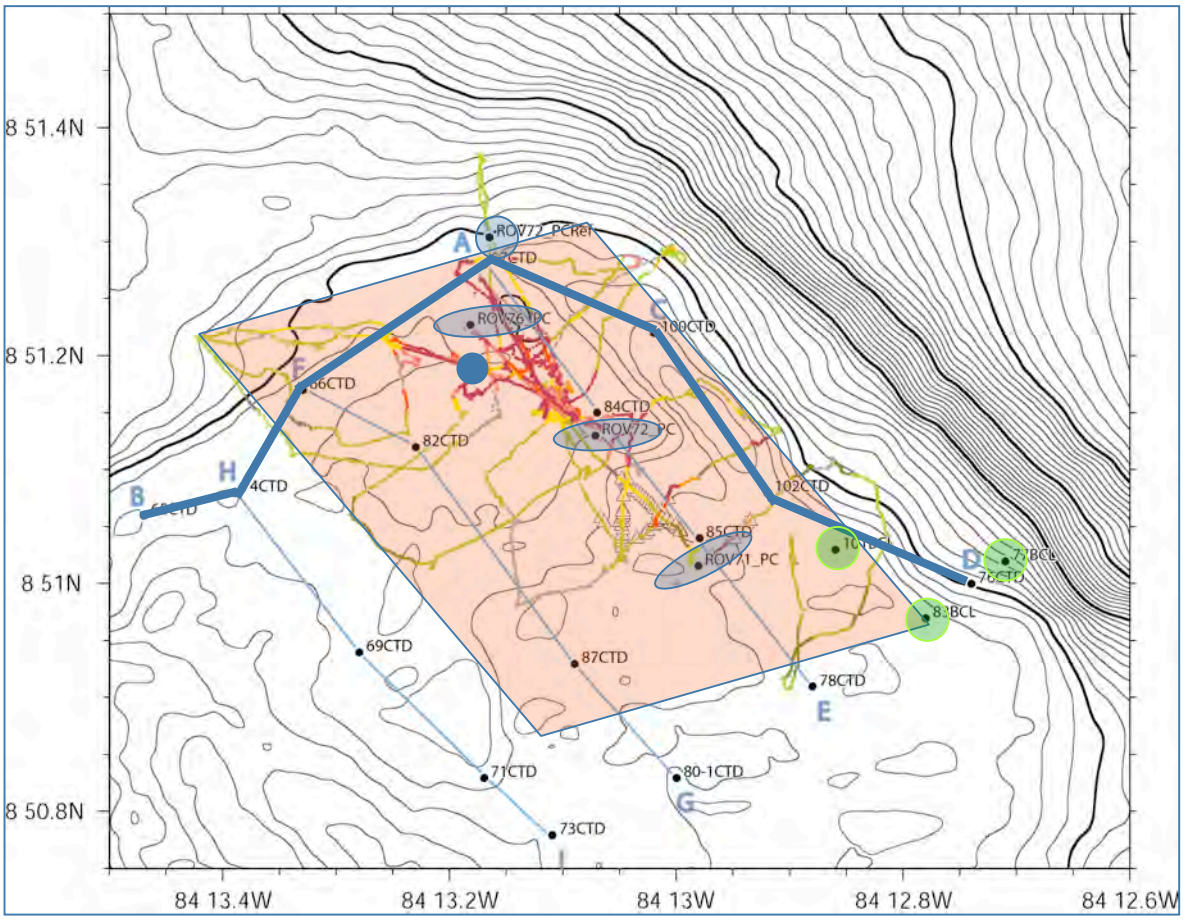


**FIG. 2.4:** Bathymetry, station positions, and ROV tracks at Quepos Slide. Color code of tracks indicated coverage by bacterial mats (red 50-100% coverage, green 0-10%). Grey shaded areas indicate positions where sediment core sections have been sampled. Green dots show positions of the BCL deployments referred to in Figs. 2.13 & 2.14. Thick blue line indicates methane concentration section shown in Figure 2.19.

***Jaco Scar:*** *Dive # 73 (St. 88 ROV), Dive # 74 (St. 92 ROV)*

Main objectives for the two dive stations at the Jaco Scar site were (i) to map the area and to possibly identify new active seeps in the E part of the structure formerly located by methane anomalies in numerous CTD casts, and (ii) to comprehensively sample known active seeping areas, characterized by large fields of vestimentiferan tube worms (*Lamellibrachia* sp.), with high spatial resolution. ROV dive # 73 explored the 'target box' with known active seeps coming from NW. Towards the northern end of the box a large field with thousands of dead, and few living, vesicomyid clams (*Calyptogena* sp.) was sampled with KIPS (# 1), and push cores PC-17 and -18. Net #1 was filled with living Calyptogena. At another place a microbial mat was sampled with PC-19 to PC-21. Further towards the south, large fields with clams and very abundant tube worms were encountered. Leaving the field and uphill again were many boulders overgrown with serpulid polychaetes and tube worm bushes, the latter with a high diversity of other species living within these bushes (crabs, snails, shrimp, fish, brittle stars, octopus, bathymodiolin mussels etc.). A sample with serpulid polychaetes was taken, two giant sea spiders (approx. 80-100 cm) were observed. Ambient water from within a tube worm bush was taken with KIPS-3 and -5 and Niskin bottle #3, and sediment from the same spot was sampled wit PC-23 and -24. Specimens of *Lamellibrachia* sp. were sampled successfully. Niskin bottle #4 was a background reference water sample.

ROV Quest dive #74 landed besides the DOS lander deployed during St. 90 DOS and explored the area with a transect to NW, later changing course to NE (see Figure 3.8.1.x). In a tube worm thicket a transect through a tube worm bush was sampled with both KIPS (#1 - #5) and the autoclave sampler (PFS-1 to -5). Serpulid polychaetes and vesicomyid clams nearby on a steep wall (KIPS-7) were sampled with NET. One spot was sampled covered with bacterial mats, bathymodiolin mussels, and tube worms. The clam field was sampled with KIPS-11, and the base of a tube worm bush with KIPS-13. Push core sampling failed due to the softness of the sediment. Another bacterial mat was successfully sampled with PC-1, taking also a polychaete sample with the manipulator. Mapping revealed extremely rough terrain in the north-eastern area of the investigation box, with almost vertical walls and abundant talus, as well as many dead vesicomyid clam fields.

***Mound Culebra****: Dive # 77 (St. 107 ROV)*

The landing site was on a crater rim with abundant massive carbonate and vesicomyid clams covering the seafloor. ELINOR was deployed on a clam field (*Calyptogena* sp.) for 7 hours (EL-1). Another clam field was sampled with both KIPS fluid sampler and PFS autoclave sampler (PFS 1, KIPS 1). The seafloor has a rough morphology here with steep carbonate cliffs. Clam fields are abundant but only a few living clams were observed within huge numbers of dead ones. Dark brown to black sponge-like organisms were observed quite frequently, a few of these were sampled with the manipulator at several occasions. From another clam field living specimen were sampled with the NET sampler. From within the same clam field push cores (PC 17, 18) were taken. Bottom sea water between the clams was sampled with the autoclave sampler (PFS 2, 3). At 0750 UTC an unusual red tube of approx 3-5 m length and 20 cm diameter appeared in front of the ROV floating in the water (video sequences from 0750 – 0800 UTC). The genus of the animal/s is unknown to us (probably a colony of radiolarians). A second deployment of ELINOR was conducted for 3 hours in background sediment (EL-2). Massive

carbonates, usually more or less sediment-covered, with abundantGorgonaria sponges, vesicomyid clam beds, echinoderms, and few serpulid polychaetes are characteristic for this site.

***Parrita Mud Pie**: Dive # 78 (St. 108 ROV)*

Dive 75 focused on the exploration of the northern rim area of the "Mud pie" structure. Landing site was in between carbonate rocks and tube worm bushes, clam fields with *Calyptogena* sp. close by. An attempt to place ELINOR on the mussel field failed, but was successful on a small bacterial mat (EL-1). Push cores were taken from this site. A new morphological feature not seen on any location before was the occurrence of circular, crater-like depressions with steep walls which closely resemble "pock marks". This was documented by video mosaicing. White bacterial mats near the wall of this pock mark were extensively sampled with KIPS (KIPS-1 to -9) and push cores (PC 21-26). ELINOR was then transferred to an area remote from the active area (EL-2). A larger 4x4 m white bacterial mat with adjacent black spot was sampled with KIPS and push cores (PC 27-30), and ELINOR was deployed on this site (EL-3). Massive carbonate was sampled nearby. Biology highlights from this dive were sightings of a 1.5 m long fish nicknamed "clown shark (*Chimera monstrosa*)", very abundant Gorgonaria, tube worms, vesicomyid clams, and floating colorless, transparent organisms of unknown genus. During ascent, a water profile was sampled with KIPS-11 to -17.

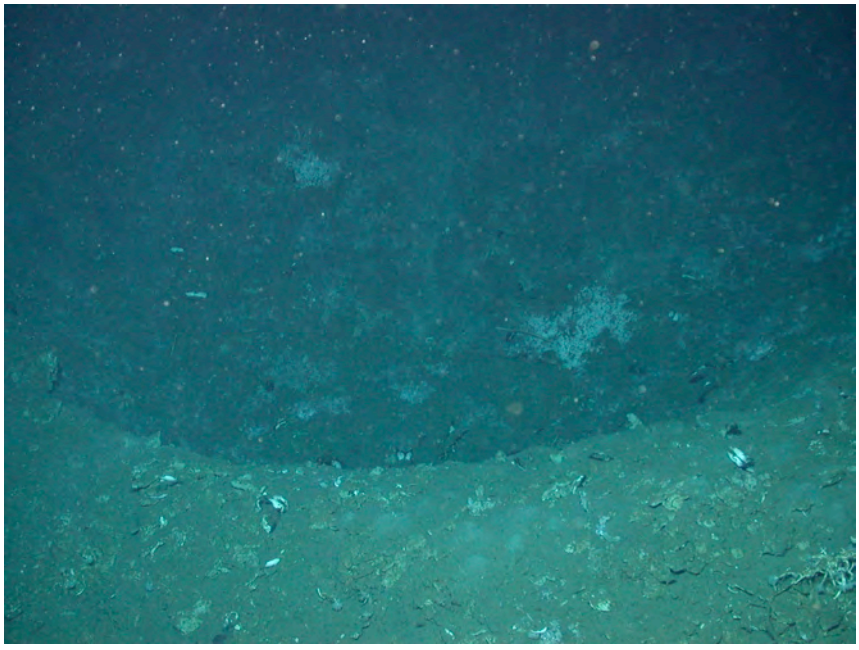

**FIG. 2.5:** Crater-like depression at "Mud Pie" discovered during dive 78, with bacterial mats at the bottom. Pockmark-like structures had not been reported in the area before.

### 2.4.2 Pore Water Geochemistry

Phosphate, nitrate, nitrite, silica, ammonia, and sulphide were determined in pore water and water samples using standard photometric procedure described in previous cruise reports (i.e. GEOMAR-reports 111, 115). Sub-samples for nutrient analysis were taken, acidified with HCl and purged with $N_2$-gas for 90 minutes to remove dissolved sulphide prior to analysis. Nitrate, chloride, bromide, and sulphate concentrations were measured using ion chromatography (IC). Total alkalinity (TA) was determined by titration with 0.02 N HCl and dissolved oxygen via Winckler titration. Selected samples were also analyzed for dissolved chloride using argentometric titration in order to control the IC results.

Bottom water samples were taken during ROV-deployments using the KIPS system (IfG Kiel), a pressurized fluid sampler (PPS), and a bottom water sampler (BWS) while the entire water column was sampled during CTD deployments. Surface sediments were taken during ROV-deployments using push corers (PC) provided by the MPI Bremen. Additional surface sediments were recovered using the TV-guided multi-corer (MUC). The benthic chamber lander (BCL) recovered both water samples taken with syringes from the enclosed chamber and surface sediments. Porewater was separated from surface sediments recovered during PC, MUC and BCL deployments by squeezing with Argon gas at 1 - 4 bar in the cold room at 4 - 6°C as described in previous cruise reports. The different sample types were analyzed for a large range of chemical parameters according to the sample size and the recovery mode.

Samples were recovered and analyzed at Mound Iguana, Mound 11, Mound 12, Quepos Slide, Jaco Scarp, and a newly discovered pockmark site. Several sections of sediment core sampling were achieved across active cold vent sites, indicated by the surface expression of bacterial mats. They allow for the first time an insight into small scale 2-dimensional flow patterns through the sediment fluid flow expression on convergent margin systems, a major achievement of this expedition. Selected results are highlighted in this section.

**Mound Iguana**

A total of 11 push cores and one TV-guided MUC were taken at Mound Iguana (s. Tab. 2). All cores taken in bacterial mats showed clear signs of anaerobic oxidation of methane (AOM). Considering the decrease in dissolved sulphate with depth, the AOM intensity increased in the following order:

ROV67PC2 < ROV67PC3 < ROC66PC30 < ROV67PC4 < MUC49 < ROV65PC9 < ROV66PC32 < ROC66PC22 < ROV65PC2 < ROV66PC31 < ROV66PC28 < ROV64PC1

Methane fuelling the AOM in surface sediments is produced by the decay of organic matter in deeper sediment layers. During this process, ammonia and other nutrients are released into the porewater. Hence, fluids from the methanogenic zone are usually enriched in dissolved nutrients. Low concentrations of nutrients were however found at the base of all studied sediment cores (5 – 40 µM ammonia) clearly indicating that methane is not transported to the surface with ascending fluids but rather as free gas. Gas bubbles from below the BSR are apparently rising through the sediment column at Mound Iguana. Similar pore water signatures were previously found at Hydrate Ridge where independent observations clearly indicate that methane bubbles formed at depth are expelled at the seafloor.

In three cores (ROV65PC2, ROV66PC32, ROV67PC3) dissolved chloride increased with sediment depth suggesting gas hydrate formation at depth. The increase was however small and close to the resolution of the analytic methods. In one core the increase in dissolved chloride with depth was confirmed by additional argentometric chloride measurements and by a coeval increase in dissolved bromide (Fig. 2.6). It seems to be likely that gas hydrates are formed in the upper few m of the sediment column at site ROV65PC2 from ascending methane gas bubbles.

Dissolved chloride did not decrease with depth in any of the cores suggesting that chloride-depleted fluids from the subducted slab are not ascending to the surface at the locations sampled on Mound Iguana. Alternatively, a shallow hydrological system may be active at this Mound mixing bottom waters into the surface sediments so that the chemical signature of the deep fluids is overprinted by the bottom water signature.

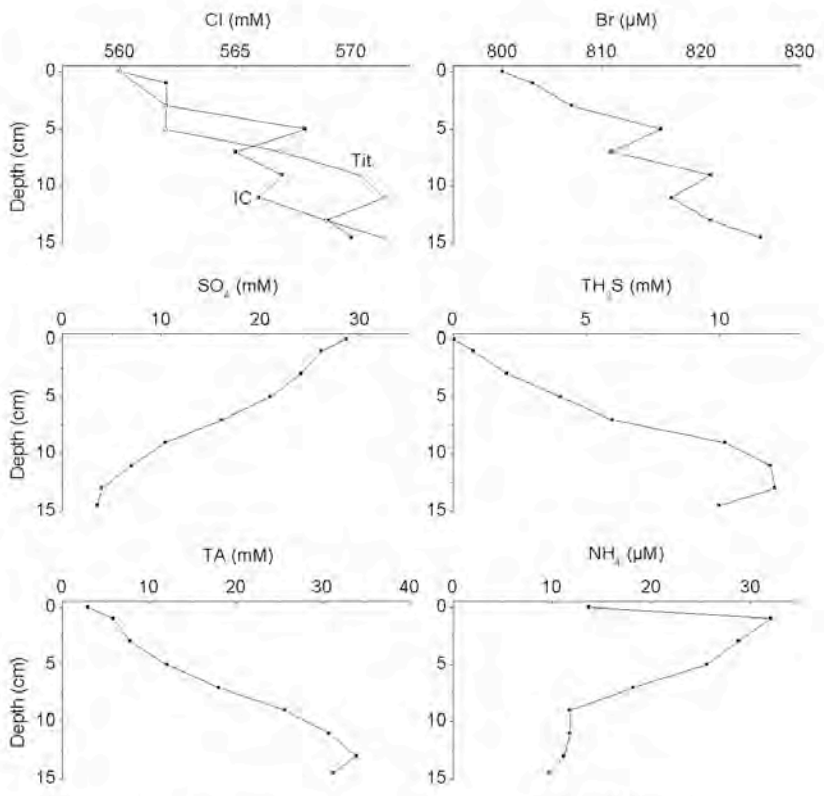


**FIG. 2.6:**
Pore water composition in surface sediments taken at Station 42 during ROV dive 65 with push core 2 in a bacterial mat on Mound Iguana.

**Mound 11**

A large bacterial mat located close to the top of Mound 11 was sampled in detail during ROV Dive 68 (M66-58). The mat had an elongated shape being approximately 3 m long while the width of the mat varied in between 0.2 and 1.5 m. A transect of push cores was taken perpendicular to the orientation of the mat across its most narrow part where the bacteria formed a particularly thick mat with an intense orange colour. The first sample was taken directly in the centre of the orange patch. The second core taken 20 cm away from its centre was already located outside of the mat. The following three cores were taken at an increasing distance to the mat centre (40, 60, and 80 cm) in soft background sediments. Distances to the mat were measured by two parallel laser pointers attached to the ROV creating two green light spots at the seafloor at a well-defined distance of 20 cm.

The core from the mat centre (M66-51-PC10) had very low concentrations of dissolved chloride at the base indicating the ascent of deep fluids originating from the subducted slab (Fig. 2.6). The chloride profile had a rather complex structure deviating from the simple exponential decay previously observed at other sites on Mound 11 where chloride is transported by upward advection and downward diffusion, only. The chloride plateau observed between 3 and 9 cm depth indicates that the upper 9 cm of the sediment column are affected by additional transport processes such as the lateral inflow of bottom waters. The rising deep fluids have a lower density than the overlying bottom water so that a convection cell may be established spontaneously in response to this unstable density layering. Hence, high-density bottom waters may penetrate into the sediment while low-density fluids are expelled into the overlying water column. The data suggest that the convection cell extends down to a sediment depth of 9 cm. The shape of the

bromide and ammonia profiles also suggest inflow of bottom water through the upper 9 cm of the sediment column. Sulphide and TA reach a maximum at 7 cm depth indicating that AOM proceeds at a high rate within the surface sediment. At that depth methane rising to the surface with the ascending fluids is mixed with sulphate which is delivered to the surface sediment by downward diffusion and convection of bottom waters. The core taken at 80 cm distance to the mat centre has higher chloride and lower ammonia concentrations indicating that the upward flow of deep fluids depleted in chloride and enriched in ammonia is restricted to the mat area. The chloride concentrations in the upper 7 - 9 cm are very close to bottom water values confirming the presence of a shallow convection system (Fig. 2.7). The AOM zone is shifted to larger depth as shown by the downward displacement of the sulphide and TA maxima.

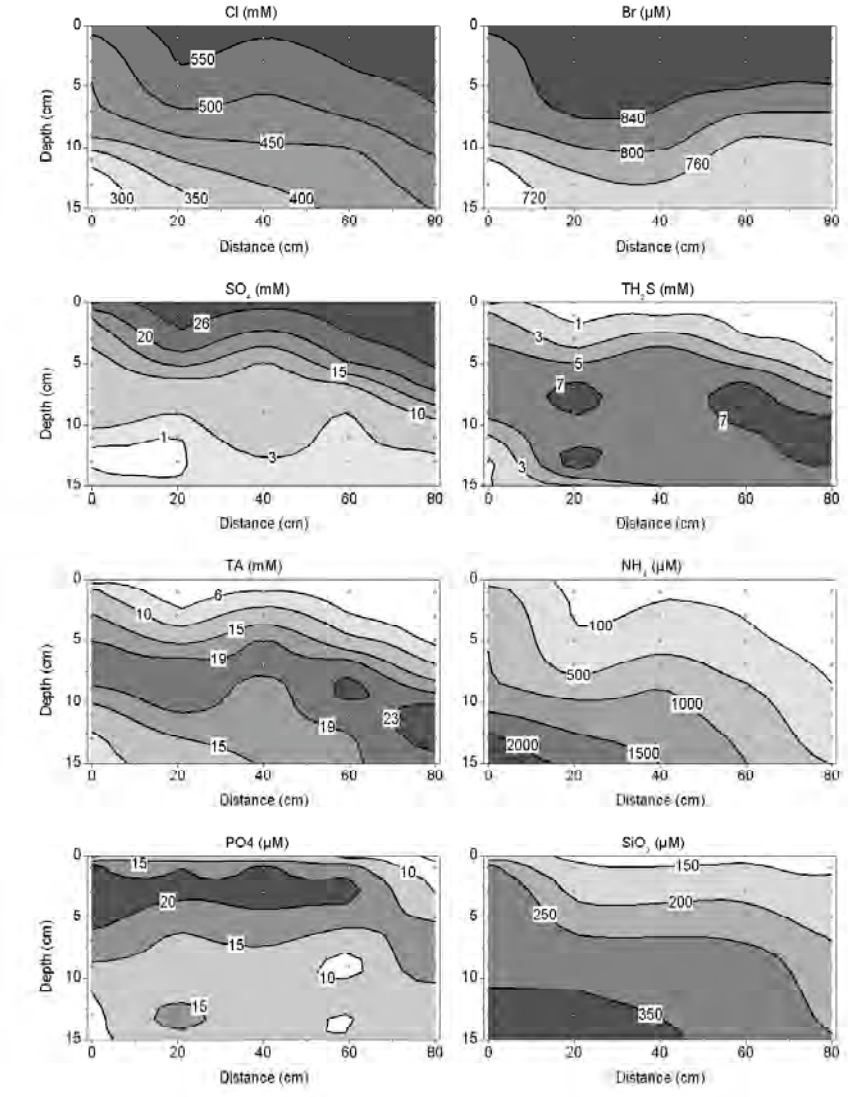


**FIG. 2.7:** Transect through a bacterial mat on Mound 11. The x-axis gives the distance to the centre of the mat. Open dots mark the positions were push core samples have been taken and analyzed.

Fig. 2.7 shows - to our knowledge - the first 2-D-distribution of dissolved species over a mat-covered cold seep at the deep-sea floor. It illustrates the structure of the convection cell indicating that the inflow of seawater is focussed at a lateral distance of 20 cm from the mat centre while the outflow occurs mainly through the mat-covered sediments.

## Jaco Scarp

Only two sediment cores were taken at Jaco Scarp because the steep morphology and the lack of soft sediments inhibited further sampling. Push core 21 taken during ROV Dive 73 within a bacterial mat proved to contain deep fluids most likely originating from the down-going slab (Fig. 2.8). The low chloride concentrations and very high dissolved silica value clearly point towards a deep origin. The extremely high N - P ratios in the fluids confirm that the fluids ascend from deep strata where phosphate is almost completely removed from solution by authigenic mineral formation. Fluids originating from clay mineral dewatering have been shown for several vent sites off Costa Rica (Hensen et al., 2004), but have been demonstrated here for the first time for a scarp created by seamount subduction. This type of geological setting is the other major group of fluid emitting sites which have been demonstrated to occur off Costa Rica.

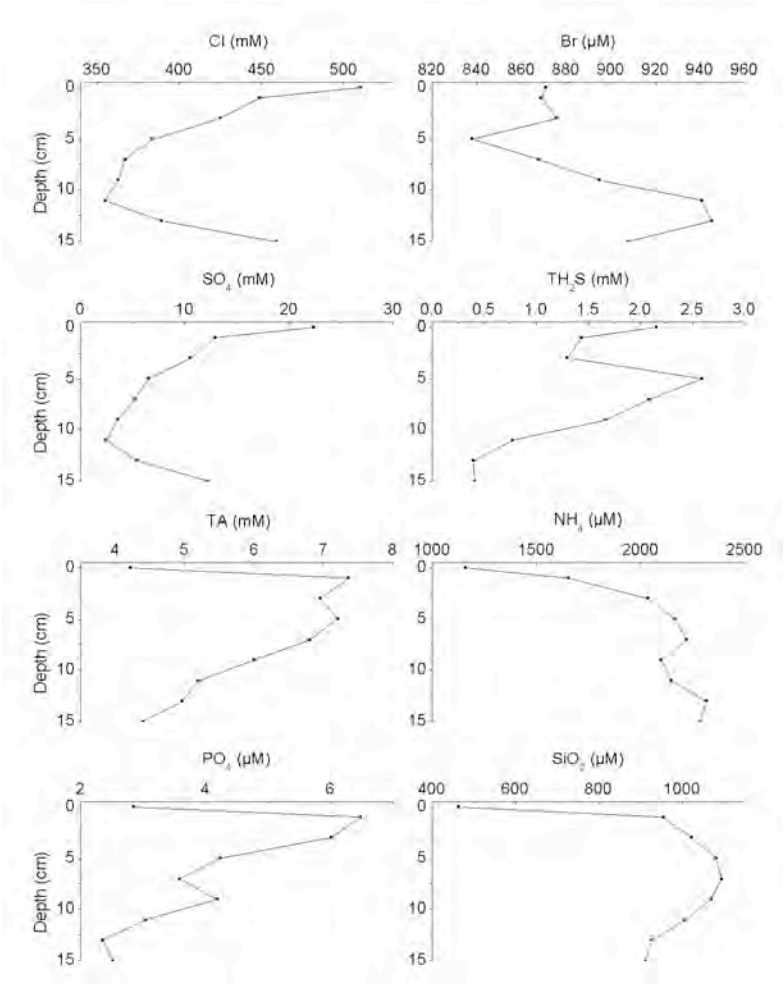


**FIG. 2.8:** Composition of pore fluids at Jaco Scarp. Core PC-21 was taken during ROV Dive 73 at the centre of a small bacterial mat located on the steep hanging wall of the scarp.

## Quepos Slide

A total of 17 push cores and numerous KIPS samples were taken at Quepos Slide during 4 ROV dives. Sediment core sections to derive 2-D sections of geochemical properties were sampled at 3 locations. In addition to this extensive coring program, samples from 3 successful deployments of the benthic chamber lander (BCL) and 2 bottom water sampler deployments (BWS) were analyzed.

Quepos Slide is located at shallow water depth (400 m) in a very productive upwelling area. Consequently, background sediments not affected by fluid ascent show strong gradients in dissolved sulphate and high concentrations of nutrients, alkalinity and sulphide reflecting the rapid degradation of organic matter via microbial sulphate reduction. In contrast, sediments from below bacterial mats are strongly depleted in dissolved chloride due to the ascent of deep fluids. They are dominated by AOM rather than sulphate reduction. In the evaluation of the mat data, it should however be considered that sulphate is not only reduced by AOM but also by the microbial degradation of particulate organic matter. Ammonia concentrations are higher below the mats while the phosphate concentrations are depleted compared to the reference site. The unusually high N : P ratios of the pore fluids below the mats reflects the loss of phosphate in the deep source region of the ascending fluids.

During ROV Dive 72 (St. M66-81), a transect of push cores was taken across a large bacterial mat. The mat had an elongated shape broadening towards the south. The transect was located across the more narrow northern part of the mat. The mat's diameter was 80 cm; the mat being orange in the centre and white at the rim. The transect was oriented perpendicular to the strike of the mat going from the centre to the east. The cores selected for pore water analysis were located at the following distances to the centre of the mat:

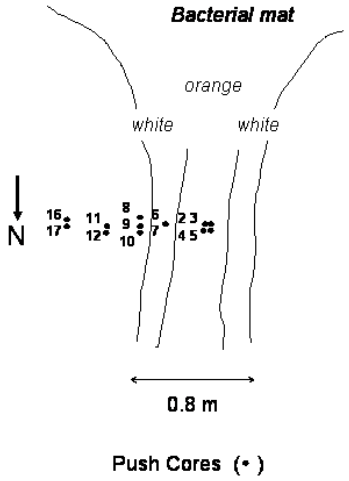


PC 2: Centre of the mat (orange)
PC 6: 30 cm to the east of the mat centre in white rim
PC 8: 60 cm to the east of the mat centre in soft sediment
PC 11: 90 cm to the east of the mat centre in soft sediment
PC 13: 120 cm to the east of the mat centre in soft sediment

Surprisingly, the minimum in dissolved chloride was found below soft sediments 1 m away from the mat' centre in the transect taken during Dive 72 (Fig. 2.9). The distribution of alkalinity and sulphide show, however, that AOM rates were highest below the mat's centre where the ammonia concentrations also reached a maximum. Dissolved phosphate was again depleted below the mat and enriched in the surrounding background sediments. The distribution of chloride and sulphate in surface sediments suggests that bottom waters penetrate the upper few centimetres of the soft sediments in the immediate surrounding of the mat.

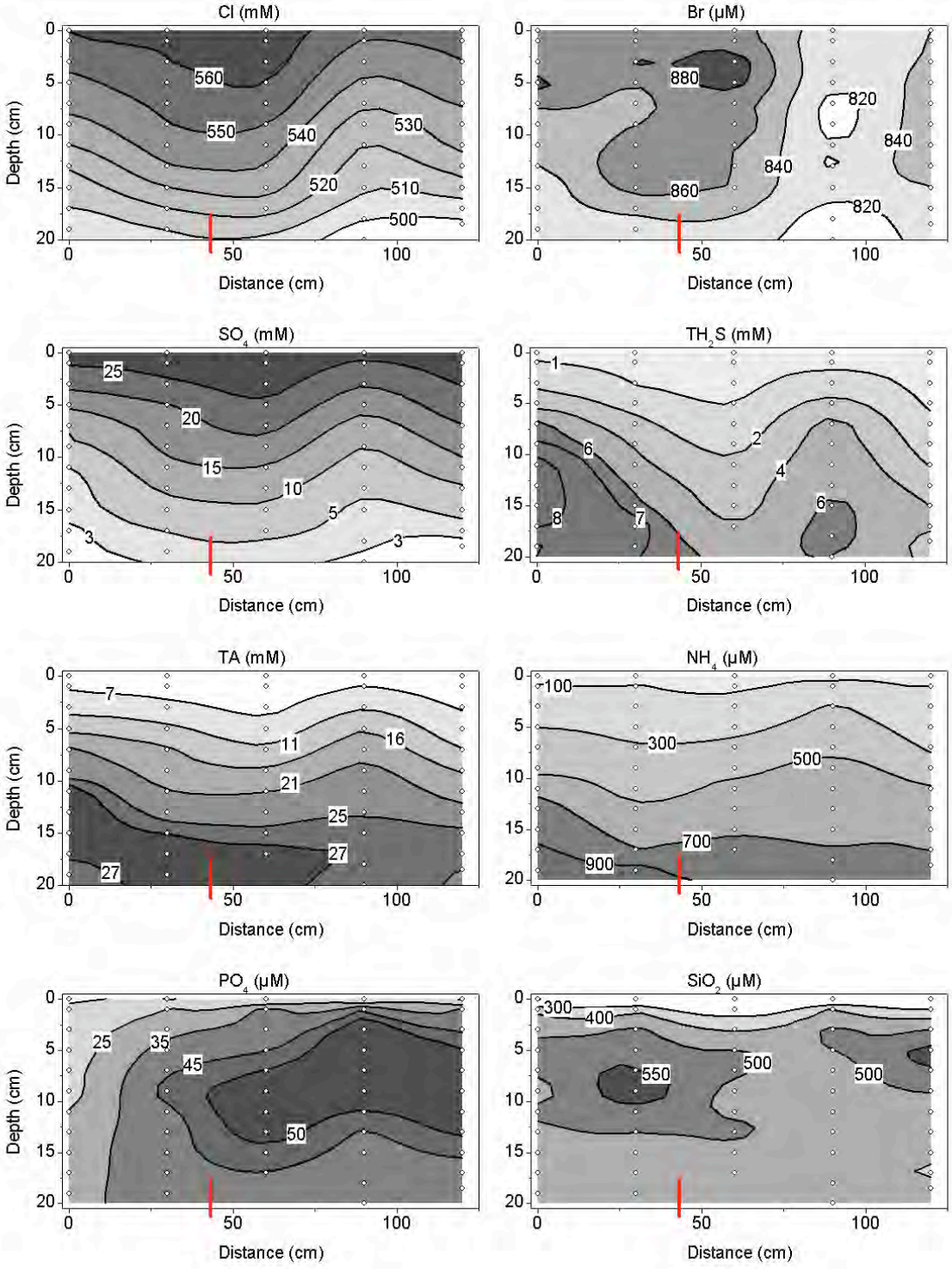


**FIG. 2.9:** Transect through a bacterial mat on Quepos Slide (ROV Dive 72). The x-axis gives the distance to the centre of the mat. Open dots mark the positions were push core samples have been taken and analyzed. The vertical bar cutting the x-axis indicates the outer boundary of the mat.

During Dive 76, a large patch of black sediment covered with a thin greyish bacterial mat was observed at the inclined flank of an extended ridge. The patch was at least 20 m long and 10 m wide. The upper two centimetre of the surface sediments recovered from this patch were cemented by a black mineral while the underlying sediments were soft and greyish. The patch

was surrounded by an inner orange rim and an outer white rim both being 30 cm wide. The colouring was caused by thick layers of orange and white bacterial mats. The cores were taken in an east – west transect starting within the black sediments:

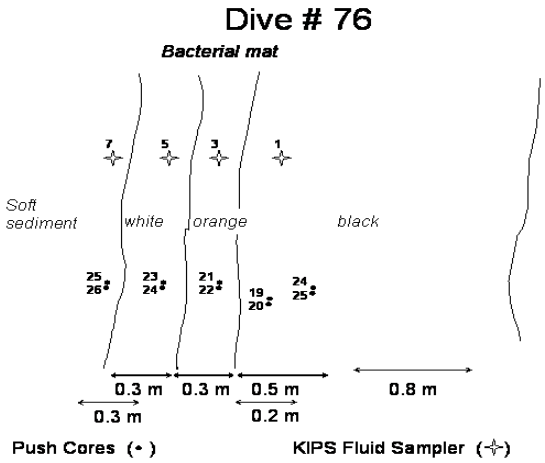


PC 17: In black patch 50 cm to the east of the inner orange rim
PC 19: In black patch 20 cm to the east of the inner orange rim
PC 21: In the centre of the inner orange rim
PC 23: In the centre of the outer white rim
PC 25: In soft sediment, 30 cm to the west of the white rim's centre

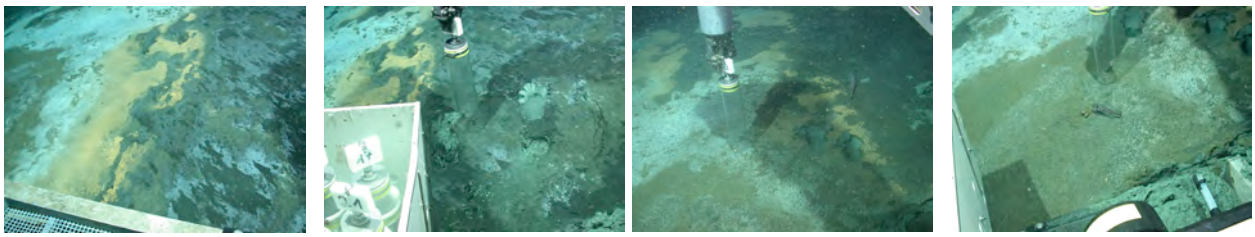

**FIG. 2.10:** Locations of the sampling positions for the sediment section recovered during Dive 76. (a): setting with the black patch to the left, (b) sampling close to the rim, (c) prior to sampling in the orange rim, and (d) samling west of white rim.

The lowest chloride concentrations and steepest chloride gradients during the entire sampling program at Quepos slide were found below the dark coloured sediments sampled during Dive 76 (Figs. 2.10a, 2.11). The black surface sediments were covered with a thin and greyish mat and were cemented by a dark-coloured authigenic mineral of unknown composition, while the underlying sediments were soft and attained a greyish colour. The nutrient contents of the chloride-depleted fluids ascending to the surface were much lower than at the other mat sites. AOM rates were low below the black sediments and high below the orange and white rim indicating an astonishing degree of decoupling between fluid flow and AOM.

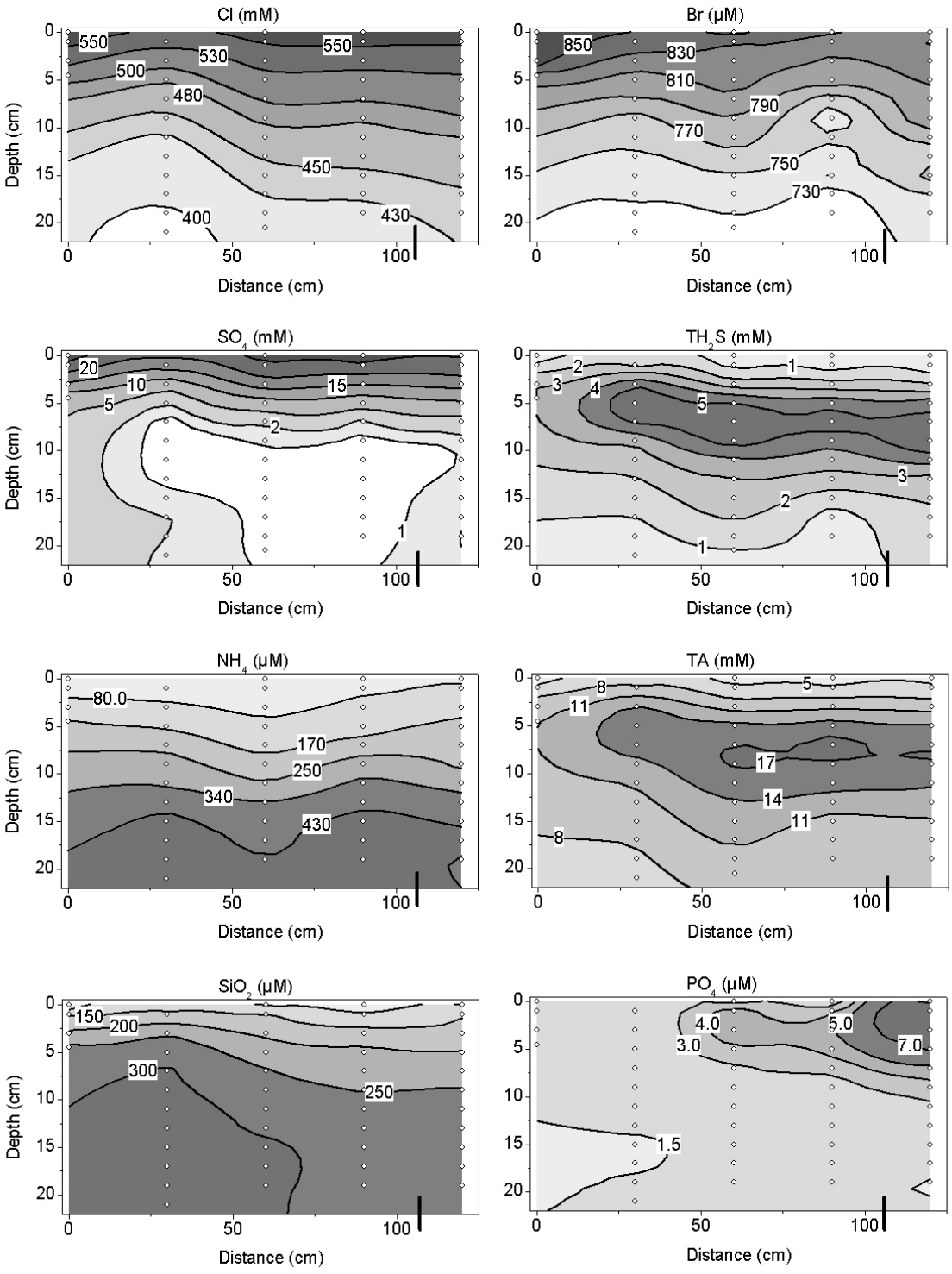


**FIG. 2.11:** Transect through a bacterial mat on Quepos Slide (ROV Dive 76). The x-axis gives the distance to the core taken within the most inner part of the mat. Open dots mark the positions were push core samples have been taken and analyzed. The vertical bar cutting the x-axis indicates the outer boundary of the mat.

### 2.4.3 Methane Oxidation Rates, Sulphate Reduction Rates, and Sampling for Microbiological Investigations

In ocean sediments, up to 80% of methane is consumed before reaching the water column (Reeburgh, 1996). The oxidation of methane under aerobic conditions by methanotrophic bacteria can hardly account as the major methane sink because the majority of methane is consumed under anoxic conditions. Although thermodynamically unfavourable, anaerobic oxidation of methane (AOM) with sulphate as the terminal electron acceptor is performed by a microbial consortium of sulphate reducing bacteria and methane oxidizing archaea (Boetius *et al.*, 2000; Elvert *et al.*, 2001; Hinrichs *et al.*, 1999; Orphan *et al.*, 2001). So far, three uncultivated archaeal lineages (ANME-1, ANME-2 and ANME-3), which are related to the *Methanosarcinales*, are known to mediate AOM (Boetius *et al.*, 2000; Michaelis *et al.*, 2002; Niemann and Lösekann unpubl.). The end products of AOM $CO_2$ and $H_2S$ may be sequestered in carbonates or consumed by thiotrophic organisms, respectively. The thiotrophs may consist of giant bacteria such as *Beggiatoa* and *Thioploca* or megafauna organisms such as pogonophoran worms and certain bivalves such as *Calyptogena* and *Bathymodiolus*. These megafauna species harbour symbiotic, thiotrophic bacteria, which profit from the motility of the host. Free-living thiotrophs are commonly found in mat-like aggregates covering sediments with comparably high sulphide concentrations where the hot spot of AOM is located just some centimetres below sea floor. Often, the metabolic activity of these bacteria, which use nitrate and/or oxygen as the terminal electron acceptor, leads to a total consumption of sulphide and thus to steep sulphide gradients. In contrast, megafauna with symbiotic thiotrophs are usually found where sulphide concentrations are lower (Sahling *et al.*, 2002). The high concentrations of sulphide found below the microbial mats are probably too toxic for these organisms. On a final level in these geo-eco-systems, megafauna species such as crabs and some fish appear to feed on the mat systems and perhaps on AOM biomass.

Well-constrained estimates of the magnitude of methane oxidation and sulphate reduction, as well as oxygen consumption are of particular importance to assess the biogeochemical dynamics in the different habitats of a given seep system. Furthermore, the identity of seep associated organisms and their potential for certain metabolic pathways, as well as the importance of seep-derived biomass in the food web are preliminary for the seep systems at the Costa Rican subduction zone.

The goals of this work were to assess turnover rates of methane and sulphate and to identify participating, free living and symbiotic microorganisms as well as to point out major microbial, metabolic pathways.

Sediment samples from Push Cores (PC) were incubated for microbially mediated methane oxidation and sulphate reduction rates as well as benthic oxygen consumption and sampled for cultivation experiments, FISH, DNA, biomarker and QPCR analysis. Several seep-related mega fauna species were collected and prepared for identification studies of microbial symbionts.

The majority of samples taken during cruise M66-2b were preserved for subsequent biological and/or chemical analysis in the home laboratory.

A total of ca. 400 AOM as well as SR rate samples were taken in triplicates during cruise M66-2. The target of push coring was to cover the range of putatively methane seeping spots such as bacterial mats and sites populated by seep megafauna species. Each sediment interval was also sampled for FISH, DNA and RNA analysis for estimations of microbial abundance,

community structure and expression of specific genes. In addition to sediment samples, seep megafauna species were preserved for subsequent analysis of symbiotic microorganisms. Several KIPS samples taken just above bacterial mats were analysed for methane turnover mediated by aerobic methanotrophic bacteria. Aerobic methane oxidation rates (MOx) were ranging between 0.08 and 4.5 pmol $l^{-1}$ $d^{-1}$.

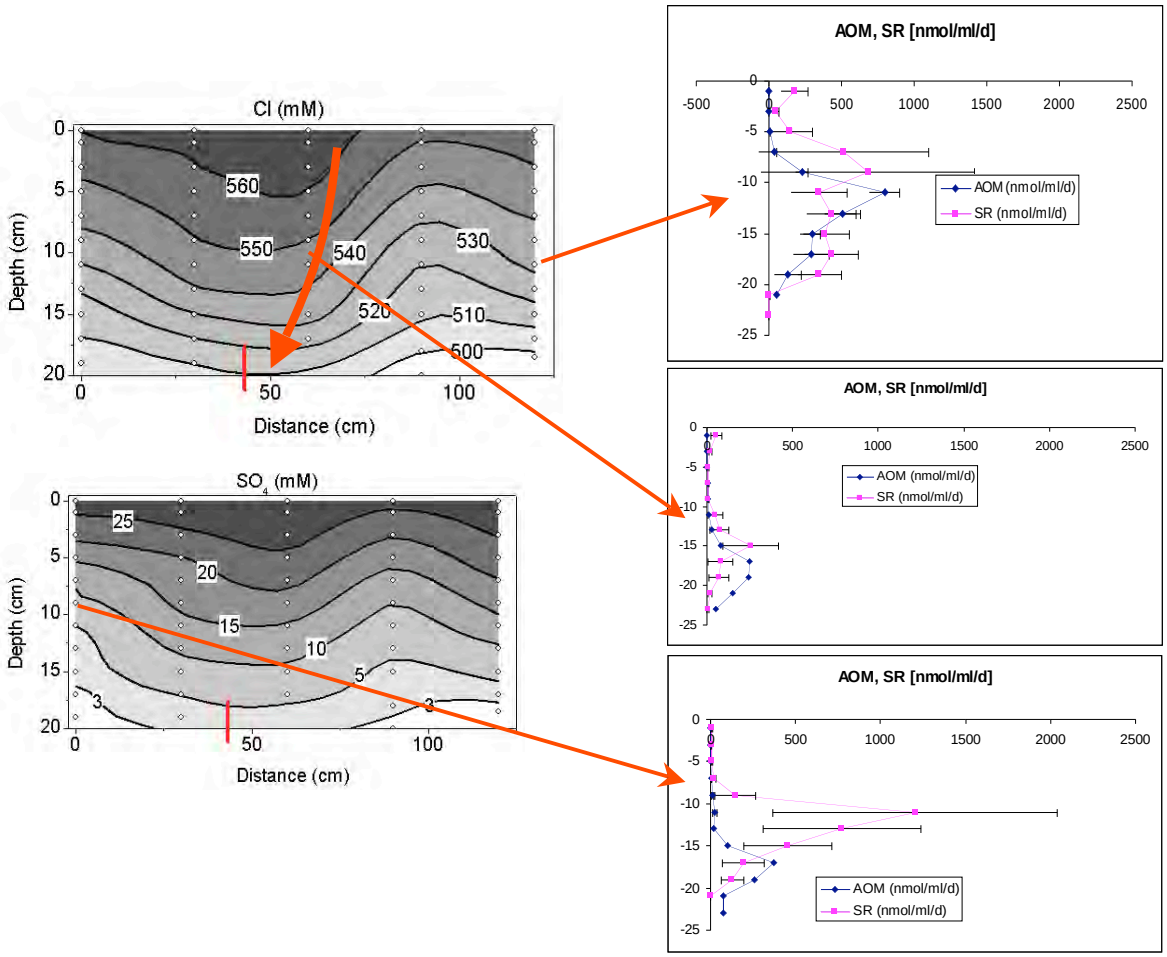


**FIG. 2.12:** AOM/SR results from a sedimentary section across a bacterial mat (for details see Figure 2.8 and referring text). The deeper layer of maximum SR/AOM is consistent with a penetration of seawater into the sediment close to the rim of the bacterial mat.

AOM and SR rates were measured on cores taken in immediate proximity to the cores taken for geochemical analysis. As an example, the data analysed for the sediment transect sampled at Quepos slide during Dive 72 is shown (Fig. 2.12), together with the chloride and sulphate results from the geochemical data. The results support the interpretation of the penetration of bottom water into the sediment close to the rim of the bacterial mat, in accordance to deeper horizon of the AOM/SR zone.

Previous oxygen consumption measurements on cruises of the SFB 574, indicated a potential oxygen net production in sediments of Quepos slide. One dive (Dive 75) was therefore dedicated for verification or falsification of the previous production measurements. A benthic chamber equipped with an optode was placed on several locations (orange *Beggiatoa*, white *Beggiatoa*, a close background and a far background). The sensor measured a slight oxygen production from roughly 2 nM to 2.3 nM (data not shown). However, because the oxygen sensor was not cross

calibrated against sea water solutes other than oxygen and the overall concentration change was very low and close to the detection limit, we could neither verify nor falsify the previous results. Furthermore, *ex situ* oxygen consumption measurements performed in hole push cores, did not show concentration changes which can be interpreted as a net oxygen production (data not shown).

### 2.4.4 Trace Elements

The chemical composition of fluids sampled during leg M 66/2b - pore water, seeping fluid above bacterial mats, bottom seawater – is the result of variable mixtures of fluid components from different sources and origins, e.g.,: (i) low-salinity/ high alkalinity fluids from deep sources, rich in sulfide and methane assumed to represent ascending fluids formed by heating of the sediments and basalt of the subducted slab; (ii) fresh water from *in-situ* gas hydrate destabilization, (iii) a local fluid source essentially pore water that interacted with local sediment; (iv) normal seawater. The distribution of selected trace elements is characteristic for the different fluid components and can be used for the identification and discrimination of the fluid components and their sources. Another aspect is the identification and quantification of one or more tracer elements in the bottom-near water column above active seeps which can be used as a (conservative) fluid tracer for mass balance calculations.

Fluid sampling during leg M 66/2b focused on evolved carbonate mounds (Mound Iguana, Mound Culebra, Parrita Mud Pie), sites with abundant bacterial mats (Mounds #11, #12), and large slides (Quepos Slide, Jaco Scarp) where active seeping of fluids is manifested by abundant bacterial mats and rich vent communities. Large methane anomalies were observed in the bottom water and overlying water column. By now, deeply sourced fluids characterized by e.g., low chlorinity, high alkalinity and sulphide concentrations could be proven at almost all sampled active sites.

The ROV Quest with the tools push corer and *in situ*-fluid sampler (KIPS) enabled us to sample fluid transects across bacterial mats with cm resolution allowing previously unknown spatial resolution of the hydrodynamic fluid regime. Redox processes occurring along gradients between anoxic, deep-sourced fluids and normal seawater overprint the original chemistry of the rising fluid, and the characterization and understanding of these processes will be one aspect of our study.

Results from previous cruises indicate that there exist systematic differences in the trace element chemistry of fluids from the northern area off Nicaragua above the subducted smooth surface plate segment when compared to fluids from the southern area off Costa Rica with seamounts and a rough surface of the subducting plate. One of the major aims for this campaign is to prove our hypothesis that the observed differences in fluid chemistry are a function of the local subduction mechanism.

Fluid samples were obtained by means of (i) pressing pore water (PW) from sediments obtained with ROV operated push corers, or from benthic chambers of landers (BCL), (ii) the ROV operated *in situ*-fluid sampler (KIPS) or the pressurized fluid sampler (PFS, autoclave sampler) sampling seeping fluids 1-3 cm above bacterial mats or from within pogonophera bushes (fluid); (iii) lander-operated bottom water sampler (BSS). In addition, (iv) time-series samples (INC) were taken from incubation experiments with ROV-handled benthic chambers (BCS) or with autonomous lander (BCL).

A total of 631 samples (pore water, fluids, bottom seawater, incubations) was taken. After return to the home labs in Kiel a selection of samples will be analysed for trace element composition (e.g., I, Br, B, Li, Al, Ti, Cs, Ba, Sr, Y-REE, Fe, Mn, Cr, V, Cu, Co, Ni, Pb, U, Mo, As, Sb, W) by ICP-mass spectrometry using both collision-cell quadrupole, and high resolution sector-field based instrumentation.

### 2.4.5 Investigations Based on Lander and Video-Guided Equipment

Numerous deployments of video- and ROV-guided instruments were conducted during cruise M66/2b (Tab. 2.1).

**TAB. 2.1:** List of video- and ROV-guided instruments deployed and recovered during M66/2. OFOS: Ocean Floor Observation System; DOS: Deep-Sea Observation System; BCL: Benthic Chamber Lander; BCS Benthic Chamber Shuttle; BWS: Bottom Water Sampler; PFS:Pressure-retaining fluid sampler; ELINOR: Benthic flux chamber.

| Instrument / Working area | OFOS | DOS #deploy./#recov. | BCL deploy./#recov. | BCS #deploy./#recov. | BWS | PFS | ELINOR |
|---|---|---|---|---|---|---|---|
| **Mt. Iguana** | | St. 43-2/52:<br>Data/pictures retrieved | | St. 44-2 & Dive 66/ St. 46:<br>Chambers fell over, no samples | | Dive 64 | |
| **Mt. Quetzal** | St. 48 | | | | | | |
| **Parrita scarp** | St. 59 | | | | | | |
| **Mound 12** | | St. 55:<br>Failure due to release malfunction<br>St. 110/198<br>Deployed until 3rd leg<br>Data/pictures retrieved | St. 61:<br>Failure due to release malfunction | St. 63-1 & Dive 70 / St. 63-2:<br>2 chambers successfully deployed<br>1 chamber<br>2 water samplers | St. 57:<br>16 water samples | | |
| **Quepos slide** | | St. 70/86:<br>Data/pictures retrieved | St. 72/77<br>1 chamber<br>1 water sampler<br>St. 80-2/83<br>2 chambers<br>2 water samplers<br>St. 98/101<br>2 chambers<br>2 water samplers | | St. 94:<br>16 water samples<br>St. 96:<br>16 water samples | | Dive 72:<br>3 depl.<br><br>Dive 75:<br>6 depl.<br><br>Dive 76:<br>2 profiles,<br>3 depl. |
| **Jaco scarp** | St. 75 | St. 90/103:<br>Data/pictures retrieved | | | | Dive 74 | |
| **Mound Culebra** | | | | | | Dive 77 | Dive 77:<br>2 depl. |
| **Mud Pie** | St. 104 | | | | | Dive 78 | Dive 78:<br>2 depl. |

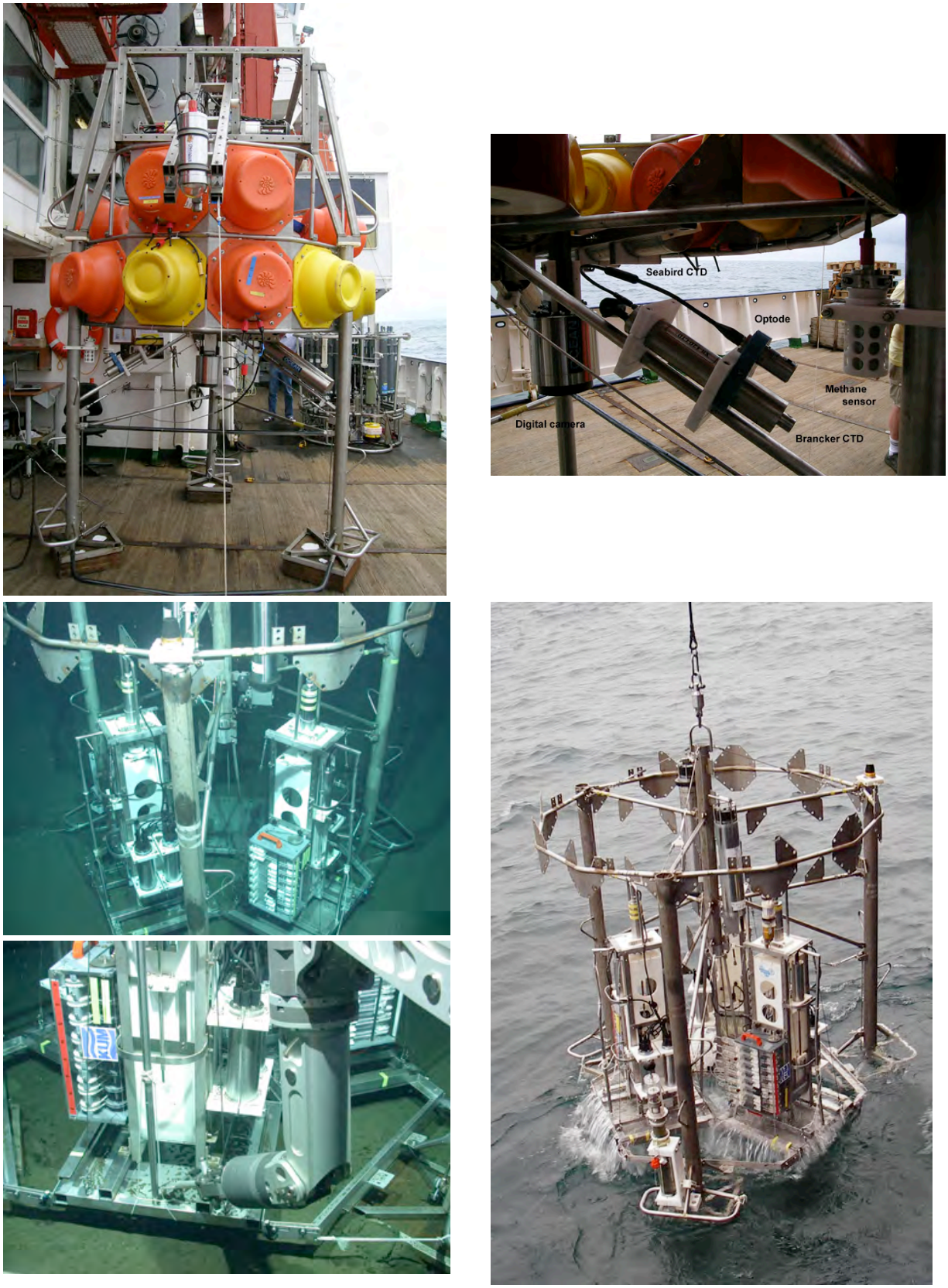


**FIG. 2.13:** DOS-Lander and Benthic Chamber Shuttle, which were deployed during M66/2. Upper left: DOS-Lander ready for video-guided deployment. Upper right: Sensor packages in the lower part of the lander. Not visible are the 3 ADCPs mounted on the back and inside of the lander. Lower frames: Benthic chamber shuttle during recovery (right), at the seafloor, and immediately before individual positioning of one of the chambers by the ROV

In the following, some of the results of the benthic chamber lander (BCL) are shown. The instrument was successfully deployed at three different bacterial mat sites in the Quepos Slide area. Both, water samples from the enclosed bottom water and the underlying incubated sediments were retrieved by the BCL. The former are shown here for the deployment at station 77 (Fig. 2.14), while the latter is shown for all three deployments in composite graphs (Fig. 2.15).

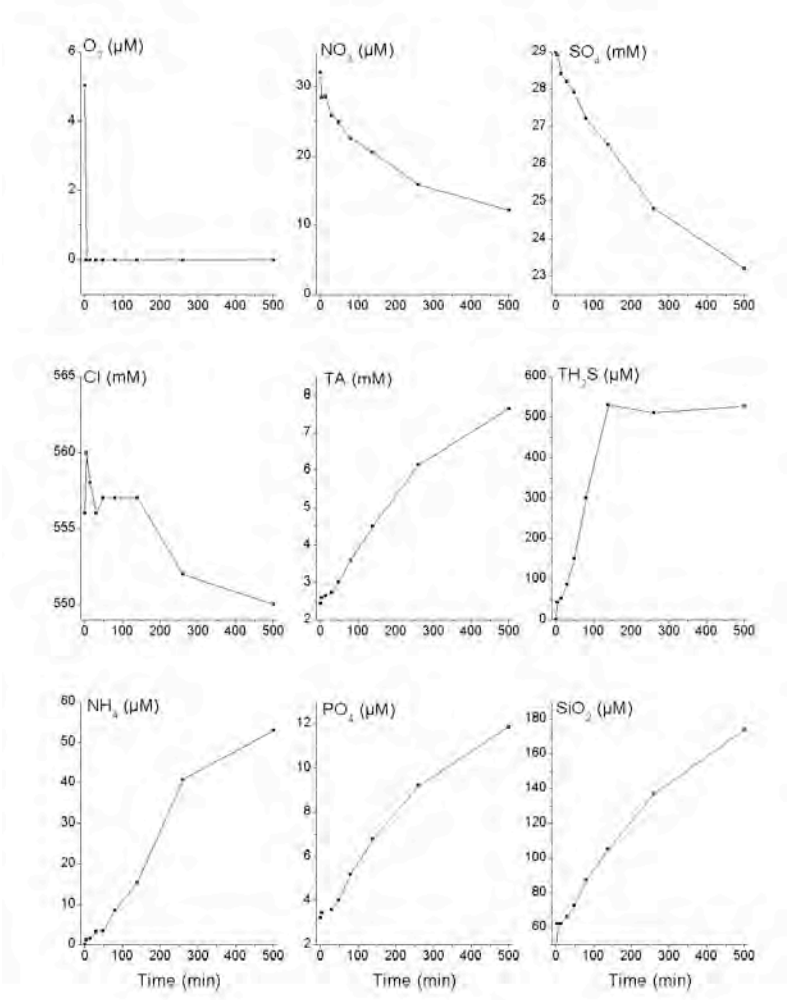


**FIG. 2.14:** Change in bottom water concentrations of various chemical species during the deployment of a benthic chamber on a bacterial mat at Quepos Slide (St. 77). Concentrations at time zero are taken from KIPS samples.

During the first deployment (St. 77) dissolved oxygen was already depleted after 5 minutes incubation time (Fig. 2.14). Nitrate, sulphate, and chloride concentrations decreased rapidly over time while the concentrations of nutrients and AOM metabolites increased during the incubation. The decrease in dissolved chloride can be used to calculate the fluid outflow velocity into the chamber. The chamber penetrated deeply into the sediments so that the volume of enclosed bottom water was as small as 0.4 $dm^3$. Hence, the products of AOM and the fluids were accumulated rapidly in the chamber water.

.

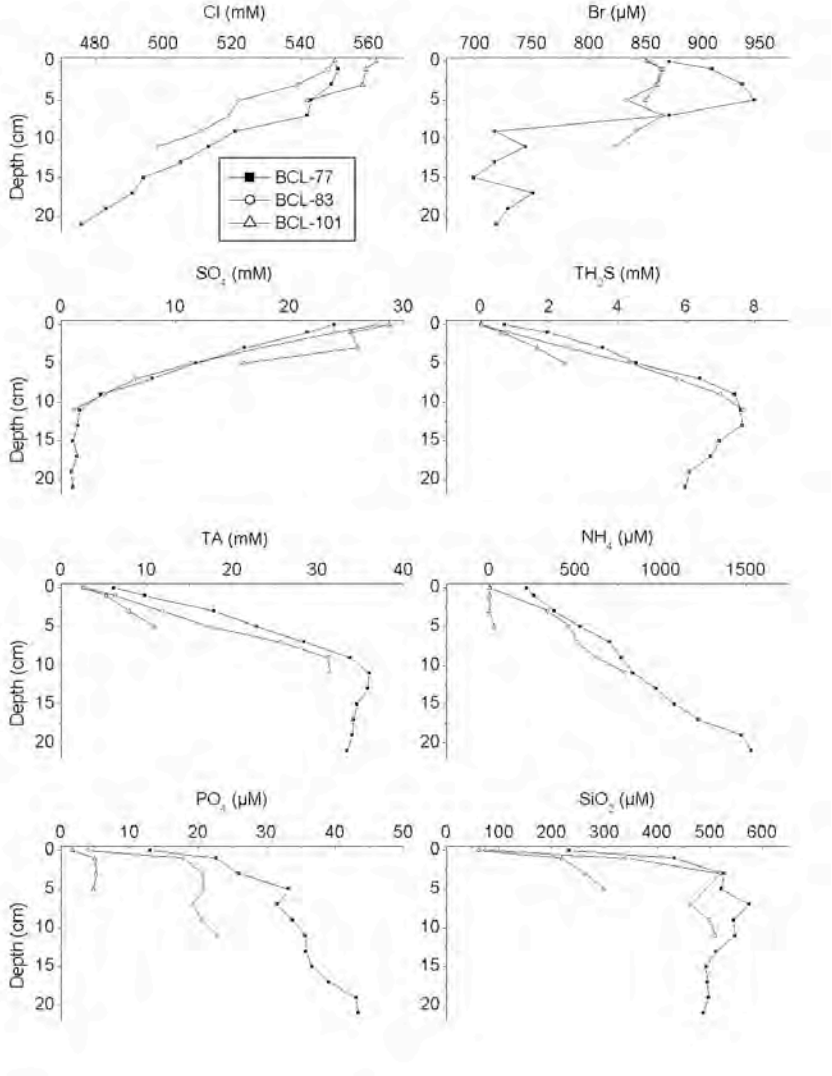


**FIG. 2.15:** Composition of pore fluids in sediments retrieved by the BCL after in-situ incubation. Sediments were taken from chamber one at each station located in the Quepos Slide

The third deployment (St. 101) showed the smallest rates of nitrate and oxygen consumption and nutrient release (Data not shown). The underlying sediments were less reactive than the sediments retrieved during the two previous deployments (Fig. 2.15). The low fluxes recorded at station 101 may thus reflect lower rates of AOM and fluid ascent in the incubated sediments.

### 2.4.6 Water Column Work and Methane Distribution

The investigation of methane in the water column provides valuable insight in the processes of dewatering at active continental margins, because methane belongs to the cycled key components. Methane injection into the water column is just one process of the carbon cycle at active seep sites. Due to its generally low background in deep water this injected methane is ideally suited to locate currently active vent sites and the dimensions of the generated methane plumes. Methane concentration in the water column and investigations of its isotopic composition yield information about its escape from the sediments, its inventory, and further development in the water column. It proves particular helpful at sites where sedimentary work is difficult because of steep morphology (i.e. scarps) or because of authigenic mineral formation hampering coring. During M66/2b, the two most important research targets of the water column methane survey were (a) the revisited sampling of stations at which interannual variability has

been observed during earlier surveys (Mau et al., 2007), and a detailed mapping of the methane inventory at Quepos slide, with the aim of quantifying the excess methane due to seepage at this morphological structure. Several deployments in order to get a first hint at methane seepage were also performed, but data are not shown here.

*(a) Repeated stations*

*Mound 12:* To investigate the inter-annual variability of seep venting over time, three CTD casts were taken at positions matching stations 99, 150 and 169 of cruise M54 (Fig. 2.16) at Md 12, which has been extensively investigated during M54 an SO 173. Highest values were found near the bottom of station 78 which corresponds to station 150 of M54 with methane concentration reaching more than 25 nmol/l (100nmol/L during M54). There is a sharp decline towards lower water depths interrupted by a positive anomaly at a water depth of 790m. This might result from a second source further up the continental slope. Station 62 (station 169 of M54) revealed values of up to 9nmol/l in the first 30m above the seafloor and a second enrichment in the upper water column ranging between 2 and 5nmol/l. This matches well with measurements during M54. A nearly homogenous profile was sampled at station 54 (station 96 of M54), with 4nmol/L and a depletion to 2nmol/l in a water depth between 750 and 800m. All profiles show an enrichment of 4 to 5nmol/l in water depths around 400m as a result of production of methane in the well-pronounced oxygen minimum zone.

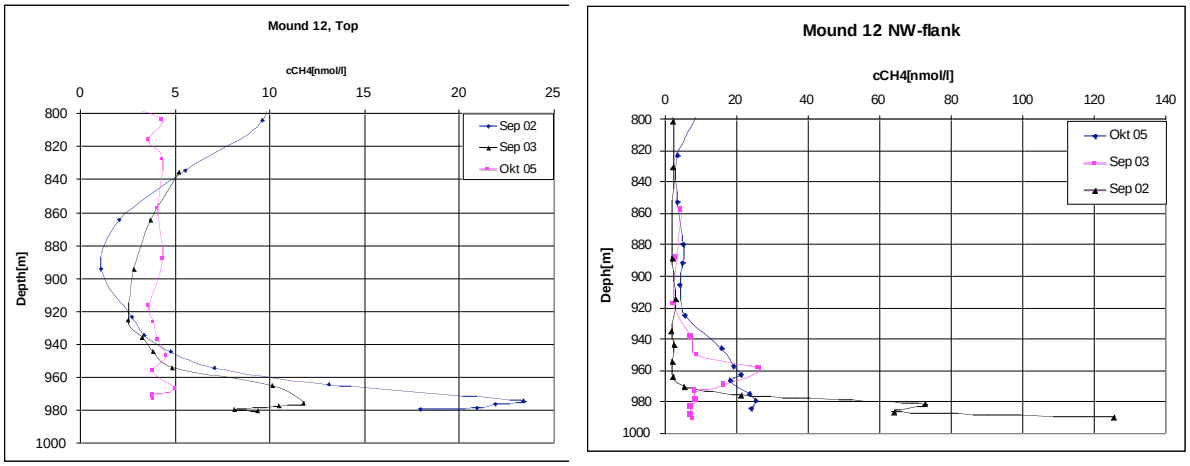


**FIG. 2.16:** Methane concentrations at stations repeatedly sampled over several years at Mound 12.

*Jaco Scarp:* This scarp was extensively sampled with a CTD program during SO 163 and M54. The aim of the reinvestigation during SO173 was to determine the time variability of two sites. One is situated at the edge of the slide, the other at the SE rim. Methane concentrations changed within a year, but the plumes were observed within the same depths. During M66, these two sites were revisited to expand the time series (station 89 and 93) (Fig. 2.17). The profiles show a maximum in 1800m with a concentration of 140nmol/l (station 89) and 25nmol/l (station 93).

An intense temporal variability is observable with concentrations varying between 280 nmol/l in April 2002 and 100 nmol/l in September 2003 within 3 years at Station 89. The values at station 93 show a strong decrease of methane content from 100nmol/l in August 2002, 70nmol/l in September 2003 to 25nmol/l in October 2005. Further investigations are required to get more information about the time scale for the changing methane inventory at these locations and their causes.

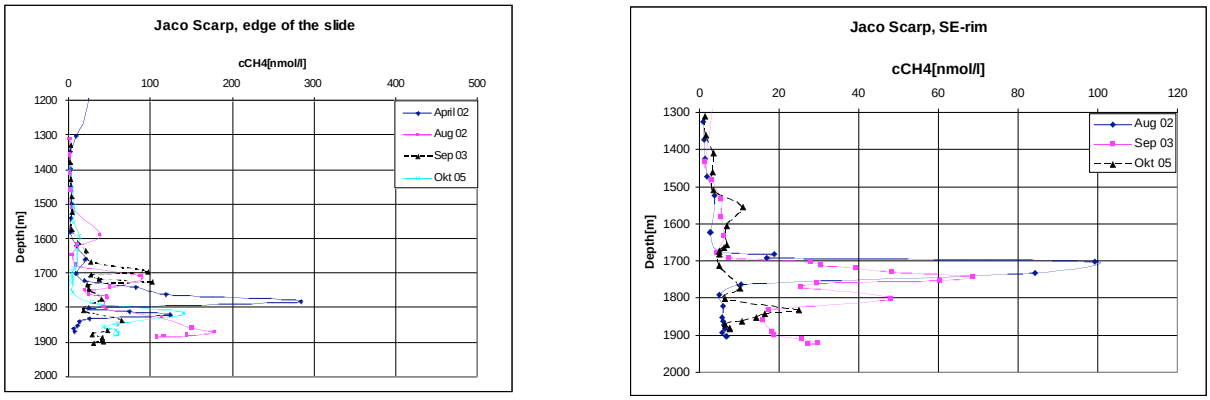


**FIG. 2.17:** Methane concentrations at stations repeatedly sampled over several years at Jaco Scarp.

*Mound Culebra:* Two sites were revisited during M66 at the same positions as during SO163, SO173 and M54 at the top and the NW-flank of the mound (Fig. 2.18) to extend the investigation of temporal variability at this site. Slightly enriched methane concentrations of 3nmol were found at station 105 close to the bottom at the north western flank. Maximum values with 7nmol/l were measured 100m above the seafloor. During cruise SO173, no increased methane concentration had been measured, in contrast to 16nmol/l in May and 45nmol/l in August 2002. Station 106 indicates a bottom source at the summit with values up to 6nmol/l. A second increase of methane concentrations was observed at 1370mbsl with values up to 5nmol/l. The latter finding indicates a second source on the higher slope not detected before. In comparison to May and August 2002, the concentrations near the bottom seem to be reduced, but increased with respect to September 2003. Mound Culebra shows distinct temporal variability. The interannual changes of the methane emission at the active vent systems off Costa Rica have been attributed to seismological activity (Mau et al., 2007).

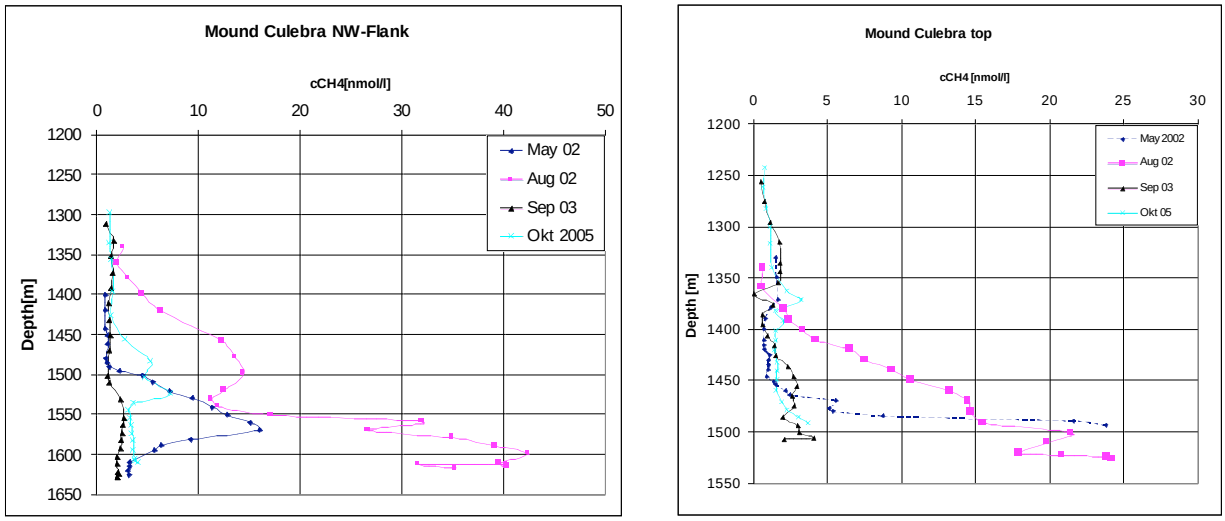


**FIG. 2.18:** Methane concentrations at stations repeatedly sampled over several years at Mound Culebra.

*(b) Methane survey of the water column above Quepos Landslide*

Quepos slide was the main working area of the CTD sampling program during M66. 17 CTD casts starting from 5m to 100m above the sea floor yielded a so far not comparable resolution of the methane plume identified during previous cruises (for locations in detail, see Fig.2.4). The survey was done laying three transects of 3-4 stations around the headwall to cover an area inside the slide structure on the slide mass. Seven stations were added later to complete a sample grid on the research area. The investigations were completed by a DOS-Lander deployment to assess information on current speed and directions. Highest values (250nmol/l) were measured close to the bottom at the most northern station (station 67). The analysis reveals a continuous decrease of methane concentrations from the northern rim of the slide to the southeast and southwest (Fig. 2.19). All stations reveal two distinct maxima in 360 and 370m depth. In all profiles methane concentrations decrease to background values of 1 to 3 nmol/l in water depths less than 300m. All profiles show a sharp decline of methane concentrations in water depths between 330 and 350 m.

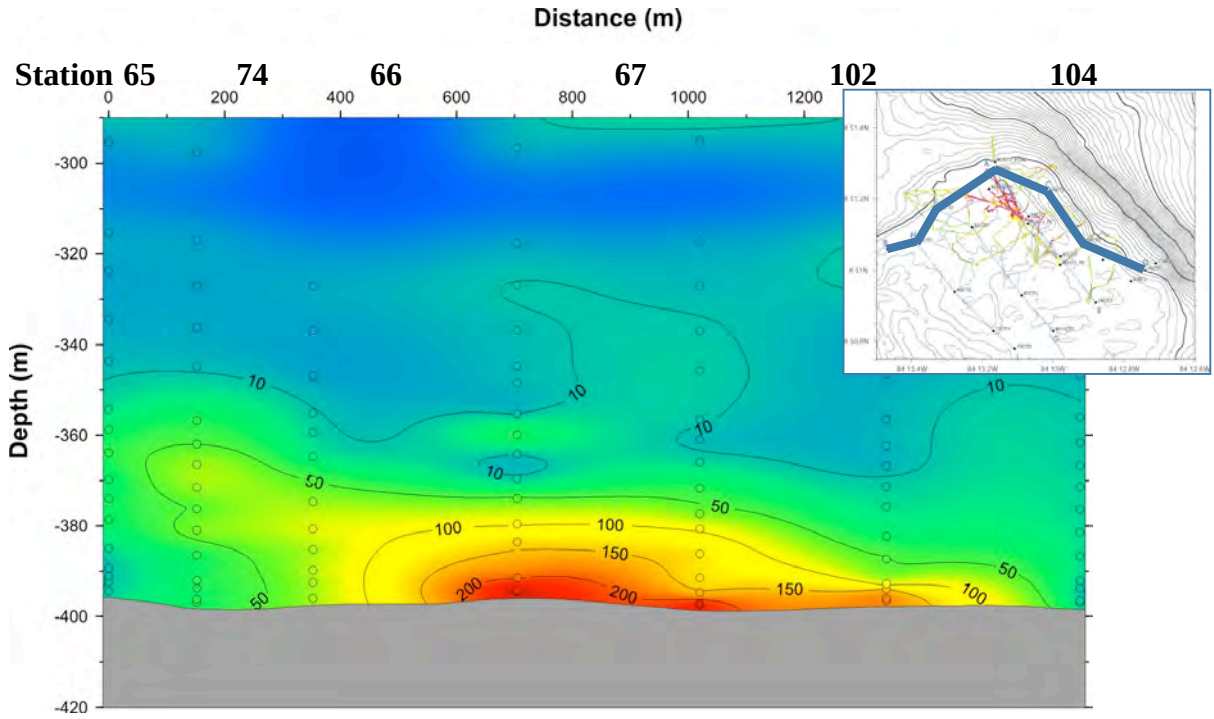


**Fig. 2.19:** Methane section along the headwall of Quepos Slide. All stations at approximately 400 m water depth.

## 2.5 Ship's Meteorological Station

While several hurricanes and tropical storms occurred over the Caribbean and the Gulf of Mexico during the cruise, some of them with devasting consequences like the hurricane Rita, which hit New Orleans on September 22nd and 23rd, the scientific work during M66/2-ab was nearly unaffected by the weather conditions during the cruise. The only exception was the 2nd of October, where the first ROV Dive of Leg 66/2b had to be postponed for 24 h because of the swell caused by the tropical storm "Stan", at that time centred over the Gulf of Campeche. The

work close to or within the ITCZ frequently led to strong rainfall within the working area, which however did not affect the scientific program of the cruise.

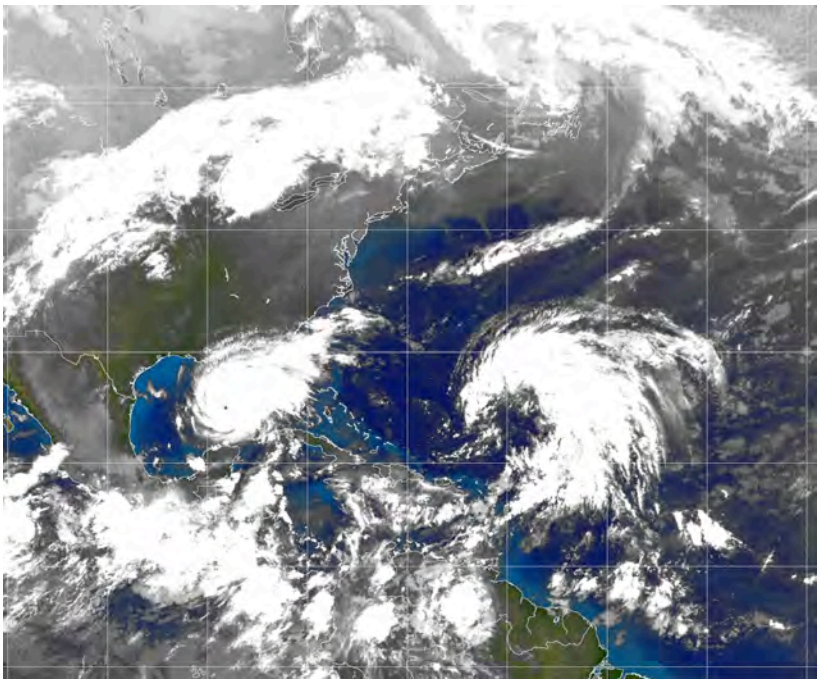

**FIG. 2.20:** Satellite image of the first day of M66/2a showing hurricane “Rita” close to the coast of New Orleans

## 2.6 List of Stations

**Meteor 66** — **Station List**

| Date | St. No. | St. No. | | Time (UTC) | | | | | Begin / on seafloor | | End / off seafloor | | | | | | |
|---|---|---|---|---|---|---|---|---|---|---|---|---|---|---|---|---|---|
| | | | | | Start Sci. | End Sci. | | Duration | Latitude | Longitude | Latitude | Longitude | Water | Recovery | Supervisor | Area | Target |
| 2005 | M66 | Meteor | Instrument | Begin | Program | Program | End | hh:mm | N° | W° | N° | W° | depth (m) | Remarks | | | Feature |
| 23.09.2005 | 1 | 620 | CTD 01 | 06:29 | 06:29 | 07:18 | 07:18 | 00:49 | 13:48.65 | 72:08.40 | 13:48.37 | 72:00.59 | 4041 | | Brentführer | Karibik | Transect |
| 23.09.2005 | 2 | 621 | CTD 02 | 17:37 | 17:37 | 18:30 | 18:30 | 00:52 | 12:49.91 | 73:51.65 | 12:49.91 | 73:51.65 | 3807 | Releaser Test | Brentführer | Karibik | Transect |
| 24.09.2005 | 3 | 622 | CTD 03 | 05:20 | 05:20 | 06:43 | 06:43 | 01:22 | 11:53.02 | 75:41.68 | 11:53.06 | 75:41.63 | 3231 | | Brentführer | Karibik | Transect |
| 24.09.2005 | 4 | 623 | CTD 04 | 17:34 | 17:34 | 18:19 | 18:19 | 00:44 | 10:56.11 | 77:32.85 | 10:56.11 | 77:32.85 | 3266 | | Brentführer | Karibik | Transect |
| 25.09.2005 | 5 | 624 | CTD 05 | 08:21 | 08:33 | 09:18 | 09:18 | 00:57 | 09:59.98 | 07:24.49 | 09:59.98 | 07:24.39 | 2228 | | Brentführer | Karibik | Transect |
| 27.09.2005 | 6-1 | 625-1 | OBS05 | | | 18:20 | | | 08:29.89 | 84:19.51 | | | 2497 | Recovery | Bialas | Quepos | Profil Breitband 2005 |
| 27.09.2005 | 6-2 | 625-2 | OBT07 | | | 18:19 | 18:57 | 00:38 | 8:30.61 | 84:19.37 | 8:30.93 | 84:19.33 | 2572 | Recovery | Bialas | Quepos | Profil Breitband 2005 |
| 27.09.2005 | 7-1 | 626-1 | OBS04 | | | 20:20 | | | 8:38.00 | 84:13.86 | 8:38.25 | 84:13.44 | 1437 | Recovery | Bialas | Quepos | Profil Breitband 2005 |
| 27.09.2005 | 7-2 | 626-2 | OBT06 | | | 20:20 | 20:58 | 00:38 | 8:37.90 | 84:13.61 | | | 1437 | Recovery | Bialas | Quepos | Profil Breitband 2005 |
| 27.09.2005 | 8 | 627 | OBS03 | | | 21:57 | | | 8:45.26 | 84:09.68 | | | 505 | Recovery | Bialas | Quepos | Profil Breitband 2005 |
| 27.09.2005 | 9 | 628 | OBS02 | | | 23:40 | 00:09 | 00:29 | 8:52.34 | 84:03.58 | | | 98 | Recovery | Bialas | Quepos | Profil Breitband 2005 |
| 28.09.2005 | 10 | 629 | OBS01 | | | 00:55 | | | 8:59.93 | 84:00.41 | 8:59.73 | 84:00.28 | 77 | Recovery | Bialas | Quepos | Profil Breitband 2005 |
| 28.09.2005 | 11 | 630 | OBS08 | 03:14 | | | | | 8:55.72 | 84:18.80 | | | 1018 | Deployment | Bialas | Costa Rica | Profil Mounds |
| 28.09.2005 | 12 | 631 | OBS09 | 03:25 | | | | | 08:55.68 | 84:18.90 | | | 1028 | Deployment | Bialas | Costa Rica | Profil Mounds |
| 28.09.2005 | 13 | 632 | OBH24 | 23:33 | | | | | 10:37.42 | 87:28.50 | | | 3292 | Deployment | Bialas | Nicaragua | Outer Rise Net |
| 29.09.2005 | 14 | 633 | OBS29 | 00:36 | | | | | 10:30.93 | 87:34.88 | | | 2913 | Deployment | Bialas | Nicaragua | Outer Rise Net |
| 29.09.2005 | 15 | 634 | OBH32 | 01:57 | | | | | 10:31.03 | 87:47.45 | | | 2996 | Deployment | Bialas | Nicaragua | Outer Rise Net |
| 29.09.2005 | 16 | 635 | OBS28 | 03:30 | | | | | 10:44.10 | 87:47.32 | | | 2967 | Deployment | Bialas | Nicaragua | Outer Rise Net |
| 29.09.2005 | 17 | 636 | OBH27 | 04:27 | | | | | 10:50.67 | 87:53.65 | | | 2980 | Deployment | Bialas | Nicaragua | Outer Rise Net |
| 29.09.2005 | 18 | 637 | OBH31 | 05:29 | | | | | 10:44.22 | 87:59.95 | | | 2894 | Deployment | Bialas | Nicaragua | Outer Rise Net |
| 29.09.2005 | 19 | 638 | OBH33 | 06:28 | | | | | 10:37.76 | 88:06.27 | | | 3020 | Deployment | Bialas | Nicaragua | Outer Rise Net |
| 29.09.2005 | 20 | 639 | OBS30 | 08:27 | | | | | 10:57.32 | 88:12.38 | | | 2820 | Deployment | Bialas | Nicaragua | Outer Rise Net |
| 29.09.2005 | 21 | 640 | OBH25 | 09:49 | | | | | 11:10.37 | 88:22.38 | | | 3440 | Deployment | Bialas | Nicaragua | Outer Rise Net |
| 29.09.2005 | 22 | 641 | OBH20 | 10:49 | | | | | 11:16.87 | 88:05.96 | | | 4170 | Deployment | Bialas | Nicaragua | Outer Rise Net |
| 29.09.2005 | 23 | 642 | OBH10 | 12:36 | | | | | 11:23.24 | 87:46.98 | | | 4840 | Deployment | Bialas | Nicaragua | Outer Rise Net |
| 29.09.2005 | 24 | 643 | OBH11 | 13:33 | | | | | 11:16.67 | 87:40.75 | | | 4984 | Deployment | Bialas | Nicaragua | Outer Rise Net |
| 29.09.2005 | 25 | 644 | OBH17 | 14:56 | | | | | 11:14.65 | 87:50.72 | | | 4863 | Deployment | Bialas | Nicaragua | Outer Rise Net |
| 29.09.2005 | 26 | 645 | OBH21 | 15:59 | | | | | 11:06.95 | 87:56.55 | | | 3771 | Deployment | Bialas | Nicaragua | Outer Rise Net |
| 29.09.2005 | 27 | 646 | OBS26 | 17:01 | | | | | 11:00.47 | 88:02.91 | | | 3160 | Deployment | Bialas | Nicaragua | Outer Rise Net |
| 29.09.2005 | 28-1 | 647-1 | OBS22 | 18:38 | | | | | 10:57.15 | 87:47.20 | | | 3445 | Deployment | Bialas | Nicaragua | Outer Rise Net |
| 29.09.2005 | 28-2 | 647-2 | CTD 06 | 18:53 | 18:58 | | 23:27 | 04:29 | 10:57.20 | 87:47.22 | 10:57.10 | 87:47.24 | 3434 | + Transponder Test | Bialas | Nicaragua | Outer Rise Net |
| 30.09.2005 | 29 | 648 | OBS18 | 00:28 | | | | | 11:03.64 | 87:40.85 | | | 4202 | Deployment | Bialas | Nicaragua | Outer Rise Net |
| 30.09.2005 | 30 | 649 | OBP19 | 00:39 | | | | | 11:03.81 | 87:41.06 | | | 4011 | Deployment | Bialas | Nicaragua | Outer Rise Net |
| 30.09.2005 | 31 | 650 | OBS12 | 01:35 | | | | | 11:10.10 | 87:34.49 | | | 5296 | Deployment | Bialas | Nicaragua | Outer Rise Net |
| 30.09.2005 | 32 | 651 | OBH13 | 02:42 | | | | | 11:03.51 | 87:28.22 | | | 5091 | Deployment | Bialas | Nicaragua | Outer Rise Net |
| 30.09.2005 | 33 | 652 | OBS14 | 03:44 | | | | | 10:56.97 | 87:22.02 | | | 4892 | Deployment | Bialas | Nicaragua | Outer Rise Net |
| 30.09.2005 | 34 | 653 | OBP15 | 03:54 | | | | | 10:57.01 | 87:22.25 | | | 4871 | Deployment | Bialas | Nicaragua | Outer Rise Net |
| 30.09.2005 | 35 | 654 | OBH23 | 05:28 | | | | | 10:49.46 | 87:30.17 | | | 3880 | Deployment | Bialas | Nicaragua | Outer Rise Net |

| | | | | | | | | | | | | | | | | | |
|---|---|---|---|---|---|---|---|---|---|---|---|---|---|---|---|---|---|
| 30.09.2005 | 36 | 655 | OBH16 | 07:10 | | | | | 10:50.41 | 87:15.71 | | | 5077 | Deployment | Bialas | Nicaragua | Outer Rise Net |
| 30.09.2005 | 37 | 656 | ROV 64 | 15:24 | 16:52 | 02:59 | 04:09 | 12:45 | 11:12.25 | 87:09.26 | 11:12.12 | 87:09.19 | 1228 | Dive | Rehder | Mt Iguana | Mound Iguana |
| 30.09.2005 | 38 | 657 | CTD 07 | 04:21 | 04:25 | 05:47 | 05:47 | 01:26 | 11:12.19 | 87:09.25 | 11:12.19 | 87:09.38 | 1231 | CTD-Bottom contact | Brentführer | Mt. Iguana | |
| 02.10.2005 | 39 | 658 | TV-MUC | 23:40 | 00:22 | 05:55 | 06:36 | 06:54 | 11:12.17 | 87:09.30 | 11:12.33 | 87:09.42 | 1249 | no cores | Linke | Mt. Iguana | Bakterial Mat |
| 03.10.2005 | 40 | 659 | Parasound | 07:01 | 07:15 | 11:43 | 11:43 | 04:41 | 11:12.10 | 87:08.90 | 11:12.38 | 87:08.82 | 1173 | no time for the last 3 lines left | Fromm | Mt. Iguana | |
| 03.10.2005 | 41 | 660 | CTD 08 | 12:07 | 12:07 | 13:06 | 13:06 | 00:58 | 11:12.16 | 87:09.21 | 11:12.16 | 87:09.21 | 1221 | Gaps failure, no ADCP | Brentführer | Mt. Iguana | |
| 03.10.2005 | 42 | 661 | ROV 65 | 14:15 | 15:10 | 12:50 | 14:03 | 23:48 | 11:12.16 | 87:09.21 | 11:12.31 | 87:09.18 | 1215 | Dive | Rehder | Mt. Iguana | |
| 04.10.2005 | 43-1 | 662-1 | DOS | 16:25 | 17:17 | 18:26 | 19:20 | 02:01 | 11:12.22 | 87:09.21 | 11:12.27 | 87:09.20 | 1216 | Deployment - Release Failure | Linke | Mt. Iguana | |
| 04.10.2005 | 43-2 | 662-2 | DOS | 20:25 | 21:21 | | 22:00 | 01:35 | 11:12.20 | 87:09.23 | 11:12.30 | 87:09.19 | 1226 | Deployment | Linke | Mt. Iguana | Position |
| 04.10.2005 | 44-1 | 663 | CTD 09 | 22:19 | 22:19 | 23:22 | 23:28 | 01:02 | 11:12.22 | 87:09.15 | 11:12.23 | 87:09.16 | 1215 | | Brentführer | Mt. Iguana | |
| 05.10.2005 | 44-2 | 664 | BCS | 00:00 | | | 01:08 | 01:08 | 11:12.27 | 87:09.20 | 11:12.27 | 87:09.20 | 1221 | Deployment | Linke | Mt. Iguana | |
| 05.10.2005 | 45 | 665 | ROV 66 | 01:40 | 02:50 | 00:12 | 01:24 | 24:04 | 11:12.27 | 87:09.21 | 11:12.11 | 87:09.29 | 1230 | Dive | Rehder | Mt. Iguana | |
| 06.10.2005 | 46 | 666 | BCS | 01:35 | | | 04:15 | 02:40 | 11:12.27 | 87:09.15 | 11:12.33 | 87:08.94 | 1181 | Recovery St.44-2- Release Failure | Linke | Mt. Iguana | |
| 06.10.2005 | 47 | 667 | CTD 10 | 05:07 | 05:09 | 06:10 | 06:15 | 01:08 | 11:12.27 | 87:10.74 | 11:12.23 | 87:10.82 | 1353 | ADCP + GAPS / no gaps | Brentführer | Mt. Quetzal | Bacteria Mat |
| 06.10.2005 | 48 | 668 | OFOS | 06:55 | 08:27 | 14:39 | 15:19 | 08:24 | 11:12.20 | 87:10.83 | 11:12.36 | 87:10.68 | 1368 | | Wallmann | Mt. Quetzal | |
| 06.10.2005 | 49-1 | 669 | TV-MUC | 17:10 | 17:15 | 17:30 | 18:07 | 00:57 | 11:12.29 | 87:09.20 | 11:12.26 | 87:09.29 | 1221 | 4 cores | Linke | Mt. Iguana | |
| 06.10.2005 | 49-2 | 670 | TV-MUC | 18:30 | 19:07 | 19:11 | 20:18 | 01:48 | 11:12.26 | 87:09.31 | 11:12.33 | 87:09.43 | 1256 | hard ground | Linke | Mt. Iguana | |
| 06.10.2005 | 49-3 | 671 | TV-MUC | 20:33 | 21:11 | 21:36 | 22:12 | 01:39 | 11:12.38 | 87:09.44 | 11:12.17 | 87:09.29 | 1225 | | Linke | Mt. Iguana | Bacteria Mat |
| 06.10.2005 | 50 | 672 | CTD 11 | 22:46 | 22:47 | 23:48 | 23:50 | 01:04 | 11:12.40 | 87:10.88 | 11:12.40 | 87:10.88 | 1327 | | Brentführer | Mt. Quetzal | Carbonat Peak |
| 06.10.2005 | 51 | 673 | ROV 67 | 03:33 | 04:23 | 12:20 | 13:19 | 09:46 | 11:12.27 | 87:09.26 | 11:12.22 | 87:09.23 | 1216 | Dive | Rehder | Mt. Iguana | |
| 07.10.2005 | 52 | 674 | DOS | 14:10 | | 14:30 | 14:40 | 00:30 | 11:12.24 | 87:09.22 | 11:12.33 | 87:09.06 | 1202 | Recovery St.43-2 | Linke | Mt. Iguana | |
| 07.10.2005 | 53 | 675 | CTD 12 | 15:13 | 15:13 | 16:13 | 16:13 | 01:00 | 11:12.25 | 87:09.18 | 11:12.27 | 87:09.19 | 1213 | ADCP | Linke | Mt. Iguana | Dos Lander Position |
| 08.10.2005 | 54 | 676 | CTD 13 | 14:02 | 14:02 | 14:51 | 14:51 | 00:49 | 08:55.82 | 84:18.64 | 08:55.70 | 84:18.70 | 1015 | without ADCP | Brentführer | Mt. 12 | |
| 08.10.2005 | 55 | 677 | DOS | 15:50 | 17:30 | 19:55 | 20:30 | 04:40 | 08:55.72 | 84:18.90 | 08:55.96 | 84:18.71 | 1021 | Deployment - release failure | Linke | Mt. 12 | |
| 08.10.2005 | 56 | 678 | CTD 14 | 20:45 | 20:46 | 21:38 | 21:38 | 00:53 | 08:55.98 | 84:18.71 | 08:55.94 | 84:18.71 | 1003 | | Brentführer | Mt. 12 | |
| 08.10.2005 | 57 | 679 | BWS | 23:23 | 00:48 | 00:59 | 01:40 | 02:17 | 08:55.79 | 84:18.85 | 08:55.77 | 84:18.67 | 1007 | 16 watersamples | Linke | Mt. 12 | |
| 09.10.2005 | 58 | 680 | ROV 68 | 01:49 | 02:35 | 14:40 | 15:46 | 13:57 | 08:55.78 | 84:18.66 | 08:55.06 | 84:18.27 | 1051 | Dive | Rehder | Mt. 11,12 | |
| 09.10.2005 | 59 | 681 | OFOS | 18:02 | 18:52 | 22:56 | 00:00 | 05:58 | 08:57.97 | 84:38.37 | 08:56.53 | 84:39.83 | 2058 | | Linke | Parrita | |
| 10.10.2005 | 60 | 682 | ROV 69 | 02:00 | 02:43 | 15:10 | 16:17 | 14:17 | 08:55.74 | 84:18.82 | 08:55.73 | 84:18.61 | 1020 | Dive | R,W,G-S | Mt. 12 | DOMS recovery + sampling |
| 10.10.2005 | 61 | 683 | BCL | 17:45 | 18:26 | 19:30 | 20:11 | 02:26 | 08:55.59 | 84:18.88 | 08:55.53 | 84:18.92 | 1030 | Deployment - release failure | Linke | Mt. 12 | |
| 11.10.2005 | 62 | 684 | CTD 15 | 20:40 | 20:40 | 21:53 | 21:53 | 01:13 | 08:55.76 | 84:18.82 | 08:55.78 | 84:18.84 | 1012 | | Brentführer | Mt. 12 | Bakterial Mat |
| 11.10.2005 | 63-1 | 685 | BCS | 23:16 | | | 23:30 | 00:14 | 08:55.67 | 84:18.82 | 08:55.66 | 84:18.83 | 1021 | Deployment | Linke | Mt. 12 | |
| 11.10.2005 | 64 | 686 | ROV 70 | 00:00 | 00:59 | 18:40 | 19:32 | 19:32 | 08:55.66 | 84:18.79 | 08:55.61 | 84:18.92 | 1022 | Dive | Rehder | Mt. 12 | |
| 11.10.2005 | 63-2 | 687 | BCS | 19:37 | | | 21:50 | 02:13 | 08:55.60 | 84:19.02 | 08:54.71 | 84:18.11 | 1022 | Recovery St.63-1 | Linke | Mt. 12 | |
| 11.10.2005 | 65 | 688 | CTD 16 | 22:43 | 22:45 | 23:14 | 23:14 | 00:31 | 08:51.06 | 84:13.47 | 08:51.08 | 84:13.47 | 404 | no ADCP | Brentführer | Quepos Slide | |
| 12.10.2005 | 66 | 689 | CTD 17 | 00:20 | 00:24 | 00:50 | 00:50 | 00:30 | 08:51.17 | 84:13.33 | 08:51.18 | 84:13.34 | 460 | no ADCP | Brentführer | Quepos Slide | |
| 12.10.2005 | 67 | 690 | CTD 18 | 01:58 | 02:02 | 02:28 | 02:28 | 00:30 | 08:51.28 | 84:13.17 | 08:51.29 | 84:13.16 | 396 | no ADCP | Brentführer | Quepos Slide | |
| 12.10.2005 | 68 | 691 | ROV 71 | 02:47 | 03:11 | 15:08 | 15:42 | 12:55 | 08:51.04 | 84:13.10 | 08:51.00 | 84:12.89 | 400 | | R,W,G-S | Quepos Slide | Mapping + Sampling |
| 12.10.2005 | 69 | 692 | CTD 19 | 16:12 | 16:13 | 16:40 | 16:40 | 00:28 | 08:50.94 | 84:13.28 | 08:50.96 | 84:13.31 | 409 | | Brentführer | Quepos Slide | |
| 12.10.2005 | 70 | 693 | DOS | 17:33 | | 17:57 | 18:18 | 00:45 | 08:51.16 | 84:13.00 | 08:51.14 | 84:13.13 | 397 | Deployment | Linke | Quepos Slide | |
| 12.10.2005 | 71 | 694 | CTD 20 | 18:48 | 18:50 | 19:22 | 19:27 | 00:39 | 08:50.83 | 84:13.17 | 08:50.87 | 84:13.24 | 404 | | Brentführer | Quepos Slide | |
| 12.10.2005 | 72 | 695 | BCL | 20:42 | | 20:59 | 21:21 | 00:39 | 08:51.11 | 84:13.00 | 08:50.96 | 84:12.98 | 408 | Deployment | Linke | Quepos Slide | |

| | | | | | | | | | | | | | | | | | |
|---|---|---|---|---|---|---|---|---|---|---|---|---|---|---|---|---|---|
| 12.10.2005 | 73 | 696 | CTD 21 | 21:39 | 21:42 | 22:07 | 22:10 | 00:31 | 08:50.78 | 84:13.11 | 08:50.77 | 84:13.15 | 404 | | Brentführer | Quepos Slide | |
| 12.10.2005 | 74 | 697 | CTD 22 | 23:00 | 23:01 | 23:27 | 23:30 | 00:30 | 08:51.08 | 84:13.39 | 08:51.11 | 84:13.42 | 396 | | Brentführer | Quepos Slide | |
| 13.10.2005 | 75 | 698 | OFOS | 03:23 | 04:21 | 11:29 | 12:24 | 09:01 | 08:05.04 | 84:49.1 | 08:07.00 | 84:50.18 | 1788 | | Rehder | Jaco Scarp | |
| 13.10.2005 | 76 | 699 | CTD 23 | 15:49 | 15:30 | 16:28 | 16:30 | 00:41 | 08:51.00 | 84:12.74 | 08:51.01 | 84:12.75 | 402 | ADCP | Brentführer | Quepos Slide | |
| 13.10.2005 | 77 | 700 | BCL | 16:32 | | 16:36 | 18:58 | 02:26 | 08:51.02 | 84:12.71 | 08:50.98 | 84:12.64 | 392 | Recovery St.72 | Linke | Quepos Slide | |
| 13.10.2005 | 78 | 701 | CTD 24 | 17:36 | 17:37 | 18:02 | 18:02 | 00:26 | 08:50.91 | 84:12.88 | 08:50.90 | 84:12.88 | 412 | ADCP | Brentführer | Quepos Slide | |
| 13.10.2005 | 79 | 702 | Parasound | 18:09 | | | 21:38 | 03:29 | 08:50.94 | 84:12.90 | 08:49.50 | 84:13.69 | 623 | | Fromm | Quepos Slide | |
| 13.10.2005 | 80-1 | 703 | CTD 25 | 22:07 | 22:08 | 22:32 | 22:32 | 00:25 | 08:50.83 | 84:13.00 | 08:50.83 | 84:13.02 | 406 | ADCP, GAPS | Brentführer | Quepos Slide | |
| 13.10.2005 | 80-2 | 704 | BCL | 22:56 | 23:12 | 23:24 | 23:35 | 00:39 | 08:51.10 | 84:13.00 | 08:51.14 | 84:13.06 | 400 | Deployment | Linke | Quepos Slide | |
| 14.10.2005 | 81 | 705 | ROV 72 | 01:04 | 01:32 | 13:12 | 14:02 | 12:58 | 08:51.26 | 84:13.26 | 08:51.13 | 84:13.09 | 400 | | R,W,G-S | Quepos Slide | |
| 14.10.2005 | 82 | 706 | CTD 26 | 14:18 | 14:19 | 14:48 | 14:51 | 00:33 | 08:51.12 | 84:13.23 | 08:51.09 | 84:13.23 | 401 | | Brentführer | Quepos Slide | |
| 14.10.2005 | 83 | 707 | BCL | 15:15 | | 15:19 | 15:40 | 00:25 | 08:50.97 | 84:12.78 | 08:50.94 | 84:12.83 | 416 | Recovery St.80-2 | Linke | Quepos Slide | |
| 14.10.2005 | 84 | 708 | CTD 26 | 16:09 | 16:09 | 16:37 | 16:40 | 00:31 | 08:51.15 | 84:13.07 | 08:51.16 | 84:13.08 | 397 | | Brentführer | Quepos Slide | |
| 14.10.2005 | 85 | 709 | CTD 27 | 17:35 | 17:36 | 18:04 | 18:09 | 00:34 | 08:51.04 | 84:12.98 | 08:51.01 | 84:13.00 | 407 | | Brentführer | Quepos Slide | |
| 14.10.2005 | 86 | 710 | DOS | 18:16 | | 18:17 | 18:45 | 00:29 | 08:51.02 | 84:12.98 | 08:50.98 | 84:12.80 | 417 | Recovery St.70 | Linke | Quepos Slide | |
| 14.10.2005 | 87 | 711 | CTD 28 | 19:19 | 19:20 | 19:40 | 19:52 | 00:33 | 08:50.93 | 84:13.09 | 08:50.96 | 84:13.11 | 403 | | Brentführer | Quepos Slide | |
| 15.10.2005 | 88 | 712 | ROV 73 | 00:25 | 01:32 | 13:44 | 14:22 | 13:57 | 09:07.39 | 84:50.88 | 09:07.07 | 84:50.60 | 1860 | | R,L,G-S | Jaco Scarp | active pogonophora |
| 15.10.2005 | 89 | 713 | CTD 29 | 15:40 | 15:42 | 17:15 | 17:19 | 01:39 | 09:06.83 | 84:50.69 | 09:06.88 | 84:50.78 | 1922 | | Brentführer | Jaco Scarp | long term observation |
| 15.10.2005 | 90 | 714 | DOS | 17:40 | 18:57 | 19:00 | 19:52 | 02:12 | 09:06.96 | 84:50.47 | 09:07.00 | 84:50.49 | 1882 | Deployment | Linke | Jaco Scarp | |
| 15.10.2005 | 91 | 715 | CTD 30 | 20:52 | 20:53 | 23:05 | 23:12 | 02:20 | 08:59.51 | 84:43.61 | 08:59.39 | 84:43.80 | 1919 | 2 Positions, CTD towed | Brentführer | Mudpie | |
| 16.10.2005 | 92 | 716 | ROV 74 | 00:21 | 01:46 | 12:19 | 13:42 | 13:21 | 09:07.00 | 84:50.51 | 09:07.32 | 84:50.77 | 1804 | Dive | R,W,G-S | Jaco Scarp | |
| 16.10.2005 | 93 | 717 | CTD 31 | 14:41 | 14:42 | 16:12 | 16:14 | 01:33 | 09:05.42 | 84:49.57 | 09:04.41 | 84:49.64 | 1916 | | Brentführer | Jaco Scarp | long term observation |
| 16.10.2005 | 94 | 718 | BWS | 19:58 | 20:07 | 20:20 | 20:47 | 00:49 | 08:51.18 | 84:13.12 | 08:51.18 | 84:13.12 | 410 | | Linke | Quepos Slide | |
| 16.10.2005 | 95 | 719 | CTD 32 | 21:02 | 21:03 | 21:30 | 21:33 | 00:31 | 09:51.19 | 84:13.13 | 08:51.19 | 84:13.12 | 398 | | Brentführer | Quepos Slide | Oxygen Profile |
| 16.10.2005 | 96 | 720 | BWS | 22:00 | 22:30 | 22:40 | 23:00 | 01:00 | 08:51.26 | 84:13.13 | 08:51.22 | 84:13.15 | 398 | | Linke | Quepos Slide | Bacteria |
| 17.10.2005 | 97 | 721 | ROV 75 | 00:00 | 00:21 | 11:22 | 11:55 | 11:55 | 08:51.15 | 84:13.11 | 08:51.19 | 84:13.17 | 397 | Dive | R,W,G-S | Quepos Slide | Bacterial Mats |
| 17.10.2005 | 98 | 722 | BCL | 22:35 | 22:59 | 22:59 | 23:10 | 00:35 | 08:51.16 | 84:13.11 | 08:51.17 | 84:13.12 | 399 | Deployment | Linke | Quepos Slide | Bacteria |
| 18.10.2005 | 99 | 723 | ROV 76 | 00:07 | 00:28 | 14:00 | 14:42 | 14:35 | 08:51.18 | 84:13.14 | 8:51.18 | 84:12.99 | 410 | | R,L,W,G-S | Quepos Slide | Bacterial Mats |
| 18.10.2005 | 100 | 724 | CTD 33 | 14:54 | 14:55 | 15:16 | 15:32 | 00:38 | 08:51.23 | 84:12.99 | 08:51.22 | 84:13.02 | 410 | | Brentführer | Quepos Slide | |
| 18.10.2005 | 101 | 725 | BCL | 15:44 | 15:46 | | 16:10 | 00:26 | 08:51.03 | 84:12.86 | 08:51.03 | 84:12.86 | 417 | Recovery Station 98 | Linke | Quepos Slide | |
| 18.10.2005 | 102 | 726 | CTD 34 | 16:31 | 16:31 | 16:59 | 17:02 | 00:31 | 08:51.08 | 84:12.92 | 08:51.08 | 84:12.90 | 417 | | Brentführer | Quepos Slide | |
| 18.10.2005 | 103 | 727 | DOS | 21:00 | 21:03 | | 21:47 | 00:47 | 09:06.97 | 84:49.99 | 09:06.92 | 84:50.36 | 1142 | Recovery Station 90 | Linke | Jaco Scarp | |
| 18.10.2005 | 104 | 728 | OFOS | 23:15 | 00:19 | 07:10 | 08:06 | 08:51 | 08:59.57 | 84:43.44 | 08:59.76 | 84:43.55 | 1930 | | R,W,L,N,G-S | Mudpie | Carbonate/Deep Fauna |
| 19.10.2005 | 105 | 729 | CTD 35 | 20:37 | 20:37 | 21:54 | 22:00 | 01:23 | 10:18.16 | 86:18.37 | 10:18.18 | 86:18.35 | 1647 | | Brentführer | Mound Culebra | long term observation |
| 19.10.2005 | 106 | 730 | CTD 36 | 22:51 | 22:52 | 00:05 | 00:08 | 01:17 | 10:17.98 | 86:18.30 | 10:17.98 | 86:18.32 | 1549 | | Brentführer | Mound Culebra | long term observation |
| 20.10.2005 | 107 | 731 | ROV 77 | 00:27 | 01:33 | 12:54 | 14:25 | 13:58 | 10:17.99 | 86:18.31 | 10:18.05 | 86:18.32 | 1585 | Dive | Rehder | Mound Culebra | |
| 21.10.2005 | 108 | 732 | ROV 78 | 00:50 | 02:33 | 13:23 | 15:02 | 14:12 | 08:59.60 | 84:43.68 | 08:59.56 | 84:43.72 | 1917 | Dive | Rehder | Mudpie | |
| 21.10.2005 | 109 | 733 | CTD 37 | 15:43 | 15:44 | 17:16 | 17:16 | 01:33 | 08:59.55 | 84:43.71 | 08:59.55 | 84:43.71 | 1919 | | Brentführer | Mudpie | |
| 21.10.2005 | 110 | 734 | DOS | 19:36 | 20:14 | 20:36 | 21:12 | 01:36 | 08:55.69 | 84:18.78 | 08:55.69 | 84:18.86 | 1023 | Deployment until M66-3 | Linke | Mt. 12 | Bacterial Mat |
| 21.10.2005 | 111 | 735 | TEST | 21:35 | | | 22:34 | 00:59 | 08:55.68 | 84:18.89 | 08:55.68 | 84:18.89 | 1031 | Test Benthos floats | Linke | Mt. 12 | |
| 22.10.2005 | 112 | 736 | Hydrosweep | 05:31 | | | 19:11 | 13:40 | 08:30.13 | 85:17.97 | 08:18.00 | 84:58.50 | 2195 | | Fromm | | |

## 2.7 Acknowledgements

We are indebted to the captain of Meteor Expedion 66/2ab, Martin Kull, and the officers and crew of RV Meteor for their assistance and dedication during every minute of the cruise. The success of this cruise would not have been possible without the willingness of the ROV team of MARUM, Bremen, to work at, and sometimes beyond the limits. We like to thank captain Berkenheger and the Leitstelle Meteor for their help before, during, and after the cruise. The logistics of this cruise were coordinated by the skilful work of Klaus Bohn, Lehnkering VTG. The coordination of M66 by Dr. Warner Brückmann considerably facilitated the planning for this cruise. Silke Schenck of IFM-GEOMAR skilfully assisted the preparation of this cruise report.

## 2.8 References

Boetius, A., K. Ravenschlag, C. Schubert, D. Rickert, F. Widdel, A. Gieseke, R. Amann, B.B. Jørgensen, U. Witte, O. Pfannkuche, 2000. A marine microbial consortium apparently mediating anaerobic oxidation of methane. Nature, 407, 623-626

Elvert, M., J. Greinert, E. Suess, M.J. Whiticar, 2001. Carbon isotopes of biomarkers derived from methane-oxidizing microbes at Hydrate Ridge, Cascadia convergent margin. In: C.K. Paull, W.P. Dillon (Eds.), Natural gas hydrates: Occurrence, distribution, and dynamics, 124 (Ed. by C.K. Paull, W.P. Dillon), pp. 115-129. American Geophysical Union, Washington DC

Grasshoff, K., M. Ehrhardt, K. Kremling, 1997. Methods of seawater analysis. Verlag Chemie, Gulf Publishing, Houston

Hensen C., K. Wallmann, M. Schmidt, C. Ranero, and E. Suess, 2004. Fluid expulsion related to mud volcanism at Costa Rica continental margin - a window to the subducting slab. Geology 32, 201-204

Hinrichs, K.-U., J.M. Hayes, S.P. Sylva, P.G Brewer, E.F. DeLong, 1999. Methane-consuming archaebacteria in marine sediments. Nature, 398, 802-805

Lammers, S., E. Suess, 1994. An improved head-space analysis method for methane in seawater. Marine Chemistry 47: 115-125

Mau, S., G. Rehder, I. Arroyo, J. Gossler, and E. Suess, 2007. Indications of a link between seismotectonics and CH4 release from seeps off Costa Rica. Geochemistry, Geophysics and Geosystems 8(4), Q04003

Michaelis, W., R. Seifert, K. Nauhaus, T. Treude, V. Thiel, M. Blumenberg, K. Knittel, A. Gieseke, K. Peterknecht, T. Pape, A. Boetius, R. Amann, B.B. Jorgensen, F. Widdel, J.R. Peckmann, N.V. Pimenov, M.B. Gulin, 2002. Microbial reefs in the Black Sea fueled by anaerobic oxidation of methane. Science, 297(5583), 1013-1015

Orphan, V.J., C.H. House, K.U. Hinrichs, K.D. McKeegan, E.F. DeLong, 2001. Methane-consuming archaea revealed by directly coupled isotopic and phylogenetic analysis. Science, 293(5529), 484-487

Reeburgh, W.S., "Soft spots" in the global methane budget. In: M.E. Lidstrom, F.R. Tabita (Eds.), Microbial Growth on $C_1$ Compounds (Ed. by M.E. Lidstrom, F.R. Tabita), pp. 334-342. Kluwer Academic Publishers, Dordrecht, 1996.

Rehder, G., R. Keir, E. Suess, M. Rhein, Methane in the Northern Atlantic controlled by microbial oxidation and atmospheric history. Geophysical Research Letters 26: 587-590, 1999.

Sahling, H., D. Rickert, R.W. Lee, P. Linke, E. Suess, Macrofaunal community structure and sulfide flux at gas hydrate deposits from the Cascadia convergent margin, NE Pacific. Marine Ecology-Progress Series, 231, 121-138, 2002.

METEOR-Berichte 09-2

# *SUBFLUX*

## PART 3

Cruise No. 66, Leg 3a
October 26 – November 10, 2005, Caldera (Costa Rica) – Caldera (Costa Rica)

Cruise No. 66, Leg 3b
November 10 - November 19, 2005, Caldera (Costa Rica) – Corinto (Nicaragua)


**Warner Brückmann,** Anke Bleyer, Oliver Bartdorff, Kristin Deppe, Bettina Domeyer, Emelina Corrales, Christine Flies, Armin Freundt, Tanja Fromm, Thomas Hammerich, Rieka Harders, Bernd Heesemann, Christian Hensen, Norbert Kaul, Steffen Kutterolf, Florian Leis, Julia Mahlke, Tobias Mörz, Wolf-Thilo Ochsenhirt, Wendy Perez-Fernandez Martin Pieper, Johannes Rogenhagen, Ulrike Schacht, Mark Schmidt, Klaus-Peter Steffen, Erik Steen, Matthias Türk, the shipboard scientific parties and Silke Schenck

Editorial Assistance:

Andreas Krell
Alfred-Wegener-Institut für Polar- und Meeresforschung, Bremerhaven

Leitstelle METEOR
Institut für Meereskunde der Universität Hamburg

2009

**Table of Contents Part 3 (M66/3)** **Page**

## 3.1 Participants M66/3

### 3.1.1 Participants Leg M66/3a

| Name | Discipline | Institution |
|---|---|---|
| 1. Brückmann, Warner, Dr. | Chief scientist | IFM-GEOMAR |
| 2. Bleyer, Anke | Pore water geochemistry | IFM-GEOMAR |
| 3. Bartdorff, Oliver | Pore water geochemistry | SFB 574 |
| 4. Ochsenhirt, Wolf Thilo | Meteorology | DWD |
| 5. Corrales, Emelina | Pore water geochemistry | NGO |
| 6. Flies, Christine | Microbiology | University Göttingen |
| 7. Fromm, Tanja | Mapping, documentation | SFB 574 |
| 8. Hammerich, Thomas | Sedimentology | SFB 574 |
| 9. Hensen, Christian, Dr. | Pore water geochemistry | SFB 574 |
| 10. Kutterolf, Steffen, Dr. | Tephra chronology | SFB 574 |
| 11. Leis, Florian | Physical Properties | SFB 574 |
| 12. Mahlke, Julia | Sedimentology, Tephra chronology | SFB 574 |
| 13. Mörz, Tobias | Sedimentology, Tephra chronology | SFB 574 |
| 14. Brett, Colin Peter | Rockdrill | BGS |
| 15. Campbell, Neil Colin | Rockdrill | BGS |
| 16. Derrick, John | Rockdrill | BGS |
| 17. Glendinning, James | Rockdrill | BGS |
| 18. Wallis, David | Rockdrill | BGS |
| 19. Wilson, Michael | Rockdrill | BGS |
| 20. Harders, Rieka | Sedimentology | SFB 574 |
| 21. Pieper, Martin | Lander technician | SFB 574 |
| 22. Schacht, Ulrike | Geochemistry | SFB 574 |
| 23. Schmidt, Mark, Dr. | Sedimentology | CAU |
| 24. Steen, Erik | Core technician | CAU |
| 25. Türk, Matthias | Lander technician | IFM-GEOMAR |
| 26. Seibold, Jörg | TV documentation | DWTV |
| 27. Kassube, Hans | TV documentation | DWTV |
| 28. Cee, Dagmar | TV documentation | DWTV |
| 29. Gómez, Eddy | Observer | CIMAR-UCR |

### 3.1.2 Participants Leg M66/3b

| Name | Discipline | Institution |
|---|---|---|
| 1. Brückmann, Warner, Dr. | Chief scientist | IFM-GEOMAR |
| 2. Bartdorff, Oliver | Pore water geochemistry | SFB 574 |
| 3. Ochsenhirt, Wolf Thilo | Meteorology | DWD |
| 4. Corrales, Emelina | Pore water geochemistry | NGO |
| 5. Fromm, Tanja | Mapping, documentation | SFB 574 |
| 6. Hammerich, Thomas | Sedimentology | SFB 574 |

| | | |
|---|---|---|
| 7. Hensen, Christian, Dr. | Pore water geochemistry | SFB 574 |
| 8. Kutterolf, Steffen, Dr. | Tephra chronology | SFB 574 |
| 9. Leis, Florian | Physical Properties | SFB 574 |
| 10. Mahlke, Julia | Sedimentology, Tephra chronology | SFB 574 |
| 11. Mörz, Tobias | Sedimentology, Tephra chronology | SFB 574 |
| 12. Harders, Rieka | Sedimentology | SFB 574 |
| 13. Schacht, Ulrike | Geochemistry | SFB 574 |
| 14. Schmidt, Mark, Dr. | Sedimentology | CAU |
| 15. Steen, Erik | Core technician | CAU |
| 16. Rogenhagen, Johannes | Heat flux measurements | FILAX |
| 17. Domeyer, Bettina | Geochemistry | IFM-GEOMAR |
| 18. Deppe, Kristin | Tephra stratigraphy | SFB 574 |
| 19. Kaul, Norbert | Heat Flow | GEOB |
| 20. Heesemann, Bernd | Heat Flow | GEOB |
| 21. Freundt, Armin | Tephra chronology | IFM-GEOMAR |
| 22. Steffen, Klaus-Peter | Airgun technician | IFM-GEOMAR |
| 23. Perez Fernandez, Wendy | Tephra chronology, observer | SFB 574 |
| 24. Rojas Arevalo, Mario Alf. | Observer | Guatemalan Navy |
| 25. Cifuentes Marckwordt, M. J. | Observer | USC |

| | |
|---|---|
| **BGS** | British Geological Survey, Murchison House, West Mains Road, Edinburgh EH9 3LA, Great Britain |
| **CAU** | Institut für Geowissenschaften der Christian-Albrechts-Universität zu Kiel, Ludewig-Meyn-Str. |
| **CIMAR-UCR** | Centro de Investigacion en Ciencias del Mar y Limnologia, Universidad de Costa Rica, San Pedro de Montes de Oca, 2060-1000 |
| **DWD** | Deutscher Wetterdienst, Geschäftsfeld Seeschifffahrt, Bernhard-Nocht-Str. 76, 20359 Hamburg, Germany |
| **DW-TV** | Deutsche Welle – TV, Voltastr. 6, 13355 Berlin, Germany |
| **FIELAX** | Gesellschaft für wissenschaftliche Datenverarbeitung mbH, Schifferstrasse 10 – 14, 27568 Bremerhaven, Germany |
| **GEOB** | Fachbereich Geowissenschaften; Universität Bremen Postfach 330440, 28334 Bremen, Germany |
| **IFM-GEOMAR** | Leibniz Institut für Meeresforschung, Wischhofstrasse, 24105 Kiel, Germany |
| **NGO** | Escuela de ciencias Biologicas, Facultad de Ciencias Exactas y naturales, Universidad Nacional Heredia, Costa Rica |
| **SFB 574** | Sonderforschungsbereich 574, Christian-Albrechts-Universität zu Kiel, Wischhofstrasse 1-3, 24148 Kiel, Germany |
| **USC** | University of San Carlos, Guatemala |

## 3.2 Research Program

The R V METEOR M 66 cruise w as of central i mportance t o t he C ooperative R esearch Center "SFB" 574. All subprojects were involved and participated in various aspects of the cruise. The main obj ective of S FB 574 i s t o unde rstand t he bud get, r eactions, a nd r ecycling o f vol atile elements in subduction zones and their role in climate forcing. In this way the SFB addresses the long- and s hort-term de velopment of t he E arth´s c limate, t he geochemical e volution of t he hydrosphere and atmosphere, and the caus es of na tural di sasters. These pr ocesses ar e al l connected i n on e w ay o r a nother with t he r eturn flow a nd i mpact of vol atiles a nd fluids f rom subduction zones.

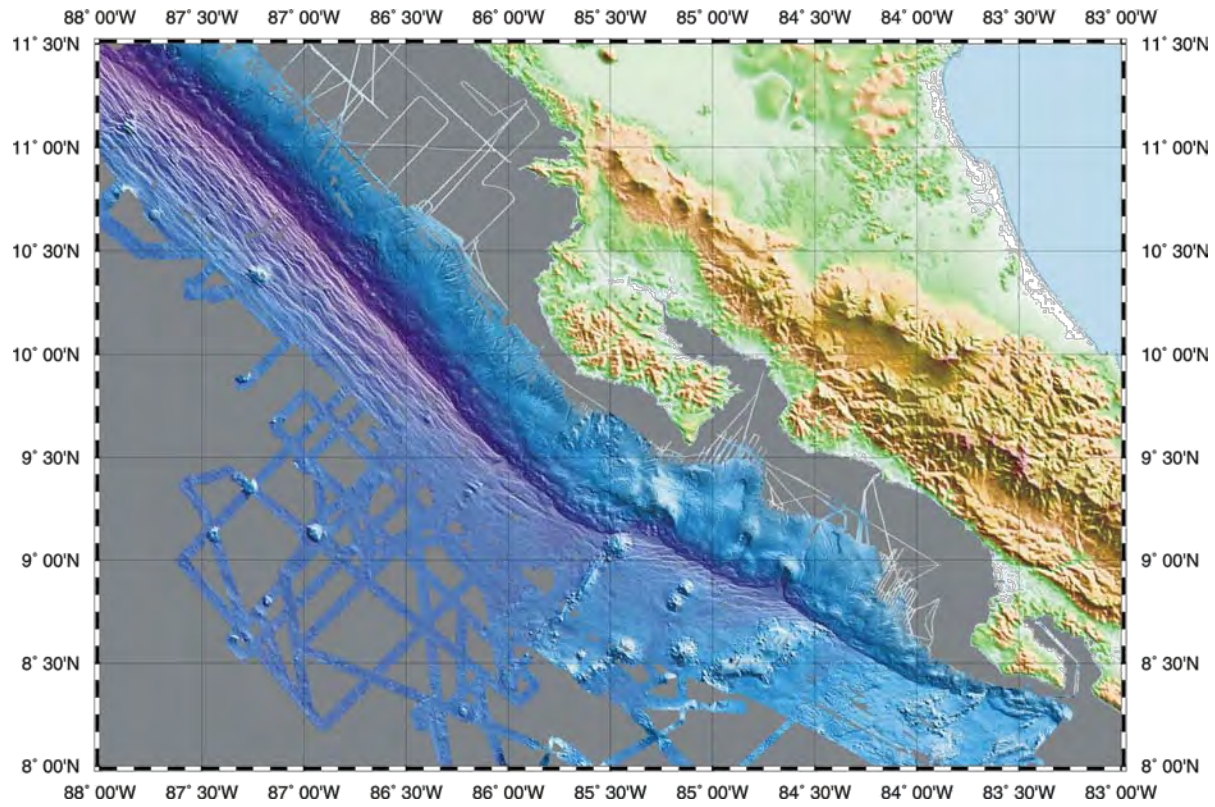


**FIG. 3.1:** The working areas of M66/3

The m ajor vol atile i nput i nto s ubduction z ones consists of s ediments, t he a ltered pr oducts oceanic crust, and the trench-fill from down-slope mass wasting. The output is via fluid venting at the deformation front, by gas hydrate formation/dissociation, and by volcanic degassing at the fore-arc. Inside t he s ubduction z one t he i ncoming m aterial i s t ransformed, m obilized or fractionated into different volatile reservoirs and phases. These phases are either ejected into the exosphere through the upper plate, accreted to the leading edge of the continental plate, or are transported into the lower mantle. The tectonic style of subduction, the structure of the margin wedge, and the properties and configuration of the down-going plate all exert a first order control on volatile budget,its transformation, and return pathway.

The ar ea of i nvestigation, the C entral A merican fore-arc o ff C osta R ica and Nicaragua (Fig 3.1), is well suited for such an investigation because of small-scale changes of features which influence t he vol atile c ycling; i .e. t he c omposition a nd a ge of t he i ncoming oc eanic c rust, t he

morphology of continental slope, and the accretionary tectonic style. Equally important are the composition of the volcanic rocks on land as well as in submarine outcrops to trace the history of volcanic emissions.

### 3.2.1 Specific Cruise Objectives Leg M66/3a

The primary objective of the work performed on this leg was deep sampling of mud diapirs and carbonate mounds, large numbers of which have been found off Costa Rica and Nicaragua. These structures are a major element in the recycling of volatiles and fluids on this erosive continental margin, therefore they are in the focus of the work of several subprojects of the SFB 574. Clear evidence has been found that fluids are transported upwards from deep sources as well as shallower sources.

Near-surface gas hydrates have been found as well as extensive "carbonate caps" of varying thickness. They render sampling of the mounds difficult or even impossible. Thus, on the past cruises of the SFB 574, when conventional coring systems such as piston corers and gravity corers were used, it was not possible to recover cores form the carbonate-covered tops of these mounds. Yet, information from the central parts of these structures, which are likely to expell volatiles, fluids and sediments from large depths, would be of special importance for a better understanding of their genesis.

Previous SFB work resulted in a differentiation between several types of authigenic carbonates: chemoherms and crusts associated with fluid expulsion at the sediment surface, gas hydrate – associated carbonates as well as limy and dolomitic concretions. Complete cores of all depths of these carbonate caps would enable a high-resolution temporal reconstruction of the devolatilisation history and fluid drainage. In addition, the pore water chemistry of the sediments can be expected to be less contaminated by sea water below the carbonate caps, as suggested by earlier samples from the marginal areas of mounds. This would allow for a better assessment of the source depth of fluids by geochemical and isotope geochemical methods, providing answers for one of the central SFB 574 objectives. Coring was performed by a portable drilling device to be deployed via METEOR's A frame, the BGS Seabed Rockdrill and Vibrocorer (description see below).

Mound Culebra, Mound 10, Mounds 11 and 12 as well as a group of large mounds off Nicaragua discovered during SONNE cruise SO173 are already well known by preliminary SFB sampling using gravity corers and piston corers as well as OFOS surveys performed on cruises SONNE 163 and SONNE 173. For Leg 3a, representative profiles from the top of each structure as well as 2 further cores on the flanks were recovered in order to examine if potential earlier phases of stagnation during the formation of the mounds are documented within the carbonate layers.

*Geochemistry*

A major goal of Leg 3a was the investigation of sediment diagenesis in the fore-arc of subduction zones and the sampling of cold vents. The quantification of organic matter mineralization, secondary redox reactions, seawater-mineral interactions, as well as the determination of fluid flow and accumulation rates of volatile species in fore-arc sediments is of central importance for the submarine cycling of carbon, nitrogen, sulfur, water, and halogens. Anaerobic organic matter degradation coupled with sulfate reduction and methane formation

releases dissolved volatiles (SCO2, NH4+, Br-, I-, SH2S, CH4) into the pore fluids and produces important carbon and sulfur reservoirs (e.g. gas hydrates, carbonates, pyrite). Other redox reactions are involved in the formation of carbonate precipitates and halogen enrichments in surface sediments. Alteration and submarine weathering of volcanic ashes, biogenic opal, and clay minerals further contribute to the water cycling and solute flows in sediments. The spatial variability and distribution of processes and compounds in the fore-arc area will help to define the volatile input into subduction zones and to constrain the submarine volatile emissions via diffusive and focused fluid flow.

*Sedimentology and Physical Properties*

Lithological core descriptions and physical parameter profiles are the basis for any further investigations on sediment cores of the SFB 574 study area off Central America. The lithological characterization will be based on core descriptions and sediment physical properties. The sediment-physical working schedule included the non-destructive logging part and sampling based determination of the sediment physical index parameter: water content, wet bulk density and grain density. The whole-core logging program includes the following parameters: core diameter, p-wave velocity, density (GRAPE) and magnetic susceptibility. Aim of the sediment physical working program was to establish coherent litho-physical sediment profiles by integrating descriptive and measured parameters.

### 3.2.2 Specific Cruise Objectives Leg M66/3b

*Tephrostratigraphy*

In Central America and other regions on Earth, highly explosive, plinian volcanic eruptions generate buoyant eruption columns consisting of solid particles (Pumice Lapilli, ash, lithics) and gases, penetrating 20-40 km high into the atmosphere up to the level of neutral buoyancy where they spread laterally in the prevailing wind directions. Eruption clouds drift with the wind and gradually drop their ash load over areas larger than 100000 $km^2$. Due to their wide distribution and the prevailing westerly winds, ashes from Central American volcanoes can reach the Pacific Ocean where they are incorporated in the marine sediments. Their wide aerial distribution across sedimentary facies boundaries, their near-instantaneous emplacement and chemical signatures facilitate stratigraphic correlations with deposits on land. Ash layers are best preserved in non-erosive marine or lacustrine environments and therefore provide the most complete record of explosive volcanic activity of one region. Additionally the eruption volumes, which grow significantly with the portion of the widely distributed distal part of the Tephra deposits, can be recalculated using the marine distribution. For this purpose, gravity cores were collected along the Central American subduction zone (El Salvador and Guatemala) through M66/3B, promising a good recovery of ash layers and complementing the former record of marine ashes in this region. Core locations were picked out with the PARASOUND to prevent irregularities in sedimentation (mass wasting processes, turbidites, slumps), and which promise undisturbed stratigraphy. Additionally core logging techniques helped to identify both distinct layers, and dispersed ashes in marine sediment cores, prior to core description. Standard core logging parameters included P-wave velocity, density from gamma attenuation and magnetic susceptibility. Later, compositional data, including mineral assemblages, mineral and glass

compositions obtained by electron microprobe, as well as bulk rock chemistry, are used for correlations between marine and on-land tephras.

## 3.3 Narrative of the Cruise

### 3.3.1 Narrative of the Cruise Leg M66/3a

Cruise M66/3a began with a call to the port of Caldera, Costa Rica, which was occupied by numerous logistical tasks. After the University of Bremen QUEST container had gone from board, laboratory containers, reefer containers, a 40-foot container and the winch for the Rockdrill system were placed on the working deck. On 25 October the loading work was finished by transferring the Rockdrill system, which had been pre-assembled on the pier, onto the ship. R/V METEOR left the port of Caldera on 26 October at 10:00 sharp. After a short "wet test" of the Rockdrill system in Nicoya Bay, we headed for our working area off Nicaragua, where we arrived in the morning of 27 October.

The first runs of the British Rockdrill system took place at a water depth of 880m on the summit of Mound Baula, a 200-m-high structure with a diameter of 2.5 km that consists of massive carbonates. While the first trials in "rotary" mode did not produce much core material, the subsequent runs in "vibrocore" mode were very successful. From the saddle region of Mound Baula we were able to retrieve cores with clastic sediment, part of which showed an extensive gas hydrate cementation. 24-hour-Rockdrill deployments were carried out on 29 and 30 October, sampling Mounds Iguana, Quetzal and Carablanca. The nights were used for the more time-consuming operations in rotary mode and the days for the vibrocore mode. In addition, we took gravity cores and performed PARASOUND mapping on the extended Massaya slide that is located directly beneath the Nicaragua Mounds and consists of several phases. The newly developed PWP lander for long-term measurements of pore pressure variations in active venting areas was deployed for the first time.

One of the highlights of the first days was the discovery that Mound Carablanca, wich had hitherto been classified as a carbonate mound due to its acoustic signature, is clearly of a young, diapiric origin, and that areas of high backscatter are characterised by clay clasts that were emplaced through diapiric transport. A further highlight was the recovery of core M66/129 the first core with authigenic carbonates, sampled from Mound Iguana using the BGS Rockdrill. Three main zones could be identified during the first examinations: The upper layer is about 16 cm thick and shows primary authigenic carbonates with fractures filled with secondary authigenic carbonate. The second zone (about 24 cm thick) consists of authigenic carbonate containing a lot of shells, with crystalline, layered palisade carbonate in cavities and cemented foraminifera and crystals. The lowermost zone (about 12 cm thick) consists of clay clasts and a matrix of authigenic carbonates.

The second week was again dedicated to the northern part of the working area off Nicaragua. Efforts were made to get BGS Rockdrill cores from massive carbonates, yet only at some of the sites in the Perezoso Mound area and the Baula massive they were successful. Here, cores of up to 100 cm in length could be recovered.

In addition, the sedimentological and geochemical work was continued. Various mound structures were sampled with the BGS vibrocorer and the gravity corer. Pore waters were examined with regard to an ascent of deep fluids which are characterised by negative chloride

anomalies, i.e. a depletion in salt in comparison to sea water. So far, such fluids have only been detected in the southern part of our working area off Costa Rica, where they can definitely be attributed to dewatering of clay minerals in the sediments of the subducting oceanic plate. In total, 8 of the 10 structures sampled off Nicaragua showed negative chloride anomalies. However, the anomalies found here are usually less significant, and there are clear differences in the concentrations of nutrients compared to the pore waters of the southern working area off Costa Rica. These differences may indicate shallow circulation systems transporting sea water deeper into the sediments and thus weakening the original fluid signal. Considering all the data, only low ascent rates can be assumed for the whole area. Preliminary modelling of the pore water data from Mound Culebrita suggests ascent rates of clearly less than 1 cm per year.

The important role the explosive volcanism that is characteristic of subduction zones plays in marine sedimentation is proven by ash layers and ash lenses found in the numerous cores sampled off Nicaragua. Based on their stratigraphic position within the cores and their appearance they were preliminarily matched to eruptions on land. As an example, the photograph in Fig. 3.2 shows an ash layer of 9 cm in thickness which we assume to be correlated to the Chiltepe eruption of the Apoyeque volcano near the Nicaraguan capital Managua which took place about 2000 years ago.

Another main object of study were the mechanisms triggering submarine landslides. Gravity cores were taken from three submarine landslides located in the deeper part of the continental margin off Nicaragua. We were able to retrieve an exemplary core, core no. M66-3a-151, from Hermosa Slide. It penetrated right through the consolidated, clayey slide plane and the discordant slided mass above it.

It is a noteworthy fact that the two sedimentary zones are separated by a thin layer of ash, which presumably was a weak interval and thus an important factor in the de stabilisation. Already on previous cruises, ash layers were identified as zones of instability at the base of slides, so that these results fit well into our previous observations.

The first pore water analyses performed on board show a marked leap of the gradient of alkalinity and thus support the results of the core classification.

Our work off Nicaragua was concluded by recovering the PWP lander, a new in situ tool developed by the SFB 574. The second deployment was very successful. Over a period of three days high-resolution pore pressure profiles have been recorded from depths of up to 2 m.

A further deployment of the PWPL is planned in the area of Mound 12 off Costa Rica, where there are already several flow meters belonging to an US group that were deployed by ALVIN as well as IFM-GEOMAR ocean bottom seismometers (OBS).

On Saturday, 5 November, R/V METEOR left the northern working area off Nicaragua. In the morning of 6 November we arrived off Costa Rica and started Rockdrill sampling at the base of the Jaco Scar slide.

In the third week of leg M66/3a we concentrated our work on the southern working area off Costa Rica. Corresponding to the northern working area off Nicaragua, we mainly focussed on drilling carbonate mounds, which are an important element in the process of volatile and fluid recycling at this erosive continental margin off Central America. It was our aim to sample authigenic carbonates from the summits of the mounds studied during our previous cruises. They were to serve as the basis for a high-resolution reconstruction of the history of devolatilisation and de fluidisation. Unfortunately, our attempts to drill carbonates from the best-examined

mounds in this area, mounds 11 and 12, were unsuccessful as we did not find carbonates that were sufficiently massive to be cored by the BGS rockdrill.

Two cores with a clear signal of deep fluids were taken from the central area of mound 12. They indicated a direct connection to the fault running NW-SW and thus to Mound 11 which is located further to the south-east. The site work on mound 11 and 12 was completed by retrieving the PWP lander developed by the SFB. Again, it was successful in collecting high-resolution in situ pore pressure profiles which are to be correlated with the data of several flow meters (Scripps, San Diego) and ocean bottom seismometers (IFM-GEOMAR, Kiel) that are currently deployed at the same site.

Our examinations of Jaco Scar, a large erosive structure created by seamount subduction, turned out a great success. Several cores were sampled from the basis of Jaco Scar using the BGS vibrocorer. They were taken in the immediate vicinity of extensive fields of tube worms. Pore water chemistry showed clear signs of deep fluids.

Above Jaco Scar, the continental slope is bulged upward by the subducting seamount. Here, we were able to observe and core thick layers of carbonate. Core M66-215 (Fig. 3.2), which is 317 cm long, is the greatest highlight of the BGS Rockdrill drilling programme.

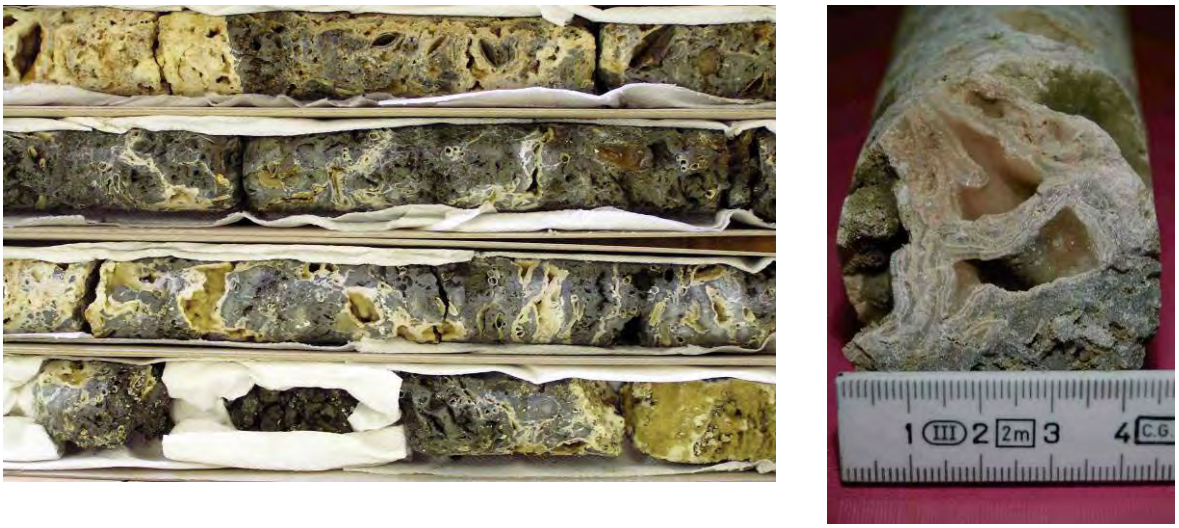


**FIG 3.2:** Overview photography and detail of M66-215.

We would like to stress the unusually good quality of the cored material: few fractures, complete core segments of up to 42 cm. The core is composed of two sequences recurring troughout the whole thickness of the material sampled: Medium grey to dark grey primary carbonates with a high content of sediments and cemented tube worms and shells alternate with light beige to white secondary carbonates (Fig. 3.2). It should be noted that this is a fossil analogue to the faunal community found recently at the basis of Jaco Scar. Thus, the core serves as a document of a dewatering process caused by seamount subduction that has not been included in quantitative assessments so far.

Leg METEOR M66/3a ended in the morning of 11 November when R/V METEOR berthed in the port of Caldera, Costa Rica. 11 members of the scientist crew left the ship. The BGS rockdrill was demobilised and taken from board, three containers left the ship. Four containers had arrived with the equipment for leg M66/4a and were unloaded. A new, 8000-m-long coaxial cable was spooled onto winch W12. Our two-day, busy port call was accompanied by an event

for presentation and representation that had been organised in collaboration with the German embassy in San José. Apart from the embassador, among the participants there were representatives of university institutes, authorities and the media. The scientist group was completed by 10 newly arrived members, and R/V METEOR left the port of Caldera in the morning of 13 November, heading north in order to start the working programme of leg M66/3b off Nicoya peninsula.

### 3.3.2 Narrative of the Cruise Leg M66/3b

The programme for the last week of M 66/3 mainly comprised sampling ash layers and performing heat flux measurements in the northern working area off Nicaragua, El Salvador and Guatemala. The first task of the final, short leg M 66/3b was the deployment of a Canadian ADCP mooring which is to record flow velocities and flow directions in the vicinity of ODP site 1255 (Leg 205) off Nicoya Peninsula, Costa Rica, over a period of several years. The resulting information will be important for interpretation of the data collected by the CORK drill hole observatory, which has been installed at site 1255.

A series of gravity cores was taken during the first days of leg M66/3b from a total of six positions parallel to the deep sea trench off El Salvador and Guatemala. All cores showed several layers of mafic and felsic ashes. Mafic ashes in the cores taken from the sites further towards the north showed an enrichment in biotite indicating an increasing alkalinity of the erupted material corresponding to the observations on land. In addition, many graded layers show characteristics that are interpreted as an indication of eruptions that were stronger than those observed off Nicaragua. The tephrastratigraphy covers more than 70ka, which is the age of the Arce ashes of Coatepeque Caldera in northern El Salvador. This layer was found in all cores at approximately the same depth, which will facilitate stratigraphic correlation. All ash layers were sampled for further chemical and petrographic examinations, especially for thermoluminescence dating.

Surprisingly, in spite of the great distance of the sampling sites to the Central American deep sea trench, all cores showed indications of numerous slides that were presumably caused by tectonic events on the flexural bulge of the Pacific plate before subduction.

In addition, leg M66/3b gave us the opportunity to extend some heat flow profile sections across the deep sea trench towards the oceanic crust in the west. Heat flux measurements performed during METEOR M54 to assess the seismic hazard potential were extended for the areas of Costa Rica (CR1) and Nicaragua (NIC1). Hardly any measurements have been performed in the area north of Nicaragua so far. So we took the chance and mapped a profile, albeit short, off Guatemala (GUA1) as an extension of earlier DSDP 84 drilling. The comparison of the thermal structure of different segments of the Pacific plate will contribute to understanding variations of seismicity along the Central American continental margin, as it is already known that the rigidity of the subducting plate to a certain degree is determined by its temperature. Unfortunately, the work on profile GUA1 had to be finished early on 18 November because the new coaxial wire was damaged so that further measurement became impossible.

Leg M 66/3b ended on 19 November when FS METEOR entered the port of Corinto, Nicaragua.

## 3.4 Preliminary Results

### 3.4.1 Coring techniques and sample analysis

#### 3.4.1.1 British Geological Survey (BGS) Vibro corer and Rockdrill

The coring programme used the BGS rockdrill with the option of vibrocoring by exchange of barrels and selection of different drilling parameters. Deployment was over the stern of R V METEOR via a combined signal/power/hoist umbilical cable on a dedicated winch system. All functions were PC controlled and two TFT monitor displays allowed the operators to observe progress and vary the coring parameters. The data on seabed operation were recorded for each coring site.

In rockdrilling mode, the tool collects a core of 49 mm diameter and a maximum length of about 5 m in a double-walled core barrel. The speed of rotation can be varied from 0-600 rpm, the bit weight control can be adjusted and either one or two flush pumps can be used. A real time video color camera gives the advantage to observe and evaluate the seafloor and search for desired drilling targets. Penetration, oil pressure and rpm are normally monitored, as being the most useful for interpretation of the drilling process. Additional sensors fitted include pitch and roll to check the stability of the frame on the seabed. The maximum possible drilling angle of the BGS rockdrill device is 25 degrees. Two different bits were used on this cruise: a stepped profile, surface set bit and a soft matrix impregnated diamond bit. Upon full penetration or refusal to drill further, the drill function is switched off and the barrel is retracted into the frame. Within the inner core barrel, the core is retained by a core spring during recovery. The core is extracted by removing the bit and reaming shell from the bottom end of the outer barrel, withdrawing the top water swivel and disconnecting the inner core barrel. The core is then removed from the inner barrel into labelled plastic guttering (A (BASE), B, C, D, E, F (TOP) - each individually sub-labelled with BASE and TOP) using controlled water pressure.

*Gravity Coring*

Sediment cores of 2 to 8 m total length where taken with a standard gravity coring system during M66 cruises in the Costa Rica, Nicaragua, El Salvador and Guatemala for-arc area. The gravity coring device was equipped with a 1.5 to weight attached to the top of a 3 to 9 m steel tube barrel surrounding an inner 3-9 m PVC-tube acting as the core liner. A valve situated at the to end of the coring barrel allows water to escape during sediment penetration. Standard outer liner diameters are 12.5 cm and average liner thickness is around 2.5 mm.

*Core handling of BGS vibrocorer & Gravity Cores*

Following the arrival of the cores on deck and retrieval of the PVC liner from the core barrel either from BGS vibrocorer or from Gravity Corer they where cut into 1 m segments. Each segment end was sampled for gas-analysis with syringes. After numbering the segments from bottom to top and marking the bottom and top ends the segments where sealed with end caps and stored in the 4°C METEOR Lab for further labeling.

*Multi Sensor Core Logging (MSCL)*

Geotechnical logging with the GEOTEK Ltd. (UK) multi sensor whole core logger consisted of standard parameters – core diameter, p-wave attenuation, gamma ray attentuation, and magnetic susceptibility - taken at a 2 cm sampling interval (for details on methods see Blum, 1997).

*Core handling after logging*

The liner of the logged core segments were opened with a saw on deck whereas splitting into archive and working halves was done in the cold lab. Still in the cold room the working halves were immediately sampled for further geochemical analysis. Following geochemical sampling the working halves where used up for geotechnical index measurements and undrained shear strength determination and further sub-sampling.

*Core description and core imaging*

Core description included grain size estimates, addressing color values based on the Munsell Color Chart and the description of sedimentological and tectonic structures. Smear slides and acid testing aided in the detection of ashes, organic residues and other exceptional particles. Digital core photos were made on a mobile rack with scale illuminated by 2500 Watt lamps set up to produce shadow free high resolution images. The digital camera was set up in timer mode to avoid camera motion resulting from manual triggering.

### 3.4.2 Gravity coring

About 200 m of sediment was recovered offshore Costa Rica, Nicaragua, El Salvador and Guatemala at the Pacific Continental Margin during METEOR cruises M66-3a and b. 31 coring stations were sucessfully conducted during M66-3a using the BGS-vibrocoring device primarily in consolidated or cemented seafloor areas (carbonate mounds, slides, scars). About 90 m of sediment was recovered by using this method. Gravity coring was used during M66-3a and b in areas were soft sediment was expected. Overall 110 m of sediment cores were recovered in 26 stations. Results are described in the context of specific studies on tephrostratigraphy, submarine slides, carbonate mounds, and with respect to geochemistry (see below).

### 3.4.3 Authigenic carbonates

Previous work shows that authigenic carbonates are excellent archives for reconstructing ancient fluid flow activity at active continental margins. The cruises SO144, SO163, SO173, M54 and M66/2 of RV SONNE and RV METEOR along the Middle American subduction zone discovered and sampled authigenic carbonates covering mud mounds, scarps and faults with an impenetrable cap offshore Nicaragua and Costa Rica (Weinrebe and Flüh 2000; Bohrmann et al. 2002). The sample techniques were limited to relatively thin surface samples obtained video controlled by TV-Guided Grab and ROV, or randomly selected by Gravity Corer and Multi Corer. As a result of this insufficient controlled sampling the chronological knowledge and the geochemical history of the formation of authigenic carbonates is poorly understood.

During cruise M 66/3 the main objective was to recover previously identified carbonate mounds and –structures and actively drill these with the video controlled BGS rockdrill. The aim was to obtain long coherent carbonate cores to get a continuous record of the authigenic carbonate origin. The second approach was to obtain carbonate cores from different geological

settings (e.g.: Nicaragua: smooth East Pacific Rise Plate, Costa Rica: rough Galapagos Rise Plate) and various depth ranges.

Authigenic carbonate cores were collected during M 66-3A with the BGS rockdrill. The working program of the cruise started in the working area offshore Nicaragua and lasted for 2/3 of the total expedition time. This was followed by another week of working offshore S Costa Rica. The drill sites were chosen considering interpreted geological and geophysical data from previous scientific cruises. At every drilling locality the BGS rockdrill was deployed and stopped approximately 5m above seafloor. While hovering, the seafloor surface was evaluated with the help of the live video pictures to search for a possible landing area. If necessary the BGS rockdrill was moved laterally by drifting of RV METEOR. Desired locations on the seafloor were indicated, where carbonate was visible on/in the sediment or hardground. At promising spots the BGS rockdrill was put down while watching closely to the pitch and roll angle. A rest period of several minutes was applied to see if the whole BGS rockdrill unit is still moving, sliding or tilting. If the conditions were stable the drilling was started. During the drilling penetration vs. time, rotation value (rpm = rotations per minute) and oil pressure were constantly moniored by telemetry. Rpm, bit weight and flush pumps were manually modified to get an ideal penetration of 1-5cm/min. With increasing drilling experience a rpm of 280 to 300 and a high flush rate turned out to be an optimum value for carbonates. After several drilling attempts with low or no core recovery (gravel and/or highly fractured material) we changed our strategy. Instead of approaching the maximum penetration depth of 5m we stopped the drilling immediately if the penetration rate per time was getting too high (>8-10cm/min; drilling into soft sediments instead of hard material) to recover core material so far drilled.

Continuous authigenic carbonate cores were drilled successfully for the first time ever. Also carbonate cores were achieved from different geological settings and depths:

-Offshore Nicaragua: Md.Congo is the northernmost-drilled mound whereas Md.Culebra, the deepest (1527 mbs) recovered drill site, is located at the southern end of the Nicaraguan working area. Md.Baula V with a water depth of 796m is both, the most shallow and with a total recovery rate of 172cm carbonate, the most successful drilled Nicaraguan mound.

-Offshore Costa Rica: Jaco Scarp is situated at the northern edge of the working area and represents with 815m water depth also the most shallow drill site. Mound 12 (979 mbs) is the deepest drilled mound station off Costa Rica and marks also the southern border of the Costa Rican working area.

During our BGS rockdrill attempts we noticed mainly three different kinds of seafloor structures resulting in three types of drillings:

1) only soft sediment visible on seafloor surface - We deployed the BGS rockdrill nevertheless. Most of the drilling was characterized by a high penetration rate (>8-10cm/min) and no hardground or carbonate rocks/stones/clasts were visible in the drilling log. No sample recovery.

2) soft sediment and carbonates occur on the seafloor - low penetration rate of 1-5cm/min, repeated intervals of increased penetration rate of >8-10cm/min. Sample recovery rare.

3) carbonate blocks and –boulders - we observed at this drilling basically very low to low penetration rates only. Intervals of increased penetration rate are rare. Core sample recovery abundant.

A slightly fractured 317cm long coherent carbonate core and a total recovery rate of 387cm carbonate accomplished at Jaco Scarp are the highlights of the BGS rockdrill campaign.

Regarding both working areas, a total of 38 BGS rockdrilling attempts were carried out with a total carbonate core recovery of 835cm. The total drilling recovery related to carbonate mounds is the following:

| | |
|---|---|
| Md.Baula V: | 7 drilling attempts, 172cm carbonate core |
| Md.Perezoso: | 2 drilling attempts, 80cm carbonate core |
| Md.Iguana: | 2 drilling attempts, 73cm carbonate core |
| Md.Culebra: | 4 drilling attempts, 44cm carbonate core |
| Md.Quetzal: | 6 drilling attempts, 36cm carbonate core |
| Md.Baula: | 5 drilling attempts, 21cm carbonate core |
| Mound 12: | 1 drilling attempt, 13cm carbonate core |
| Md.Congo: | 1 drilling attempt, 9cm carbonat core |

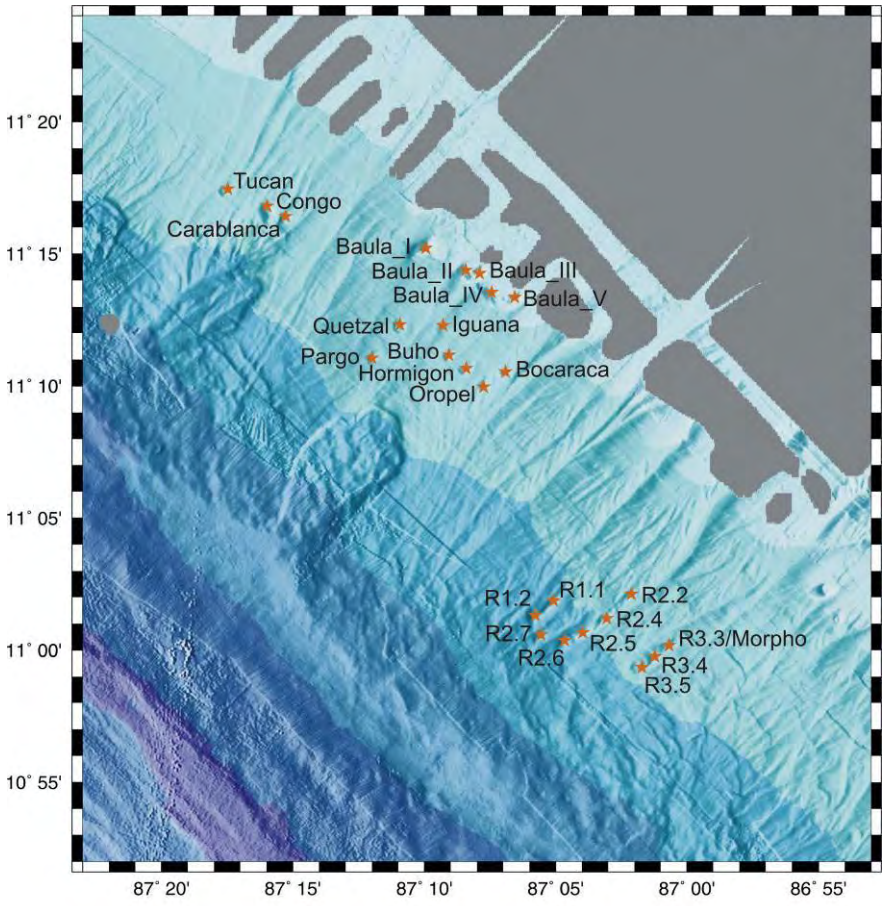


**FIG. 3.3:** Location map of Nicaragua Mound Province.

Many of the recovered cores are highly fractured (up to a drilling breccia) and possess therefore a high amount of gravel and other broken material. The most parts of the stations M66/3-129, -156, -157, -184, -185, -210 and -214 are only slightly to moderately fractured and the best drilling results with a fair to good carbonate core sample quality.

The recorded data of penetration vs. time of the BGS rockdrilling result in an advanced knowledge about the thickness and distribution of known carbonate coverage. The carbonate thickness is less than expected from OFOS and ROV observations. In addition the distribution of carbonate pavements is much smaller than indicated by geophysical data.

Looking at the BGS rockdrill localities we notice that we recovered less fractured and more continuous core samples from shallow stations like the Nicaraguan Mounds Perezoso (80cm core) and Baula V (90cm core) as well as the 317cm core from Jaco Scarp (Costa Rica area). All these stations have a similar depth of about 800m bsl. Only exception from a deeper station where we recovered one continuous core sample is Mound Iguana (65cm core) at 1225m bsl water depth. From previous OFOS observations we know that mounds offshore Nicaragua are generally larger than those off Costa Rica. This fits with our investigations from Nicaraguan drill sites compared to Mound 11a,b and Mound 12 from Costa Rica. So chances to recover carbonate cores seems to be much higher offshore Nicaragua. Although we have to take into account that we drilled 9 sites in Nicaragua and 4 Costa Rican sites only. The shallower mounds and carbonate structures seem to be more dense and solid and more suitable for the BGS rockdrilling device.

The carbonate core M 66/3-210 and -214 were both drilled at the top of the Jaco Scarp formation. We found fossil vestimentiferan tubeworms cemented inside the grey carbonate layers. These tubeworms are the fossil ancestors of living tubeworm fauna colonies from the deeper part of the Jaco Scar formation. The tubeworm colonies were observed during previous Alvin dives and also at coring attempts with BGS vibrocorer. Considering this observation we are able to show for the first time that Jaco Scar is a previously unaccounted site of fluid dewatering caused by seamount subduction.

The thickness and distribution of carbonate coverage on mounds is not as abundant as interpreted by OFOS and ROV seafloor observations. Previously collected and interpreted side-scan sonar data show extensive high reflectivity (backscatter) on or around the topography of the outcropping mounds. During all of our drilling attempts we selected sites inside these backscatter anomalies and drilled every time several meters deep (up to the max. penetration depth of 5m). We never found hardground, massive carbonate or buried carbonate layers where soft sediments were visible on the seafloor only. We came to the conclusion that at type 1 stations the high backscatter is not caused by or necessarily associated with the occurrence of (massive) authigenic carbonates hidden under a thin layer or inside the sediment.

At Type 2 drillings we observed a low penetration rate with repeated intervals of high penetration. This leads to the interpretation that there are carbonate layers with intermediate layers of soft sediment or extended voids. Also possible are bigger carbonate rocks and -stones inside the soft sediment that got hit by the drilling bit. An alternative explanation is drilling through soft sediments with intermediate layers of consolidated clay clasts. But because of the rare carbonate sample recovery and the total missing of mixed consolidated/soft sediment samples as well as continuous core samples, open questions remain. We found soft sediment with intermediate layers of semicemented to hard carbonate granules and pebbles in some of the BGS vibrocores. But these granules and pebbles formed not coherent solid layers instead these were loosly connected. Also observed were the semi consolitated/compacted clay clasts in some of the vibrocores and Gravity Cores.

Summarising all the observations we come to the conclusion that the carbonate coverage on mounds is not as continous, solid and thick as interpreted before. The carbonates consist mostly of blocks/rocks and stones, highly porous material with voids and cracks. Only at type 3 stations the carbonate material, consisting of bigger blocks and boulders, is dense and solid enough to be drilled and recovered.

### 3.4.4 Marine Tephras offshore Southern and Central Middle America – preliminary results from METEOR cruise M66/3

In Central America and other regions on Earth, highly explosive, plinian volcanic eruptions generate buoyant eruption columns rising 20-40 km high into the atmosphere up to the level of neutral buoyancy where they spread laterally (Kutterolf et al. 2006). The Central American Volcanic Arc (CAVA), an area with one of the largest densities of active volcanoes in the world, cause eruption clouds drifting to the West with the prevailing wind and gradually drop their ash load over areas up to $10^6$ km$^2$ in the Pacific Ocean (Fig. 3.4). The CAVA formed in response to subduction of the Cocos plate beneath the Caribbean plate since the late Cretaceous.

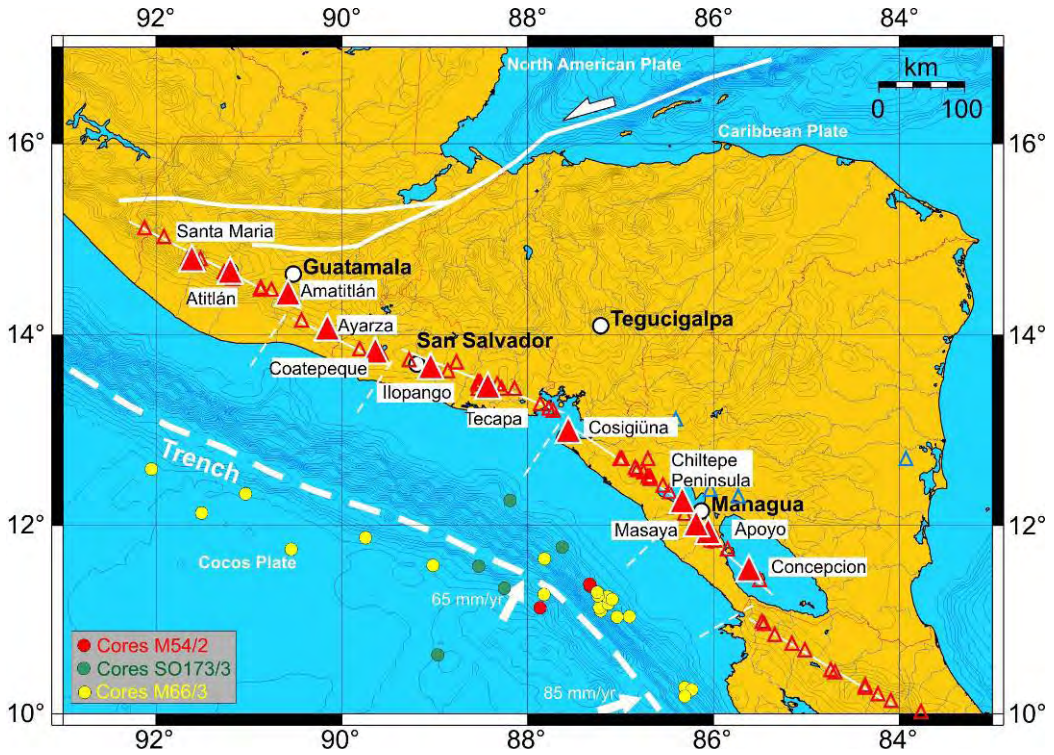


**FIG. 3.4:** Overview map of Middle and Central Middle America with core locations of M66/3, M54/2 and SO173/3.

Ash layers are best preserved in non-erosive marine or lacustrine environments and therefore provide the most complete record of volcanic activity. Wide aerial distribution across sedimentary facies boundaries, near-instantaneous emplacement, chemical signatures, facilitating stratigraphic correlations and the presence of minerals suitable for radiometric dating make ash layers excellent stratigraphic marker beds for marine geoscience (Kutterolf et al. 2006). Therefore marine ash layers of M66/3a are used to date submarine erosion and deposition processes, submarine mound structures, and submarine landslides. Marine tephrostratigraphy also provides constraints on the temporal evolution of both, the volcanic source region and the ash-containing sediment facies, and should be a good feature to correlate different sediment successions from on-land and marine environments of the whole Central American region with each other. The latter was the major goal of the second leg of the M66/3 cruise.

Due to sedimentation conditions gravity cores of 6 to 9 m length reach only up to 7 m depth in soft sediments. Therefore, tephrostratigraphy is limited to ages of around $10^6$ years concerning evaluated sedimentation rates of *c.* 6 cm/ka at the incoming plate and *c.* 20 cm at the slope

(Kutterolf et al. 2006). At the first part of the cruise (M66/3a) only slope sediments have been sampled, whereas in the second leg (M66/3b) mainly the sediments from the incoming plate have been the targets.

Visual identification of ash layers is easy when the ash forms mm to cm thick distinct and undistorted layers. In slope settings, however, mass wasting processes redistribute ashes and therefore visual recognition in core sections can be difficult and many ash lenses occur within the core. If these ash lenses that are concentrated in confined areas of the core and the compositions are unique, insitu reworking of ash layers can be assumed with nearly no offset regarding the stratigraphic location of the primary ash layers.

Core logging techniques allow identifying both, distinct layers, and dispersed ashes in marine sediment cores, prior core description. Standard core logging parameters include P-wave velocity, density from gamma attenuation and magnetic susceptibility. Logging the magnetic susceptibility of ashes could closely be linked to density values of marine ashes. Bulk slice samples are easily cut from ash layers with thickness in the cm-range whereas samples from very thin ash layers are usually mixed with sediment. Even primary fallout layers usually contain some biogenic and clastic debris. Thus Laboratory techniques need to be employed to separate the volcanic material before geochemical analyses.

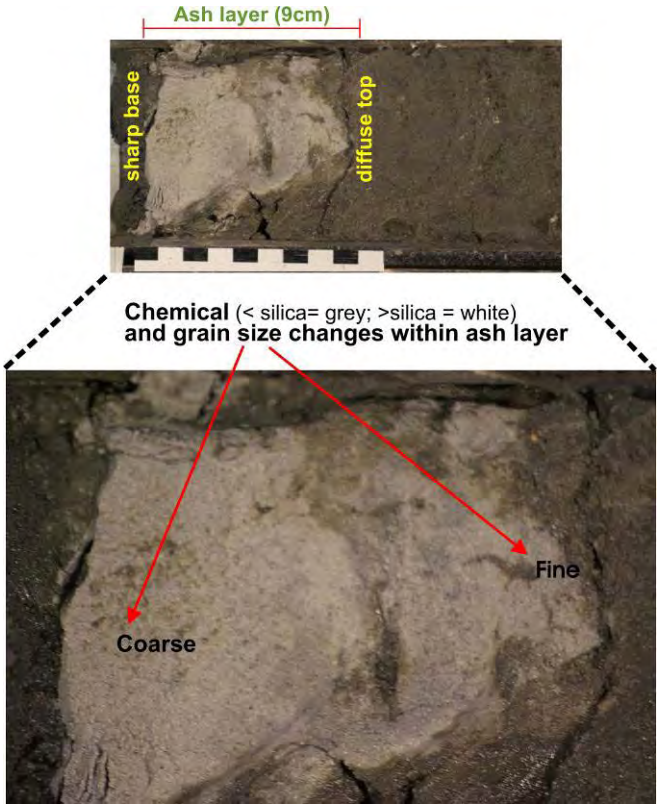


**FIG. 3.5:** Detail picture of prominent ash layer from core M66/3-179 with sharp base and diffuse top. The 8-cm-thick ash layer shows gradation from coarse ash to fine ash and an interbedded horizon with grayish ash material

Petrographic, structural studies and compositional data - including mineral assemblages, mineral and glass compositions obtained by electron microprobe and LA-ICP-MS - as well as bulk rock chemistry, are used for correlations between marine and onland tephras. Micro analytical methods of glass shards may also allow detecting components of compositional zoning of magma chambers or of ash beds containing material from different eruptions mixed by reworking. Potassium-bearing minerals can be used for single-crystal $^{40}Ar/^{39}Ar$ dating at ages greater than $10^4$ years. Dating of younger ash layers is based on constraints from the interbedded sediments, or $^{14}C$-ages as determined from organic material of correlated tephra on land. Another possibility for dating is thermoluminescence dating, where the amount of radiation from background sediment that affected the glass shards during the time of storage at the ocean bottom, is determined and transferred to depositional ages. All ash layers were sampled for further chemical and petrographic examinations, and especially for thermoluminescence dating.

**TAB. 3.1:** Smear slides description

| Core | Area | Ash layer | Color | Layer borders | Grain sizes | Sediment proportion | Crystall content | Color of glass shards | Glass shards specifications | Minerals (% of total) | Fossils % |
|---|---|---|---|---|---|---|---|---|---|---|---|
| **M66/3-222** | South Salvador | 29-32 | White | sharp base, diffuse top | medium ash | 5-10% | 20% | transparent | > elongated pum remenants, > cuspate and angular shards> y-shards | plag (10-15%), ass: opx, cpx, ap | <1% |
| | | 86-89 | Black | lenses | fine ash | <5% | 5-7% | dark brown | angular | plag (~5%), ass:ol, px | 1-5% |
| | | 91-94 | Black | sharp base, diffuse top | medium ash | ~10% | 2-5% | dark brown | irregular shapes (Hawaiin particles), spheres od sideromelan | plag (2-3%), ass:ol | |
| | | 203-205 | Black | sharp base, diffuse top | medium ash | 5-10% | ~30% | light brown | spheres with round vesicles, | plag (25-30%), ass: ol, px, chlorite, ox | ~20% |
| | | 225-232 | White | sharp base, diffuse top | coarse ash | 1-3% | 1-5% | transparent | elongated pum rmenants = blocky = y-glass shards | plag = px = amph; ass:ap | <1% |
| | | 425-427 | White | sharp base, diffuse top | fine ash | ~10% | 5-10% | transparent | angular > elongated pum remnants | plag (~5%), amph (<1%), ass:ap, px, qz? | <1% |
| | | 436-440 | Gray | sharp base, diffuse top | coarse and fine ash | ~10 | <1% | light brown | trachylite clasts (50%), vesicular sideromelan, angular shards in matrix | plag (5-10%), px(<1%), ass: ol | 1-2% |
| | | 478-480 | light gray | sharp base, diffuse top | fine ash | ~5% | 40-50% | transparent-light brown | elongated pum remnants = blocky = y-structures | plag (>30%), ass:px, ap | 1-2% |
| | | 517-518 | Black | lenses | coarse to medium ash | ~5% | 2-5% | pale brown > transparent | elongated pum remnants = blocky = y-structures | plag (2-3%) | ~5% |
| **M66/3-223** | Middle Salvador | 0-8 | White | lenses | medium ash | ~5% | 8-11% | transparent | elongated pum remnants = blocky = y-structures | plag (8-10%), <1% amph | 3% |
| | | 65-68 | Black | sharp base, diffuse top | coarse ash | ~5% | 1-5% | dark brown | moderatley vesicular glass > some elongated pum remnants | plag (10-20), px, ass:ol | ~5% |
| | | 93-98 | White | sharp base, diffuse top | medium ash | <1% | ~3% | transparent | elongated pum remnants = blocky = y-structures | plag (~2%), <1% other (opx, ol, amph) | <1% |
| | | 122-125 | Black | sharp base, diffuse top | coarse and fine ash | <1% | 10-15% | dark brown | > elongated pum remenants, > blocky and angular shards | plag (1-5%), px (<1%), ass: ap | <1% |
| | | 153-155 | Gray | sharp base, diffuse top | medium ash | <1% | 2-3% | pale brown > transparent | moderatley vesicular glass > some elongated pum remnants | plag (2%), ass:px | ~5% |
| | | 185-187 | light gray | lenses | medium to fine ash | 30% | ~2% | transparent | elongated pum remenants = blocky and angular shards > y-shards | plag (1-2%) | ~5% |
| | | 202-204 | Gray | sharp base, diffuse top | medium ash | ~15% | 10% | pale brown > transparent | moderatley vesicular glass > some elongated pum remnants | plag (1-5%), px (<1%), ass: ap | 5-10% |
| | | 205-206 | Gray | sharp base, diffuse top | | 60% | 10% | light brown | moderatley vesicular glass > some elongated pum remnants | plag (1-5%), px (<1%), ass: ap | ~10% |
| | | 227-234 | Gray | lenses | coarse ash | 40-50% | 10% | light brown | moderatley vesicular glass | plag (~1%), ass: ol, px | <1% |
| | | 245-246 | Gray | lenses | fine ash | 50-60% | <5% | transparent>light brown | elongated pum rmenants = blocky | plag (1-2%) | ~5-10% |
| | | 303 | Gray | sharp base, diffuse top | fine ash | 20% | 5-15% | light brown | moderatley vesicular glass, blocky shards > elongated pum remnants | plag (5-10%), px(<1%), ass: ol | |
| | | 305 | Black | sharp base, diffuse top | coarse and fine ash | 5% | 10-20% | dark brown | moderatley vesicular glass, blocky shards >> elongated pum remnants | plag (10%), px(<1%), ass: ol | |
| | | 378 | Black | lenses | fine ash | ~50% | <2% | pale brown > transparent | rounded sideromelan shards>> vesicular elongated pum remnants | plag (~1%), ass: ol, px | ~5% |
| **M66/3-225** | South Guatemala | Core catcher | White | lenses | fine ash | <1% | 5-10% | transparent | elongated pum remnants = blocky = y-glass shards | plag (1-5%), px (<1%), ass: ol | |

| | | | | | | | | | | | |
|---|---|---|---|---|---|---|---|---|---|---|---|
| **M66/3-226** | South Guatemala | 16 | light gray | lenses | medium ash | 60% | 2-5% | transparent | > elongated pum remenants, > cuspate and angular shards> y-shards | plag (1-2%), ass: px, ol | 10-20% |
| | | 47-48 | White | lenses | coarse to medium ash | <1% | 2-5% | transparent | >> elongated pum remenants, > cuspate and angular shards> y-shards | plag (~2%), <1% other (bi, px) | |
| | | 57-61 | Gray | sharp base, diffuse top | coarse ash | 10-15% | 1-5% | pale brown > transparent | moderatley vesicular glass = blocky > some elongated pum remnants | plag (~2%), <1% px, ol | ~20% |
| | | 61-63 | light gray | sharp base, diffuse top | fine ash (some coarse) | <1% | 5-10% | transparent>>light brown | elongated pum remenants, = cuspate and angular shards = y-shards | bi (~5%), 1-2% plag, <1 % amph | 1-2% |
| | | 68-72 | White | sharp base, diffuse top | coarse ash | <<1% | 1-2% | transparent | > elongated pum remenants, > cuspate and angular shards> y-shards | plag (~1%), ass: amph | |
| | | 74-79 | White | sharp base, diffuse top | coarse ash | ~3% | ~5% | transparent | cuspate and angular blocky shards > y-shards > elongated pum remenants | crystall, Hyph? (2-3%), plag (<1%), bi (<1%), ass: amph | <1% |
| | | 84-88 | Gray | sharp base, diffuse top | coarse ash | 70% | 1-5% | transparent-light brown | elongated pum remenants = blocky and angular shards > y-shards | plag (~1%); ass: px | ~10% |
| | | 104 | White | sharp base, diffuse top | coarse ash | <1% | 5-10% | transparent | elongated pum remenants >> blocky and angular shards > y-shards | bi (~5%), 1-2% plag, <1 % amph, ass: qz? | |
| | | 109 | white-light gray | sharp base, diffuse top | coarse and fine ash | <1% | ~10% | transparent | > elongated pum remenants, > cuspate and angular shards> y-shards | bi (~5%), 1-2% plag, <1 % amph, ass: px, qz? | |
| | | 120-122 | greenish gray | sharp base, diffuse top | coarse ash | 50% | 0-2% | light brown > transparent | moderatley vesicular glass > some elongated pum remnants | plag (~1%); ass: qz? | 5-10% |
| | | 134-137 | Dark gray | sharp base, diffuse top | coarse and fine ash | 10% | ~1% | light brown > dark brown | moderatley vesicular glass | plag (~1%), ass:ol | |
| | | 154-157 | Black | sharp base, diffuse top | medium ash | 5-10% | 1-2% | light brown > dark brown | moderatley vesicular glass > some elongated pum remnants | plag (~1%) | <5% |
| **M66/3-227** | North Guatemala | 0-30 | greenish gray | lenses | fine ash | 60% | <1% | transparent | elongated pum remnants = blocky = y-structures | plag, amph | ~30% |
| **M66/3-228** | North Guatemala | 67 | greenish black | lenses | medium ash | 80% | <1% | transparent | moderatley vesicular glass > some elongated pum remnants | plag, amph | ~20% |
| | | 147-151 | greenish gray | diffuse | coarse and fine ash | <5% | ~1% | dark brown | elongated = blocky = y-structures | plag (~1%), ass:px, ol | <1% |
| | | 151-157 | White | sharp base, diffuse top | coarse ash | <1% | <1% | transparent | > elongated vesicular > cuspate and angular shards> y-shards | plag (~1%), ass:qz, bi, amph | <2% |
| | | 225-229 | White | sharp base, diffuse top | medium ash | ~5% | ~2% | transparent | > elongated vesicular, > cuspate and angular shards> y-shards | plag (~1%), amph (~1%), ass:bi, qz | 5% |
| | | 239-246 | White | sharp base, diffuse top | fine ash | ~3% | <1% | transparent | cuspate and angular shards> elongated pum remenants, > y-shards | plag, bi, amph | <1% |
| | | 292-293 | White | sharp base, diffuse top | coarse ash | <1% | 2-3% | transparent | elongated pum remenants = blocky and angular shards > y-shards | plag (~1%), amph, bi (~1%), ass: px | |
| | | 298-297 | White | sharp base, diffuse top | coarse and fine ash | <10% | <1% | transparent | elongated pum remenants = blocky and angular shards > y-shards | plag (~1%), ass: amph, bi, px | <1% |
| | | 312-311 | White | sharp base, diffuse top | medium ash | <1% | ~5% | transparent | elongated = blocky and angular shards > y-shards> vesicular | plag (~2%), bi (~2%), ass: amph, px | |
| | | 315-313 | White | sharp base, diffuse top | coarse to medium ash | <1% | ~5% | transparent | > elongated vesicular, > cuspate and angular shards> y-shards | plag (~2%), bi (~2%), ass: amph, px | |

| | | | | | | | | | | | |
|---|---|---|---|---|---|---|---|---|---|---|---|
| | | 317-315 | White | sharp base, diffuse top | coarse ash | <1% | 10-15% | transparent | > elongated vesicular, > cuspate and angular shards> y-shards | plag (~5%), bi (~5%), amph (1-2%), ass: px | |
| | | 376-377 | white-greenish | sharp base, diffuse top | fine ash (some coarse) | ~75% | <1% | transparent | cuspate and angular shards> elongated pum remenants, > y-shards | Plag | ~20% |
| | | 387-390 | Dark gray | sharp base, diffuse top | coarse ash | <10% | 1-2% | dark brown | cuspate and angular shards, vesicular > elongated pum remenants, > y-shards | plag (~1%), px (<1%), ass:ol | <1% |
| | | 443-451 | White | sharp base, diffuse top | fine ash | <1% | ~1% | transparent | > elongated vesicular, > cuspate and angular shards> y-shards | plag (~1%), ass: bi, px | |
| **M66/3-229** | Middle Guatemala | 51 | greenish gray | lenses | medium ash | ~75% | <<1% | light brown > transparent | cuspate and angular shards> elongated pum remenants, > y-shards | Plag | ~15% |
| | | 352-361 | White | sharp base, diffuse top | coarse ash | 1-2% | 1-2% | transparent | elongated pum remenants = blocky and angular shards > y-shards | plag (~1%), ass: bi, amph, px | |
| | | 409-411 | White | lenses | fine ash | 2-3% | 2-3% | transparent | > elongated > cuspate and angular shards> y-shards> vesicular | plag = amph = bi = px | |
| | | 422-426 | White | sharp base, diffuse top | fine ash | <1% | ~2% | transparent | cuspate and angular shards> elongated > y-shards> vesicular | plag (1-2%), ass: amph, bi, px | |
| | | 429-435 | Black | sharp base, diffuse top | fine ash (some coarse) | <5% | ~1% | light brown > dark brown | cuspate and angular shards= vesicular = elongated pum remenants = y-shards | plag (~1%), ass: px, ol | <1% |
| | | 524-534 | White | sharp base, diffuse top | coarse ash | <1% | ~2% | transparent | cuspate and angular shards> elongated > y-shards> vesicular | plag (~1%), bi (~1%), ass:px, amph | |
| **M66/3-230** | North Salvador | 203-207 | Black | sharp base, diffuse top | fine ash (some coarse) | <5% | 1-2% | light brown > dark brown | cuspate and angular shards= vesicular = elongated pum remenants = y-shards | plag (~1%), ass:px, ol | <1% |
| | | 213-219 | light gray | sharp base, diffuse top | fine ash (some coarse) | <1% | ~1% | transparent | > elongated vesicular, > cuspate and angular shards> y-shards | plag (~1%), ass: bi, px | <2% |
| | | 228-229 | White | sharp base, diffuse top | coarse ash | <1% | 2-3% | transparent | cuspate and angular shards= vesicular = elongated pum remenants = y-shards | plag (~1%), bi (~1%), ass: amph, qz | |
| | | 272 | White | sharp base, diffuse top | medium ash | <1% | ~2% | transparent | cuspate and angular shards= vesicular = elongated pum remenants = y-shards | plag (~1%), bi (~1%), ass: amph, px, qz | |
| | | 274-273 | White | sharp base, diffuse top | coarse ash | <1% | 2-5% | transparent | angular and vesicular>> elongated pum remenants = y-shards | plag (~2%), bi (~2%), ass: amph, px, qz | |
| | | 347-360 | White | sharp base, diffuse top | medium ash | <1% | 1-2% | transparent | angular >> vesicular and tubular = y-shards | plag (~1%), amph (~1%) ass: qz, px | |
| | | 358-362 | White | sharp base, diffuse top | coarse ash | <1% | <1% | transparent | elongated pum remenants = blocky and angular shards > y-shards | plag (~1%), ass: amph, bi, px | |
| | | 396 | White | sharp base, diffuse top | fine ash (some coarse) | <1% | <1% | transparent | vesicular and tubular or angular > elongated = y-shards | plag (~1%), ass: bi, px | |
| | | 399 | White | sharp base, diffuse top | medium ash | <1% | <<1% | transparent | tubular to elongated >> vesicular | plag (~1%), ass: amph, bi, px | |
| | | 412-415 | White | sharp base, diffuse top | fine ash (some coarse) | <1% | ~10% | transparent | vesicular and tubular or angular > elongated = y-shards | plag (3-5%), bi (~2%) amph (~1%) | |
| | | 436 | White | lenses | medium ash | 3-5% | <1% | transparent | elongated and angular and tubular | plag (~1%), ass: amph, bi, px | |
| | | 468-471 | White | sharp base, diffuse top | medium ash | <1% | <<1% | transparent | blocky and angular shards > y-shards | plag (~1%), ass: amph, bi | ~5% |
| | | 472-475 | White | lenses | coarse ash | 10-15% | <<1% | transparent | blocky and angular shards > y-shards > tubular and vesicular | plag (~1%), ass: amph, bi, px | ~10% |

### 3.4.5 Sediment Analyses and Seismic Investigations on submarine Landslides offshore Nicaragua and Costa Rica (Pacific)

Since bathymetry data, collected by former cruises M54 and SO173, revealed many individual slope failures along the erosive continental margin off Costa Rica and Nicaragua, a major goal of METEOR cruise M66/3 was the investigation of submarine landslides.

Slides along the Central American (CA) subduction zones should be predominantly characterized by the different geological settings. Nicaragua with a morphologically smooth incoming plate, penetrating deeply into the lithospheric mantle, should have different effects on slope stabilities and therefore the formation of slides, than the area offshore Costa Rica with a rough, seamount dominated subducting plate and a flat subducting angle. Another driving force for slope failures is an overloading by sediments. Since the geological settings in the study area are different, sediment input on the slope of Nicaragua and Costa Rica is variable as well. Explosive volcanism in Nicaragua produces large amounts of ashes that are rapidly deposited on the slope. In contrast Costa Ricas recent volcanism is less explosive and sediments are dominated by terrigenous input from the continent. Comparing the slides of these different areas and also incorporating the changing geological settings (input, slope angle, tectonic, morphology, seismic activity) in our considerations is therefore one major goal of this study.

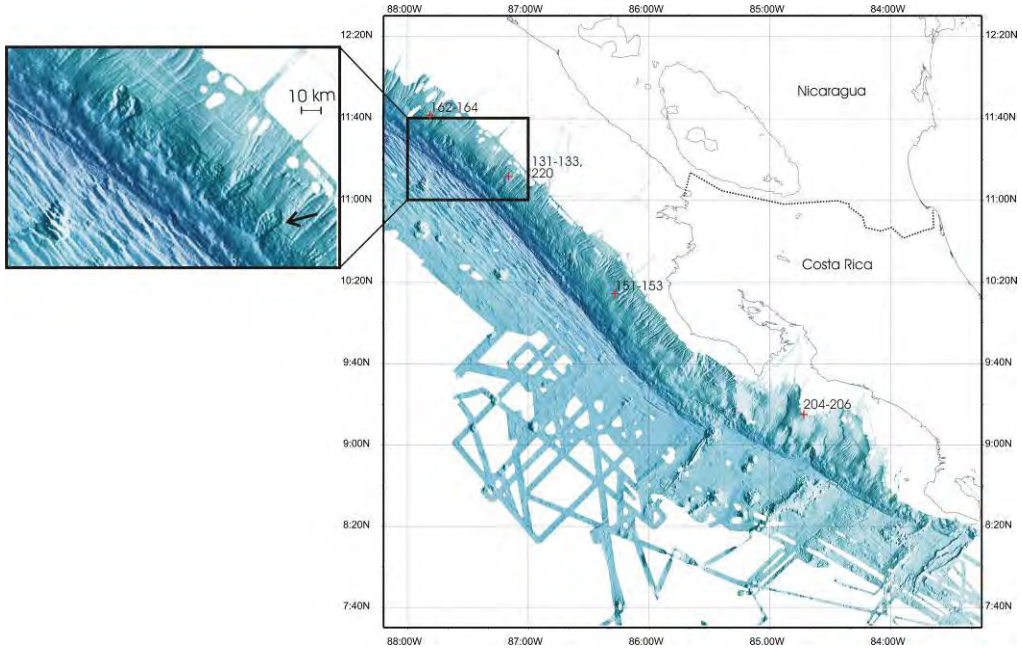


**FIG. 3.6a:** Continental margin along Costa Rica and Nicaragua: Numbers and crosses mark core stations (see Table 1).

**FIG. 3.6b:** Inset: Masaya Slide(little arrow) at water depth around 2000-3000 m and unnamed neighbouring slides to the north west.

Another focus will be the identification of weak layers within the sediment successions that can act as sliding planes and the evaluation of their relevance for slope destabilization during earthquakes or volcano activities. Therefore the work is going to include analyses of physical and sedimentary properties from sediments of the slide areas and their undisturbed surroundings.

For this purpose a total of four submarine landslides on the continental slope of Costa Rica and Nicaragua were chosen during the cruise M66 3a/3b. PARASOUND data of each slide were

recorded and 13 gravity cores were taken. Determination of some physical properties, analyses of pore water chemistry as well as core photography and core description were done immediately on board. From locations offshore Nicaragua in the north to the south off Costa Rica the slides were named Telica, Masaya, Hermosa and Lira Slide (Fig. 3.6, Tab. 3.2).

**TAB. 3.2:** Locations of slides with extension, headwall sizes, core numbers and water depths.

| Name | Location | Station No. | Size | Headwall | Water depth |
|---|---|---|---|---|---|
| Telica | 11:39.19/87:49.49 Nicaragua | 162-164 | 1.5x 1. 5km | 40m | 2400-2600m |
| Masaya | 11:09.07/87:13.22 Nicaragua | 131-133, 220 | 12x6km | 100-150m | 1600-3700m |
| Hermosa | 10:12.35/86:18.07 Costa Rica | 151-153 | 9x3km | 25m | 1900-2500m |
| Lira | 9:12.18/84:44.03 Costa Rica | 204-206 | 3.5x1.5km | 30m | 500-700m |

The continental slope off Nicaragua differs from Costa Rica not only in tectonic setting, but also in average slope angles. Especially within the critical water depth of 1000 to 3000 m where the majority of slides occur one can find a typical decrease in the angles from Nicaragua to Costa Rica (Fig. 3.7).

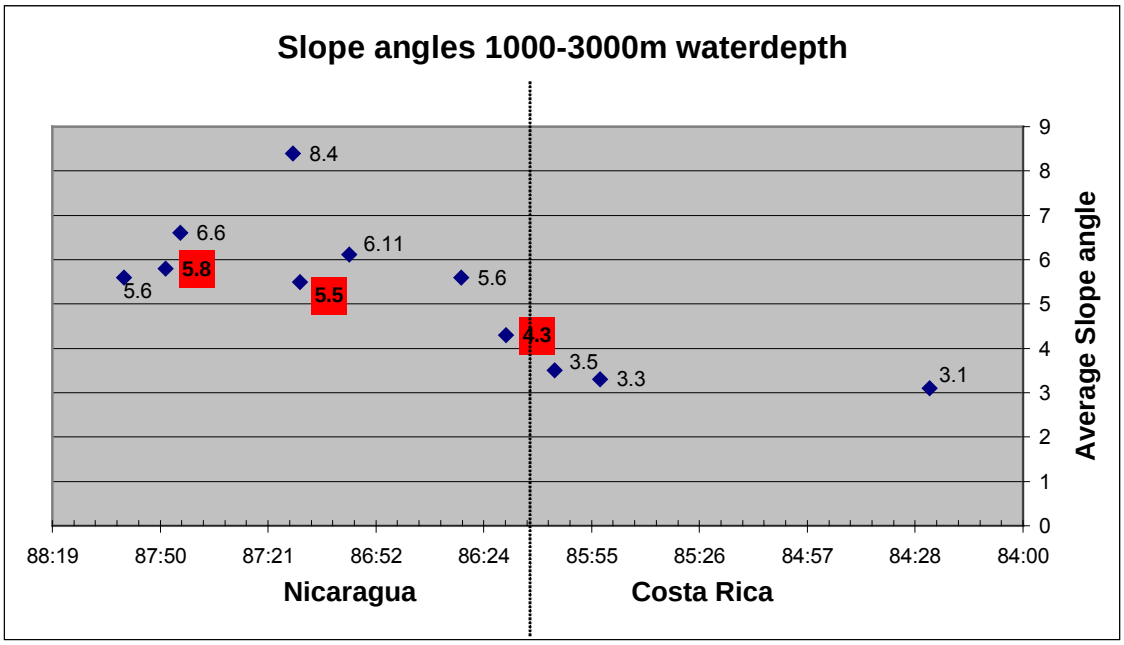


**FIG. 3.7:** Average slope angles of fshore Nicaragua and Costa Rica in water depths between 1000-3000m. Numbers in red are slope angles in the nearest surrounding of the slides. Dotted line marks the geographic border from Nicaragua to Costa Rica.

### 3.4.5.1 Masaya Slide

This slide is the largest one investigated (Fig. 3.8). Masaya Slide is located in 2000-3000 m water depth on the steep continental slope offshore Nicaragua in association with several other slides of the same size and shape (inset of Fig.3.6). The headwalls of these neighboring slides are placed in the same water depth. In contrast to the other slides, bathymetry data show a conspicuous fresh shape with sharp distinct edges.

Upslope of Masaya Slide, *c*. 6 km to its northwest, there are two mud mounds that have been named Mound Iguana and Quetzal in former cruises .

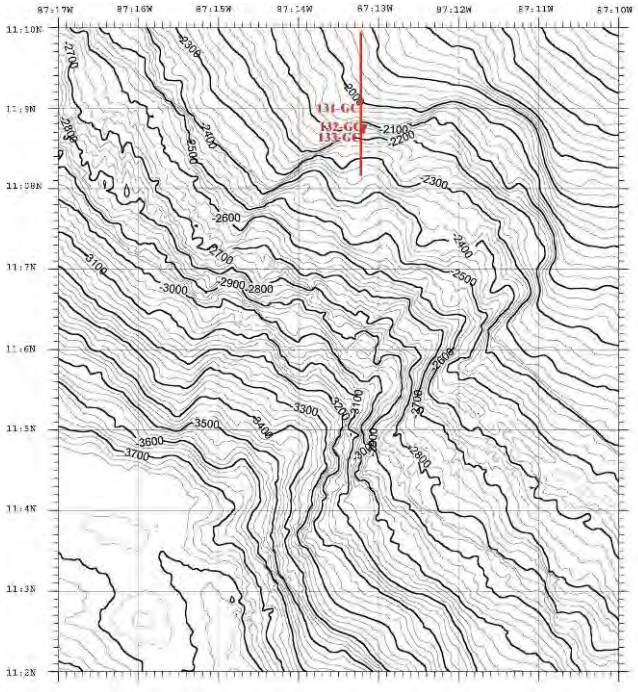


**FIG. 3.8:**
Bathymetric data of Masaya Slide. Vertical line shows the PARASOUND profile at the headwall and the location of coring stations.

Masaya slide appears to be generated by multiple slide events since bathymetry data shows some smaller steps and headwalls on different levels all over the collapsed area (e.g. Fig.3.8).

The average angle of the slope in the area of the headwall is around 5.5°. The headwall is up to 200 m high and the slope angle is about 25°, respectively. Since the data acquisition with the PARASOUND system is difficult on surfaces with an angle greater than 4°, we did not deliver good data for the headwall area. Nevertheless the sonograph in Figure 3.9 shows the surface morphology of the slide and some meters within the sediment succession in vertical resolution.

Four Gravity cores were taken (cores 131-133, 220; see Fig. 3.8) but none of them reached a mélange horizon or a consolidated layer, which indicate a slide plane, respectively.

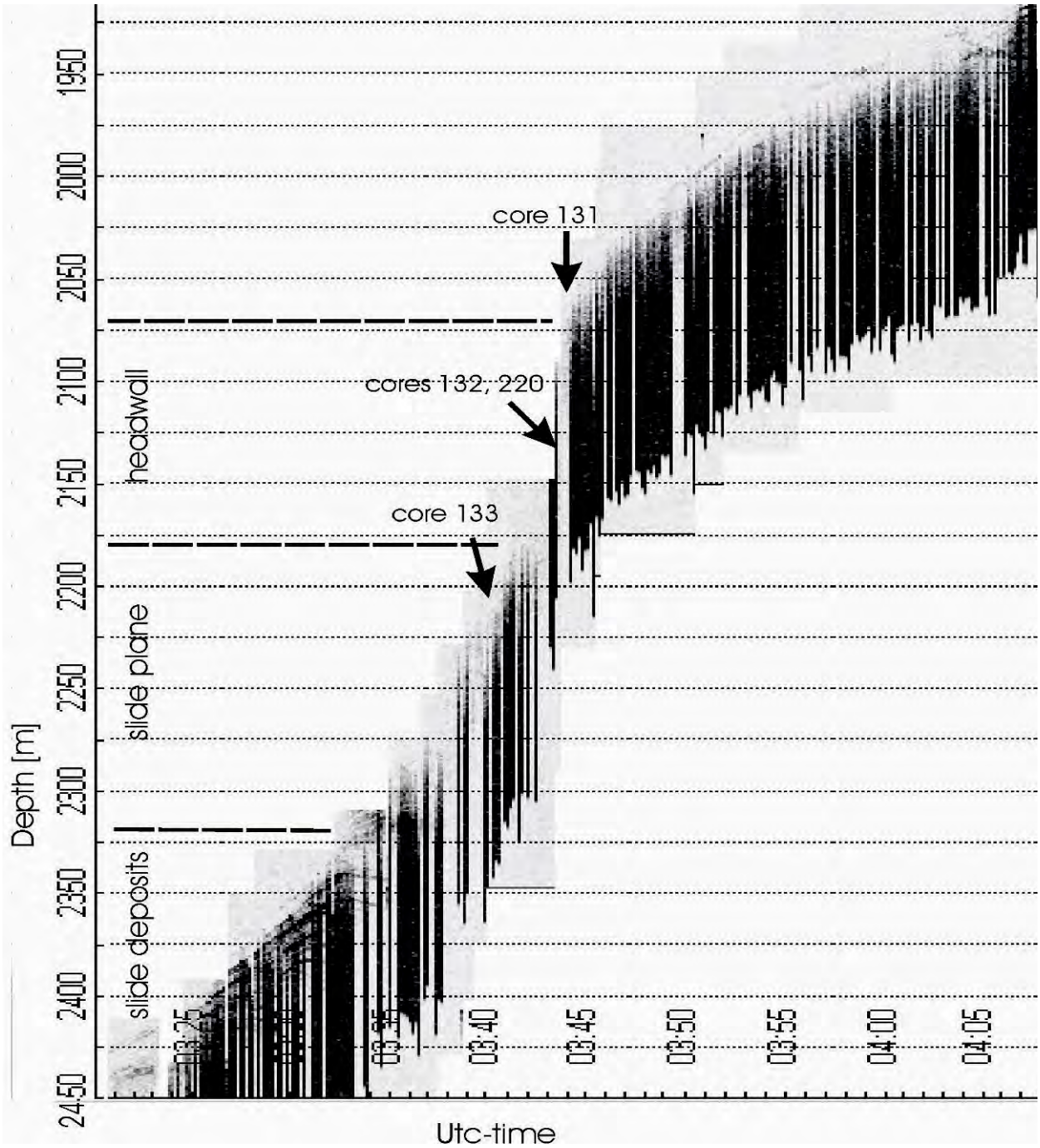


**FIG. 3.9:** PARASOUND image of Masaya Slide and core stations 131-133, 220. The main morphological features are shown on the left side. (Ship velocity ± 2 knots; 5 Minutes of UTC time on the x-axis are ± 300 m).

The cores mainly consist of reworked brown to greyish silty clays with few intercalations of mafic or felsic ash layers. The tephras are more mafic near the top of the core and more felsic near the bottom. In general felsic ash layers are thicker than the mafic ones. Often, they are also associated with an accumulation of foraminifers within the layers. Since, the cores 131-133 and 220 from Masaya Slide look similar only core 132 is shown here in detail. Logging data in Figure 6 show, that the density of the material is increasing typically with depth throughout the core. The only significant change in the gradients is between 2,18 m and 2,30 m concerning values of porosity and shear strength. It can be seen, that shear strength and porosity are acting

inversely proportional to each other. When shear strength is decreasing with depth, porosity is increasing, respectively.

As a first approximation the alkalinity gives information how long digenetic processes have been active in the sediments of the cores. Strong changes within alkalinity suggest a rapid change in sedimentation conditions like it will happen when younger sediment material slides onto older. Together with a sharp change regarding the density gradient, it gives information about possible movements, linear stratification and non-linear stratification, respectively. The cores taken from Masaya Slide did not show any significant gradient changes within alkalinity and shows a continuous increase with depth. This is the usual case in sediments, which are vertically affected by diagenetic processes. The only anomaly which can be observed concerns the gradient for $H_2S$, $NH_4$ and Chloride between 2.18 cm -2.30 cm (bsf). This is within the same depth interval where changes in the values of shear strength, porosity and p-wave velocity can be seen in the logging data.

### 3.4.5.2 Hermosa Slide

This slide located in 1900 to 2500 m water depth (Fig. 3.10). Its headwall is about 25 m high with a slope angle of 12,7°. The surrounding area of the continental slope has an average angle of 5,7°. Eleven kilometers to its northwest, at around 1500 m water depth, there are two mud mounds, called Md. Culebrita and Md. Culebra.

On a larger scale its morphology looks more like an erosion channel caused by terrigeneous sedimentation than a distinct triangle shaped collapsed area comparable to Masaya, Hermosa or Telica Slide. The relatively long and narrow shape as well as the water depth is similar to its neighbouring BGR and GEOMAR slides in the southeast. Lira slide is located on the top of a plateau, which is in the extension of Jaco Scarp, nine kilometres to the southeast.

PARASOUND data from Lira slide show parallel reflectors in the area of the undisturbed layers.

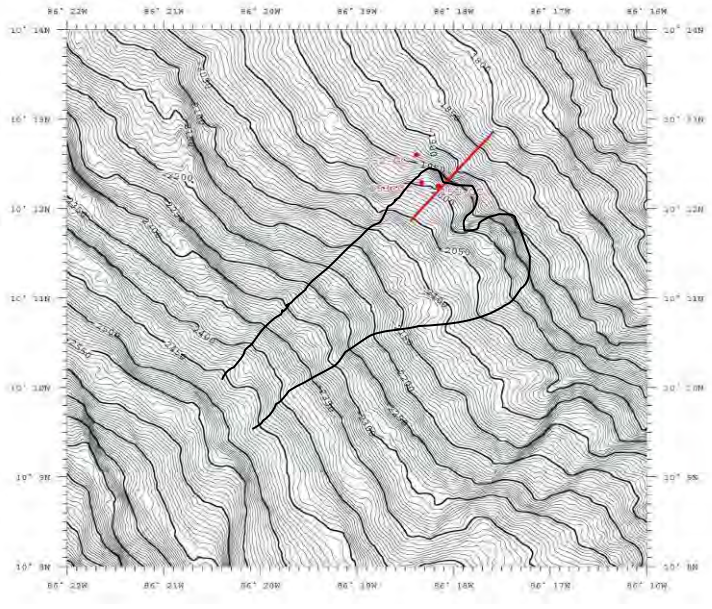

**FIG. 3.10:**
Bathymetry data of Hermosa Slide. The red line shows the conducted Parasound profile and the coring stations. Schematic contour of Hermosa Slide.

The PARASOUND images showed disturbed layers in water depths greater than 2000 m. Sediment layers above the headwall have more parallel reflectors. Nevertheless, in a bigger scale they have a wavy character and can be divided in three units with amplitudes of 300 – 400 m. Core Number 151 was taken in front of the headwall. Cores 152 and 153 were taken from the neighboring areas and are supposed to be reference cores and therefore not described in detail here. Core 151 consists of olive gray silty and clayey layers with embedded ash layers and intercalations of ashe lenses. A unconformity at 147 cm below seafloor is remarkable. In the subjacent bed, a zone of reworked material occurs, which consist of consolidated carbonate mud clasts in a silty to clayey matrix. At the depth of 156 cm this zone is limited by an ash layer having volcanic particles of fine-sand grain size. In the following units a rapid increase in density occurs, which is obvious in the core description as well as in the physical properties.

### 3.4.5.3 Telica Slide

Telica slide has the most indistinct appearance in the bathymetry data, since it is really small and the resolution of the bathymetric data is limited. Nevertheless, it is possible to look for smaller slides like Telica by scanning the continental slope from different points of view. It is reasonable to investigate also these smaller slides since there is a better chance to penetrate a slide plane in smaller slides than in the larger ones, because the overlying sediments are thinner. At Masaya Slide it was impossible to break through the thick overlying deposits. It is also important to understand the processes that cause slides are operating over a variety of scales.

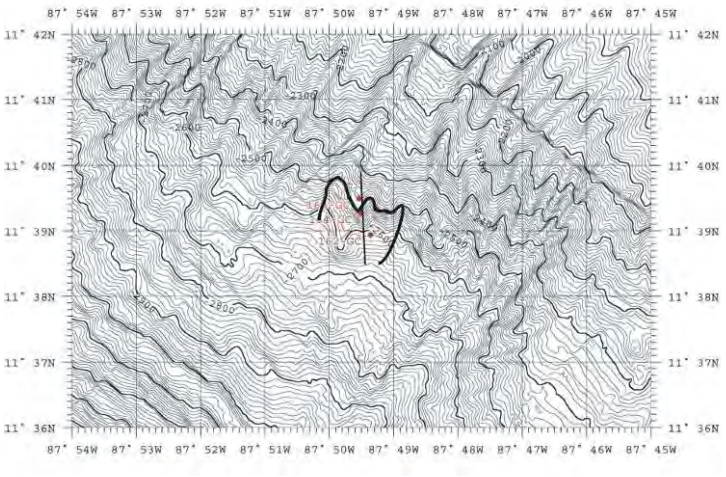


**FIG. 3.11:**
Bathymetry data of Telica Slide with the PARASOUND profile at the headwall and applied core stations. Schematic contour of Telica Slide.

The core location is an approximation since the exact position is difficult to determine due to the movements of the ship and the 2.5 km long rope of the gravity core. This is a common problem with locations situated in water depth greater than 2000 m. Nevertheless, from water depth, lithology, pore water chemistry and logging data it can be assumed that core 164 is located near the headwall.

### 3.4.5.4 Lira Slide

This was the last slide to be sampled during the M66-3 cruise. It is the only one, which had been taken from the erosive continental slope off middle Costa Rica. The continental slope is rough in contrast to Nicaragua and is marked with scars from seamount subduction. Maximum water depths and the deepest parts of the trench respectively are much shallower than offshore

Nicaragua. Average slope angles next to Lira Slide (3 °)are much smoother than in the north of the working area. Lira Slide is located on the upper part of the slope between 500 and 700 m of water depth (Fig. 3.12 a and 3.12 b).

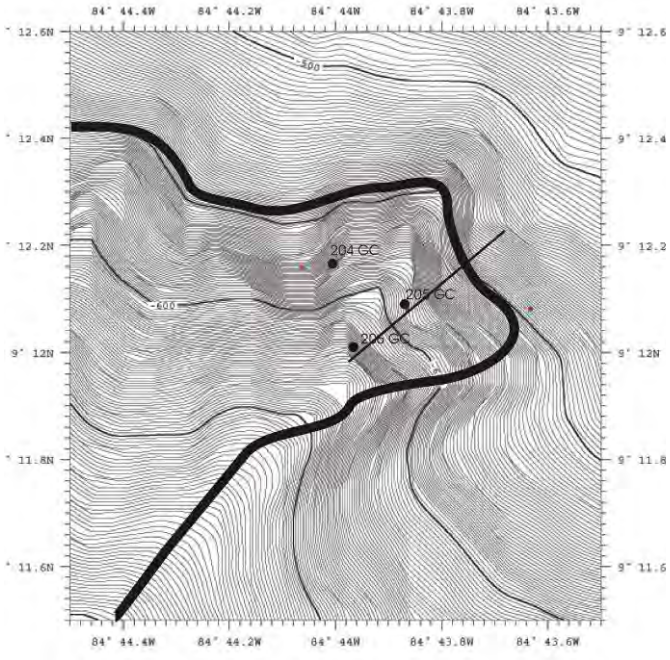


**FIG. 3.12:**
Bathymetry data of the headwall area of Lira Slide with PARASOUND profile and core stations. Schematic contours of the headwall area of Lira Slide.

On a larger scale its morphology looks more like an erosion channel caused by terrigeneous sedimentation than a distinct triangle shaped collapsed area comparable to Masaya, Hermosa or Telica Slide. The relatively long and narrow shape as well as the water depth is similar to its neighbouring BGR and GEOMAR slides in the southeast. Lira slide is located on the top of a plateau, which is in the extension of Jaco Scarp, nine kilometres to the southeast.

PARASOUND data from Lira slide show parallel reflectors in the area of the undisturbed layers (Fig. 3.13).

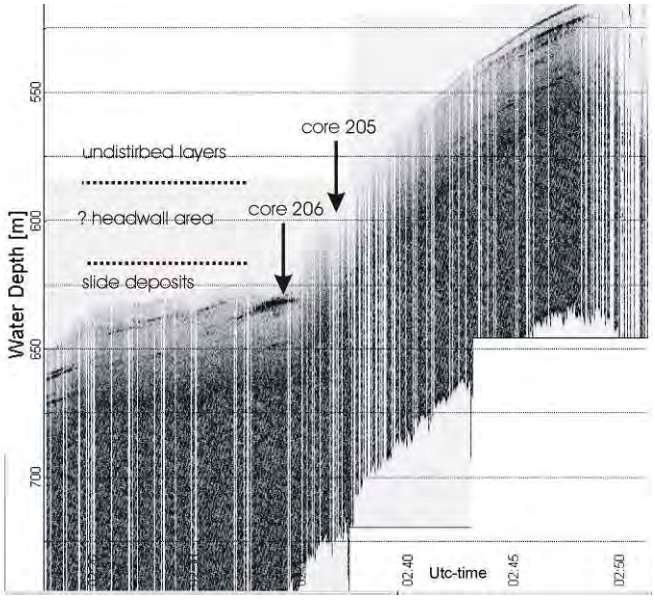


**FIG. 3.13:**
PARASOUND profile over Lira Slide and core stations 205 and 206 with the main morphological features described on the left side. Data of the headwall are incomplete, due to an slope angle of > 2° .(Ship velocity ± 3 knots. 5 Minutes of UTC time on the x-axe are ± 450 m.)

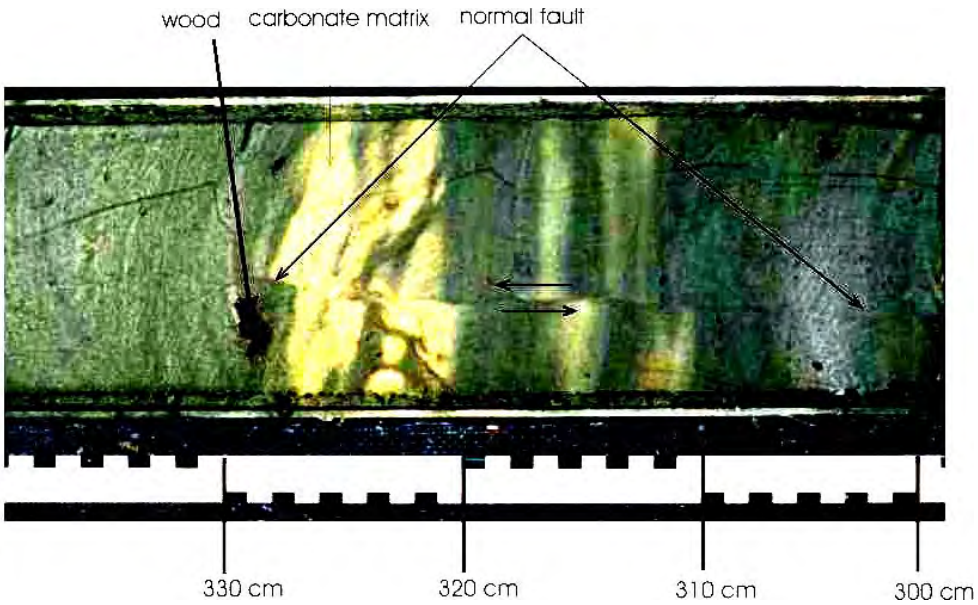


**FIG. 3.14:** Sediment succession between 300 to 340 cm bsf of Core 205 from Lira Slide. An unconformity can be seen that is well developed throughout the whole core showing normal faulting in the sediment layers.

A major result of cruise M66-3a/3b concerning slides is that slide characteristics along the Costa Rican slope differ from slides offshore Nicaragua similarly to the varying slope morphology and tectonic settings. The water depth, where the slides occur is in average much shallower off Costa Rica than at the Nicaraguan slope and in addition, the sediments and their bedding are also more variable. This implicates also, that the trigger mechanisms and pre-failure history of a slide could be different as well. In the following results for each slide are discussed in detail.

*Masaya Slide*

Masaya Slide shows no anomaly regarding the alkalinity gradient, which would represent a discordance in the chronology of the sediment succession and therefore could indicate slide deposits. In contrast, Masaya Slide has typically values for alkalinity regarding the increasing depth, and represents a diagenetic process in undisturbed layers in deeper parts of the core sediments.

Only from bathymetry data it is obvious, that these sediments are not undisturbed. The reason for the relatively inconspicuous physical and chemical properties could be that a gravity core of only about 6 m records no remarkable changes within the sediment succession since Masaya slide deposits are too thick and were not able to be intersected. It can be assumed, that the core caught a thick layer, which collapsed at the headwall and slided as a relatively undisturbed sediment package downslope.

*Hermosa Slide*

Hermosa Slide has a similar morphology like Masaya but is much smaller. Within the PARASOUND profile it is conspicuous that in contrast to Masaya, Hermosa has no slide plane exposed at the surface. Since slide deposits at Hermosa Slide are thinner, they were caught with gravity core 151 and one can see a sharp bend in the gradient for alkalinity. This is an evidence for a slide event, which brought two different sediment units together. In this case alkalinity

increased with a relatively sharp bend and relatively young deposits have been slided over older deposits.

Interpretation of the lithology and physical properties support this assumption. Additionally an ash layer marks the point where density and alkalinity are increasing rapidly. This ash layer is likely to be the slide plane with smaller values in shear strength and higher values for porosity. In the superposed area, intercalated between the ash layer and less denser younger material, a horizon with reworked sediments occurs, marking a melange where both sediment packages have been mixed during sliding.

#### 3.4.5.5 Telica Slide

Bathymetry data of Telica Slide seem to indicate a slide structure with a short run out and a relatively vast headwall area. Physical properties of core 164 show a peak in shear strength and a decreasing porosity simultaneously at around 350 cm bsf. This marks the boarder to a much younger, subjacent sediment body. This interpretation is supported by the alkalinity gradient that also shows a bend with a following reversal of values in that horizon. The explanation for this result could be, that some old material from the slides vertical truncated headwall area dropped in an "after slide event" over fresh and young slide deposits lying in deeper parts of the slide scar. Remarkable are the concentrations for chloride and $PO_4$, which also show a break in their normal diagensis gradients in the similar horizon where the anomalies in physical properties occur. This might represent the exchange of young sediments with salt water before a failure happened. In this core a mafic ash layer between 170 cm to 173 cm bsf has higher shear strength and lower porosity values than its surrounding clayey to silty sediments.

#### 3.4.5.6 Lira Slide

Lira slide is situated at much shallower water depth and had a completely different sediment succession in its cores recovered. Many small discordances were common within the deposits. As the whole structure is smaller and has a more elongated appearance it might be assumed that it is more likely an erosion channel, being highly dependent on terrestric sedimentation.

There are no slides at the continental slope of Costa Rica, which are comparable with the morphology of those found off Nicaragua. Shapes and sizes are less reminding of avalanches than they do offshore Nicaragua. It seems that sedimentation of fC ostaR ica i s m ore inhomogeneous and therefore facilitates more frequent smaller collapse events without creating a triangle shaped large slide scar. In average, the carbonate content is higher within the cores 204-206 offshore Costa Rica compared with cores from Masya, Hermosa and Telica Slide.

### 3.4.6 Sedimentology of Mounds (General physical properties)

In general, the observations made from the material of M 54 and S O 173 have been corroborated: Material extruded off the north of Nicoya Peninsula and Nicaragua is more rigid than material extruded off southern Costa Rica (see cores from Carablanca, Costa Rica). This indicates that the source of the material is deeper in the north.

Information on the thickness of massive carbonate covers on the mound can only be obtained indirectly. On the mounds, the maximum drilling depth achieved was <1.5 m, while Jaco Scar yielded a ~4-m-long core. An indirect conclusion is that the carbonate cover on the mounds is

only partial and that – as far as can be judged from the drilling protocols – softer sediment follows quite soon.

There is no clear trench-parallel trend concerning age and activity. In the south, active structures were only found at Mound 11 (Alvin dives), while in the north there is a close vicinity of more active structures and rather passive structures. For example, Mound Culebrita has almost no hemipelagic cover above extruded material while the cover on Mound Culebra is already ~ 100 cm thick. Another example is Mound Baula, the largest mound off Nicaragua and Costa Rica. None of the cores taken here contained material extruded from deeper sources, while nearby Mound Carablanca is characterized by only thin or no carbonate and sediment covers.

The assumed correlation between carbonate cover, size and activity of the mounds appears to be supported by the new data. Large, heavily "carbonated" mounds are less active than small structures with only a thin or no carbonate cover.

### 3.4.7 Pore Water Geochemistry

*Sampling, processing, and analyses*

Surface sediments were taken using a TV-guided vibrocorer (RDV) from BGS (Edinburgh) and a gravity corer (GC). To prevent a warming of the sediments after retrieval all cores were immediately placed in a cooling room and maintained at a temperature of about 5°C. Each core was cut lengthwise after recovery. Sample intervals between 10-50 cm were taken for pressure filtration. At sampling locations where methane was expected to be present, syringe samples were taken on deck from every cut segment surface. Occasionally, higher resolution sampling for methane analysis was carried out in the cooling laboratory. Syringe samples of 3 ml sediment were injected into 24 ml septum vials containing 9 ml of a concentrated NaCl-solution. Porewater was separated from the sediments using PE-squeezers. The squeezers were operated with argon at a pressure gradually increasing up to 5 bar. Depending on the porosity and compressibility of the sediments, up to 30 ml of pore water were received from each sample. The pore water was retrieved through 0.2 µm cellulose acetate membrane filters.

Dissolved phosphate, silica, ammonia, and sulphide were determined in pore water samples using standard photometric procedures (i.e. Grasshoff, 1997). Sub-samples for nutrient analysis were taken, acidified with HCl and purged with $N_2$-gas for 90 minutes to remove dissolved sulphide prior to analysis. Total alkalinity (TA) was determined by titration with 0.02 N HCl. Most samples were also analysed for dissolved chloride using argentometric titration in order to control the IC results. Methane concentrations were measured using standard GC methods. Acidified sub-samples (35µl suprapure HCl + 3 ml sample) were prepared for ICP analyses of major ions (K, Li, B, Mg, Ca, Sr, Mn, Br, and I) and trace elements. Sulfate, DIC, $\delta^{18}O$ and $\delta^{13}C$ of $CO_2$ will be determined on selected sub-samples in the shore-based laboratories.

*Results and Discussion*

In total, 47 RDVs and GCs were processed and investigated for pore water processes. The results shown below are subdived into 4 subsections with regard to the major goals in the different working areas: (1) Nicaragua Mounds, (2) Costa Rica Mounds, Jaco Scar and Parita Mud Pie, (3) Slide Cores, and (4) Ash cores.

### 3.4.7.1 Nicaragua Mounds

The major focus on M 66/3a was to perform an intense sampling program in the Nicaragua Mounds area and in the vicinity of Mound Culebra off Nicoya Peninsula, northern Costa Rica. In total, 25 cores were taken at Mound Baula, Iguana, Carablanca, Congo, Quetzal, Perezoso, Colibri, Mosquito, and the Mound Ridge off Nicaragua as well as Mound Culebra and Culebrita off northern Costa Rica. The major intention was to identify and sample locations of intense fluid seepage and/or to drill through authigenic carbonate crusts, which were known to occur widespread in the northern Mound areas, in order to get clear information on the specific fluid composition. In particular, it should be tested, if a similar type of deep fluids as unequivocally determined at Mound 11 and Quepos Slide is also expelling and driving mud volcanism in the northern part of the studied area. Data obtained on earlier cruises were not suitable to either prove or disprove this hypothesis.

Deep fluid signatures as known from the sites off southern Costa Rica (Hensen et al. 2004) are typically depleted in chloride and strongly enriched in nutrients, specifically in phosphate and ammonia. Methane fuelling the anaerobic methane oxidation (AOM) in surface sediments is generally produced by the decay of organic matter in deeper sediments. During this process nutrients are released into the pore water. Hence, fluids from the methanogenic zone are usually enriched in dissolved nutrients. In most cases, these sites represent active upward migration of methane-enriched fluids. This is documented by high levels of methane and peaks of alkalinity and hydrogen sulphide within the zone of AOM. Unfortunately, sulphate data are not available yet so that the location of the AOM could not be determined precisely, where plots of alkalinity and hydrogen sulphide are too scattered to allow a good approximation. Gas hydrates could be sampled only at Mound Baula, specifically at stations 134 and 135 larger pieces could be sampled from the cores. In addition, we suspected that small amounts of finely dispersed gas hydrate must have been present at station 139 at Mound Carablanca.

In total, negative chloride anomalies could be observed at all structures with the exception of Mound Iguana and Mound Colibri (Table 1). Considering the potential occurrence of gas hydrate at a some sites, artificial freshening of pore fluids by decomposing gas hydrate cannot be ruled out as reason for these observations. Overall, clear evidence for the advection of nutrient-rich, deep fluids could only be from Mound Perezoso and a couple of locations on the Mound Ridge. At all other sites, low concentrations of nutrients were found indicating that either methane is not transported to the surface with ascending fluids but rather as free gas or that shallow hydrological systems may be active at those locations, mixing bottom waters into the surface sediments so that the chemical signature of the deep fluids is overprinted by the bottom water signature. The latter hypothesis seems to fit better to the observations for two reasons: (1) Gas bubbles escaping from the sediment were not observed at any of the locations and (2) the chloride depletions are less pronounced (i.e. compared to many sites in southern Costa Rica) and appear as continuous curves in the depth plots. Usually, inherent signatures, as for example the chloride depletions, appear as continuously decreasing curves as they reflect the advective upward flow of the fluid and the mixing with seawater by diffusion as they approach the very sediment surface. In contrast, the dissociation of gas hydrates causes more scattered profiles as it may be suggested for some sites at Mound Baula and Carablanca.

Since the majority of the cores show more or less continuous chlorinity plots, we may preliminarily conclude that the observed mineralization processes are largely driven by the advection of deep, chloride-depleted fluids.

**TAB. 3.3:** Chloride anomalies at various Mounds in the northern working area.

| Mound | Chloride Anomaly |
|---|---|
| Congo | ↓ |
| Carablanca | ↓ (Gas hydrate?) |
| Baula | ↓↓ (Gas hydrate) |
| Quetzal | ↓↓ |
| Iguana | no |
| Perezoso | ↓ |
| Colibri | no |
| Mosquito | ↓ |
| Culebra | ↓↓ |
| Culebrita | ↓ |

### 3.4.7.2 Costa Rica Mounds, Jaco Scar and Parrita Mud Pie

Due to the extensive preceding work in the southern working area off Costa Rica, only specific targets were sampled on this cruise. Particularly, we aimed at getting more information on the composition of the fluids expelling at the slide plain of Jaco Scar, a region which turned out to be extremely difficult to sample on past cruises because of the steep slope and out cropping consolidated sediments. Overall 4 cores could be retrieved using the TV-guided vibrocorer. Three of those cores consisted of extremely consolidated, outcropping sediments and could not been sampled for pore water. Although they were located in the vicinity of areas extensively covered by tubeworm and calyptogena associations, they contained no methane and no smell of $H_2S$ was noticed. Obviously, the sites of fluid expulsion are very distinct and irregularly distributed. Only core 190 was possible to sample and showed clear evidence for the advection of deep chloride-depleted fluids.

The pockmark (Mud Pie) located north of seamount subduction of Parrita Scar, was extensively sampled during cruise M66-2 and revisited in order to collect information from deeper layers by using the Rockdrill device (RDV). Two cores (191 and 199) were taken at this structure. Whereas core 191 obviously failed to sample an active site, core 199 recovered about 4 m of gas hydrate bearing sediments. Although gas hydrate was present all over the core and specifically enriched between 1-2 m, the chloride curves show an exponential decrease with depth, indicating - in combination with highly elevated ammonia concentrations – the advection of a deep fluid. As observed at the Jaco Scar site, the exponential decrease of the chloride profile clearly indicates increased levels of upward advection.

Two cores (197 and 213) were taken close to the summit of Mound 12. Up to this cruise, only two cores from the NW-flank of Mound 12 revealed evidence for the advection of chloride-depleted, deep fluids. The whole area southwest of the summit, which is largely covered by bacterial mats and has been extensively studied by lander deployments and TV-multicorer, does

not show any indications of pore water freshening. In contrast, all cores from the nearby-located Mound 11 do show significant negative chloride anomalies. As Mound 12 is supposed to be connected by a NW-SE striking fault this has been extremely puzzling. Cores 197 and 213 were supposed to be located on the extension of the Mound 11 fault and obviously exhibit clear evidence for the advection of chloride-depleted fluids. Inasmuch both types of venting areas at Mound 12 are structurally connected needs to be clarified by future studies.

*Slide Cores*

Pore waters were analyzed from a total of 11 gravity cores taken in the vicinity of slope failures of different dimensions in both, the northern and the southern working area. The slide areas were named Massaya (132, 220), Hermosa (151, 153, 154), Telica (162, 163, 164), and Lira (204, 205, 206). At least in one core of each site, pore water profiles show slight discontinuities indicating small-scale disruptions of the sedimentary sequence. Most interestingly, the core 220 taken on M 663b clearly shows the rise of chloride-depleted fluids (deep fluid signature as at the Mound sites), which allows the conclusion that at least some of the slide events have been triggered by fluid advection as well.

Ash Cores

In total, pore water of all of the six cores from the incoming plate off El Salvador and Guatemala was analysed. As they are located away from active seeping sites and do not receive significant input of organic material from export production, generally indicate low mineralization intensities. Hence, no methane sampling and titration for chloride anomalies was performed on these samples. At several locations, small kinks in the pore water profiles have been observed (i.e. at ~300 cm). These were discussed of either being related to small scale slide events or were caused by compression of the sediment sequence by coring.

## 3.5 List of Stations

**Meteor 66-3** **Station list**

| | | | | Time (UTC) | | | | | Begin / on seafloor | | End / off seafloor | | | |
|---|---|---|---|---|---|---|---|---|---|---|---|---|---|---|
| Date 2005 | St. No. M66 | St. No. Meteor | Instrument | Begin | Start Sci. Program | End Sci. Program | End | Duration hh:mm | Latitude N° | Longitude W° | Latitude N° | Longitude W° | Water depth (m) | Area |
| 27.10.2005 | 113 | 737 | RDR | 14:05 | 14:35 | 15:35 | 16:10 | 02:05 | 11:15.34 | 87:09.83 | 11:15.34 | 87:09.83 | 876 | Md. Baula |
| 27.10.2005 | 114 | 738 | RDV | 17:25 | 18:00 | 18:15 | 18:45 | 01:20 | 11:15.33 | 87:09.83 | 11:15.33 | 87:09.83 | 882 | Md. Baula |
| 27.10.2005 | 115 | 739 | GC | 19:45 | 20:04 | 20:04 | 20:28 | 00:43 | 11:15.58 | 87:09.64 | 11:15.55 | 87:09.68 | 973 | Md. Baula |
| 27.10.2005 | 116 | 740 | RDV | 21:00 | 21:25 | 21:27 | 22:10 | 01:10 | 11:15.30 | 87:09.86 | 11:15.30 | 87:09.86 | 876 | Md. Baula |
| 27.10.2005 | 117 | 741 | RDV | 23:10 | 23:35 | 23:50 | 00:25 | 01:15 | 11:15.29 | 87:09.90 | 11:15.29 | 87:09.90 | 880 | Md. Baula |
| 28.10.2005 | 118 | 742 | RDV | 00:45 | 01:15 | 01:25 | 01:45 | 01:00 | 11:15.29 | 87:09.89 | 11:15.29 | 87:09.89 | 874 | Md. Baula |
| 28.10.2005 | 119 | 743 | RDR | 02:15 | | | 03:55 | 01:40 | 11:15.22 | 87:09.91 | 11:15.22 | 87:09.91 | 874 | Md. Baula |
| 28.10.2005 | 120 | 744 | RDR | 04:30 | 05:32 | 07:14 | 07:40 | 03:10 | 11:15.33 | 87:09.77 | 11:15.33 | 87:09.77 | 874 | Md. Baula |
| 28.10.2005 | 121 | 745 | RDR | 08:45 | 09:25 | 11:15 | 11:49 | 03:04 | 11:15.34 | 87:09.75 | 11:15.32 | 87:09.73 | 872 | Md. Baula |
| 28.10.2005 | 122 | 746 | RDR | 13:00 | 13:45 | 15:03 | 15:40 | 02:40 | 11:15.22 | 87:09.01 | 11:15.20 | 87:09.96 | 864 | Md. Baula |
| 28.10.2005 | 123 | 747 | RDV | 16:15 | 16:40 | 16:50 | 17:40 | 01:25 | 11:12.22 | 87:09.27 | 11:12.10 | 87:09.29 | 1240 | Md. Iguana |
| 28.10.2005 | 124 | 748 | RDV | 18:05 | 18:40 | 18:55 | 19:30 | 01:25 | 11:12.21 | 87:09.29 | 11:12.21 | 87:09.28 | 1230 | Md. Iguana |
| 28.10.2005 | 125 | 749 | RDV | 20:00 | 20:25 | 20:40 | 21:15 | 01:15 | 11:12.28 | 87:09.21 | 11:12.27 | 87:09.21 | 1210 | Md. Iguana |
| 28.10.2005 | 126 | 750 | RDV | 21:40 | 22:40 | 22:35 | 23:20 | 01:40 | 11:12.59 | 87:09.33 | 11:12.49 | 87:09.30 | 1236 | Md. Iguana |
| 28.10.2005 | 127 | 751 | RDV | 23:55 | 00:35 | 00:45 | 01:40 | 01:50 | 11:12.18 | 87:09.22 | 11:12.80 | 87:09.26 | 1226 | Md. Iguana |
| 29.10.2005 | 128 | 752 | RDR | 02:15 | 02:45 | 03:11 | 03:50 | 01:35 | 11:12.21 | 87:09.27 | 11:12.21 | 87:09.27 | 1226 | Md. Iguana |
| 29.10.2005 | 129 | 753 | RDR | 05:20 | 05:40 | 06:55 | 07:50 | 02:30 | 11:12.22 | 87:09.28 | 11:12.22 | 87:09.28 | 1225 | Md. Iguana |
| 29.10.2005 | 130 | 754 | RDR | 08:30 | 09:00 | 09:31 | 10:10 | 01:40 | 11:12.23 | 87:09.28 | 11:12.20 | 87:09.27 | 1225 | Md. Iguana |
| 29.10.2005 | - | 755 | Parasound | 11:06 | | | 12:36 | 01:30 | 11:08.18 | 87:13.16 | 11:09.62 | 87:12.09 | 1830 | ?? |
| 29.10.2005 | 131 | 756 | GC | 13:00 | 13:30 | 13:31 | 14:15 | 01:15 | 11:09.07 | 87:13.22 | 11:09.06 | 87:13.16 | 2017 | Masaya Slide |
| 29.10.2005 | 132 | 757 | GC | 14:38 | 15:14 | 15:15 | 15:50 | 01:12 | 11:08.77 | 87:13.18 | 11:08.77 | 87:13.20 | 2147 | Masaya Slide |
| 29.10.2005 | 133 | 758 | GC | 16:05 | 16:35 | 16:37 | 17:10 | 01:05 | 11:08.71 | 87:13.20 | 11:08.71 | 87:13.20 | 2184 | Masaya Slide |
| 29.10.2005 | 134 | 759 | RDV | 18:00 | 19:05 | | 19:37 | 01:37 | 11:15.30 | 87:09.88 | 11:15.33 | 87:09.35 | 894 | Md. Baula |
| 29.10.2005 | 135 | 760 | RDV | 20:42 | 21:05 | | 22:00 | 01:18 | 11:15.28 | 87:09.87 | 11:15.29 | 87:09.86 | 902 | Md. Baula |
| 30.10.2005 | 136 | 761 | PWPL | 05:48 | | 06:25 | 06:56 | 01:08 | 11:15.58 | 87:09.61 | 11:15.58 | 87:09.61 | 989 | Md. Baula |
| 30.10.2005 | 137 | 762 | RDR | 09:50 | 10:15 | 11:00 | 17:00 | 07:10 | 11:12.25 | 87:10.78 | 11:12.25 | 87:10.78 | 1353 | Md. Quetzal |
| 30.10.2005 | 138 | 763 | RDR | 12:20 | 12:58 | 13:34 | 14:30 | 02:10 | 11:12.36 | 87:10.85 | 11:12.36 | 87:10.65 | 1323 | Md. Quetzal |
| 30.10.2005 | 139 | 764 | RDV | 13:17 | 13:45 | 14:00 | 14:50 | 01:33 | 11:16.42 | 87:15.25 | 11:16.42 | 87:15.23 | 1448 | Md. Carablanca |

| | | | | | | | | | | | | | | |
|---|---|---|---|---|---|---|---|---|---|---|---|---|---|---|
| 30.10.2005 | 140 | 765 | RDV | 15:25 | 16:01 | 16:21 | 17:00 | 01:35 | 11:16.35 | 87:15.16 | 11:16.35 | 87:15.16 | 1465 | Md. Carablanca |
| 30.10.2005 | 141 | 766 | RDR | 17:39 | | | 20:47 | 03:08 | 11:16.35 | 87:15.16 | 11:16.44 | 87:15.30 | 1445 | Md. Carablanca |
| 30.10.2005 | 142 | 767 | GC | 21:08 | | | 21:56 | 00:48 | 11:16.51 | 87:15.32 | 11:11.00 | 87:15.30 | 1442 | Md. Carablanca |
| 30.10.2005 | 143 | 768 | GC | 22:10 | 22:30 | 22:31 | 22:59 | 00:49 | 11:16.49 | 87:15.31 | 11:16.45 | 87:15.30 | 1443 | Md. Carablanca |
| 31.10.2005 | 144 | 769 | GC | 00:10 | 00:23 | 00:24 | 00:40 | 00:30 | 11:15.29 | 87:09.86 | 11:15.31 | 87:09.88 | 893 | Md. Baula |
| 31.10.2005 | 145 | 770 | Parasound | 02:04 | | | 07:51 | 05:47 | 11:08.18 | 87:13.43 | 11:09.90 | 87:12.06 | 2366 | Masaya Slide |
| 31.10.2005 | 146 | 771 | RDV | 21:00 | 21:48 | 22:10 | 23:10 | 02:10 | 10:17.88 | 86:18.37 | 10:17.87 | 86:18.40 | 1528 | Md. Culebra |
| 31.10.2005 | 147 | 772 | RDV | 23:30 | 00:40 | 01:05 | 01:54 | 02:24 | 10:17.86 | 86:18.37 | 10:17.84 | 86:18.34 | 1526 | Md. Culebra |
| 01.11.2005 | 148 | 773 | RDR | 02:38 | 04:10 | 05:23 | 06:12 | 03:34 | 10:17.90 | 86:18.42 | 10:17.84 | 86:18.37 | 1523 | Md. Culebra |
| 01.11.2005 | 149 | 774 | RDR | 06:45 | 08:13 | 09:10 | 09:50 | 03:05 | 10:17.92 | 86:18.26 | 10:17.90 | 86:18.21 | 1527 | Md. Culebra |
| 01.11.2005 | 150 | 775 | Parasound | 10:55 | | | 12:24 | 01:29 | 10:12.04 | 86:18.57 | 10:12.87 | 86:17.56 | 1812 | |
| 01.11.2005 | 151 | 776 | GC | 13:06 | 13:32 | 13:44 | 14:18 | 01:12 | 10:12.35 | 86:18.07 | 10:12.25 | 86:18.16 | 2006 | Hermosa Slide |
| 01.11.2005 | 152 | 777 | GC | 15:48 | | | 17:00 | 01:12 | 10:12.41 | 86:18.34 | 10:12.60 | 86:18.38 | 1939 | Hermosa Slide |
| 01.11.2005 | 153 | 778 | GC | 17:35 | | | 18:55 | 01:20 | 10:12.35 | 86.18.37 | 10:12.29 | 86:18.33 | 2012 | Hermosa Slide |
| 01.11.2005 | 154 | 779 | GC | 19:50 | | | 20:55 | 01:05 | 10:17.92 | 86:15.84 | 10:17.93 | 86:15.94 | 1290 | Md. Culebrita |
| 01.11.2005 | 155 | 780 | RDR | 21:45 | 23:30 | | 00:11 | 02:26 | 10:17.97 | 86:18.30 | 10:17.91 | 86:18.31 | 1520 | Md. Culebra |
| 02.11.2005 | 156 | 781 | RDR | 01:20 | 02:15 | | 03:54 | 02:34 | 10:17.94 | 86:18.31 | 10:17.93 | 86:18.33 | 1520 | Md. Culebra |
| 02.11.2005 | 157 | 782 | RDR | 09:20 | 09:59 | 12:15 | 12:45 | 03:25 | 11:02.21 | 86:54.73 | 11:02.22 | 86:54.70 | 783 | Md. Perezoso |
| 02.11.2005 | 158 | 783 | RDR | 13:10 | 13:40 | | 14:32 | 01:22 | 11:02.22 | 86:54.70 | 11:02.20 | 86:54.67 | 784 | Md. Perezoso |
| 02.11.2005 | 159 | 784 | RDV | 15:00 | 15:45 | 15:55 | 16:25 | 01:25 | 11:00.86 | 86:54.33 | 11:00.86 | 86:54.33 | 1009 | Md. Mosquito |
| 02.11.2005 | 160 | 785 | PWPL | 18:22 | 18:28 | | 18:48 | 00:26 | 11:15.45 | 87:09.26 | 11:15.51 | 87:09.57 | 990 | |
| 02.11.2005 | 161 | 786 | RDV | 19:40 | 21:23 | 21:51 | 22:30 | 02:50 | 11:16.40 | 87:15.22 | 11:16.40 | 87:15.22 | | Md. Carablanca |
| 03.11.2005 | 162 | 787 | GC | 02:20 | 03:00 | 03:01 | 21:40 | 19:20 | 11:38.74 | 87:49.48 | 11:38.94 | 87:49.36 | 2262 | Telica Slide |
| 03.11.2005 | 163 | 788 | GC | 04:00 | 04:35 | 04:37 | 05:35 | 01:35 | 11:39.34 | 87:49.55 | 11:39.49 | 87:49.54 | 2490 | Telica Slide |
| 03.11.2005 | 164 | 789 | GC | 05:35 | | | 07:00 | 01:25 | 11:39.19 | 87:49.49 | 11:39.27 | 87:49.51 | 2528 | Telica Slide |
| 03.11.2005 | 165 | 790 | Parasound | 07:24 | | | 08:38 | 01:14 | 11:38.68 | 87:49.58 | 11:33.86 | 87:49.34 | 2400 | |
| 03.11.2005 | 166 | 791 | RDR | 12:55 | 14:00 | 15:07 | 15:49 | 02:54 | 11:16.74 | 87:15.89 | 11:16.79 | 87:15.91 | 1414 | Md. Congo |
| 03.11.2005 | 167 | 792 | RDV | 16:00 | 16:50 | 17:00 | 17:45 | 01:45 | 11:16.75 | 87:15.89 | 11:16.73 | 87:15.88 | 1422 | Md. Congo |
| 03.11.2005 | 168 | 793 | RDV | 18:45 | 19:45 | 20:05 | 20:40 | 01:55 | 11:12.28 | 87:10.82 | 11:12.24 | 87:10.77 | 1326 | Md. Quetzal |
| 03.11.2005 | 169 | 794 | RDR | 21:15 | 21:52 | 22:35 | 23:15 | 02:00 | 11:12.38 | 87:10.83 | 11:12.38 | 87:10.83 | 1327 | Md. Quetzal |
| 04.11.2005 | 170 | 795 | PWPL | 00:07 | | | 01:05 | 00:58 | 11:15.00 | 87:05.00 | 11:15.02 | 87:05.04 | 687 | Nicaragua Slope |
| 04.11.2005 | 171 | 796 | RDR | 01:58 | 02:28 | 03:19 | 04:05 | 02:07 | 11:12.37 | 87:10.87 | 11:12.37 | 87:10.87 | 1324 | Md. Quetzal |
| 04.11.2005 | 172 | 797 | RDR | 04:25 | 04:50 | 07:05 | 07:45 | 03:20 | 11:12.36 | 87:10.82 | 11:12.36 | 87:10.82 | 1319 | Md. Quetzal |
| 04.11.2005 | 173 | 798 | RDR | 08:10 | 09:10 | 09:20 | 10:10 | 02:00 | 11:12.36 | 87:10.84 | 11:12.02 | 87:10.30 | 1354 | Md. Quetzal |
| 04.11.2005 | 174 | 799 | RDV | 12:00 | 13:00 | 13:20 | 13:50 | 01:50 | 11:02.25 | 86:54.71 | 11:02.31 | 86:54.65 | 805 | Md. Perezoso |

| | | | | | | | | | | | | | | |
|---|---|---|---|---|---|---|---|---|---|---|---|---|---|---|
| 04.11.2005 | 175 | 800 | RDV | 14:22 | 14:49 | 15:00 | 15:30 | 01:08 | 11:02.25 | 86:54.71 | 11:02.45 | 86:54.68 | 780 | Md. Perezoso |
| 04.11.2005 | 176 | 801 | RDR | 15:55 | 16:36 | 17:10 | 17:40 | 01:45 | 11:02.25 | 86:54.71 | 11:02.28 | 86:54.68 | 791 | Md. Perezoso |
| 04.11.2005 | 177 | 802 | RDR | 18:05 | 19:05 | 19:50 | 20:15 | 02:10 | 11:02.29 | 86:54.65 | 11:02.30 | 86:54.68 | 802 | Md. Perezoso |
| 04.11.2005 | 178 | 803 | RDV | 20:45 | 21:25 | 21:40 | 22:00 | 01:15 | 11:01.12 | 86:54.39 | 11:01.18 | 86:54.24 | 958 | Md. Colibri |
| 05.11.2005 | 179 | 804 | RDV | 22:40 | 23:05 | 23:20 | 23:25 | 00:45 | 11:01.30 | 86:54.17 | 11:01.29 | 86:54.17 | 920 | Md. Colibri |
| 05.11.2005 | 180 | 805 | RDV | 01:10 | 01:55 | 02:15 | 03:10 | 02:00 | 11:02.45 | 87:02.12 | 11:02.45 | 87:02.11 | 1707 | Nica Ridge |
| 05.11.2005 | 181 | 806 | RDR | 04:30 | 04:50 | 05:22 | 05:50 | 01:20 | 11:13.58 | 87:07.46 | 11:13.76 | 87:06.91 | 858 | Baula IV |
| 05.11.2005 | 182 | 807 | RDV | 06:20 | 06:53 | 08:10 | 08:30 | 02:10 | 11:13.37 | 87:06.52 | 11:13.32 | 87:06.56 | 811 | Baula V |
| 05.11.2005 | 183 | 808 | RDR | 08:53 | 09:20 | 10:10 | 10:35 | 01:42 | 11:13.37 | 87:06.53 | 11:13.37 | 87:06.54 | 800 | Baula V |
| 05.11.2005 | 184 | 809 | RDR | 10:50 | 11:26 | 12:59 | 13:24 | 02:34 | 11:13.36 | 87:06.53 | 11:13.37 | 87:06.54 | 799 | Baula V |
| 05.11.2005 | 185 | 810 | RDR | 14:16 | 14:45 | 16:14 | 16:45 | 02:29 | 11:13.36 | 87:06.53 | 11:13.27 | 87:06.54 | 796 | Baula V |
| 05.11.2005 | 186 | 811 | RDR | 17:06 | 17:35 | 19:40 | 20:02 | 02:56 | 11:13.38 | 87:06.52 | 11:13.38 | 87:06.55 | 797 | Baula V |
| 05.11.2005 | 187 | 812 | PWPL | | | 22:30 | 22:45 | 00:15 | 11:15.07 | 87:05.00 | 11:15.07 | 87:05.00 | 703 | |
| 05.11.2005 | 188 | 813 | RDR | 21:27 | 21:50 | 22:05 | 22:28 | 01:01 | 11:13.39 | 87:06.55 | 11:13.38 | 87:06.54 | 803 | Baula V |
| 06.11.2005 | 189 | 814 | RDV | 15:30 | 16:10 | 16:15 | 18:10 | 02:40 | 09:07.18 | 84:50.54 | 09:07.18 | 84:50.53 | 1766 | Jaco Scar |
| 06.11.2005 | 190 | 815 | RDV | 21:00 | 22:02 | 22:04 | 23:07 | 02:07 | 09:06.99 | 84:50.49 | 09:07.40 | 84:50.54 | 1857 | Jaco Scar |
| 07.11.2005 | 191 | 816 | GC | 00:15 | 00:50 | | 01:21 | 01:06 | 08:59.56 | 84:43.77 | 08:59.56 | 84:43.71 | 1927 | Parrita |
| 07.11.2005 | 192 | 817 | PWPL | 04:15 | 04:50 | | 07:20 | 03:05 | 08:56.05 | 84:18.88 | 08:55.74 | 84:18.73 | 1007 | Md. 12 |
| 07.11.2005 | 193 | 818 | RDR | 07:50 | 10:01 | 10:59 | 11:05 | 03:15 | 08:55.87 | 84:18.60 | 08:55.61 | 84:18.51 | 979 | Md. 12 |
| 07.11.2005 | 194 | 819 | RDR | 11:56 | | 13:39 | 14:06 | 02:10 | 08:55.32 | 84:18.24 | 08:55.33 | 84:18.22 | 1023 | Md. 11a |
| 07.11.2005 | 195 | 820 | RDR | 14:22 | 15:00 | 15:40 | 16:07 | 01:45 | 08:55.19 | 84:18.18 | 08:55.26 | 84:18.21 | 1038 | Md. 11b |
| 07.11.2005 | 196 | 821 | RDV | 16:50 | 17:40 | 17:50 | 18:15 | 01:25 | 08:55.84 | 84:18.62 | 08:55.72 | 84:18.54 | 1013 | Md. 12 |
| 07.11.2005 | 197 | 822 | RDV | 18:45 | 19:25 | 19:40 | 20:10 | 01:25 | 08:55.86 | 84:18.62 | 08:55.80 | 84:18.56 | 1013 | Md. 12 |
| 07.11.2005 | 198 | 823 | DOS | 20:10 | | 20:15 | 20:50 | 00:40 | 08:55.82 | 84:18.53 | 08:56.01 | 84:18.97 | 1014 | Md. 12 |
| 07.11.2005 | 199 | 824 | RDV | 23:10 | 00:11 | 00:23 | 01:52 | 02:42 | 08:59.57 | 84:43.65 | 08:59.59 | 84:43.64 | 1937 | Parrita |
| 08.11.2005 | 200 | 825 | RD-Test | 02:35 | | | 05:17 | 02:42 | 08:59.38 | 84:43.63 | 08:59.31 | 84:43.59 | 1953 | Parrita |
| 08.11.2005 | 201 | 826 | RDR | 06:20 | 07:10 | 08:40 | 09:55 | 03:35 | 09:07.08 | 84:50.57 | 09:07.10 | 84:50.47 | 1832 | Jaco Scar |
| 08.11.2005 | 202 | 827 | RDV | 10:10 | 12:33 | 13:27 | 15:50 | 05:40 | 09:07.07 | 84:50.45 | 09:07.09 | 84:50.49 | 1795 | Jaco Scar |
| 08.11.2005 | 203 | 828 | RDV | 16:05 | 20:00 | 20:30 | 22:30 | 06:25 | 09:07.10 | 84:50.51 | 09:07.05 | 84:50.55 | 1849 | Jaco Scar |
| 08.11.2005 | 204 | 829 | GC | 22:55 | | | 23:20 | 00:25 | 09:12.18 | 84:44.03 | 09:12.17 | 84:44.00 | 576 | Lira Slide |
| 08.11.2005 | 205 | 830 | GC | 23:45 | | | 00:13 | 00:28 | 09:12.08 | 84:43.87 | 09:12.10 | 84:43.87 | 592 | Lira Slide |
| 09.11.2005 | 206 | 831 | GC | 00:40 | | | 01:04 | 00:24 | 09:12.02 | 84:43.98 | 09:12.02 | 84:43.97 | 623 | Lira Slide |
| 09.11.2005 | 207 | 832 | Parasound | | | | | 00:00 | | | | | | |
| 09.11.2005 | 208 | 833 | RDR | 04:15 | 04:45 | 06:16 | 06:45 | 02:30 | 09:09.00 | 84:49.21 | 09:09.04 | 84:49.10 | 817 | Jaco Scar |
| 09.11.2005 | 209 | 834 | RDR | 06:58 | | | 08:25 | 01:27 | 09:09.05 | 84:49.14 | 09:09.01 | 84:49.16 | 833 | Jaco Scar |
| 09.11.2005 | 210 | | RDR | 09:01 | 10:28 | 12:58 | 13:19 | 04:18 | 09:09.02 | 84:43.17 | 09:09.07 | 84:49.16 | 815 | Jaco Scar |

| | | | | | | | | | | | | | | |
|---|---|---|---|---|---|---|---|---|---|---|---|---|---|---|
| 09.11.2005 | 211 | 835 | RDV | 14:20 | 16:10 | 16:45 | 18:00 | 03:40 | 09:06.99 | 84:50.42 | 09:06.94 | 84:50.42 | 1845 | Jaco Scar |
| 09.11.2005 | 212 | 836 | PWPL | 21:07 | | 21:11 | 21:40 | 00:33 | | | 08:55.82 | 84:19.04 | 1025 | Mound 12 |
| 09.11.2005 | 213 | 837 | RDV | 22:50 | 23:40 | 23:50 | 00:20 | 01:30 | 08:55.84 | 84:18.60 | 08:55.85 | 84:18.39 | 980 | Mound 12 |
| 10.11.2005 | 214 | 838 | RDR | 03:30 | 04:27 | 10:05 | 10:28 | 06:58 | 09:09.04 | 84:49.19 | 09:09.08 | 84:49.15 | 828 | Jaco Scar |
| 10.11.2005 | 215 | 839 | Hydrosweep | | | | | | | | | | | |
| 14.11.2005 | 216 | | ADCP Mooring | | 00:26 | | | | | | 09:39.04 | 86:11.78 | 4386 | Costa Rica |
| 14.11.2005 | 217-1 | | HF-1 | | 05:54 | 06:09 | | | | | 09:35.51 | 86:14.49 | 3942 | Costa Rica |
| 14.11.2005 | 217-2 | | HF-1 | | 07:01 | 07:15 | | | | | 09:35.10 | 86:14.84 | 3908 | Costa Rica |
| 14.11.2005 | 217-3 | | HF-1 | | 08:03 | 08:18 | | | | | 09:34.69 | 86:15.19 | 3799 | Costa Rica |
| 14.11.2005 | 217-4 | | HF-1 | | 09:14 | 09:20 | | | | | 09:34.27 | 86:15.55 | 3748 | Costa Rica |
| 14.11.2005 | 217-5 | | HF-1 | | 10:09 | 10:23 | | | | | 09:33.86 | 86:15.90 | 3725 | Costa Rica |
| 14.11.2005 | 217-6 | | HF-1 | | 11:15 | 11:23 | | | | | 09:33.44 | 86:16.24 | 3664 | Costa Rica |
| 14.11.2005 | 218 | | GC | 21:00 | | | 22:00 | 01:00 | 11:02.36 | 87:02.20 | | | 1719 | Nicaragua |
| 14.11.2005 | 219 | | GC | 22:25 | 22:50 | | 23:25 | 01:00 | 11:02.45 | 87:02.16 | | | 1710 | Nicaragua |
| 15.11.2005 | 220 | | GC | 00:40 | 01:09 | 01:11 | 01:45 | 01:05 | 11:08.75 | 87:13.23 | 11:08.76 | 87:13.24 | 2158 | Masaya Slide |
| 15.11.2005 | 221-1 | | HF-2 | | 06:48 | 06:55 | | | | | 10:52.92 | 87:50.78 | 3072 | Nicaragua |
| 15.11.2005 | 221-2 | | HF-2 | | 07:44 | 07:56 | | | | | 10:53.31 | 87:50.42 | 3045 | Nicaragua |
| 15.11.2005 | 221-3 | | HF-2 | | 08:31 | 08:38 | | | | | 10:53.70 | 87:50.05 | 3066 | Nicaragua |
| 15.11.2005 | 221-4 | | HF-2 | | 09:19 | 09:23 | | | | | 10:54.10 | 87:49.67 | 3162 | Nicaragua |
| 15.11.2005 | 221-5 | | HF-2 | | 10:09 | 10:23 | | | | | 10:54.49 | 87:49.30 | 3325 | Nicaragua |
| 15.11.2005 | 221-6 | | HF-2 | | 11:14 | 11:27 | | | | | 10:54.84 | 87:48.90 | 3339 | Nicaragua |
| 15.11.2005 | 222 | | GC | 20:30 | 21:30 | 21:32 | 22:29 | 01:59 | 11:37.35 | 89:07.37 | 11:37.34 | 89:07.45 | 3630 | South Salvador |
| 16.11.2005 | 223 | | GC | 02:15 | 03:12 | 03:14 | 04:20 | 02:05 | 11:54.78 | 89:46.61 | 11:54.66 | 89:46.99 | 3882 | Middle Salvador |
| 16.11.2005 | 224 | | GC | 07:59 | 08:53 | 08:55 | | | 12:10.66 | 90:23.61 | 12:10.70 | 90:23.49 | 4003 | North Salvador |
| 16.11.2005 | 225 | | GC | 13:50 | 14:56 | 15:05 | | | 12:22.62 | 91:04.45 | | | 3707 | |
| 16.11.2005 | 226 | | GC | 17:15 | | | | | 12.22.40 | 91:05.91 | | | 3732 | |
| 16.11.2005 | 227 | | GC | 21:20 | 22:15 | 22:22 | | | 12:42.77 | 91:48.13 | | | 3965 | |
| 17.11.2005 | 228 | | GC | 03:15 | 04:15 | 04:17 | 05:15 | 02:00 | 12:33.96 | 92:02.01 | | | 3838 | |
| 17.11.2005 | 229 | | GC | 08:45 | 09:50 | 09:52 | 10:25 | 01:40 | 12:15.06 | 91:30.65 | 12:15.06 | 91:30.54 | 3703 | |
| 17.11.2005 | 230 | | GC | 17:15 | 18:04 | 18:05 | | | 11:44.92 | 90:31.23 | | | 3593 | |
| 18.11.2005 | 231 | | HF-3 | 00:10 | 01:23 | 06:21 | 08:00 | 07:50 | 12:25.55 | 91:00.00 | | | 4148 | Guatemala |

## 3.6 Acknowledgements

The scientific party gratefully acknowledges the friendly cooperation with Captains Kull and Jakobi, the officers and crew of FS METEOR. Their tireless support and superb technical assistance was crucial to making this cruise a scientific success. We also appreciate the continuing support by the Leitstelle FS METEOR at the University of Hamburg. Cruise METEOR M66 was generously supported by the Deutsche Forschungsgemeinschaft DFG in the framework of the Collaborative Research Center (SFB) 574 "Volatiles and Fluids in Subduction Zones".

## 3.7 References

Blum, P., 1997. Physical properties handbook: A guide to the shipboard measurement of physical properties of deep-sea cores. ODP Tech. Note, 26. available from http://www-odp.tamu.edu/publications/tnotes/tn26/INDEX.HTM

Grasshoff, K., M. Ehrhardt and K. Kremling, 1997. Methods of seawater analysis. Verlag Chemie

Hensen C., K. Wallmann, M. Schmidt, C. R. Ranero, and E. Suess, 2004 Fluid expulsion related to mud extrusion of f Costa Rica continental margin - a window to the subducting slab. Geology, 32, 201-204

Hansbo, S., 1957. A new approach to the determination of the shear strength of clay by the fall-cone test. Proceedings of the Royal Swedish Geotechnical Institute, 14, 5-47

Houlsby, G.T., 1982. Theoretical analysis of the fall cone test. Géotechnique, v. 32, p. 111-119

Hunt, C., B.M. Moskowitz and S.K. Banerjee, 1995. Magnetic properties of rocks and minerals. In Rock Physics and Phase Relations. AGU Ref. Shelf 3, 189–204

Kutterolf, S., U. Schacht, H. Wehrmann, A. Freundt and T. Mörz, 2006. Onshore to offshore tephro-stratigraphy and marine ash layer diagenesis in Central America. In: Alvarado, G. and J., B., (eds): Central America, Geology, Resources and Hazards. Balkema, Lisse, Niederlande, Tokio, Japan

Skinner, A.C., 2000. BAS Cruise JR48: HILATS Millennium Cruise, coring and geophysical survey; RRS James Clark Ross. BGS Technical Report WB/00/6C

Soeding, E., K. Wallmann, E. Suess and E. R. Flueh, Eds., 2003. Cruise Report M54/2+3: Fluids and Subduction Costa Rica 2002., 111, Geomar, Kiel

METEOR-Berichte 09-2

# *SUBFLUX*

## PART 4

Cruise No. 66, Leg 4a
November 21 – December 10, 2005, Corinto (Nicaragua) – Guayaquil (Ecuador)

Cruise No. 66, Leg 4b
December 11 - December 21, 2005, Guayaquil (Ecuador) – Talcahuano (Chile)


**Jörg Bialas, Achim Kopf,** Dietmar Bürk, Eduardo Contreras-Reyes, Anke Dannowski, Juan Diaz-Naveas, Aysun Nilay Dinc-Akdogan, Yvonne Dzierma, Ulrich Doormann, Jürgen Goßler, Ingo Grevemeyer, Monika Ivandić, Ingo Klaucke, Marten Lefeldt, Karen Meißner, Pedro Perez, Jörg Petersen, Klaus-Peter Steffen, Asrarur Talukder, Martin Thorwart, Ricardo Sanchez Vega, Silvia Stegmann, the shipboard scientific parties and Silke Schenck

Editorial Assistance:

Andreas Krell
Alfred-Wegener-Institut für Polar- und Meeresforschung, Bremerhaven

Leitstelle METEOR
Institut für Meereskunde der Universität Hamburg

2009

**Table of Contents Part 4 (M66/4)** **Page**

## 4.1 List of Participants M66/4

### 4.1.1 List of Participants Leg M66/4a

| Name | Discipline | Institution |
|---|---|---|
| 1 . Bialas, Jörg, Dr. | Chief scientist | IFM-GEOMAR |
| 2 . Bürk, Dietmar | Side Scan Sonar | SFB 574 |
| 3 . Contreras-Reyes, Eduardo | Seismics | IFM-GEOMAR |
| 4 . Dannowski, Anke | Seismics | IFM-GEOMAR |
| 5 . Dinc-Akdogan, Aysun Nilay | Seismology | SFB 574 |
| 6 . Dzierma, Yvonne | Seismology | SFB 574 |
| 7 . Doormann, Ulrich | Technician | KUM |
| 8 . Goßler, Jürgen, Dr. | Geophysics | KUM |
| 9 . Grevemeyer, Ingo, Dr. | Seismics | IFM-GEOMAR |
| 10. Ivandić, Monika | Seismics | SFB 574 |
| 11. Klaucke, Ingo, Dr. | Side Scan Sonar | IFM-GEOMAR |
| 12. Lefeldt, Marten | Seismics | SFB 574 |
| 13. Meißner, Karen | Seismics | IFM-GEOMAR |
| 14. Perez, Pedro | Technician | INETER |
| 15. Petersen, Jörg, Dr. | Deep Tow Seismics | SFB 574 |
| 16. Steffen, Klaus-Peter | Airgun | IFM-GEOMAR |
| 17. Talukder, Asrarur, Dr. | Seismics | SFB 574 |
| 18. Thorwart, Martin, Dr. | Geophysics | SFB 574 |
| 19. Wellhöner, Jens | Press documentation | DLF |
| 20. Sanchez Vega, Ricardo | Technician | I.C.E |

### 4.1.2 List of Participants Leg M66/4b

| Name | Discipline | Institution |
|---|---|---|
| 1 . Kopf, Achim | CPT | GEOB |
| 2 . Stegmann, Silvia | CPT | GEOB |
| 3 . Diaz-Naveas, Juan | CPT | UCV |

**DWD** Deutscher Wetterdienst, Geschäftsfeld Seeschifffahrt, Bernhard-Nocht-Str. 76, 20359 Hamburg, Germany

**DLF** Deutschlandfunk, c/o NDR 1 - Welle Nord, Redaktion Heimat und Kultur, Am Wall 67, 24033 Kiel, Germany

**GEOB** Fachbereich Geowissenschaften; Universität Bremen Postfach 33044 0, 28334 Bremen, Germany

**ICE** Instituto Costarricense de Electricidad, Sismologia y Vulcanologia, Apdo. 10032-1000, San José, Costa Rica

**IFM-GEOMAR** Leibniz Institut für Meeresforschung, Wischhofstrasse, 24105 Kiel, Germany

| | |
|---|---|
| **INETER** | Instituto Nicaragüense de Estudios Territoriales, Dirección General de Geofísica, Frente a la Policlinica Oriental, Apdo. 2110, Managua, Nicaragua |
| **KUM** | Umwelt- und Meerestechnik Kiel GmbH, Wischhofstrasse 1-3, Gebäude D5, 24148 Kiel, Germany |
| **SFB 574** | Sonderforschungsbereich 574, Christian-Albrechts-Universität zu Kiel, Wischhofstrasse 1-3, 24148 Kiel, Germany |
| **UCV** | Escuela de Ciencias del Mar, Pontificia Universidad Catolica de Valparaiso, Av. Altamirano 1480, Valparaiso, Chile |

## 4.2 Research Program

### 4.2.1 Research Program of Leg M66/4a

The major aim of the cruise is to understand the processes occurring in the outer rise. To study the impact of outer rise faulting on the hydration of the oceanic crust approaching the Middle America trench offshore Nicaragua two different techniques were used. (i) a network of ocean bottom seismometers and hydrophones was left on the seafloor to record the natural seismicity in the outer rise area during leg M66/2a. The aim of this approach is to define active faults and the depth down to which the faults are active. This depth may provide an initial assessment of the depth down to which fluids can penetrate into the upper mantle. (ii) active seismic wide-angle and refraction work can be used to test the hypothesis that the mantle is hydrated or serpentinized. Typically, the upper mantle has velocities between 8.0 to 8.2 km/s. If hydrated or serpentinized, seismic velocities are much lower. A serpentinization of 20 % would change seismic velocities in the mantle to 7.6 km/s. Three seismic lines were shot seaward of the trench in the outer rise area. Profile 1 runs in the trench axis, profile 2 parallel to the strike of the trench axis at a distance if 60 km from the trench, and profile 3 runs normal to the trench, intersecting profile 1 and 2.

Further on high resolution active seismic profiling is applied along three profiles to support deep towed seismic streamer data analysing the structure and formation of mound structures along the continental margin. Cruise SO173-1 mapped a large number of mound locations by deep towed sidescan and multichannel seismic streamer recordings. Seismic images of the structures indicate that they are related to faults or ridge like tectonic features. A BSR has been mapped within the entire area of investigation with varying amplitude strength. Additional seismic data should verify the variability of the BSR reflectivity and investigate the causes of BSR uplift or disappearance underneath the various mound structures and the relation to the tectonic setting.

A short-term seismic network was deployed on the outer rise offshore Nicaragua (M66/2a) to record the local seismicity generated by the bending of the Cocos plate prior to its subduction to find possible fluid paths through the crust into the uppermost mantle which are bounding conditions for serpentinization models. The network comprised of 22 OBH and OBS stations, which were recovered during leg M66/4a.

A long-term network of 20 short-period seismometers and hydrophones was installed offshore Nicaragua in extension of the land stations that were deployed in October 2005. The stations will be recovered in summer 2006. The data will be used for local earthquake tomography, with the aim of exploring the detailed structure of the subduction zone in terms of $v_p$, $v_p/v_s$ velocity ratio and attenuation.

In addition to this, four broadband stations were deployed in continuation of the broadband transect across southern Costa Rica, and will also be operating until summer 2006. A receiver function analysis of the data will yield insight into the crustal and mantle structure by imaging discontinuities and giving a second estimate of the velocity ratios.

The combination of the two experiments will help to create a more detailed picture of the subduction process and may explain some changes in the subduction zone along the plate boundary, such as the jump in the volcanic chain.

### 4.2.2 Research Program of Leg M66/4b

Leg M66/4b was dedicated entirely to testing a new CPT (cone penetration testing) free fall lance. The overall objective when studying active convergent margins is to unravel the complex fluid processes and their ramifications for natural hazards such as submarine landslides and earthquakes. The understanding of such processes may be severely deepened if the crucial controlling parameters are measured *in situ*. For that purpose, a free fall-CPT lance has been built. This device allows a time- and cost-effective characterization of both pore pressure and sediment strength in the uppermost ocean floor sediments. CPT measurements are usually carried out with a cylindrical lance, either motor-driven or as free fall instrument. Penetration depth is controlled by sediment composition/grain size as well as the weight of the lance. In our case, it is a few meters. During penetration, frictional forces at the tip and along the sleeve of the lance are measured. The amount of frictional resistance allows for a classification of the sediment. In addition to these first order strength measurements, a piezometric cell is measuring pore pressure in the sediment. The RCOM free fall CPT is a seagoing modification of a standard industrial CPT tip (Geomil, NL). Pore pressure is measured in u1 and u3 position.

During earlier research cruises, landslide scars and sedimentary trench successions with abundant turbidites have been found off Chile. As a result of these cruises, wide areas along the Chilean continental margin are geophysically well characterized. These data, namely the bathymetric charts, have allowed researchers to measure in situ-heat flow along three profiles using the Chilean vessel *Vidal Gormaz* in 2003. Along the northernmost of these profiles, CPT experiments measuring sediment physical properties such as strength, pore pressure, as well as tilt of the probe were conducted with the new device during Leg M66/4b.

## 4.3 Narrative of the cruise

### 4.3.1 Narrative of the cruise Leg M66/4a

RV METEOR docked in the port of Corinto Nicaragua on 19th Nov. 2005 when Cruise M66-3b terminated. Two containers with research equipment were unloaded, while a container of the seismic group was returned from stowage area to the vessel. Unfortunately the deep-sea cable, which was replaced 10 days ago in Caldera was broken during the previous leg at 4000 m length

and needed to be replaced during this port call again. The intensive support of the crew ensured replacement without time delay.

The majority of the scientists arrived in time at Managua airport, apart from a group of three members. These people are from non-European countries and had chosen to fly across Caracas avoiding visa problems during the few hour transit that would have been necessary if they flew across the USA. As their arrival was announced for 24 hours delay departure of the vessel was not shifted to an earlier time as previously hoped. Nevertheless it turned out that the carrier Air France did not guaranteed the continued travel of the persons and hence they had to stay in Caracas another day. Due to the dense time schedule METEOR left the port of Corinto on the 21st Nov. 08:20. As the next working area of the cruise is located close to Corinto it was decided to try later for a meeting between a shuttle boat and METEOR, once the scientist had arrived in Managua.

RV METEOR used the time to deploy 7 OBH/S along the planned profile 1. The instruments were positioned between long term recording hydrophones and seismometers deployed during leg M66-2a, seven weeks ago. Further on, time was used to start picking up instruments that were not planed to record active seismic profiling later on. During 22nd Nov. we received message that our missing colleagues arrived in Managua and could welcome them in the evening onboard. After a few hours transit we reached the starting point of our first airgun profile. After 14 hours of airgun shots we recovered all instruments from this line.

A second profile was deployed parallel to the trench on the outer rise on 24th Nov. All airguns worked without problems during the 65 nm long line. During OBH/S recovery two close by instruments from the seismology network were picked up as well.

In the morning of the 26th Nov. we started the deployment of line 3. Together with 5 instruments from the seismology network 13 additional OBH/S covered this NE-SW striking profile over a length of 75 N.M. Airgun shooting was completed on 27th Nov. 12:00 without any complications.

After recovery of all instruments METEOR set course towards the first DeepTow area at 12° N on the slope of the Nicaragua continental margin. At 13: 40 hr s local time Sidescan and Depressor were lowered to the water. At 14: 00 hr s the telemetry system showed unusual amplitudes in the electric current consumption, followed by a power break down. The winch was stopped immediately, and as a restart showed abnormal high currents the system was switched off again. The winch was asked to retrieve the system onboard when a sudden drop in weight measure of the winch indicated that we had lost at least the 2 tons depressor weight. Immediately emergency release of the Sidescan indicated that the instrument sank to bottom (2300 m depth) with the depressor. Exact positioning of the instrument showed that the system must be floating 30 m above ground. Consequently we started to dredge for the system using the 18 mm deep sea working wire of METEOR. Two attempts using up to 7500 m of cable failed.

Following on METEOR headed for some swath mapping courses in order to complete the existing map in the regions of the upper terminations of the observed canyons cutting into the slope. This course reached up to 12°19' N.

In the afternoon of Dec. 1st we returned to the ground position of the Sidescan and prepared for another attempt to dredge the system. This time 9500 m of cable were used to circle the estimated position. About 5000 m of cable had been dragged in when a flash light and the radio signal verified the release and return to surface of the tow fish.

**FIG. 4.1:**
DeepTow Streamer and Sidescan with 2-ton-depressor weight.

After recovery of the Sidescan we continued our program with deployment of profiles 4 & 5 in the morning hours of 2nd Dec. These lines were dedicated to resolve high resolution data and deeper structure of Mound Baula Massive. Two perpendicular profiles were occupied by 22 instruments, which recorded shots from a 250 cinch GI gun and a 2080 cinch G-gun array of two clusters. Besides one OBH all instruments were recovered until 4th Dec. As the remaining unit rests at 1014 m depth it was decided to try another dredge attempt. As the release replies clearly verified internal motion of the motor drive it was assumed that the hook axis was not turned simultaneously. This assumption was derived from a unique point onboard with the same malfunction. Unfortunately this dredge did not result in a recovery and due to time limits no further attempts for recovery were undertaken. During the night hours of 4th and 5th Dec. a short wide angle profile was shot crossing a ridge structure identified by Sidescan sonar and deep towed streamer during cruise SO173-1.

In the afternoon of 5th Dec. we started deployment of 20 instruments for long time seismological observations off Nicaragua and Costa Rica in the vicinity of Nicoya peninsula. In between a short PARASOUND profile was recorded crossing the Hermosa slide. Upon transit to Mound 11&12 another PARASOUND profile was recorded above the Lira slide. In the morning of the 7th Dec. we deployed one Tiltmeter station, an OBH and an OBS on Mound 12. Positions were chosen close to the locations of long-term water samplers deployed by US colleagues. The afternoon hours were used for the deployment of four additional seismometers off Osa peninsula. These instruments were equipped with broadband seismometers and form the marine prolongation of a land traverse across Costa Rica.

During preparations for deployments of a final high resolution seismic line a fishing boat approached METEOR and reported about a small fishing boat which was about to sink some 20 N.M. away. Of course research activities were stopped immediately and METEOR headed towards the given location. The helpless fishing boat was found drifting on its side completely washed over while a second boat in standby rescued the crew. After two hours METEOR succeeded to move the boat in upright position again and pumps were installed to empty the boat. At about 20: 00 hrs the fishing boat departed from METEOR towed by a supporting colleague. As the remaining work time did not allow any seismic work METEOR left southwards for HYDROSWEEP mapping courses, before transit to Guayaquil in the morning of 08th Dec.

**FIG. 4.2:**
Rescue operations.

### 4.3.2 Narrative of the cruise Leg M66/4b

Leg M66/4b was primarily dedicated to transit. However, there was an opportunity to deploy the CPT in the afternoon of 21 December. Test runs were performed during the whole night, until the device was recovered in the early morning of 22 December. Cruise M66 ended in the port of Talcahuano on 22 December.

## 4.4 Preliminary Results

### 4.4.1 Instrumentation

*IFM-GEOMAR Ocean Bottom Hydrophone/Seismometer (OBH/S)*

19 ocean bottom hydrophones (OBH) and 22 ocean bottom seismometers (OBS) were available for the M66/4a project.

The instruments are deployed in a free falling manner and their exact seafloor position will be deduced later by an $L^2$ approximation of the direct water wave records. Up to four data channels are recorded on flash disks, with an accuracy of time better than 0.05 ppm over temperature. Setting and synchronising the time as well as monitoring the drift is carried out automatically by synchronisation signals (DCF77 format) from a GPS-based coded time signal generator.

After recording the flashcards need to be copied to a PC workstation, where they will be provided in standard SEG-Y format. Relocation, frequency filtering and deconvolution processes

are applied. Next arrival times were picked and interactive MacRay code or inversion routines (e.g. Corenaga code) were used to achieve first p-wave velocity depth models.

*Seismic sources: G-gun arrays*

During this cruise IFM-GEOMAR operated two 5 m long arrays with G-gun clusters. One gun cluster is build by two 520 cinch G-guns which are offset by 1 m. All guns were synchronized using the IFM-GEOMAR LongShot airgun source controller. The gun carriers were deployed through the inside of the A-frame, while towing was realized by the aft mooring winches, which cables were guided through blocks on the outside ends of the A-frame. For lifting purposes a triangle shaped hoisting rope was attached to the ends of the carrier, while the towing cable was attached to the front end where the support hoses of the guns were lead in as well. During the first profile three guns need to be switched off. Their air hoses were leaking and avoided to build up the requested 207 bar pressure after a shot. During all other lines the deployed guns were operated without further malfunction.

*Seismic sources: GI-gun*

For M66/4a cruise a GI-Gun (Generator-Injector gun; manufactured by Sercel Marine Seismic Sources, former Sodera) for high-resolution surveys, with a generator volume of 250 cinch and an injector volume of 105 cinch was available.

**TAB. 4.1:** GI-gun configuration.

| Mode | Generator Volume ($in^3$) | Injector Volume ($in^3$) | Delay (ms) | Discharge Port |
|---|---|---|---|---|
| Harmonic | 250 | 105 | 70 | large |

With the LongShot sensor display, the near field source wavelet was controlled and remained constant over the entire survey. A single gun hanger towed the GI-Gun approximately 20 m behind the ship's stern in a water depth of 2.5 m. Following the recommendation of the Sodera handbook, the gun was operated at a pressure of 207 bar and an shot interval of 14 s, and worked without problems.

*Seismic Sources: External Trigger*

For wide angle and surface streamer profiling the trigger signal was supplied from the ship's Glonas receiver operating in GPS mode, which can provide a 5 V -TTL pulse at selectable intervals. As the LongShot triggered on the falling flank the ships trigger signal was inverted. The source controller verifies that all guns are fired at the pre-selected aim point after the external trigger is detected. The ignition pulse is sent out to each gun according to the trigger delay time prior to this aim point. Exact position calculation for the shot time was done by post-processing using shot time and UTC time values stored with D-GPS coordinates in the ship's database. Time stamps of the coordinates were synchronized with GPS time receiver at all times during the cruise.

**TAB. 4.2:** Airgun configuration.

| | shot interval (s) | aim point (ms) | injector delay (ms) |
|---|---|---|---|
| G gun Array | 60 | 60 | N/A. |
| GI gun | 14 | 60 | 70 |

*Sidescan sonar*

The DTS-1 sidescan sonar is a dual-frequency, chirp sidescan sonar (EdgeTech Full-Spectrum) working with 75 and 410 kHz centre frequencies (giving a range resolution of 1.5 m and 1.8 cm). In addition the DTS-1 contains a 2-16 kHz chirp subbottom profiler providing a choice of three different pulses of 20 ms pulse length each. A Honeywell attitude sensor providing information on heading, roll and pitch is connected via a serial RS232 port and a second port is used for a pressure sensor. Finally, there is the possibility of recording data directly in the underwater unit through a mass-storage option with a total storage capacity of 60 GByte.

The 2.8 m x 0.8 m x 0.9 m towfish houses two titanium pressure vessels containing the sonar electronic and underwater part of the telemetry system (SEND DSC-Link) and the Linux-based Bottom-PC (SEND) of the seismic streamer data acquisition system (cf. sect. 5.3.2). In addition, a releaser capable to work with the USBL positioning system POSIDONIA (IXSEA-OCEANO) and an emergency flash and radio beacon (NOVATECH) are included in the towfish. The towfish is connected to the sea cable via the depressor through a 43-m long umbilical cable.

HydroStar Online, a multibeam bathymetry software developed by ELAC Nautik GmbH and adapted to the acquisition of EdgeTech sidescan sonar data allows onscreen presentation of the data, of the tow fish's attitude, and the tow fish's navigation when connected to the POSIDONIA USBL positioning system. It also allows setting the main parameters of the sonar electronics, such as selected pulse, range, power output, gain, ping rate, and range of registered data.

*Deep-Tow Seismic Steamer*

The hybrid multichannel digital deep-tow seismic streamer improves lateral in- and cross-line resolution particularly in regions of special interest for gas hydrate research. In this context, hybrid system means that conventional marine seismic sources like air-, GI or waterguns shot close to the surface are still used, whereas the streamer is lowered to the seafloor towed behind the above described sidescan sonar system.

The streamer is a modular digital seismic array (*HTI, High Tech, Inc.*) which can be operated in water depths up to 6000 m. It consists of a 50 m lead-in cable towed behind the sidescan sonar fish and single modules for each channel. Digital acoustic modules (AM) with a single hydrophone are used in majority, while three engineering modules (EM) which additionally include a compass, a pressure and a motion sensor (*Crossbow*) provide information on the depth orientation (magnetic heading) and on its roll and pitch during the survey. Modules are interchangeable and can arbitrarily be connected by cables of 1 or 6.5 m length. The sample interval is set to 0.25 ms.

All bottom and top side components as well as air gun shooting were synchronized by D-GPS time-based trigger signals generated by the Linux Top-PC via the LPT10 link. Additionally, all surface and underwater components controlling the deep-tow device are linked via ethernet with the Linux Top-PC as gateway and form a small PC cluster.

*Geometrics Stratavisor NX* software is used to display the complete shot gathers, their amplitude spectra and a continuous single-fold profile onscreen, to print the continuous singlefold profile on an online printer and to store the acquired data on hard disc or the two connected *DLT 8000* devices in standard seismic SEG-D, SEG-Y or SEG-2 format.

Due to unsolved problems within the synchronisation of the digital streamer and the controlling PC it was decided that the sidescan was deployed without the streamer cable in the

first working area. After the loss and successful recovery of the sidescan no further deployments were undertaken.

*Ultra Short Base Line (USBL) Positioning System POSIDONIA*

Underwater navigation, depth and position measurement of the sidescan sonar tow fish is carried out by the ultra-short base line (USBL) system *POSIDONIA* (*IXSEA-OCEANO*). It mainly consists of a deployable acoustic array (antenna) installed in the moon-pool, and a responder with remote receiver head mounted on the sidescan sonar fish housing an additional pressure sensor. The four reception hydrophones of the antenna receive the reply ping from the towfish, and by measuring the phases and the reply time the geographical position of the transponder is calculated. After lowering the moonpool a calibration run must be completed to calculate offset angles between antenna and motion sensor.

During this cruise it turned out that the connection between the Abyss PC, running the control software and the processing unit was unstable. Further tests with another PC identified the processing unit to be unreliable. As no spare systems were available *POSIDONIA* was not calibrated during this cruise.

### 4.4.2 Seismology: Outer Rise Seismic Network

*Processing of Earthquake Data*

The initial data processing of earthquake data is identical to the processing sequence for wide angle data, i.e., reading of the flashcards, conversion into the PASSCAL Reftek format, and further on into a pseudo SEGY format (PASSCAL SEGY).

The occurrence of time slips (extra or missing samples) due to a mismatch of the desired and actual sample rates has to be corrected. After unslipping, the PASSCAL SEGY files have to be cut into 25 hours records with one hour overlap between adjacent records to reduce files sizes. Next the timing of each 25 hours SEGY record has to be corrected for the slow drift of the internal clock relative to GPS time. The data quality is controlled using the pql (PASSCAL Quick Look) seismogram viewer. Only those stations and channels were used for triggering that were found to have sufficiently high data quality, see Table 4.3.

A short-term-average versus a long-term-average (STA/LTA) trigger algorithm is then applied to the data to search for seismic events. A 5-20 Hz band-pass filter must be applied prior to triggering, because of strong long-period noise around 0.2-0.5 Hz that shows up not only on broad-band sensors like DPG pressure sensors and Spahr-Webb seismometers, but also on many hydrophone channels (Fig. 4.4). After finding event triggers the events are cut from the 25 hours files with windows of 3 minutes, starting 60 s prior to trigger time. The SEGY traces in the event directories are converted into SEISAN waveform format. After conversion the data are registered into the SEISAN database (Havskov and Ottemöller, 2001).

**TAB. 4.3:** Channels used for triggering the events of the Outer Rise Network (ORN).

| **channels used for triggering** | **station** |
|---|---|
| Hydrophone | OBH10, OBH11, OBS12, OBH13, OBH16, OBH17, OBS18, OBH20, OBH23, OBH24, OBH25, OBH27, OBH28, OBH33 |
| Channel 2 | OBS22, OBS28, OBS29 |

**TAB. 4.4:** Trigger parameters as defined in the *text* to search the continuous recordings for seismic events.

| Parameter | s | l | m | t | d | S | M |
|---|---|---|---|---|---|---|---|
| Value | 0.5 s | 60 s | 500 s | 2.8 | 0.8 | 6 | 30 s |

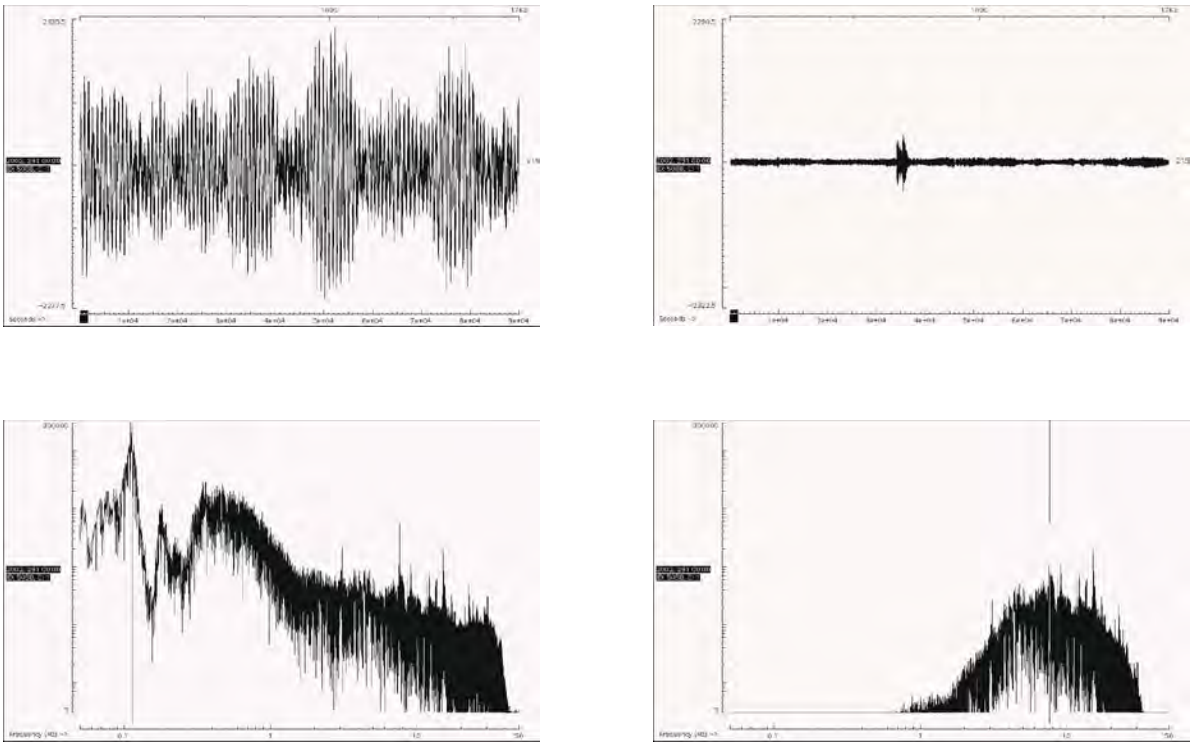

**FIG. 4.3:** Seismogram example recorded by a hydrophone. The raw seismogram (top left) contains strong long-period noise covering all higher frequency details. The noise frequency of ~ 0.1 Hz produces a large dominating peak in the raw spectrum (bottom left). On the 5–20 Hz band-pass filtered seismogram (top right) a small earthquake can be identified, that can only be detected by the trigger routine if a prefilter is applied. The filtered seismogram spectrum (bottom right) does not contain low frequencies any more.

At last, P and where possible S phases are picked and events are preliminarily located with the program HYP, which employs an iterative solution to the nonlinear localization problem (Lienert and Havskov, 1995). A 1-D velocity model, which is given in Table 4.5, is used for the preliminary location. When picking S phases on hydrophone channels it must be carefully figured out not to pick the water multiple (Fig. 4.4).

**TAB. 4.5:** 1-D velocity model offshore Nicaragua derived from profile P01 of this cruise.

| Depth [km] | $V_p$ [km/s] | $V_s$ [km/s] |
|---|---|---|
| 0.0 | 2.10 | 0.37 |
| 0.5 | 4.20 | 2.20 |
| 1.0 | 4.90 | 2.50 |
| 1.4 | 5.50 | 3.10 |
| 2.2 | 6.70 | 3.65 |
| 3.6 | 7.00 | 4.00 |
| 6.4 | 7.80 | 4.40 |
| 12.0 | 8.00 | 4.65 |
| 26.0 | 8.40 | 4.80 |
| 80.0 | 8.40 | 4.80 |

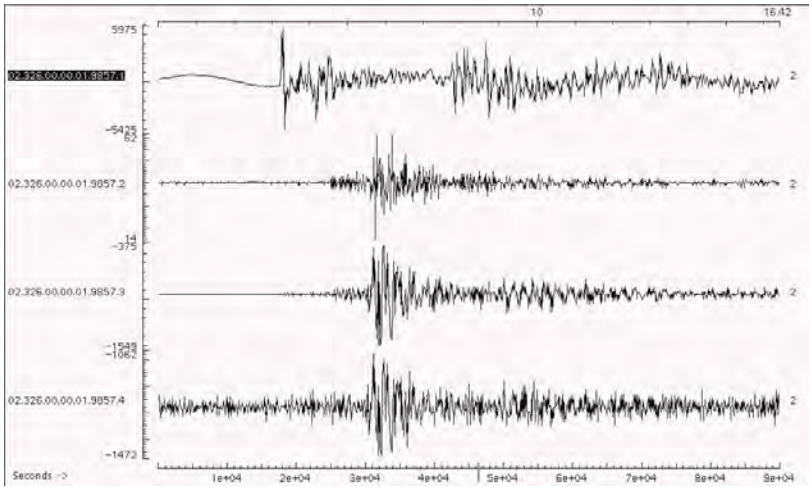


**FIG. 4.4:** Seismogram example of an OBS that shows the water multiple on the hydrophone channel (top) at about 8 seconds (top scale). The S phase can be clearly identified on the seismometer channels (2-4) at about 5.5 seconds .

*The Outer Rise Network (ORN) offshore Nicaragua*

A short-term seismic network was deployed on the outer rise offshore Nicaragua to record the local seismicity generated by the bending of the Cocos plate prior to its subduction to find possible fluid paths through the crust into the uppermost mantle which are bounding conditions for serpentinization models. The network of 22 stations operated for 2 months starting 28 Sep 2005 until 28 Nov 2005. Station locations and sensor types are given in Table 4.6.

In general data quality of the recordings was good. A major problem was the off-scaling of the hydrophones and the generally low gain of the Owen sensors. Cleaning of the connectors before deployment is suggested, as it appears to have decreased the off-scaling of the hydrophones. Off-scaling still occurred in several cases, but lasted only for a number of days.

Because of the low gain of the Owen sensors, small earthquakes were often under-amplified to allow phase picking (Fig. 4.5), especially on the vertical channels. For the deployment of the new network offshore Nicaragua (see below), we therefore changed the resistors on four of the preamplifiers of the MLS recorder to increase the gain. The data quality was checked on a one

day test run and seemed to be improved. A further check will be done after the recovery of the network and will help to decide whether more recorders should be changed.

**TAB. 4.6:** Station locations and sensor types of ORN. Hyd: Hydrophone; Seism: 3-C Seismometer; PMD: Broadband Seismometer

| Station | Latitude (N) | Longitude (W) | Depth (m) | Sensors |
|---|---|---|---|---|
| OBH 10 | 11°23.24’ | 87°46.98’ | 4840 | Hyd |
| OBH 11 | 11°16.67’ | 87°40.75’ | 4984 | Hyd |
| OBS 12 | 11°10.10’ | 87°34.49’ | 5296 | Hyd + Seism |
| OBH 13 | 11°03.51’ | 87°28.22’ | 5091 | Hyd |
| OBS 14 | 10°56.97’ | 87°22.02’ | 4892 | Hyd + Seism |
| OBH 16 | 10°50.41’ | 87°15.71’ | 5077 | Hyd |
| OBH 17 | 11°15.65’ | 87°50.78’ | 4863 | Hyd |
| OBS 18 | 11°03.64’ | 87°40.85’ | 4202 | Hyd + PMD |
| OBH 20 | 11°16.87’ | 88°05.96’ | 4170 | Hyd |
| OBH 21 | 11°06.95’ | 87°56.55’ | 3771 | Hyd |
| OBS 22 | 10°57.15’ | 87°47.20’ | 3445 | Hyd + Seism |
| OBH 23 | 10°49.46’ | 87°30.17’ | 3880 | Hyd |
| OBH 24 | 10°37.42’ | 87°28.50’ | 3292 | Hyd |
| OBH 25 | 11°10.37’ | 88°12.36’ | 3440 | Hyd |
| OBS 26 | 11°00.47’ | 88°02.91’ | 3160 | Hyd + Seism |
| OBH 27 | 10°50.67’ | 87°53.65’ | 2980 | Hyd |
| OBS 28 | 10°44.10’ | 87°47,32’ | 2967 | Hyd + Seism |
| OBS 29 | 10°30.93’ | 87°34.88’ | 2913 | Hyd + Seism |
| OBS 30 | 10°57.32’ | 88°12.38’ | 2820 | Hyd + Seism |
| OBS 31 | 10°44.22’ | 87°59.95’ | 2894 | Hyd + Seism |
| OBH 32 | 10°31.03’ | 87°47.45’ | 2996 | Hyd |
| OBH 33 | 10°37.76’ | 88°06.27’ | 3020 | Hyd |

The PMD seismometer of OBS 18 had very low gain on the vertical component. It was found that the resistor in the input cable of this channel was different from the horizontal channels, which may be the reason for the low gain. After changing the resistor, the behaviour of the vertical and horizontal channels appeared to be similar. Also a timing error occurred in OBS 18. Since this mistiming was present during the whole data recording period, therefore the traces were shifted by 30 seconds in the positive direction to correct the timing error.

The hydrophone components of OBS 22 and 30 were off-scaled, so that the hydrophone traces were removed completely for station OBS 22 and for the days 279 to 295 for OBS 30. For OBS 22 this was expected because of a bad pressure tube connector that could not be changed before deployment.

Before triggering, a 5 –20 Hz band-pass filter is applied to reduce the long-period noise between 0.03 and 0.5 Hz that often prevents the seismic events from being detected. For triggering we selected 14 channels from 13 stations that produced good data. Just three horizontal seismometer components were included because of the low signal-to-noise ratio. After

triggering, a total of 1892 events were obtained on 58 days of recording, with an average of 33 events per day (Fig. 4.6).

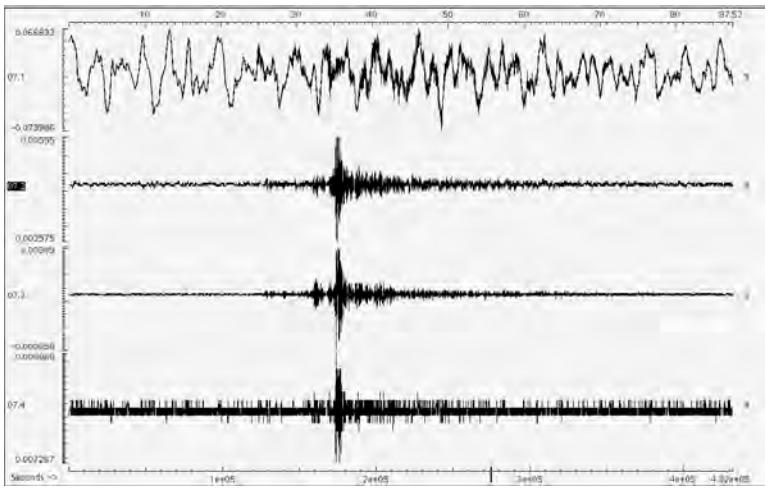

**FIG. 4.5:** Example for a small local earthquake. Traces are normalized individually. While the S-phase is visible on all seismometer components (trace 2-4), the P-arrival cannot be identified. The gain of the seismometer channels is by a factor ~100 smaller than on the hydrophone.

After picking P- and S-arrivals the events were located using the 1-D velocity model defined above (Table 4.6). A data example for an event inside the network is shown in Fig. 4.7. Clear P onsets can be seen on the hydrophone components and clear S onsets are visible on the horizontal seismometer components.

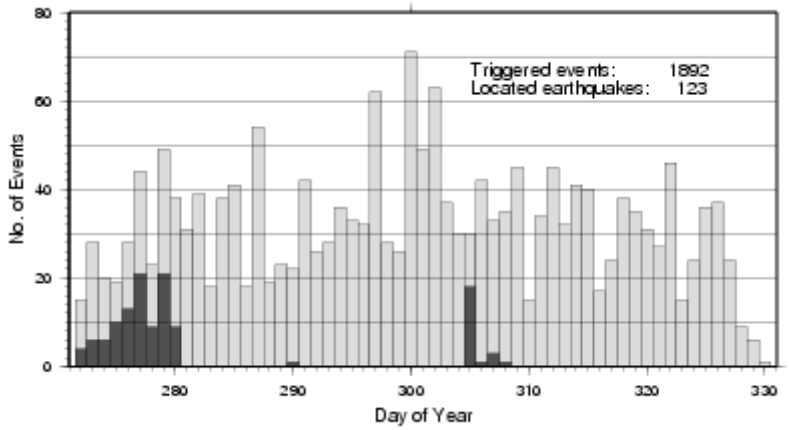


**FIG. 4.6:** Daily number of triggered events (grey bars) and located earthquakes (black). From 29 Sep 2005 (DOY 272) until 26 Nov 2005 (DOY 330) a total of 1892 events were detected, and 123 earthquakes have been located so far.

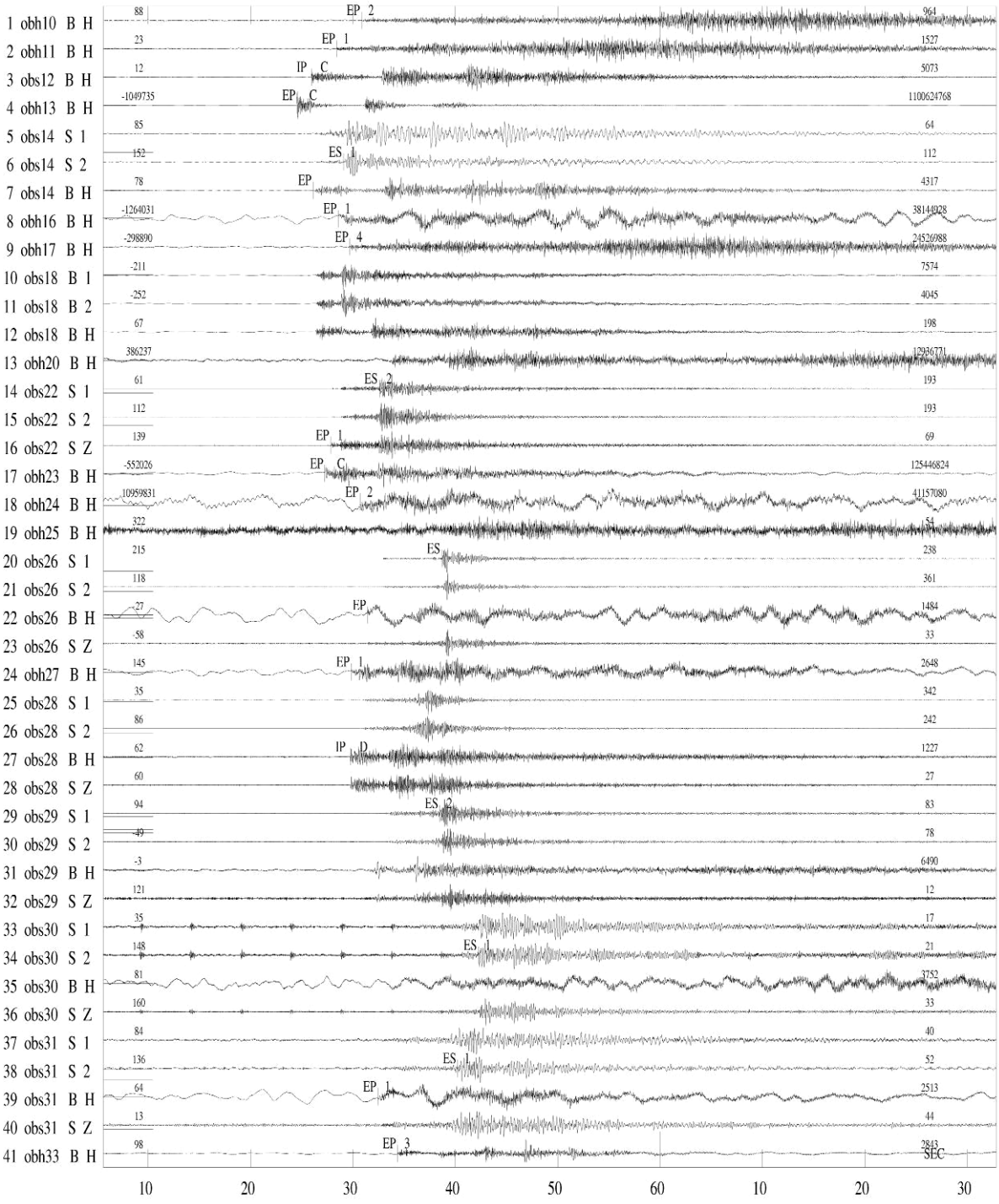


**FIG. 4.7:** Data example from the 1st Oct 2005 earthquake at 11.033°N; 87.515° W within the network. Where it was possible P and S first arrivals are indicated.

In Fig. 4.8 the seismicity recorded from the Outer Rise Network (ORN) is shown. Most of the 123 already located earthquakes occurred north of the network beneath the continental margin. The 20 events that occurred within the network are the most interesting for the outer rise study.

The focal depths of the located earthquakes vary between 0 km at the sea floor and 30 km in the mantle, however an accurate hypocentre determination is prevented by the still unknown 3D velocity structure.

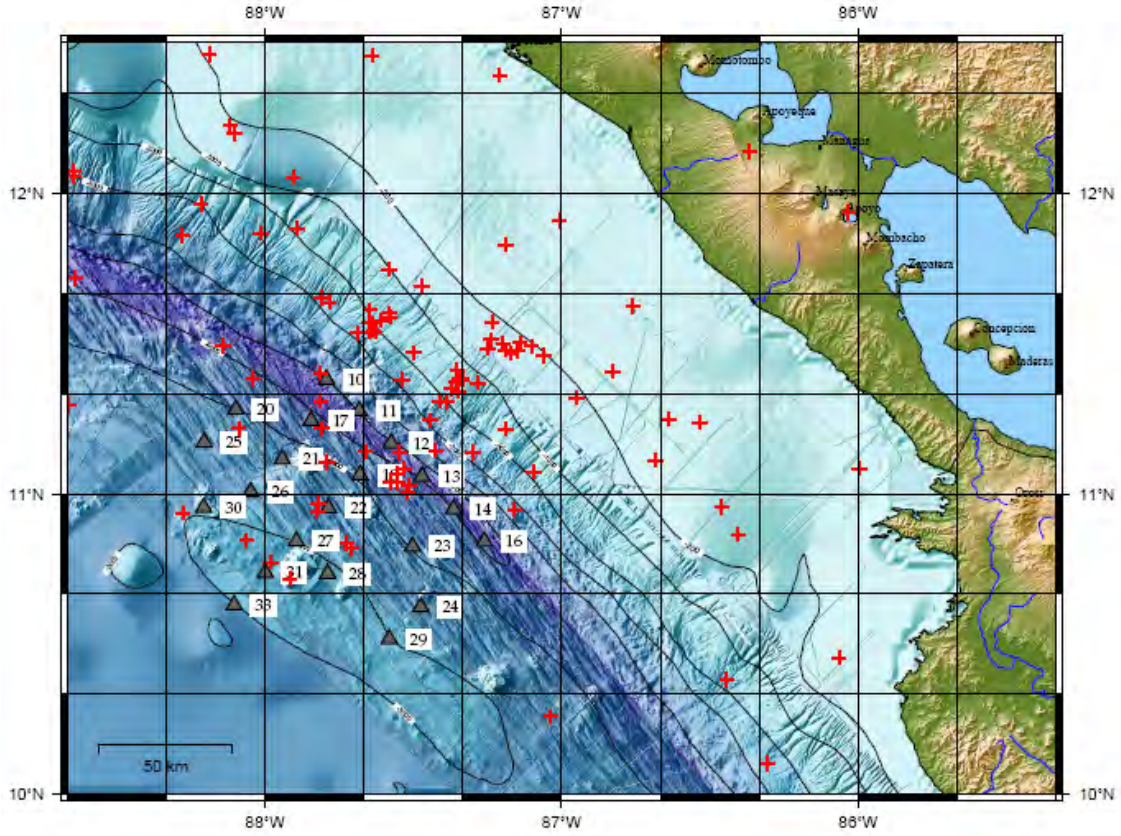


**FIG. 4.8:** Epicentres from earthquakes located so far by the Outer Rise Network. Most of the seismicity happened outside the network. However, only a small fraction of the triggered events have been evaluated so far.

### 4.4.3 Seismic Profiling in the Outer Rise

During the cruise three seismic wide angle and refraction lines were shot in the outer rise area (Fig. 4.9) using the G-gun cluster array described above. Profiles P01 and P02 run parallel to the continental slope. P01 is located in the trench itself and line P02 roughly 50 km seaward of the trench. The third profile runs perpendicular to the trench along Ewing Profile NIC80 shot in the year 2000.

Data passed an anti-aliasing filter of 50 Hz and were continuously recorded with a sampling rate of 200 Hz on all OBH and OBS stations. The data were played back and split into single shot records stored as a receiver gather in SEG-Y format. The instruments were deployed by free fall, using Global Positioning System (GPS) for drop-point positioning; instrument locations were further constrained using water-path travel times from the shots collected while the ship was navigated with GPS. Spectral analysis and filter tests show that the seismic energy is in a band ranging from 5 to 30 Hz. We ran this test for both near-offset and far-offset traces and chose a time- and range-dependant bandpass filtering approach. In addition, amplitudes were multiplied by distance to partly compensate the spherical divergence, simultaneously showing the level of both seismic signal and ambient noise.

*Profile 01*

During M 66/4a several seismic profiles perpendicular to the previously existing in the area offshore Nicaragua were acquired in order to investigate the process of serpentinization in the incoming oceanic plate. The 68 nm long profile p01 intersects the trench at 11°N ending in the margin wedge at the northwestern part of the line (Fig. 4.9).

To determine crustal and upper mantle structure and provide a detailed velocity model 12 OBH/S instruments were used to collect a deep seismic and wide angle dataset. Seismic velocities along the line will be used to estimate the amount of serpentinization in the upper ocean mantle. The instruments were deployed at intervals between 4.5 and 9 nm. Four GI-Guns were used for shooting along the line. They were fired at intervals of 60 s, which at speed of 4.5 kn results in an average spacing of 130 m. Figure 4.10 and 4.11 show examples of the data quality available for interpretation.

The preliminary velocity model (Fig. 4.12) has been constrained using MacRay 2.0 (Luetgert, 1992), an interactive conventional 2_D raytracing system, based on a trial and error approach. The modelling has been done from top to bottom applying a layer-stripping strategy, working towards the centre of the profile from both ends. Shipboard forward modelling suggests 1.2-1.3 km thick sedimentary layer at the margin wedge and 350-400 m at the trench (1.5-1.85 km/s), underlain by app. 5 km thick oceanic crust with velocities ranging from 4.5-6.7 km/s. Best-fit model yields mantle velocities ranging from 7.4 km/s at the Moho of the subducting plate and 7.5 km/s of the margin wedge, which is an indication for a serpentinized zone.

*Profile 02*

Profile P02 runs parallel to the continental slope ~50 km from the trench axis (Fig. 4.9). 12 OBS and OBH stations operated successfully (Fig. 4.13). A first seismic model was obtained from forward modelling using travel time data from each second station. Crustal thickness is ~5 km. Seismic velocities in the uppermost mantle are significantly reduced compared to normal oceanic crust. Velocities are between 7.5 to 7.6 km/s and thus may indicated that bending related faulting has affected the mantle structure by serpentinization.

*Profile 03*

15 seismic ocean bottom instruments provided data useful for geophysical interpretation. For the on-board data analysis we ignored instruments sitting on the lower slope and used 13 stations seaward of the trench. We picked crustal arrival (Pg), reflections from the crust mantle boundary (PmP) and energy diving through the uppermost mantle (Pn). Unfortunately, the most seaward seismometers provide only crustal phases of good quality. Most other stations have good Pn, PmP and Pg arrivals. Examples of the seismic sections achieved are displayed in Figures 4.14 and 4.15.

In our approach to derived the velocity structure we used the joint refraction and reflection travel time inversion method of Korenaga et al. (2000). This tomographic method allows to determine a two-dimensional velocity field and the geometry of a floating reflector from the simultaneous inversion of first arrival and wide-angle reflection travel times. The floating reflector is represented as an independent array of linear segments with only one degree of freedom (vertical) for each reflector node. We used the floating reflector to model the crust-mantle boundary, i.e., the Moho. Using normal oceanic crust as starting model (5 km thick crust, for

layer 2, layer 3 and upper mantle velocities of 4.5-6.5, 6.6-7.1, 8.1-8.3 km/s, respectively) we obtained seismic velocities within the uppermost mantle that are significantly reduced with respect to the starting model and hence much lower than elsewhere in the ocean's (Fig. 4.15) However, it is interestingto note the seismic velocity in the mantle is reasonably low along the entire line, even seaward of the outer rise. In the post-cruise data inversion we have to carefully re-analyse the dataset. For the inversion we forced a constant crustal thickness along the profile. The misfit for the PmP arrivals increases seawards and thus may suggest that the crustal thickness increases. Therefore, due to a trade-off between seismic velocity and layer thickness the low values for the upper mantle might be caused by an increase in crustal thickness and a lack of reversed seismic Pn arrivals on the most seaward instruments. Nevertheless, a profound feature from all three profiles is a clearly reduced seismic velocity in the uppermost mantle, suggesting that serpentinization is indeed an important process changing the seismic structure in deep sea trenches and hence facilitates the flux of water into the deep subduction zone and the Earth's interior.

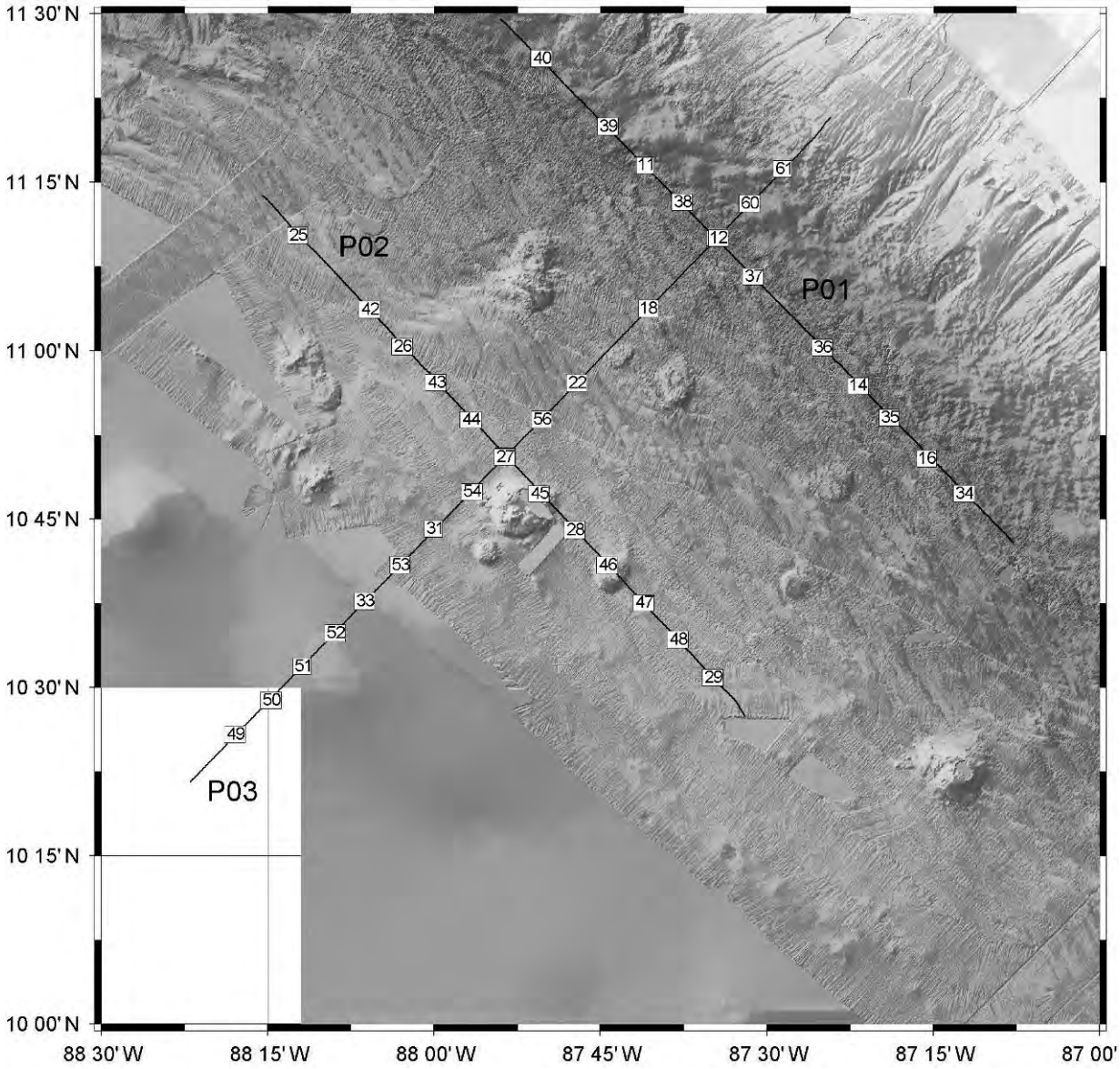


**FIG. 4.9:** Map of the three seismic profiles deployed for the active source outer rise study.

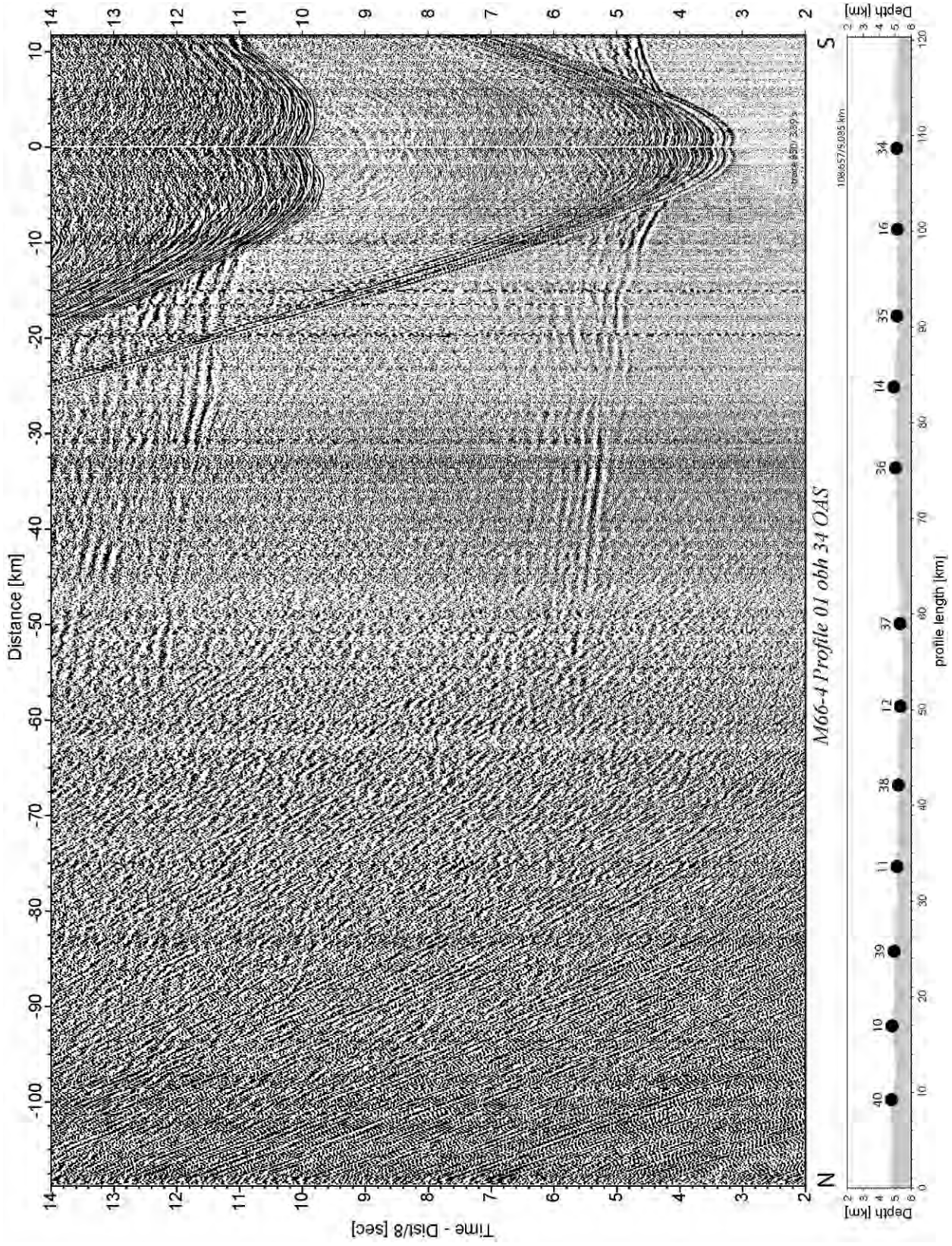


**FIG. 4.10:** Data example of station 34 observing the entire spread of profile 01. Refracted energy can be tracked as far as 60 km offset. Within 30 km offset reflected energy is observed between 5.5 and 7 sec.

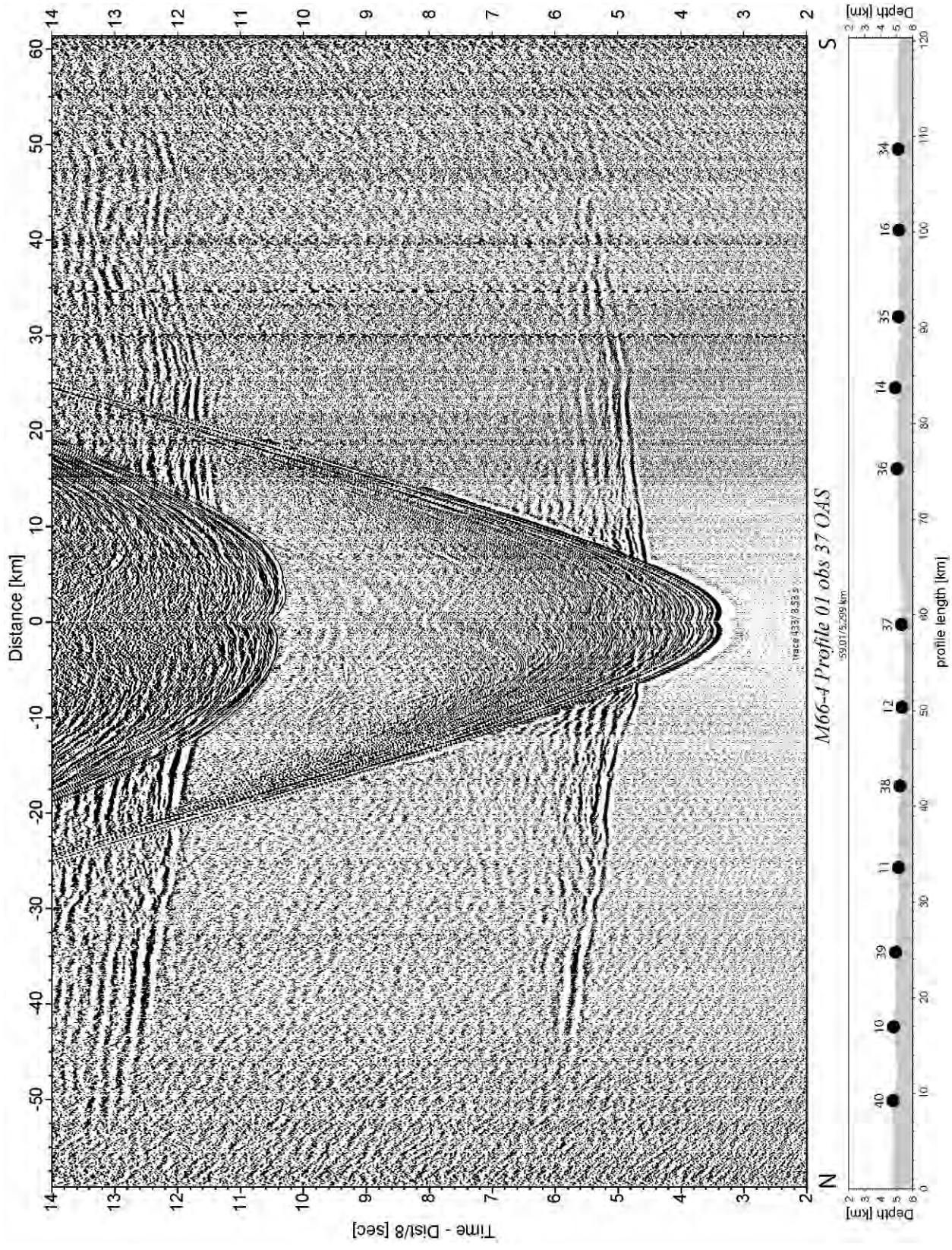


**FIG. 4.11:** Data example from the centre of profile 01.Reflection events are observed in the time interval between 6 and 8 sec. Strong amplitudes between 40 km and 50 km offset argue for Moho reflections

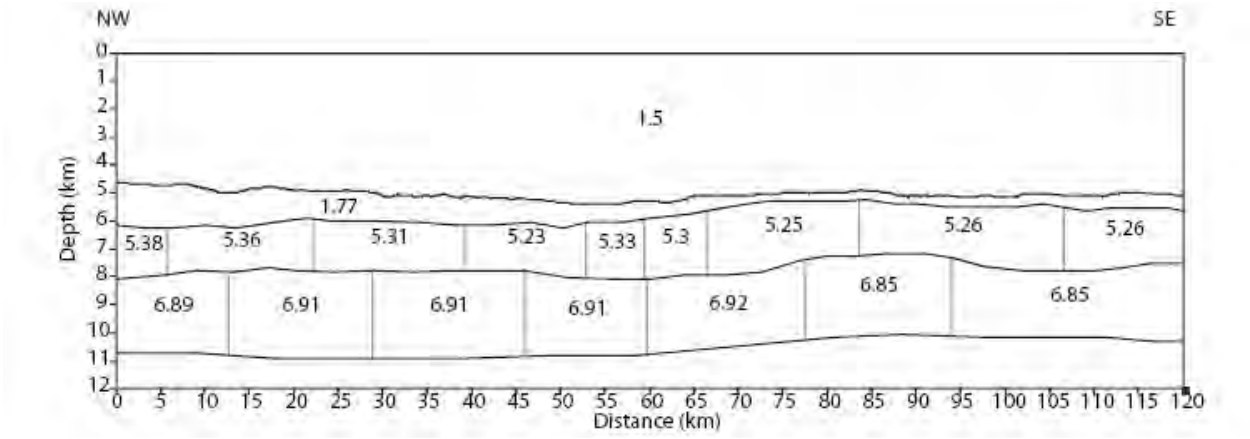


**FIG. 4.12:** 2-D velocity –depth profile derived by forward ray tracing.

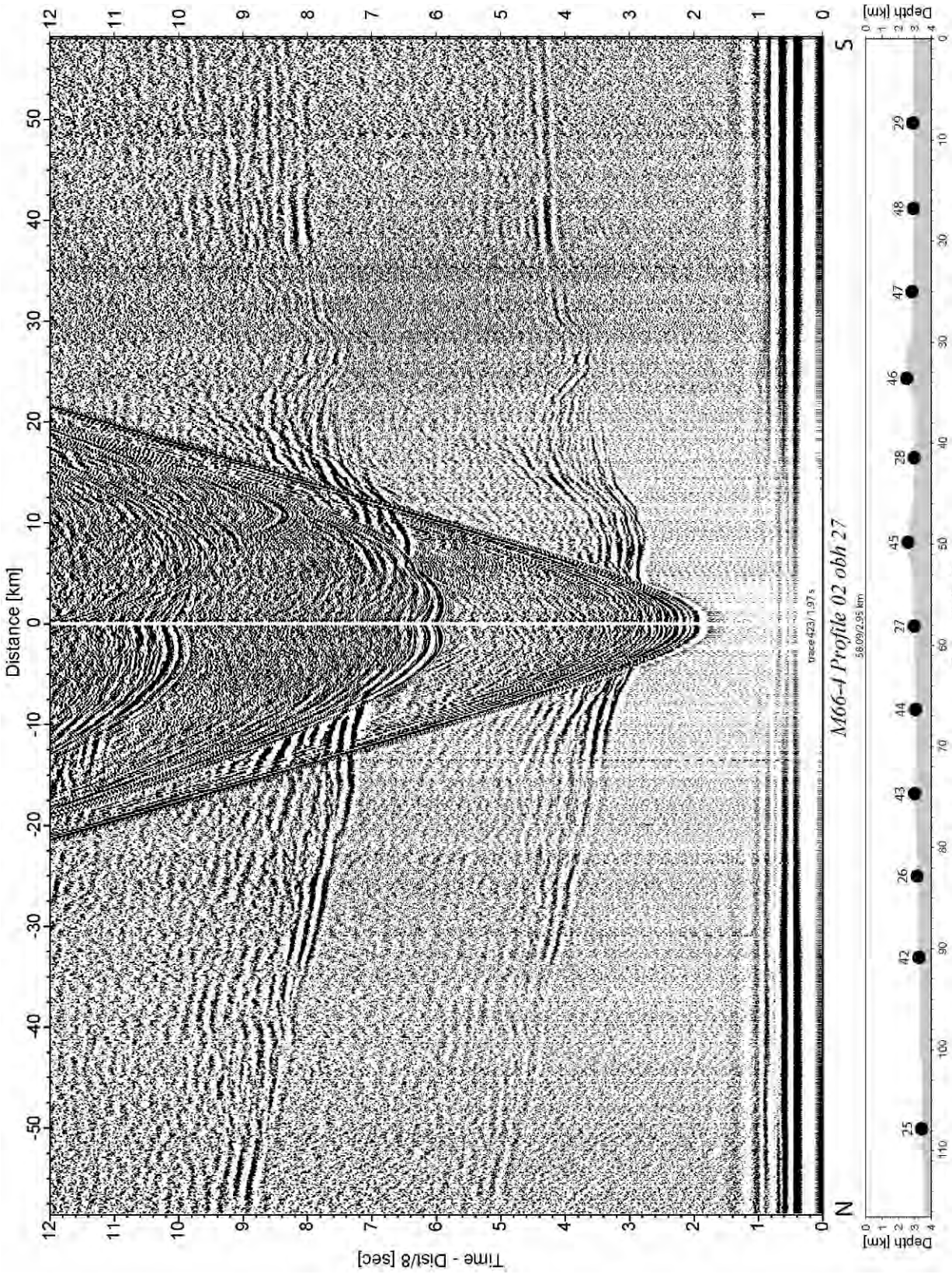


**FIG. 4.13:** Data example from station 27 located in the centre of profile 02. Refracted energy is observed as far as 60 km offset. Reflection events at later traveltimes will support the velocity model with good depth control.

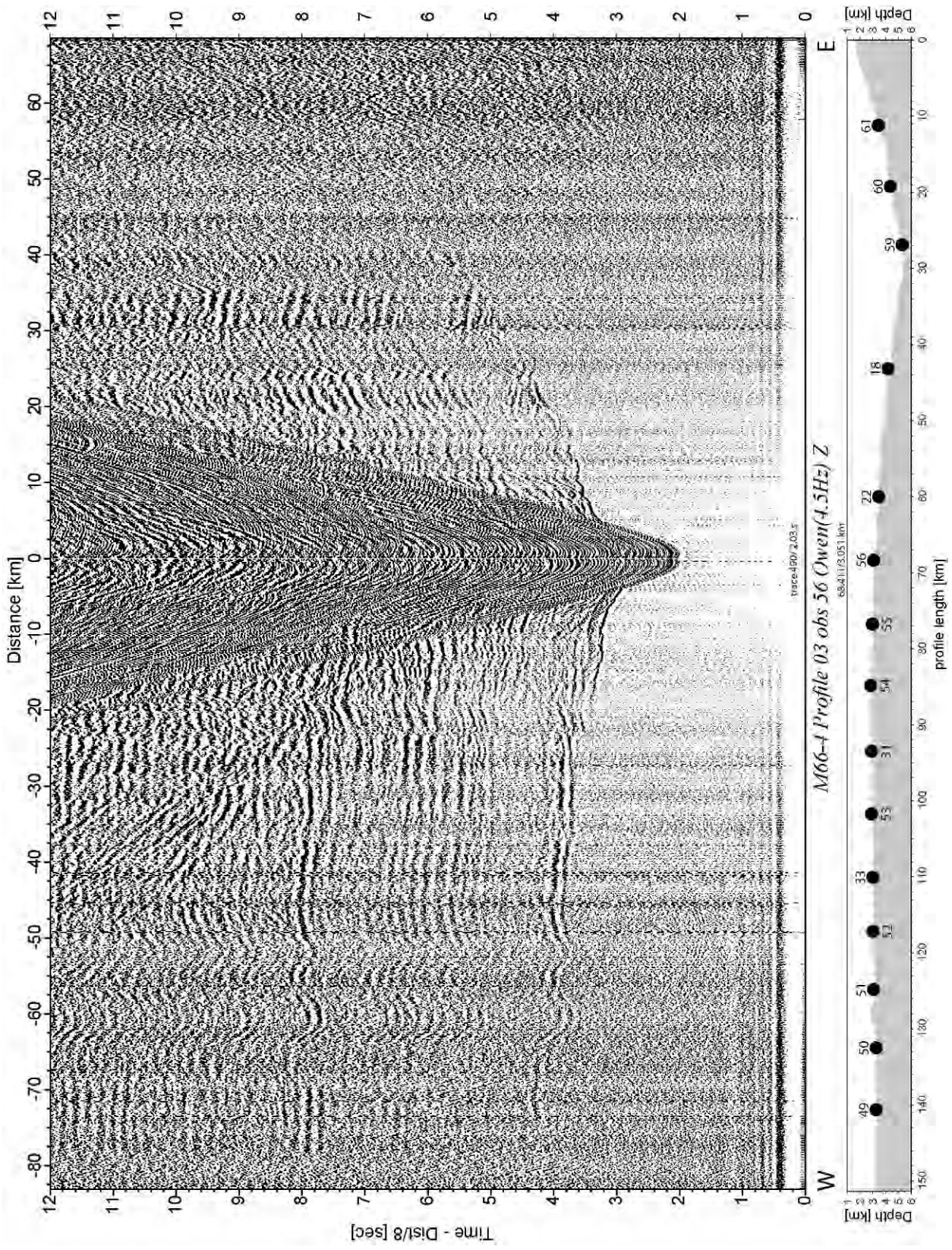


**FIG. 4.14:** Data example from station 56 located right above the outer rise. Refracted energy observed as far as 85 km offset wil provide good depth coverage for velocity-depth modelling.

.

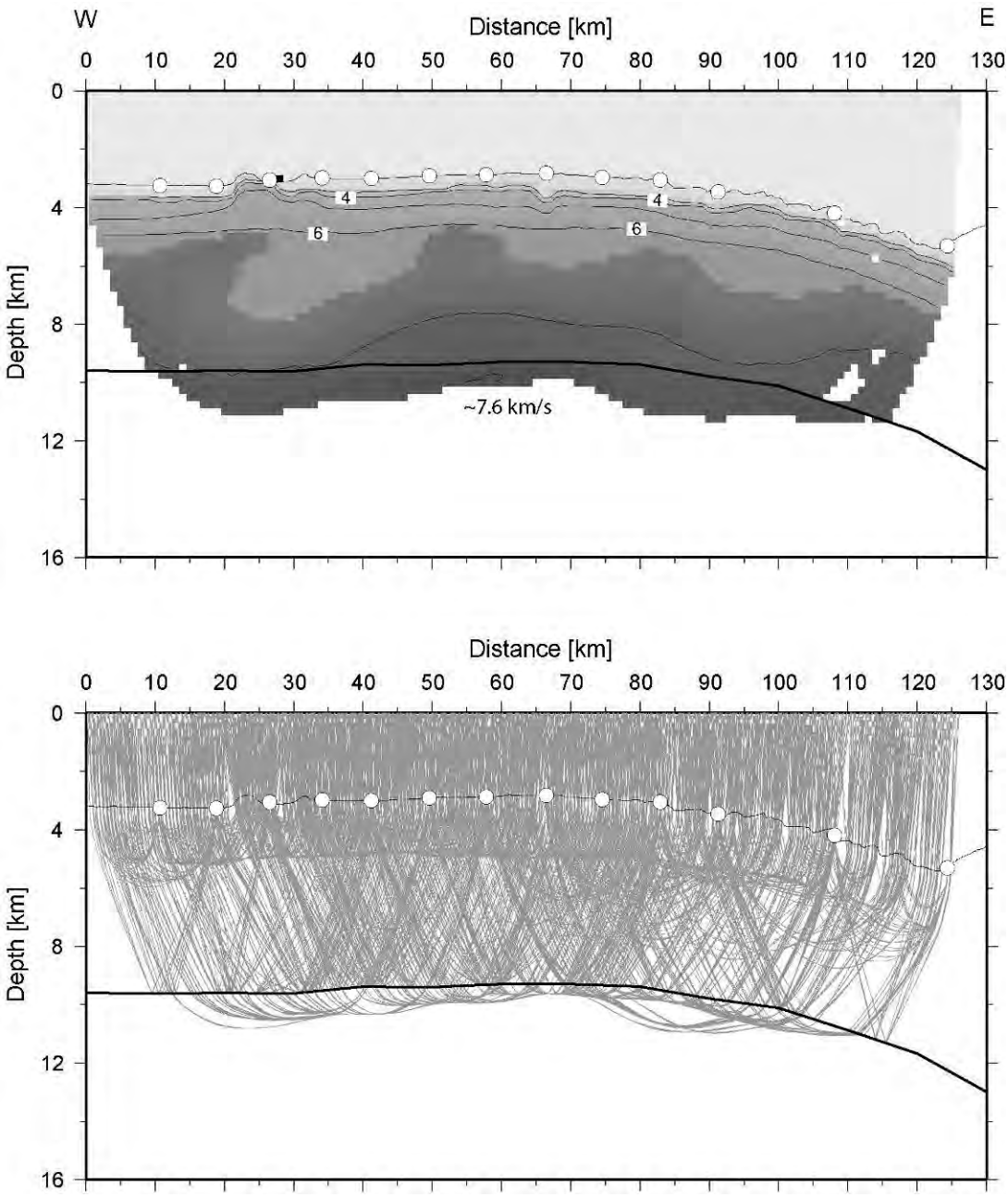


**FIG. 4.15:** Tomographic velocity model of profile 03

### 4.4.4 Seismic Profiling Across Mound Structures

During cruise SO-173 of RV SONNE a high resolution seismic survey was carried out using a deep towed multichannel seismic streamer (DTMS) and sidescan (DTS) to image the numerous submarine mud mounds and associated BSR in the continental slope off Nicaragua. Numerous mud mounds and a widespread occurrence of BSR had been discovered. The proximity of the streamer to the seafloor of the deep towed system allows recoding of wide angle reflection data and permits imaging beneath the carbonate crusts. The data have shown that the BSR in many cases continued along the mound chimneys with or without considerable loss of amplitudes. Another remarkable feature in the area is the occurrence of numerous mud mounds, which seem to be controlled by the locations of the faults.

It was planned to extend the existing profiles with additional cross lines in order to identify the relation of faults in the process of the observed diapirism and mound formation. In addition the use of a GI gun source with increased volume should enable to record seismic events from below the BSR to make sure the disappearance of the BSR is real and not caused by not penetrated energy. Due to the loss of the sidescan (see chapter 4. 4.6 for details) these investigations were cancelled.

As an alternative OBS were deployed along three profiles (Fig. 4.16) crossing prominent mound structures. The first profile runs parallel to the slope of the margin, it starts at the Masaya Slide and continues upslope crossing Mound Baula. This line should provide wide angle information from the point of origin of the slope as well as slope parallel information about the deeper structure of Mound Baula. The next line was lead out along the Mound Baula massiv perpendicular to the slope, on top of one of the older deep tow survey lines. The third profile was chosen to cross a ridge like structure in the vicinity of Mound Morpho. Along these ridge several mounds were identified by multichannel deep towed seismic and side scan sonar mapping. OBS were deployed with an overall offset of 1 nm. In the vicinity of the mounds the offset was reduced to 150 m in order to enable high resolution inversion at these sites. For high resolution investigation all three profiles were shot with a 150/250 ci. GI gun, fired at 14 s interval (P4, P5 and P9; Fig. 4.17 and Fig. 4.19). In a second run 2 G gun clusters (1040 ci each) were used to record seismic events from greater depth in order to investigate the deeper roots of the mound structures (P6, P7 and P8; Fig. 4.17).

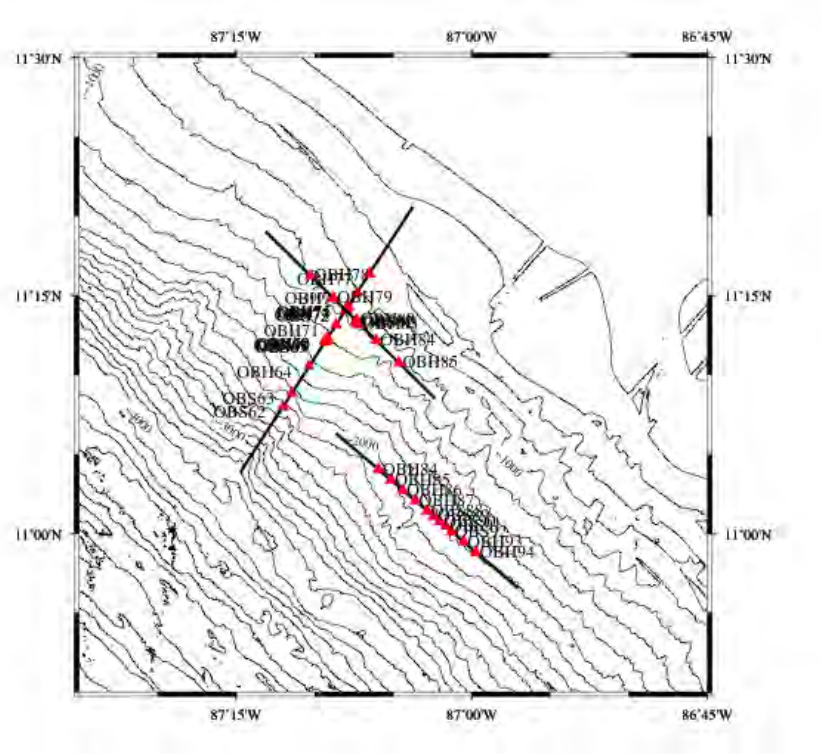


**FIG. 4.16:** Map of the high resolution seismic profiles.

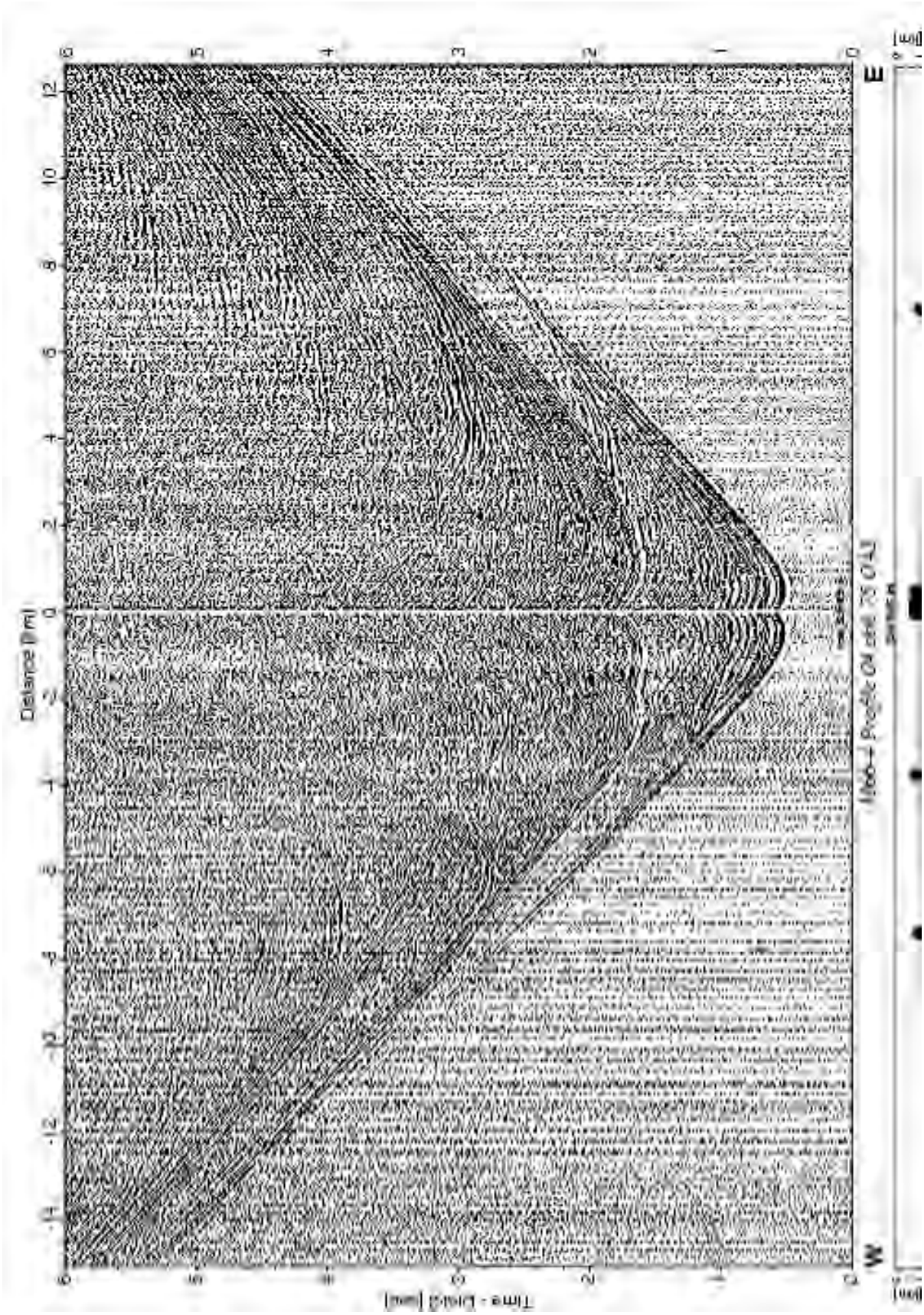


**FIG. 4.17:** Wide angle seismic record of GI airgun shots at station 78. The higher frequent GI guns allow to identify near-vertical reflections up to 8 km offset, while refracted energy is very weak.

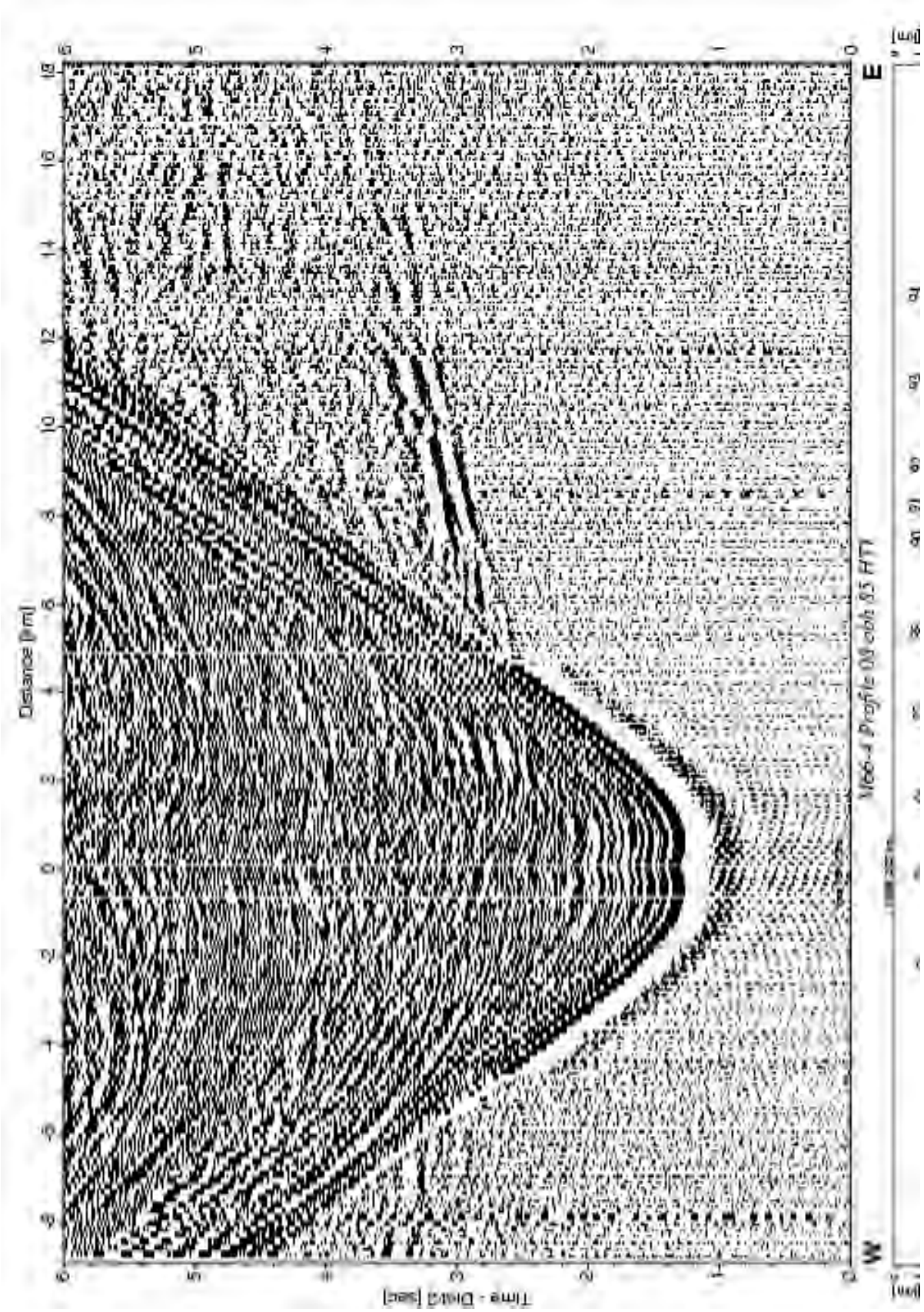


**FIG. 4.18:** Wide angle airgun shots of the G-gun array recorded at station 85. Increased source energy of the G-gun array provides observations to up to 18 km offset, which will supplement the high-resolution GI gun data with additional depth coverage.

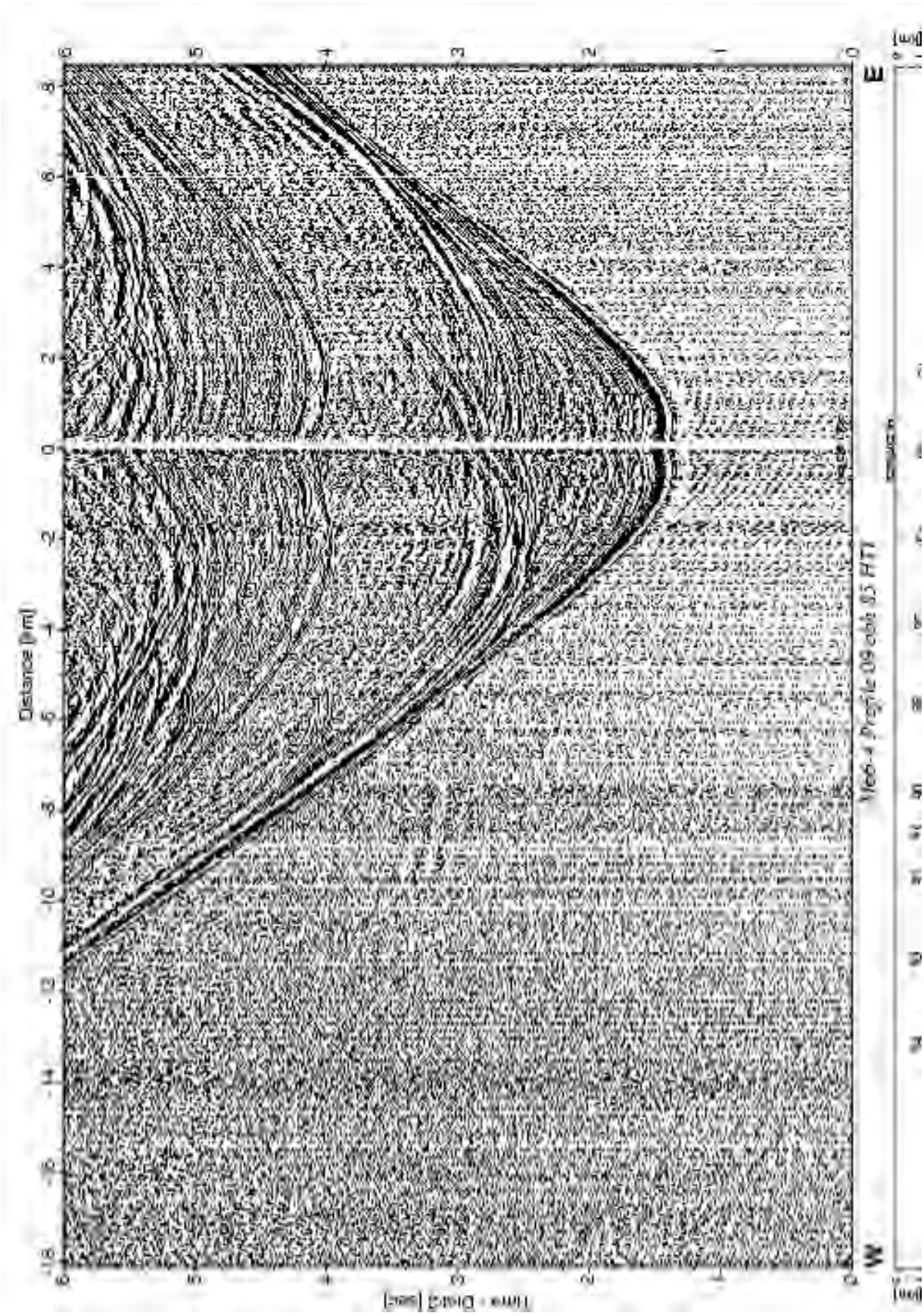


**FIG. 4.19:** Wide angle airgun shots of the GI-gun recorded at station 85. The GI guns with higher frequency allow to identify near vertical reflections up to 8 km offset, while refracted energy is very weak.

### 4.4.5 Side Scan Deployment

The first deployment of the DTS-1 sidescan sonar was targeted at imaging the continental slope offshore El Salvador. Here the orientation of the continental slope changes from roughly NW-SE to an orientation more closely to WNW-ESE (Fig. 4.20). Bathymetric data show two different segments of the slope separated by a broad canyon. The segment south of the canyon still shows indications for mound-like structures while such structures appear to be absent north of the canyon. The intention was to map this area with 75 kHz sidescan sonar in order to determine whether indeed fluid-escape structures exist south of the canyon but are absent north of it. In addition sidescan sonar images together with subbottom profiler and PARASOUND records would allow establishing the down slope sediment transfer in comparison with the continental slope off Nicaragua and off Costa Rica.

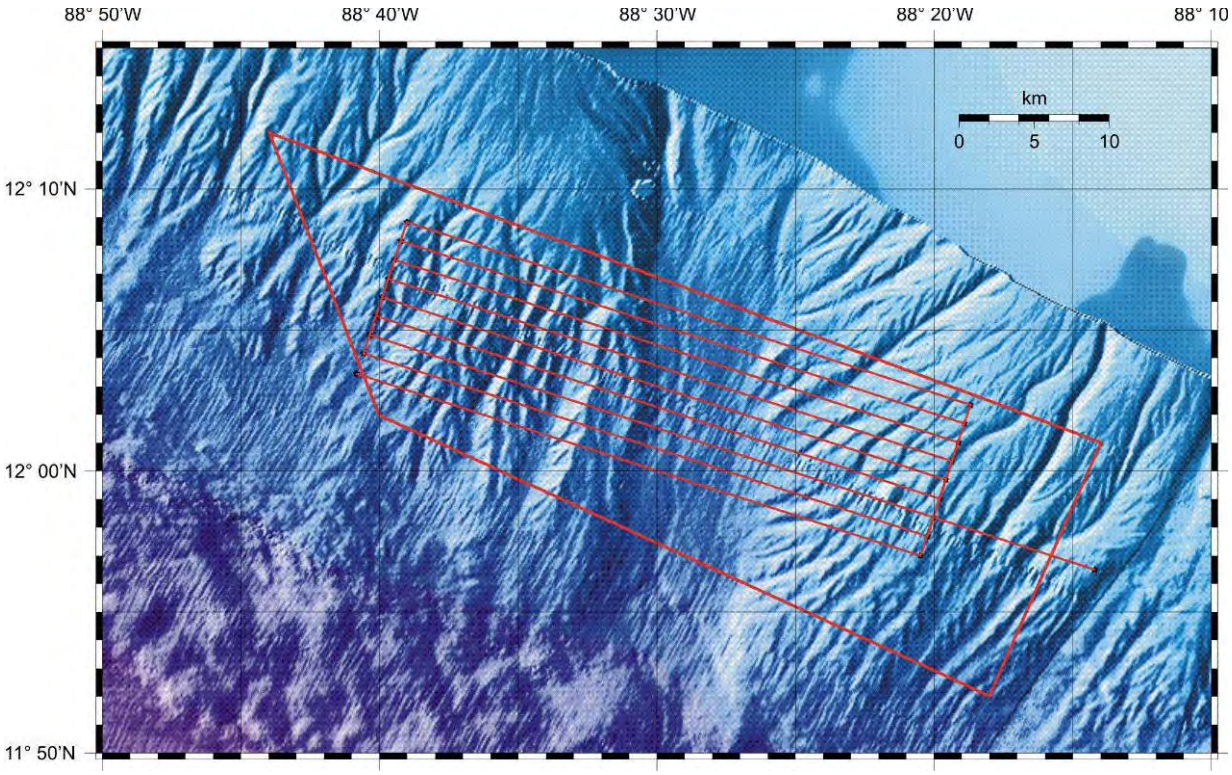


**FIG. 4.20:** Map of the desired tracks for the sidescan survey.

*Deployment and loss*

The sidescan has been deployed in its usual configuration at Nov 28, 19:40 UTC with the ship heading towards the current. At 19:52 UTC the depressor has been lowered into the water and the winch veered with 0.2 m/s while the ship slowly turned towards the correct course. The sidescan was started from its dry unit and all systems worked. At 20:11 UTC the data connection to the sidescan was interrupted, but the sidescan was still under power. After checking for a short-circuit, the sidescan was restarted. Shortly after restart at 20:13 UTC the power connection to the sidescan failed (no more current). At the time the pull on the cable dropped from 22 kN to 5 kN and we expected the sidescan sonar to have fallen off the cable. A hydrophone was lowered into the water as quickly as possible in order to release the towfish from the depressor. Range data, however, indicated that the sonar was already lying on the ground. The cable was pulled in

without its termination. Only four of the spirals of the cable stopper were still attached to the cable (Fig. 4.21).

**FIG. 4.21:** The broken cable termination.

*Recovery*

Attempts to recover the sidescan sonar started with determining its exact position. The releaser of the sidescan sonar answered perfectly allowing the determination of the range to the sidescan sonar from different positions. These data together with the water depth yield the position of the sidescan sonar on the seafloor using the law of Pythagoras (Fig. 4.22). The releaser appeared to have freed the towing rope, but the sidescan sonar probably was still connected to the power cable leaving it floating in 2270 metres water depth, some 40 metres above the seafloor.

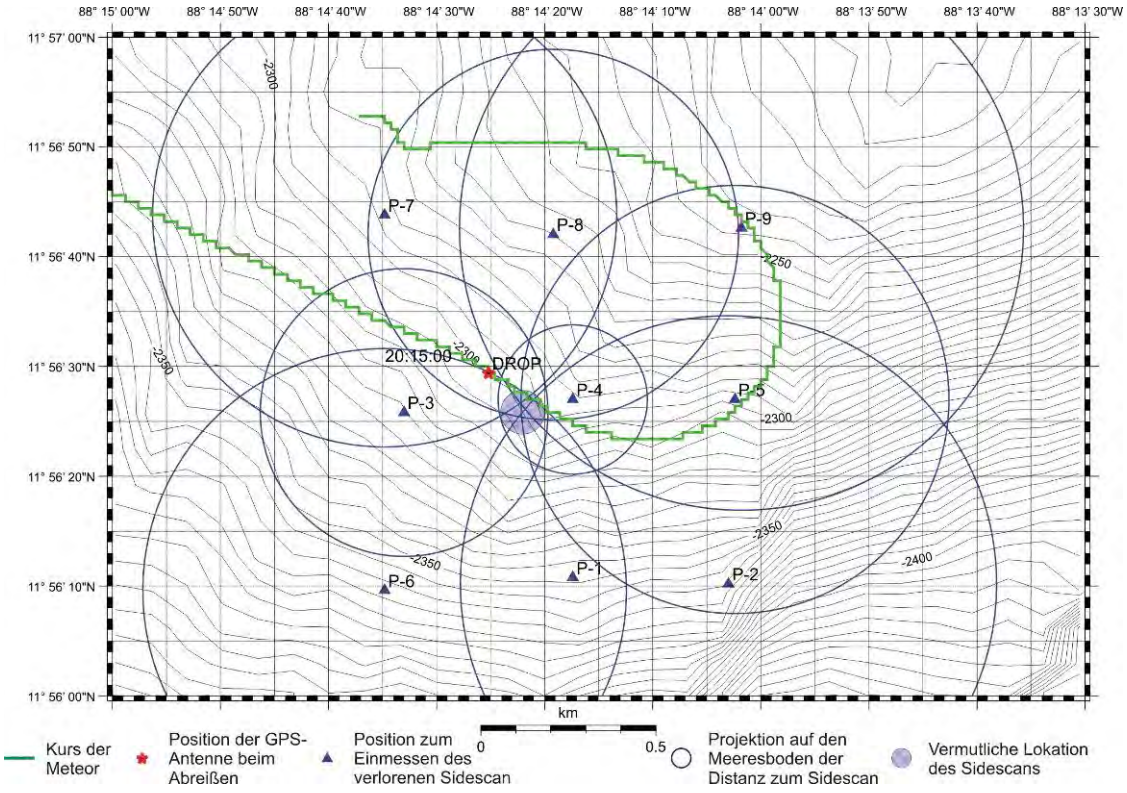


**FIG. 4.22:** Map showing the course of RV METEOR and estimated drop position of the fish.

For the recovery attempts an improvised dredge gear was set up consisting of a 200 m long precurser cable fitted with „search dragons“ and other hooks. This precurser cable was then attached to the 11 km long geology cable. Three attempts for dredging the sidescan sonar were made (29.11.05 at 14:35 UTC until 30.11.05 at 01:12 UTC; 30.11.05 at 01:16 UTC until 30.11.05 at 11:54 UTC; 01.12.05 at 22:30 until 02.12.05 at 13:47 UTC). After the first two unsuccessful attempts the precursor cable was extended to 400 metres and additional weight was attached to the towing cable once 500 metres of the cable had been paid out. During this third attempt a spiral was laid out around the estimated position of the sidescan (Fig. 4.23). Then with 9500 metres of cable paid out the ship moved away from the estimated position by another 1500 metres in order to increase chances that the dredging cable will actually scratch over the seafloor. Acoustic communication with the releaser on the sidescan sonar was no longer possible during the dredging attempts, but at 09:35 UTC a seaman spotted a blinking light on the horizon and soon later the ship received an acoustic signal from the sidescan sonar. At 14:15 UTC the sidescan sonar was back on deck with no other damage than a broken umbilical cable.

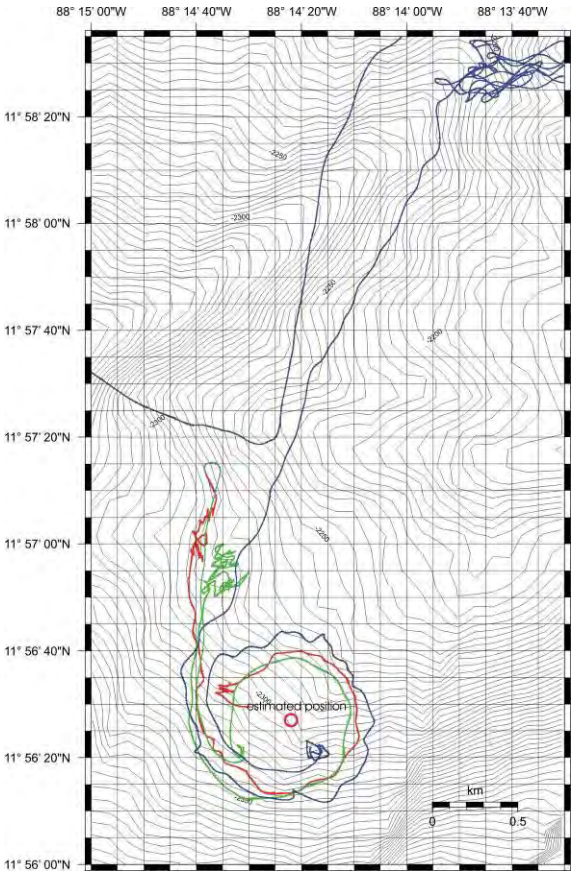


**FIG. 4.23:**
Map showing the tracks of RV METEOR during the dredge operation.

## 4.4.6 CPT Testing During Leg M66/4b

The CPT measurements at the Chilean continental slope focused on the northernmost profile to complement the earlier heat flow transects (Fig. 4.25). A total of 8 individual tests were carried out along the transect. The range of water depths was 1018 – 1824 meters below sea level. Initial results indicate two things:

1) The sediments along this section of the Chilean margin are well indurated, because the lance penetrated the sediment only by up to 1-2 meters. In some cases, repeated attempts were required to penetrate at all since the instrument fell on its side upon seafloor contact.

2) Despite the difficulties to penetrate the seafloor, pore pressure signals showed nice peaks upon impact, and a rapid decay. Measured $t_{50}$-parameters ranged between 10 and 40 minutes.

**FIG. 4.24:**
Picture of the instrument during deployment from RV METEOR.

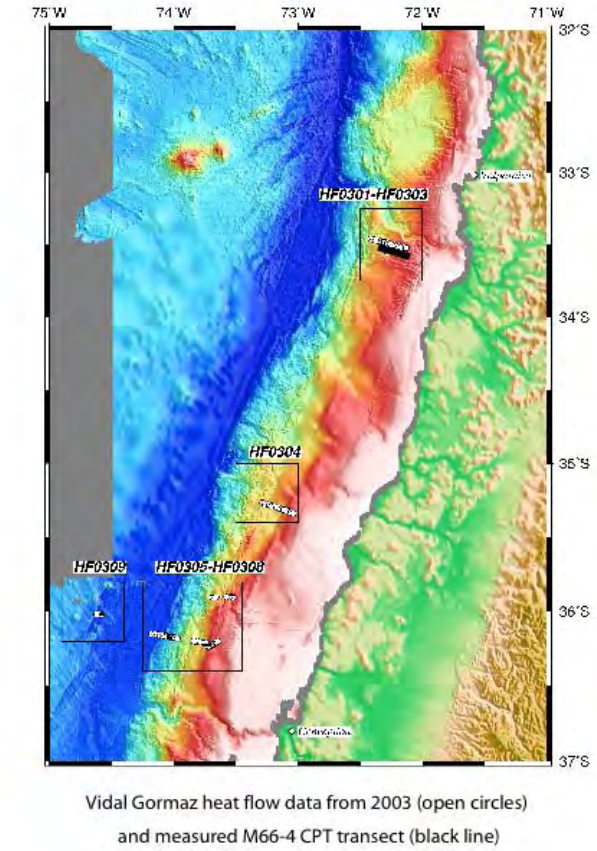


Vidal Gormaz heat flow data from 2003 (open circles)
and measured M66-4 CPT transect (black line)

**FIG. 4.25:**
Bathymetric map of the study area off Chile including heat flow and CPT locations.

## 4.5 Ship's Meteorological Station

RV METEOR left the port of Corinto in the morning of November 21 on time, heading for the investigation area off Nicaragua in fair weather with variable winds of Bft 2 to 3.

One day later the weather situation got worse by many clouds and isolated showers. On November 23 the wind from northeast to east increased up to 5 and 6 Bft and persisted in this force for the first week in the research area. During this period several small tropical depressions moved from Columbia and Panama south of METEOR´s position in westerly direction. From November 24 the clouds became scattered, on some days no clouds were observed. During the second week in the area up to 13° N 89°W the wind speed decreased to a range between 1 and 3 Bft and the wind direction became more northerly, some spells were calm.

From December 03 in the southern investigation area north of the peninsula „Nicoya" (Costa Rica) from December 03 the wind veered easterly and the speed increased to 5 and 6 Bft with some peaks of 7 Bft. The clouds were mainly scattered with translucent Altocumulus and Cirrus. On the last but one day of reasearch after passing the peninsula Nicoya a first short period of shower activity began and continued south of the peninsula.

METEOR left the area off Costa Rica in fair weather with westerly winds of about 3 Bft and steered for Guayaquil on December 08. During the following night and day the ITCZ (Inter tropical Convergence Zone) was passed with few and short but heavy showers and winds of Bft 3, backing from west to south. Until the arrival in Guayaquil (end of M66/4a) on December 11 the weather was cloudy without precipitation and the winds encountered came from south to southwest about 4 Bft.

After leaving Guayaquil for leg M 66/4b on December 12 and during the next days the weather was fair associated with southerly winds about 3 Bft, for a short time up to Bft 6 during the following night due to orographical coastal effects. The further course was affected by few, later variable mostly broken trade wind clouds.

The wind came from south to southeast with 3 to 4 Bft and increased to 5 to 6 Bft after passing the 25$^{th}$ degree of latitude. The voyage ended on December 21 in Talcahuano/Chile for repair in the shipyard.

## 4.6 List of Stations

**OBH: Ocean-Bottom-Hydrophone** **OBS: Ocean-Bottom-Seismometer**

| INSTRUMENT | LATITUDE (N) D:Min | | LONGITUDE (W) D:Min | | DEPTH (m) |
|---|---|---|---|---|---|
| **Nicoya** | | | | | |
| **OBH 95** | 11 : | 08,380 | 86 : | 48,560 | 188 |
| **OBS 96** | 10 : | 55,740 | 86 : | 40,730 | 405 |
| **OBS 97** | 10 : | 49,770 | 86 : | 54,000 | 2344 |
| **OBS 98** | 10 : | 42,550 | 86 : | 40,830 | 1309 |
| **OBH 99** | 10 : | 45,580 | 86 : | 28,990 | 210 |
| **OBS 100** | 10 : | 47,360 | 86 : | 10,840 | 193 |
| **OBH 101** | 10 : | 34,200 | 86 : | 15,600 | 255 |
| **OBS 102** | 10 : | 34,200 | 86 : | 28,220 | 924 |
| **OBH 103** | 10 : | 29,940 | 86 : | 40,970 | 3236 |
| **OBS 104** | 10 : | 29,950 | 86 : | 54,060 | 4919 |
| **OBH 105** | 10 : | 13,760 | 86 : | 48,130 | 4200 |
| **OBS 106** | 10 : | 12,570 | 86 : | 28,880 | 3435 |
| **OBH 107** | 10 : | 23,360 | 86 : | 28,840 | 2175 |
| **OBS 108** | 10 : | 23,370 | 86 : | 15,610 | 904 |
| **OBH 109** | 10 : | 12,590 | 86 : | 15,570 | 1668 |
| **OBS 110** | 10 : | 16,560 | 86 : | 04,760 | 212 |
| **OBS 111** | 10 : | 07,220 | 85 : | 55,790 | 248 |
| **OBH 112** | 10 : | 01,210 | 86 : | 06,040 | 1537 |
| **OBH 113** | 9 : | 49,260 | 85 : | 57,020 | 1762 |
| **OBH 114** | 9 : | 56,400 | 85 : | 49,190 | 317 |
| **Mound 12** | | | | | |
| **OBH 115** | 8 : | 55,710 | 84 : | 18,850 | 1017 |
| **OBH 116** | 8 : | 55,710 | 84 : | 18,810 | 1012 |
| **OBT 117** | 8 : | 55,760 | 84 : | 18,820 | 1008 |
| **Dominical** | | | | | |
| **OBS 118** | 8 : | 38,260 | 84 : | 13,610 | 1436 |
| **OBS 119** | 8 : | 43,280 | 84 : | 11,290 | 758 |
| **OBS 120** | 8 : | 48,200 | 84 : | 07,340 | 322 |
| **OBS 121** | 8 : | 33,050 | 84 : | 17,410 | 2731 |

| INSTRUMENT | LATITUDE (N) D:Min | | LONGITUDE (W) D:Min | | DEPTH (m) |
|---|---|---|---|---|---|
| **OBH 34** | 10 : | 47,210 | 87 : | 12,380 | 4997 |
| **OBH 16** | 10 : | 50,410 | 87 : | 15,710 | 5077 |
| **OBS 35** | 10 : | 54,040 | 87 : | 19,150 | 5070 |
| **OBS 14** | 10 : | 56,970 | 87 : | 22,020 | 4892 |
| **OBP 15** | 10 : | 57,010 | 87 : | 22,250 | 4871 |
| **OBS 36** | 11 : | 00,260 | 87 : | 25,170 | 5012 |
| **OBH 13** | 11 : | 03,510 | 87 : | 28,220 | 5091 |
| **OBS 37** | 11 : | 06,730 | 87 : | 31,280 | 5292 |
| **OBS 12** | 11 : | 10,100 | 87 : | 34,490 | 5296 |
| **OBS 38** | 11 : | 13,410 | 87 : | 37,590 | 5143 |
| **OBH 11** | 11 : | 16,670 | 87 : | 40,750 | 4984 |
| **OBS 39** | 11 : | 20,260 | 87 : | 44,070 | 4862 |
| **OBH 10** | 11 : | 23,240 | 87 : | 46,980 | 4840 |
| **OBH 40** | 11 : | 26,060 | 87 : | 50,290 | 4738 |
| **OBH 25** | 11 : | 10,370 | 88 : | 12,360 | 3440 |
| **OBS 41** | 11 : | 07,130 | 88 : | 09,060 | 3325 |
| **OBH 42** | 11 : | 03,750 | 88 : | 05,800 | 3263 |
| **OBS 30** | 10 : | 57,320 | 88 : | 12,380 | 2820 |
| **OBS 26** | 11 : | 00,470 | 88 : | 02,910 | 3160 |
| **OBS 43** | 10 : | 57,250 | 87 : | 59,800 | 2985 |
| **OBS 44** | 10 : | 53,940 | 87 : | 56,700 | 3047 |
| **OBH 27** | 10 : | 50,670 | 87 : | 53,650 | 2980 |
| **OBH 45** | 10 : | 47,490 | 87 : | 50,550 | 2591 |
| **OBS 28** | 10 : | 44,100 | 87 : | 47,320 | 2967 |
| **OBS 46** | 10 : | 40,850 | 87 : | 44,390 | 2441 |
| **OBS 47** | 10 : | 37,530 | 87 : | 41,130 | 2884 |
| **OBS 48** | 10 : | 34,260 | 87 : | 38,050 | 2932 |
| **OBS 29** | 10 : | 30,930 | 87 : | 34,880 | 2913 |
| **OBH 32** | 10 : | 31,030 | 87 : | 47,450 | 2996 |
| **OSB 49** | 10 : | 25,910 | 88 : | 17,960 | 3248 |
| **OSB 50** | 10 : | 28,960 | 88 : | 14,700 | 3264 |
| **OBH 51** | 10 : | 32,000 | 88 : | 11,810 | 3064 |
| **OBS 52** | 10 : | 34,910 | 88 : | 08,920 | 2996 |
| **OBH 33** | 10 : | 37,760 | 88 : | 06,270 | 3020 |
| **OBS 53** | 10 : | 40,960 | 88 : | 03,040 | 2918 |
| **OBS 31** | 10 : | 44,220 | 87 : | 59,950 | 2894 |
| **OBH 54** | 10 : | 47,500 | 87 : | 56,620 | 2830 |
| **OBS 55** | 10 : | 50,710 | 87 : | 53,610 | 2971 |
| **OBS 56** | 10 : | 53,900 | 87 : | 50,320 | 3046 |

| INSTRUMENT | LATITUDE (N) D:Min | | LONGITUDE (W) D:Min | | DEPTH (m) |
|---|---|---|---|---|---|
| **OBS 22** | 10 : | 57,150 | 87 : | 47,200 | 3445 |
| **OBS 57** | 11 : | 00,000 | 87 : | 44,000 | 3627 |
| **OBS 18** | 11 : | 03,640 | 87 : | 40,850 | 4202 |
| **OBP 19** | 11 : | 03,810 | 87 : | 41,060 | 4011 |
| **OBH 58** | 11 : | 07,250 | 87 : | 37,280 | 4814 |
| **OBH 59** | 11 : | 10,120 | 87 : | 34,580 | 5339 |
| **OBS 60** | 11 : | 13,130 | 87 : | 31,640 | 4402 |
| **OBS 61** | 11 : | 16,230 | 87 : | 28,520 | 3439 |
| **OBS 62** | 11 : | 7,98 | 87: | 12,06 | 2298 |
| **OBS 63** | 11 : | 8,88 | 87: | 11,52 | 1981 |
| **OBS 64** | 11 : | 10,60 | 87: | 10,37 | 1470 |
| **OBS 65** | 11 : | 12,09 | 87: | 09,37 | 1248 |
| **OBS 66** | 11 : | 12,19 | 87: | 9,30 | 1226 |
| **OBS 67** | 11 : | 12,26 | 87 | 9,22 | 1215 |
| **OBH 68** | 11 : | 12,33 | 87: | 9,18 | 1217 |
| **OBH 69** | 11 : | 13,15 | 87: | 8,66 | 1147 |
| **OBS 70** | 11 : | 14,07 | 87: | 8,05 | 839 |
| **OBH 71** | 11 : | 14,22 | 87: | 7,99 | 825,6 |
| **OBS 72** | 11 : | 14,24 | 87: | 7,90 | 802,6 |
| **OBH 73** | 11 : | 14,31 | 87: | 7,84 | 838,7 |
| **OBH 74** | 11 : | 15,17 | 87: | 07,29 | 801,7 |
| **OBH 75** | 11 : | 16,32 | 87: | 6,51 | 703,7 |
| **OBH 76** | 11 : | 16,26 | 87: | 10,21 | 1031 |
| **OBH 77** | 11 : | 14,83 | 87: | 8,83 | 927 |
| **OBH 78** | 11 : | 13,44 | 87: | 07,360 | 861,3 |
| **OBS 79** | 11 : | 13,39 | 87: | 7,30 | 871 |
| **OBS 80** | 11 : | 13,32 | 87: | 7,26 | 874 |
| **OBH 81** | 11 : | 13,21 | 87: | 7,18 | 902 |
| **OBH 82** | 11 : | 12,18 | 87: | 6,14 | 1010 |
| **OBH 83** | 11 : | 10,74 | 87: | 4,65 | 1130 |
| **OBH 84** | 11 : | 04,030 | 87 : | 05,980 | 2087 |
| **OBH 85** | 11 : | 03,410 | 87 : | 05,120 | 2014 |
| **OBH 86** | 11 : | 02,710 | 87 : | 04,440 | 1985 |
| **OBH 87** | 11 : | 02,130 | 87 : | 06,650 | 1950 |
| **OBS 88** | 11 : | 01,410 | 87 : | 02,860 | 1866 |
| **OBS 89** | 11 : | 01,100 | 87 : | 02,440 | 1857 |
| **OBS 90** | 11 : | 00,750 | 87 : | 02,020 | 1814 |
| **OBS 91** | 11 : | 00,450 | 87 : | 01,650 | 1807 |
| **OBS 92** | 11 : | 00,100 | 87 : | 01,300 | 1825 |
| **OBH 93** | 10 : | 59,450 | 87 : | 00,510 | 1777 |
| **OBH 94** | 10 : | 58,790 | 86 : | 59,760 | 1768 |

## 4.7 Acknowledgements

We thank Captain Niels Jakobi and the entire crew of RV METEOR for their excellent support during the cruise. Cruise M66/4a was funded by the DFG (Deutsche Forschungsgemeinschaft) through the SFB574 and the M66/4a Subflux grant.

## 4.8 References

Gutenberg, B., C.F. Richter, 1954. Seismicity of the earth and associated phenomena. Princeton University Press, pp. 310

Havskov, J., L. Ottemöller (eds), 2001. SEISAN: The earthquake analysis software for Windows, Solaris and LINUX, version 7.2. Institute of Solid Earth Physics, University of Bergen, Norway

Lay, W., T.C. Wallace, 1995. Modern Global Seismology. Academic Press

Lee, W.H.K., R.E. Bennet, L. Meagher, 1972. A method for estimating magnitude of local earthquakes from signal duration. U.S.G.S. Open file report

Lienert, B.R., J. Havskov, 1995. A computer program for locating earthquakes both locally and globally. Seismological Res. Letters, 66, pp. 26-36